THE MECHANISMS OF FRETTING WEAR OF MISALIGNED SPLINES IN THE PRESENCE OF A LUBRICANT

by

RICHARD ANDREW NEWLEY

A thesis submitted for the degree of

DOCTOR OF PHILOSOPHY

of the University of London

and also for the

DIPLOMA OF MEMBERSHIP OF IMPERIAL COLLEGE

March 1978

Lubrication Laboratory, Department of Mechanical Engineering,
Imperial College of Science and Technology,
London, SW7 2BX.

The Mechanisms of Fretting Wear of Misaligned Splines in the Presence of a Lubricant. By Richard Andrew Newley

ABSTRACT

The mechanism of fretting in lubricated contact is investigated using a spline wear tester. This rig is described in Part I of this thesis. Experiments with an ester and with a hydrocarbon lubricant show that the fretting wear rate is proportional to the activity of Oxygen dissolved in the lubricant. An oxygen electrode is used to measure the activity of Oxygen in the oil; the development of this technique is described. Studies of the worn surfaces demonstrate that wear is caused by abrasive action. It is proposed that high rates of wear are the result of the predominance of three-body abrasion.

Experiments conducted to elucidate the chemical processes involved in fretting wear in lubricated contact are described in Part II. The mechanisms of oil oxidation and of antioxidant additive action are discussed. Several ways of monitoring oil oxidation are considered and titration methods for measuring oil acidity and peroxide concentration are described. Experiments performed with antioxidant additives show both reduced oil oxidation and reduced wear.

The extent to which the fretting wear rate is determined by the dissolved Oxygen activity and the degree of oil oxidation leads to the conclusion that peroxy radicals are responsible for oxidation of the metal. The nature of the oxide formed under different conditions of fretting is investigated. It is shown that at high rates of wear there is a greater proportion of the harder oxide (Fe_2O_3) in the debris than during low wear tests.

ACKNOWLEDGEMENT

I am most grateful to Professor Cameron, Dr. Macpherson, and Dr. Spikes for their valuable aid and advice. Many thanks are due to the members of the Lubrication Laboratory for creating a working environment which was both intellectually and physically challenging, and to Mr. R. Dobson and Mr. T. Wymark for their technical advice and philosophical guidance. I greatly appreciate the encouragement given by family and friends.

I would like to thank Westland Helicopters Ltd., for providing the funds for this project.

C O N T E N T S

Title page	1
Abstract	2
Acknowledgement	3
Contents	4
Index of figures and plates	15
Index of tables	18
Index of fretting tests	19
Guide to abbreviations	20
PART I	pages 22 - 188
PART II	pages 189 - 323
References	pages 324 - 337

CHAPTER 1

Fretting Wear

1.1	General Introduction	22
1.2	Fretting - A Definition of Terms and Introduction	22
1.3	Fretting Mechanisms	25
	1.3.1 Adhesive Wear	25
	1.3.2 A Note on the Adhesive Theory of Wear	26
	1.3.3 A Note on the Delamination Theory of Wear	30
	1.3.4 Fretting and Fatigue	33
	1.3.5 Abrasive Wear	34
	1.3.6 Corrosion	35
1.4	Combination of Mechanisms	37
1.5	Effect of Various Parameters on Fretting Wear	40
1.6	Interaction Between Metals, Lubricant and Atmosphere	42
	1.6.1 Fretting	42
	1.6.2 Sliding Wear I	47
	1.6.3 Sliding Wear II	52
	1.6.4 Fatigue	54
	1.6.5 Summary	55
1.7	Corrosion by Oxidised Lubricants	57
1.8	Summary of Chapter One	62

CHAPTER 2

Description of the Spline Wear Tester

2.1 Introduction 63

2.2 The Test Specimens 63

2.3 The Components of the Tester 66

2.3.1 The Gyrator 66

2.3.2 The Specimen Chamber 68

2.3.3 The Oil Circulation System 72

2.3.4 The Loading System 74

2.3.5 Wear Monitoring 76

2.4 Cleaning Procedures 77

2.4.1 The Specimen Cleaning Procedure 77

2.4.2 Cleaning of the Rig 78

2.5 Theoretical Determination of Fretting Conditions Within a Spline Tooth Contact 79

2.5.1 Calculation of Slip Amplitude 79

2.5.2 Calculation of Hydrodynamic Film Thickness 82

2.5.3 Surface Temperature in the Fretting Contact 85

2.6 Summary 88

CHAPTER 3

Oxygen Determination

3.1	Introduction	93
3.2	Methods of Determination of Oxygen Concentration	93
3.3	The Oxygen Electrode	100
	3.3.1 Description	100
	3.3.2 Experimental Procedure	104
	3.3.3 Calibration	111
	3.3.4 Sampling from the Rig	114
	3.3.5 Summary	120
3.4	Atmosphere Control	120

CHAPTER 4

Fretting tests in Ester

4.1	Introduction	123
4.2	A comparison of the results with those of P. M. Ku	124
4.3	Properties of the ester base stock	124
	4.3.1 Composition of the ester	124
	4.3.2 Lubricant performance	128
4.4	Oxidation of the ester	129
	4.4.1 Oxidation mechanisms	129
	4.4.2 Oxidation of the Ester - reaction rate	133
4.5	Experimental Conditions	135
4.6	Experimental Procedure	137
4.7	Experimental Results	138
4.8	Discussion	146
4.9	Wear rates at long times	148
4.10	Examination of the Worn Surfaces	152
	4.10.1 Introduction	152
	4.10.2 The Unworn Surface	154
	4.10.3 Low Wear	159
	4.10.4 Mild Wear	159
	4.10.5 Severe Wear	164
	4.10.6 Conclusions from surface studies	171
4.11	Conclusions	176

CHAPTER 5

Fretting Tests in Hexadecane

5.1	Introduction	177
5.2	The Oxidation of Hexadecane	178
5.3	Purification Procedure for Hexadecane	180
5.4	Experimental	180
5.5	Results and Discussion - General Remarks	181
5.6	Results and Discussion - Initial Wear Rates	183
5.7	Results and Discussion - Wear Rates at Long Times	187
5.8	Summary	187

INTRODUCTION TO PART II 189

CHAPTER 6

Methods of Monitoring Oil Oxidation

6.1 Introduction 191

6.2 Methods Which Were Considered But Not Used 191

6.2.1 Interfacial Tension 191

6.2.2 Viscosity 194

6.2.3 Oil Insoluble Product Determination 194

6.2.4 Chemical Analysis 194

6.3 Methods Which Were Tested 194

6.3.1 Introduction 194

6.3.2 Chromatography 195

6.3.3 Infra-red Spectroscopy 201

6.3.4 Mass Spectroscopy 203

6.4 Acid Titration 209

6.4.1 The Method 209

6.4.2 Experimental 210

6.5 Redox Titration - Peroxide Determination 214

6.5.1 Introduction 214

6.5.2 Experimental 216

6.6 Summary 217

CHAPTER 7

The Effect of Some Oil Oxidation Products on Fretting Wear

7.1 Introduction 219

7.2 A survey of previous investigations of acidity and peroxide content of oxidised oils. 219

7.3 Results of tests with Ester Base stock 227

7.4 Discussion of Ester Results 232

7.4.1 Summary of results 232

7.4.2 Metal catalysis of oil oxidation 232

7.4.3 Adsorption of acid by debris 236

7.4.4 The role of hydroperoxides as pro-wear agents 239

7.4.5 The nature of the wear reaction 243

7.5 Conclusions to Part A - Ester Lubricant 244

7.6 Results of tests with Hexadecane - Introduction 245

7.7 Tests using purified Hexadecane 245

7.8 Tests with acid added to Hexadecane 249

7.8.1 Introduction 249

7.8.2 Tests with a low acid content 249

7.8.3 Tests with a high acid content 256

7.9 Conclusions to Section B - Hexadecane 258

7.10 General Conclusions 258

7.10.1 Similarities in behaviour of the ester and hexadecane lubricants 260

7.10.2 Differences in behaviour of the ester and hexadecane lubricants 260

7.10.3 The mechanism of metal oxidation within a lubricated contact - a hypothesis 262

CHAPTER 8

Fretting Tests with Antioxidant Additives

8.1 Introduction 263

8.2 Antioxidant Types 265

8.2.1 Oxidation of Hydrocarbons 265

8.2.2 Metal Deactivators 265

8.2.3 Free Radical Inhibitors 266

8.2.4 Hydroperoxide Decomposers 268

8.2.5 The Modes of Action of the Inhibitor and the Hydroperoxide Decomposer Antioxidants Contrasted 269

8.3 Experimental 271

8.4 Results 271

8.4.1 Preliminary Tests 271

8.4.2 Tests with a Hydroperoxide Decomposer 272

8.4.3 Tests with an Inhibitor 278

8.4.4 Results of Acidity Tests 281

8.5 Discussion of Results 284

8.5.1 Introduction 284

8.5.2 Alternative Modes of Action of the Additives 284

8.5.3 The Relationship Between Antioxidant Action and Wear Reduction 287

8.5.4 The Relationship Between Oxygen Activity and Wear Rate 289

8.6 Conclusions 291

CHAPTER 9

OXIDATION OF THE STEEL SURFACE

9.1	Introduction	293
9.2	The nature of the oxides	293
9.3	Factors affecting the oxide composition	297
9.4	Experimental techniques	301
	9.4.1 Introduction	301
	9.4.2 Electron probe microanalysis	303
	9.4.3 Electron spectroscopy for chemical analysis	303
9.5	Debye-Scherrer x-ray powder diffraction analysis of fretting debris	305
	9.5.1 Introduction	305
	9.5.2 The method	307
	9.5.3 Experimental procedure and results	309
	9.5.4 Assessment of the relative quantities of the oxides	310
9.6	Conclusions	316

CHAPTER 10

CONCLUSIONS AND SUGGESTIONS FOR FURTHER WORK

10.1	Conclusions	319
10.2	Practical relevance of Fretting wear results	320
10.3	Suggestions for further work	320
10.4	Investigation of additive combinations	321

INDEX OF FIGURES AND PLATES

Chapter One

1.3.1	A simplified model of asperity contact	27
1.3.2	" " " "	27
1.3.3	Abrasive wear of a chalk pin: after ref 91.	36
1.6.1	Spline fretting wear : after ref. 12.	39
1.6.2	The effect on spline wear of various additives. after ref. 12.	45
1.6.3	Four-ball wear in a highly refined paraffinic oil : after ref. 5.	48
1.6.4	Four-ball wear in ester. After ref. 5.	48
1.6.5	Effect of oxygen concentration on wear rate of ball-on-cylinder rig : after ref. 14.	50
1.6.6	Fatigue life of roller bearings run in fresh and oxidised oil : after ref. 62.	56
1.7.1	Bearing metal corrosion in an oxidising oil : after ref.92.	59
1.7.2	Oxidation and corrosion curves of a white oil : after ref. 63.	61

Chapter Two

2.2.1	Spline specimen design.	64
2.3.1	The spline wear tester.	67
2.3.2	" " " "	67
2.3.3	Diagram illustrating gyrator design.	69
2.3.4	Diagram of the specimen chamber.	70
2.3.5	The specimen chamber.	71
2.3.6	" " "	71
2.3.7	The oil circulation system.	73
2.3.8	Diagram of the loading linkage.	75
2.5.1	Calculation of the magnitude of shank bending	81
2.5.2	The simplified sliding pad model.	84
2.5.3	Variation of flash temperature with load : after ref. 72.	87
2.5.4	Variation of flash temperature with load : after ref. 73.	87
2.5.5	Location of thermocouple to measure surface temperature.	89

Chapter Three

3.2.1	Diagram of a gas chromatograph.	95
3.2.2	Diagramatic representation of electron excitation and decay processes.	98
3.3.1	The Oxygen Electrode.	101
3.3.2	Diagram of the Cell-type oxygen electrode.	103
3.3.3	Variation of cell current with voltage and oxygen concentration.	103
3.3.4	Electrical circuit for the oxygen electrode.	105
3.3.5	Variation of measured voltage with time.	106
3.3.6	Hayward's gas extraction apparatus : ref. 82	112
3.3.7	Calibration graph.	116
3.3.8	Variation of electrode sensitivity with temperature : after ref. 81.	118

3.3.9 Variation of measured voltage and oil sample temperature. 119
3.4.1 Gas flow system for low oxygen concentrations. 121

Chapter Four

4.2.1 Comparison of results with Ku et al., ref. 12,13 125
4.4.1 Reaction sequence in hydrocarbon oxidation. 131
4.6.1 The Nitrogen purging system. 139
4.7.1 Wear curves in Ester. 141
4.7.2 Wear rate versus oxygen activity. 142
4.7.3 Results of regression analysis. 145
4.8.1 Linear plot of wear rate against oxygen activity. 149
4.9.1 Wear without a lubricant 151
4.9.2 Successive tests with the same spline specimen. 151
Plate 4.1 The worn surface. 153
Plate 4.2,4.3 The unworn surface (SEM). 157
Plate 4.4 A section through the unworn surface. 158
4.10.1 Talysurf trace of unworn surface. 158
4.10.2 Talysurf traces of low wear specimens. 160
4.10.3 Diagram of low wear areas. 161
Plate 4.5,4.6 Low wear (SEM). 162
Plate 4.7,4.8 Low wear (SEM and section). 163
Plate 4.9,4.10 Mild wear (SEM). 165
Plate 4.11 Mild wear (SEM). 166
4.10.4 Mild wear. Talysurf trace. 167
Plate 4.12,4.13 Severe wear (SEM). 168
Plate 4.14,4.15 Severe wear (SEM and section) 169
4.10.5 Schematic representation of initiation and spreading of fretting damage : after ref. 45 170
4.10.6 Severe wear. Talysurf trace. 172
4.10.7 Talysurf traces illustrating conformation of the worn surfaces. 173
4.10.8 Illustration of direction of debris flow. 175

Chapter Five

5.6.1 Wear rates in Hexadecane. 185
5.6.2 Wear curves in Hexadecane. 186

Chapter Six

6.3.1 Diagram of a Thin Layer Chromatography plate 197
6.3.2 Representation of T.L.C. results. 199
6.3.3 Representation of T.L.C. results. 200
6.3.4 The Infra-red spectrum of Hexadecane. 202
6.3.5 Summary of measurements of acid and peroxide concentration during Test G 206
6.4.1 Spectrophotometric titration apparatus. 211
6.4.2 End point determination. 213

Chapter Seven

7.2.1	Relationship between peroxide concentration and corrosion rate : after ref. 92,63.	220
7.2.2	Corrosion results with engine oils : after ref.63.	222
7.2.3	Effect of metal catalyst on oil oxidation : after ref. 93.	223
7.2.4	Increase of oil acidity during a wear test : after ref. 10.	226
7.3.1	Fretting wear with Ester.	228
7.3.2	Increase in acidity during fretting tests.	229
7.3.3	Increase in peroxide concentration during fretting tests.	230
7.4.1	Reaction sequence during hydrocarbon oxidation.	235
7.4.2	Adsorption of acid molecules onto a surface.	238
7.7.1	Variation of acidity with time.	248
7.7.2	Variation of peroxide concentration with time.	248
7.8.1	Wear rates in Hexadecane with added acid (0.01 M).	250
7.8.2	Wear and acidity measurements, Test L	251
7.8.3	" " " Test M	252
7.8.4	" " " Test N	253
7.8.5	Wear rates in Hexadecane with added acid (0.19 M).	257

Chapter Eight

8.2.1	Structure of the antioxidants.	267
8.2.2	The action of Zinc diethyl dithiocarbamate : after ref. 109.	270
8.4.1	Effect of additive concentration on wear.	272
8.4.2	" " " "	274
8.4.3	Wear curves - Zinc diethyl dithiocarbamate.	276
8.4.4	Wear rate versus oxygen concentration.	277
8.4.5	Build-up of peroxide concentration.	279
8.4.6	Wear curves - Phenyl-α-naphthylamine.	280
8.4.7	Wear rate versus oxygen concentration.	282
8.4.8	Increase of acidity when inhibited by Phenyl-α-naphthylamine.	285
8.5.1	Reaction sequence during hydrocarbon oxidation.	288

Chapter Nine

9.2.1	Diagram of a duplex iron oxide film: after ref. 112.	295
9.3.1	Ellingham Diagram.	299
9.3.2	Variation of wear rate with temperature : after ref. 115.	299
9.4.1	A SEM image of the fretting debris.	302
9.4.2	Illustration of the mounting of spline teeth for ESCA.	306
9.5.1	Diagram of an X-ray film.	308
9.5.2	A comparison of densitometer recordings.	314

Chapter Ten

10.3.1	Wear graph from test with increased load.	322

INDEX OF TABLES

1.1	A survey of reported fretting mechanisms.	39
2.1	Properties of EN 36 C steel.	65
2.2	The extent of test oil contamination.	80
3.1	The results of the electrode calibration.	115
4.1	Physical properties of the Ester.	126
4.2	Relative oxidation rates of C-H bonds : after ref. 87	134
4.3	A summary of measurements of wear rate - Ester	143
4.4	A key to the plates of section 4.10.	155,156
5.1	A summary of measurements of wear rate - Hexadecane.	184
6.1	Techniques for monit oring oil oxidation.	192,193
6.2	Identification of peaks in Mass Spectra.	208
7.1	Summary of acid and peroxide observations during wear tests.	233
7.2	A summary of the processes occurring during a typical fretting test.	241
7.3	Results of acid and peroxide determinations during Hexadecane tests.	247
7.4	Summary of observations - Hexadecane tests.	259
8.1	Summary of results - Ester plus Zinc diethyl dithiocarbamate.	275
8.2	Summary of results - Ester plus Phenyl-α -naphthylamine.	275
8.3	Results of measurements of final acidity.	283
9.1	Oxides identified in the debris.	311
9.2	Diffraction pattern index.	312
9.3	A comparison of diffraction patterns.	315

INDEX OF FRETTING TESTS

Test Code	Atmosphere	Lubricant	Additive	Additive conc^{n}. (moles / litre)
A	Nitrogen	Ester	-	-
B	Nitrogen	Ester	-	-
C	air	Ester	-	-
D	air	Ester	-	-
E	Oxygen	Ester	-	-
F	Nitrogen	Hexadecane	-	-
G	air	Hexadecane	-	-
H	air	Hexadecane	-	-
I	Oxygen	Hexadecane	-	-
J	Oxygen	Hexadecane	-	-
K	Oxygen	Ester	(no fretting)	
L	Nitrogen	Hexadecane	Lauric acid	0.01
M	air	Hexadecane	Lauric acid	0.01
N	Oxygen	Hexadecane	Lauric acid	0.01
O	Nitrogen	Hexadecane	Lauric acid	0.19
P	Nitrogen	Hexadecane	Lauric acid	0.19
Q	air	Hexadecane	Lauric acid	0.19
R	Nitrogen	Ester	Phenyl- α -naphthylamine	0.16
S	air	Ester	"	0.16
T	air	Ester	"	0.16
U	Oxygen	Ester	"	0.16
V	Oxygen/air	Ester	"	0.16
W	air	Ester	Zinc diethyl dithiocarbamate	0.04
X	Oxygen	Ester	"	0.04
Y	Oxygen	Ester	"	0.04

A Guide to the Abbreviations and Symbols used in the text

conc^{n}.	concentration
e.p.	extreme pressure
ESCA	Electron Spectroscopy for Chemical Analysis
M	Molar
mmoles	millimoles
nm	nanometer
N	Newton
PαN	Phenyl-α-naphthylamine
ROOH; ROOR'	Peroxides
ROOH	Hydroperoxide
SEM	Scanning Electron Microscope
TLC	Thin Layer Chromatography
ZDDC	Zinc diethyl dithiocarbamate
μ	Coefficient of friction
μm	micron
$\Rightarrow$	it follows that
$\propto$	proportional to

Chapter 1 - Fretting Wear

1.1 General Introduction

This thesis concerns the study of fretting wear in misaligned splines: just one of many different fretting problems. Although it is generally agreed that fretting damage is caused, in all cases, by a combination of the same three or four mechanisms, there is unfortunately no universal solution. The first aim was therefore to establish the mechanism of debris formation. In the past there have been relatively few studies of fretting in the presence of a lubricant so the second aim was to investigate the mechanism of oxidation of the metal and debris under lubricated conditions, particularly as oxidation proved to be an important factor in wear.

The thesis thus falls naturally into two parts. The first (Chapters One to Five) is concerned with establishing the physical mechanism of wear. The test rig and experimental procedure are described. Fretting wear results obtained with two base lubricants are presented together with studies of the worn tooth surfaces. It is concluded that abrasion by debris is the major cause of wear.

The second part (Chapters Six to Ten) describes the investigation into the chemical interactions between the metal, the lubricant and the atmosphere during the fretting tests.

In the course of this study it was necessary to consult a wide range of published work on fretting and wear mechanisms. A selection of the literature is reviewed in this Chapter.

1.2 Fretting - A Definition of Terms and Introduction

When defining "fretting" it is important to distinguish the different terms that may be applied. Waterhouse[1] gives perhaps the clearest set of definitions:

FRETTING "The small amplitude oscillatory relative motion which may occur between contacting surfaces."

FRETTING WEAR "The damage resulting from fretting. N.B. In some circumstances fretting may occur without damage."

FRETTING FATIGUE "The combined action of fretting and fatigue."

FRETTING CORROSION "The type of fretting damage when the debris produced is a chemical reaction product between constituents of the surface and the environment."

There is general agreement that "small amplitude" means a distance of less than about 150 μm. At amplitudes greater than this damage is similar to that resulting from sliding wear[4].

Fretting has been found to be a severe problem in many different circumstances as varied as the fretting fatigue failure of nuclear fuel element cases to the fretting corrosion of surgical implants. As a result

there is a vast amount of published literature on fretting systems and mechanisms. However, such an abundance does not lead to a clear description of the fretting process, since in any given system a combination of the above three fretting mechanisms, peculiar to that system, will operate. Fortunately, the literature has been comprehensively reviewed in a number of recent publications. "Fretting Corrosion" by R. B. Waterhouse[1] (published 1972) gives an authoritative survey of the fretting process summarising much of the published work under the categories: adhesive and abrasive wear, fatigue and corrosion. Fretting mechanisms have lately been reviewed by Hurricks [2] (1970). A wide variety of fretting problems are surveyed in the report of the AGARD Conference: "Fretting in Aircraft Systems"[3].

Most investigations of fretting have looked at the wear or failure of high strength metals and alloys. Relatively little study has been made of the fretting of non-metallic materials although damage has been found to occur with glass, polythene and carbon fibre. The studies on metals may be divided into three groups characterised by different damage mechanisms. It is interesting to note that within each group certain metal alloys predominate.

(1) Fretting in situations of high loading, for instance power transmission. Ferrous alloys particularly - often in lubricated contact - wear by adhesion or abrasion.

(2) Fretting in highly stressed structures, for instance, airframes. Alloys with high strength to weight ratios, such as the alloys of aluminium and titanium -

unlubricated - damage due to fretting fatigue.

(3) Fretting in corrosive environments, for instance surgical implants. The metals studied (e.g. stainless steel) are those normally protected from the environment by a passivating film which breaks down under the fretting action leading to corrosion.

The fretting of splines falls into the first of the above categories, but corrosion or fatigue processes cannot be ruled out. Each of these mechanisms is therefore considered in detail in the next section.

1.3 Fretting Mechanisms

The possible mechanisms of wear (as opposed to fatigue and corrosion) are adhesion and abrasion. Recently the Delamination Theory of wear has been proposed as an alternative to the adhesive theory of wear, so this too is considered.

1.3.1 Adhesive Wear

It is generally agreed that an adhesive mechanism predominates in the early stages of fretting wear[19, 20, 21, 22] once the removal of any protective oxide layer has laid bare the nascent metal. Adhesion results in tearing and roughening of the contact surfaces. There is a lot of metal transfer although there is not necessarily a high rate of debris generation. In the later stages of fretting the accumulation of debris may lead to a reduction in adhesion to fairly low levels[53]. Buckley[22] has shown that those properties which reduce the adhesion of metals also reduce the fretting wear rate e.g.

(a) Orientation of the crystal lattices in the opposing surfaces.

(b) Crystal structure type.

(c) Differences in the crystal structure type or the lattice spacing between the two contacting metals.

Thus Cobalt with a hexagonal close packed structure has low adhesion with itself and with other metals and has good adhesive wear resistance under fretting[23].

1.3.2 A Note on the Adhesive Theory of Wear

Early work on sliding wear showed that the wear volume, V, was related to the load, L, the distance of sliding, S, and the flow pressure of the material, Pm, by

$$V = \text{Constant} \times \frac{LS}{Pm} \quad (24)$$

Archard[25] has proposed a theoretical analysis of this result based on the assumption that wear was due to the adhesion between metal surfaces. In the development of his simplified theory the contact between a plain non-deformable surface and a nominally flat surface made up of deformable spherical asperities of radius R is considered. He assumes a linear distribution of peak heights i.e. the density of asperities per unit depth is a constant, (in reality a skewed Gaussian distribution of height is more likely). The argument proceeds as follows:

If the surfaces move together under a load L a distance x then the area of contact of a typical asperity of height r

$$\delta A_r = 2 \quad R \ (x - r) \qquad \text{(fig. 1.3.1)}$$

$$\text{The total area of contact} = M \sum_{r=0}^{r=x} \delta A_r$$

$$\text{in the limit} \qquad = 2\pi RM \left[xr - r^2/2 \right]_0^x$$

$$= \pi R.M.x^2$$

Figure 1.3.1

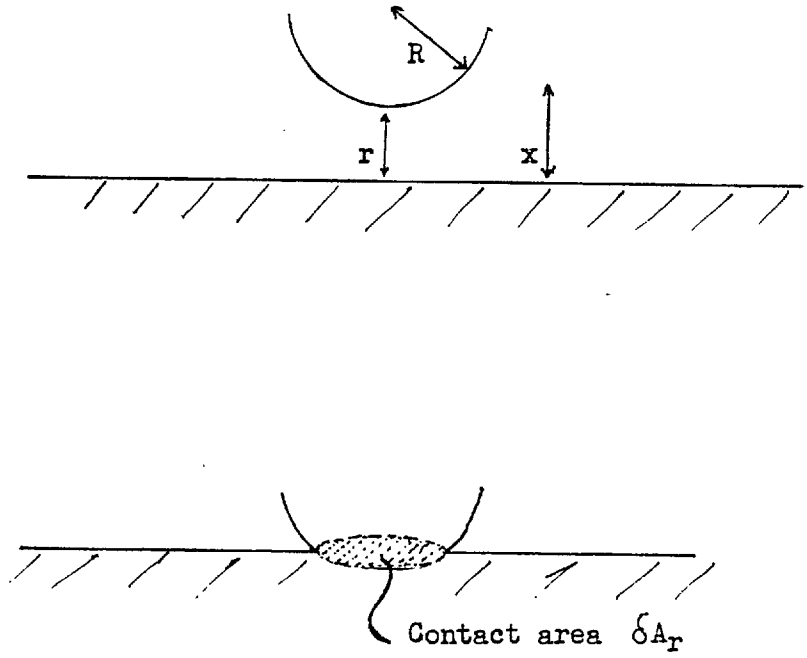

Figure 1.3.2

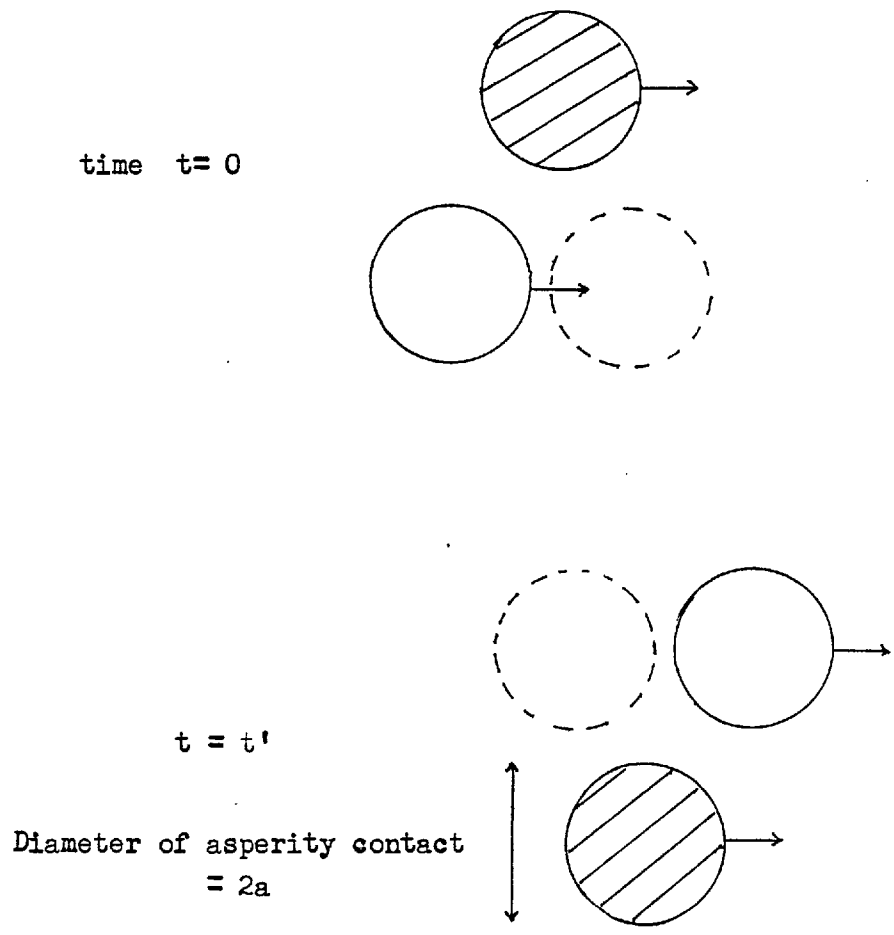

Where M is the number of asperities per unit area at height r. The load carried by each asperity will be a function of its deformation, $(x - r)$.

That is $$\delta L_r = C\,(x - r)^p$$

where the constant, C, and the power, p, depend on the nature of the deformation (elastic or plastic).

For instance for plastic deformation $C = 2\pi R.Pm$

$p = 1$

i.e. the load carried is equal to the contact area times the yield pressure, Pm.

The total load carried by all the asperities, L is given by

$$L = C.M \sum_{r=0}^{r=x} (x - r)^p$$

In the limit

$$L = C.M\left[\frac{(x-r)^{p+1}}{p+1}\right]_0^x$$

$$= C.M.\frac{1}{p+1}.x^{p+1}$$

$$= D\,x^{p+1} \qquad \text{where} \qquad D=\frac{CM}{(p+1)}$$

In order to produce a model for wear Archard made four assumptions:

(1) Asperities of the above type are present in both surfaces.

(2) Each contact is between two asperity peaks. At time t = 0 they completely cover eachother and at time t = t' they have completely separated at which time another two asperities have moved into complete contact to maintain the load. Fig. 1.3.2.

(3) That adhesion in the contact causes formation of a wear particle the size of which is some function of

the maximum radius of contact a_r.

a_r is related to the contact area by $\delta A_r = a_r^2$ and to the contact time by $t' = \frac{2ar}{U}$, U being the sliding velocity.

(4) That there is a probability factor, K, of a wear particle being produced as a result of any one contact.

Assumption (2) implies that the number of contacts per unit sliding distance $\propto 1/a_r$

Assumption (3) implies that the volume of a wear particle $\propto (a_r)^{\gamma}$, where γ for "layer" removal equals 2 and for "lump" removal equals 3.

Hence V_x, the volume of material removed per unit sliding distance due to contacts at height x is such that:

$$V_x \propto a_r^{\gamma-1}$$

now $$a_r = \sqrt{\frac{\delta A_r}{\pi}} = \sqrt{\frac{2\pi R\,(x-r)}{\pi}}$$

$$\Rightarrow \quad V_x = \propto . K\,(x-r)^q$$

where $q = \frac{\gamma-1}{2}$ and $\propto$ is a constant.

The total wear volume, $V = M K \propto \sum_{r=0}^{r=x} (x-r)^q$

$$= M K \propto \frac{1}{q+1} . x^{q+1}$$

$$= E\, x^{q+1}$$ where E is a constant.

substituting for x in terms of the applied load, $x^{p-1} = \left(\frac{L}{D}\right)$:

$$V = E \left(\frac{L}{D}\right)^{\frac{q+1}{p+1}}$$

Thus the following wear volume - load relationships are predicted:

DEFORMATION	PARTICLE SHAPE	RELATION
Elastic ($p = 2/3$)	Layer ($q = \frac{1}{2}$)	$V \quad L^{9/10}$
Elastic	Lumps ($q = 1$)	$V \quad L^{6/5}$
Plastic ($p = 1$)	Layer	$V \quad L^{3/4}$
Plastic	Lump	$V \quad L$

The exponent of the load also varies with the asperity model used. Whilst Archard's theory has been criticised for its somewhat arbitrary assumptions[26] the method of derivation of a wear equation forms the basis of most other more elaborate theories. Although Archard specified adhesion it is possible that other interactions between the asperities are responsible for the generation of a wear particle. Again the probability factor K determines the number of interactions required for particle production.

1.3.3 A Note on the Delamination Theory of Wear

The delamination theory of wear has been proposed by Suh (1973[26] and recently reviewed in a series of papers [121]) as an alternative to the "adhesive wear" models. It is an attempt to explain the production of debris by the propagation of microfatigue cracks as a result of metallurgical changes observed to take place in response to the functional stresses set up during sliding. It is postulated that microcracks propagate parallel to the surface below the wear track at a depth determined by the properties of the material and the loading conditions. As a result plate-like debris is produced. The theory is

particularly relevant to fretting wear because high coefficients of friction are commonly observed in the initial stages of wear and the frequent stress reversals would rapidly propagate the postulated microcracks. The development of the Ferrograph[15] has facilitated the examination of debris and many cases of plate-like debris have been reported.

The factors which affect the wear plate thickness are a matter of some dispute[122]. It was originally proposed that the plate debris was formed by cracking just beneath the dislocation-free zone (d.f.z.). The dislocation-free zone arises because dislocations adjacent to a free surface experience an attraction towards it (the "image" force) - by moving towards the surface the energy stored in the stress field of the dislocation is reduced[39]. In a layer close to the surface this attractive force is greater than the Pieirls stress and any dislocations in this layer are annihilated at the surface. The thickness of the d.f.z. is therefore given by

$$\text{thickness } h = \frac{G.b}{4\pi(1-\nu)\sigma_f}$$

where σ_f is the stress required for dislocation movement

ν is Poisson's ratio

b is the Burgers vector

G is the bulk modulus of the material.

It was proposed that fatigue cracks could not propagate in the d.f.z. because of the absence of dislocations but would run just beneath it.

There are a number of objections to this hypothesis

notably that the d.f.z. in most hardened metals and alloys is much thinner than the thickness of the plate-like debris that have been reported.

Hirth and Rigney[122] propose that softening at the surface extends to a greater depth - of the order of 3 grains at low plastic strains. At strains higher than 0.1, the appearance of dislocation cell structure[40] may limit the softening to a thickness of the order of the cell dimension.

It is not clear however, how the thickness of the softer layer of Hirth or the dislocation free zone, is affected by the presence of a continuous or discontinuous oxide on the surface - a consideration of great practical importance.

A third theory is that the cracks nucleate and propagate a fixed distance beneath the surface determined by the position of the maximum reversed stress[121]. The thickness of the wear plate is therefore influenced by the contact load and coefficient of friction, as well as the material properties.

Having determined the criteria governing plate thickness the wear equation is developed in much the same way as Archard's theory[25], i.e. there is a critical sliding distance for generation of a particle and the area of the wear plate is a function of the asperity contact area. Thus the combined wear between two different metals is given by:

$$V = \left[\frac{k_1 \cdot h_1}{So_1} + \frac{k_2 \cdot h_2}{So_2} \right] . L.S \qquad (26)$$

k_1 and k_2 are constants which depend on surface topography

So = the critical sliding distance for particle generation.

S = total sliding distance.

h_1 and h_2 are the delamination depths for each metal.

This equation is applicable to fretting wear if S is substituted by 2Nxa (2 x number of cycles x slip amplitude). Waterhouse and Taylor[30] found evidence of delamination-type wear in studies on mild steel. In this case the plate thickness observed is much greater than the d.f.z.

1.3.4 Fretting and Fatigue

The reduction in fatigue life of metals by fretting action is well documented (reference (1) chapter 8). ~~Figure 1.3.3 illustrates the order of the reduction.~~ Fatigue cracks nucleate at fretting scars because of the combination of frictional and adhesive forces with the tensile stress increases the maximum resolved shear stress.

It is not clear, however, whether a fatigue process occurs in situations where the externally imposed reversed stressing is absent. Where fatigue has been identified[27, 28, 29] it is generally on a microscopic scale - "Microfatigue". Microfatigue is the mechanism by which debris delamination takes place according to Suh. The direction in which the microcracks propagate is

determined by the stress fields resulting from the loading and frictional forces. Apart from the evidence of metallurgical examination further evidence that in many cases fretting damage is due to fatigue processes is given by the superior wear resistance of surface treatments which introduce compressive stress into the surface over those that simply increase the surface hardness[16]. Examples of such treatments are shot-peening or nitriding [31].

1.3.5 Abrasive Wear

Abrasive wear of two types may occur in fretting. In the early stages one surface abrades the other ("two body abrasion"). When the two surfaces are of different hardnesses, the harder material abrades the softer[34]. Such abrasive action may result in the removal of oxide layers leading to adhesion. As wear proceeds the production of debris, which may well be harder than the substrate owing to work hardening or oxidation, leads to "three body abrasion" - the debris acts as an abrasive "grit" between the two surfaces[32].

The rate of wear, therefore, depends not only on the load and slip amplitude but also on the relative hardness of the contacting surfaces and the debris. The different oxides of iron for instance have very different hardnesses. Thus under conditions which favour the formation of Fe_3O_4 a significantly lower wear rate is observed than under those which favour the formation of the harder oxide Fe_2O_3 [33, 115, 116].

Under certain conditions the two types of wear may co-exist. Godet[91] has studied the following model of

abrasive wear: a chalk pin is lightly loaded against a frosted glass disc through which the wear process may be observed (fig. 1.3.3). Debris produced at the front of the contact passes through towards the rear.

At the rear of the contact the accumulated debris separates the surfaces and supports the load. Wear in this region is three-body abrasion. There is a distinct boundary between these regions of two and three body abrasion.

Abrasion is most significant in the later stages of fretting. One of the main benefits of a liquid lubricant is that it aids dispersion of the debris from a fretting contact and so reduces abrasion. Grease lubricants on the other hand tend to retain debris within the contact and accentuate wear(11).

In fretting fatigue conditions abrasive wear plays a very small part as the cracks, generally initiated when adhesion predominates, are quickly propagated in fatigue. However, in certain circumstances the abrasive wear has been observed to occur at a higher rate than initial crack growth (thus removing the crack) with a resulting increase in fretting fatigue life(35).

1.3.6 Corrosion

Except under conditions of high vacuum, corrosion of nascent metal revealed by wear is always occurring. In highly corrosive environments the action of fretting is to increase the rate of corrosion by activation of the surface layers in the contact. Waterhouse et al.(reference (1) chapter 10) has performed many investigations of fretting in NaCl solutions and has shown an increase in the e.m.f.

Figure 1.3.3

after Godet, ref. 91

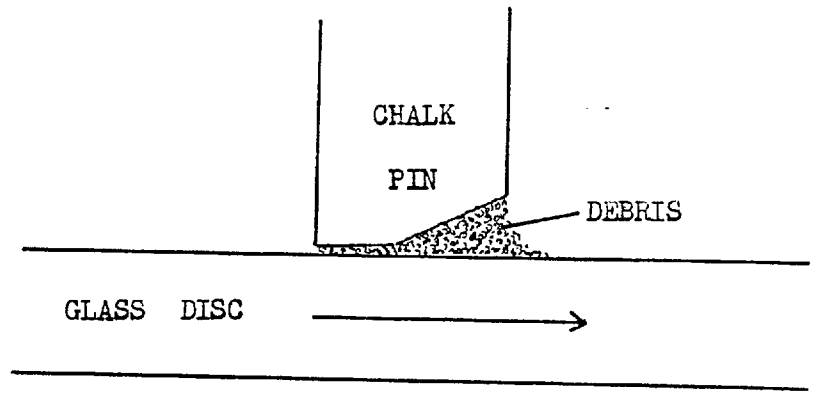

View of pin through glass

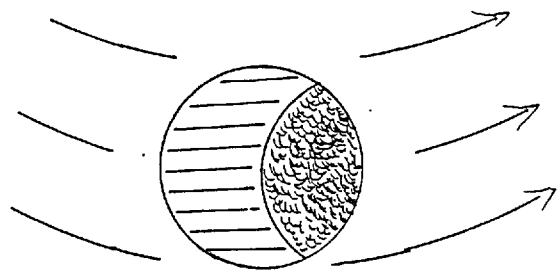

note separation of

areas of wear.

of a corrosion cell when fretting takes place (i.e. the electrode potential of the metal becomes more negative). Kostetskii[36] describes a process of "dynamic oxidation" in fretting. The chemical activity of metal surfaces is increased because of the production of a high density of crystal defects and the reduction of the electron emission energy. Fretting may also remove the passivating oxide layers formed on stainless materials, re-exposing them to a corrosive environment[37].

Less corrosive conditions, such as oxidation, play a part in enhancing the mechanisms of abrasion and fatigue. It has been stated above that oxide debris is generally harder and more abrasive than the nascent metal. The degree of oxidation is an important factor. For instance, Fe_3O_4 is relatively soft and ductile compared with the oxide Fe_2O_3. The oxide hardnesses are 600VPN and 1100VPN respectively[38]. The enhancement of fatigue in corrosive environments is well known.

1.4 Combination of Mechanisms

Attempts have been made to derive a universal wear equation for fretting in which the contributions of the above mechanisms are combined. Notably, Uhlig[41] has proposed an equation to sum corrosive and mechanical damage. The mechanism is assumed to be one of removal of oxide layers from the metal surface, and removal of nascent metal, by the ploughing action of asperities. The weight loss, W_{corr} as oxide per fretting cycle is given by:

W_{corr} = C x area swept out by asperity x number of asperities

x logarithm* of time between successive contacts

The weight loss as a result of mechanical action:

W_{mech} = k_2 x ratio of applied load over yield pressure x sliding distance.

Since the number of asperities is related to the normal load (L) the corrosion term may be simplified:

$W_{corr} = (k_o L^{\frac{1}{2}} - k_1 L)/f$

where f = the frequency of oscillation and C, k_o, k_1 and k_2 are constants. The wear after N cycles is expressed as:

$W_{TOTAL} = (k_o L^{\frac{1}{2}} - k_1 L) \frac{N}{f} + k_2 S.L.N.$

where S is the slip amplitude.

Uhlig derived values for the constants in the above equation applicable to his test conditions[50] and was able to show good agreement with his experimental results. In the general case, however, the conditions of fretting are too complex for wear to be analysed either as a single mechanism (e.g. by Archard's equation for adhesive wear) or even by a simple combination of mechanisms.

Table 1.1 lists a variety of combinations of mechanisms that have been reported in the literature. In addition to those listed there are numerous references to fretting fatigue. These have been omitted because a discussion of this mode of failure is beyond the scope of this work and furthermore, fretting fatigue failure of the

---

*A logarithmic rate of oxidation is assumed.

TABLE 1.1

A survey of some of the mechanisms of Fretting damage that have been reported in the literature.

Worker	Reference	Configuration of fretting apparatus	Wear mechanism
Bethune	20	Rider on flat	Adhesion
Bill	23	Ball on flat	Adhesion microfatigue corrosion/abrasion
Buckley	22	Rider on flat	Adhesion
Burton	27	Ball against flat	Microfatigue
Desetret	37	Fretting in Saline	Corrosion, abrasion
Godfrey	42	Ball on flat	Adhesion, corrosion abrasion
Golego	43	Fretting in electrolyte	Corrosion, fatigue
Halliday	32	Cylinder on flats	Adhesion corrosion abrasion
Hildebrand	34	Hydraulic actuator gland	Adhesion abrasion
Hirano	44	Rider on flat	Microfatigue
Hurricks	2,28	Flat on flat	Adhesion microfatigue
Kostetskii	36		Adhesion, corrosion
McDowell	16	Flat on flat	Abrasion, microfatigue
Muller	46	Flat on flat	Adhesion, corrosion
Ming Feng	45	Flat on flat	Adhesion abrasion
Pitroff	29	Cylinder against flat	Microfatigue, corrosion
Stowers	21	Flat on flat	Adhesion not abrasion
Taylor	47	Ball on flat in Saline	Corrosion
Vaessen	48	Pin on flat	Adhesion
Waters	35	Bridges on fatigue test piece	Fatigue masked by abrasion
Weatherford	12	Spline coupling	Corrosion, abrasion

splines was not observed in these tests.

Table 1.1 makes it clear that various combinations of the four basic mechanisms have been found to be responsible for wear. Adhesion is generally the initial wear process whilst abrasion becomes severe in the later stages of fretting with the accumulation of fretting debris.

1.5 Effect of Various Parameters on Fretting Wear

It will be shown that fretting mechanisms are conditioned by several factors. The variation of wear as conditions are altered has often been used as a means of elucidating wear mechanisms.

On the spline fretting rig described in chapter 2, the following variables may be altered in a controlled way:

(1) Fretting frequency

(2) Fretting amplitude

(3) Load

(4) Temperature

(5) Specimen hardness

(6) Atmosphere

These are discussed below. Clearly when testing a proposed mechanism it is best to vary individually those parameters which have the greatest effect on the primary mechanism.

(1) Frequency. When fretting occurs in an oxidising or corrosive atmosphere the effect of increasing frequency is to decrease the wear incurred in a given number of cycles(49, 50, 51). As the frequency is increased there is less time for adsorption and/or reaction to occur. A

frequency effect would therefore indicate corrosive wear. Generally, variations in frequency have been found to have only a very small effect except at very low frequencies.

(2) Amplitude. Fretting damage increases with amplitude[35, 48, 49, 50, 52, 53] until at large amplitudes the wear resembles sliding wear[4]. The above is true for all the fretting mechanisms.

(3) Load. Increasing the load is found to increase the wear rate provided it does not lead to a reduction in slip amplitude[29, 49, 50, 54]. Increasing the load would not be expected to affect the rate of corrosion directly although it might increase the activity of the metal.

(4) Temperature. The spline fretting rig could be operated with the bulk oil temperature maintained anywhere in the range 40° to 140°C. Changes in fretting wear rate over this range for unlubricated contact are small[55]. However, in lubricated contact the coefficient of friction between rubbing surfaces will vary widely as additives or impurities in the oil adsorb or desorb at their characteristic temperatures[67, 56]. The coefficient of friction determines both adhesive wear and fatigue rates. Moreover, in lubricated contact corrosive wear will be dependent on temperature (both the rates of reaction and the centres of diffusion of a reacting species will be increased with temperature). For these reasons it is to be expected that temperature effects are difficult to interpret. This has proved to be the case in sliding wear[33].

(5) Specimen Hardness. Changing the specimen hardness promises to be a method of differentiating between fatigue and abrasion or adhesion. Increasing the hardness

increases the abrasion resistance[16, 17, 29, 57] and by decreasing adhesion reduces adhesive wear (ref. (1) p. 163 ff.). The surface hardness of the spline specimens may be increased by carburising - a process which lowers resistance to fatigue crack propagation. Corrosive wear is relatively unaffected by changes in hardness.

(6) Atmosphere. The atmosphere primarily affects corrosive wear, but also indirectly influences adhesion, abrasion and fatigue. Adhesive wear is decreased if the atmosphere becomes more corrosive because there is more rapid film formation on clean metal surfaces, whilst fatigue is likely to be enhanced by any increase in corrosion unless this corrosion serves to reduced friction significantly. Abrasive wear is only affected in certain circumstances. For instance, a decrease in oxygen partial pressure favours formation on steel of the less abrasive Fe_3O_4[115]. A lubricant has two effects. Firstly it modifies the environment experienced by the fretting materials - a lubricant restricts the access of a corrosive agent to the surface. Secondly it may react with the atmosphere and the metals as is suggested by the results of Weatherford and Ku[12] which are outlined in the following section. These results prompted the experimental tests on the fretting of splines in controlled atmospheres described in the first part of this thesis.

1.6 Interaction Between Metals, Lubricant and Atmosphere

1.6.1 Fretting

An early study of lubricated fretting wear was made by Godfrey[42] (1956). His apparatus was a ball vibrating

on a flat in a controlled atmosphere. The contact was lubricated by a single drop of oil. After a time the oil was displaced by accumulated debris and severe wear ensued, but before this stage the effect on lubricated wear of oil additives and humidity were observed. Whilst humidity affected unlubricated wear it was found to have very little influence on lubricated wear, indicating the role that a lubricant plays in isolating metals from the atmosphere.

Of the additives, those of the boundary type, Octadecanol and Stearic acid gave slight wear reduction. Phosphorous antiwear additives were most beneficial (notably diethyl hydrogen phosphate) but e.p. additives were ineffective. There was evidence that increasing concentrations of surface active agents (above 5%) led to increased rather than decreased wear.

Pitroff[29] investigated how oils of different viscosities modified the fretting of roller bearings. The cylindrical rollers were vibrated at right angles to the bearing race, the tangental movement of the deforming ball causing wear. The wear was estimated from the width of the "flutes" worn in the track. Oils reduced wear by about 30 times (twice the reduction obtained with greases) and those oils with highest viscosities gave least wear. High viscosity lubricants have low oxygen diffusivities, but it is not clear whether it was this property or merely that the oil was retained in the contact that caused the high viscosity lubricants to have a better performance.

Waterhouse has pointed out that fretting configurations of this kind, when lubricated, give somewhat confusing results, instanced by the results of Burton and Russell[27] which conflict directly with those above. The formation of entrapments and the forcing of lubricant into cracks under pressure enhances fatigue rather than fretting as the main damage mechanism.

In an important pair of papers[11, 12] (published 1966 and 1968) Weatherford, Valtierra and Ku observed the effect of different atmospheres and lubricants on the fretting of splines. When lubricated with certain greases in air, the wear for an initial period was very low before reversion to a rate similar to that of unlubricated wear (see fig. 1.6.1). The period of low wear was termed an "induction period". It was proposed that the maintenance of a lubricant film in the contact during the induction period prevents oxygen access to the surface[11]. The exclusion of oxygen from the atmosphere (by running tests under nitrogen) had the effect of extending the induction period[12].

While no induction period for unlubricated specimens was observed in air, there was a suggestion of an induction period in both dry and moist nitrogen (0.6 and 0.2 hours respectively, compared with 14 hours in dry air when grease lubricated). Moisture in the atmosphere appears to improve the lubricating characteristics of the grease by extending the induction period, but otherwise acts as a pro-wear agent. Thus it was found that both oxygen and moisture separately had a detrimental effect

Figure 1.6.1 after Weatherford et al., ref. 12

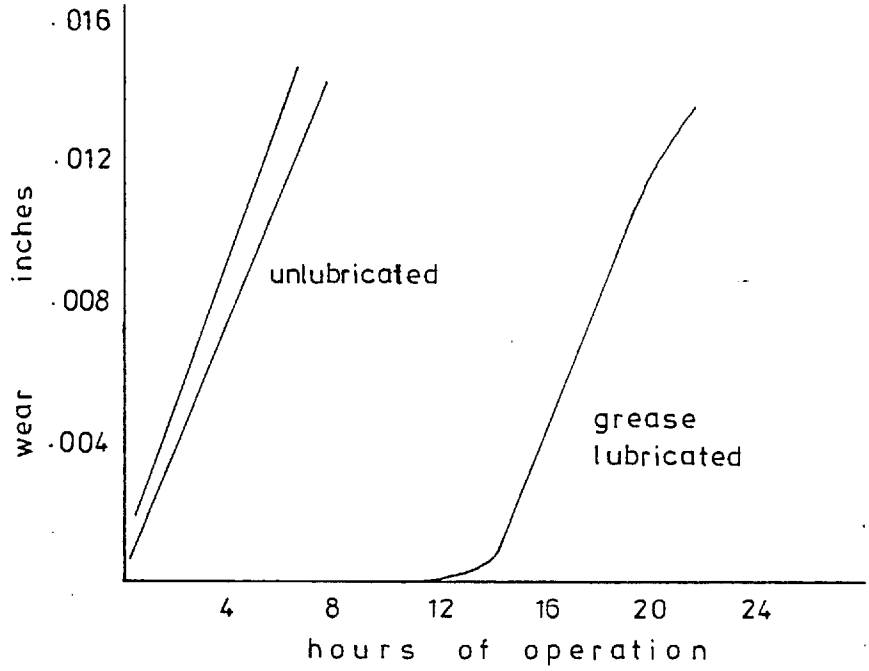

Figure 1.6.2 after Weatherford et al., ref. 12

The effect on spline wear of various additives.

Concentration of additives : 4×10^{-2} mols/litre

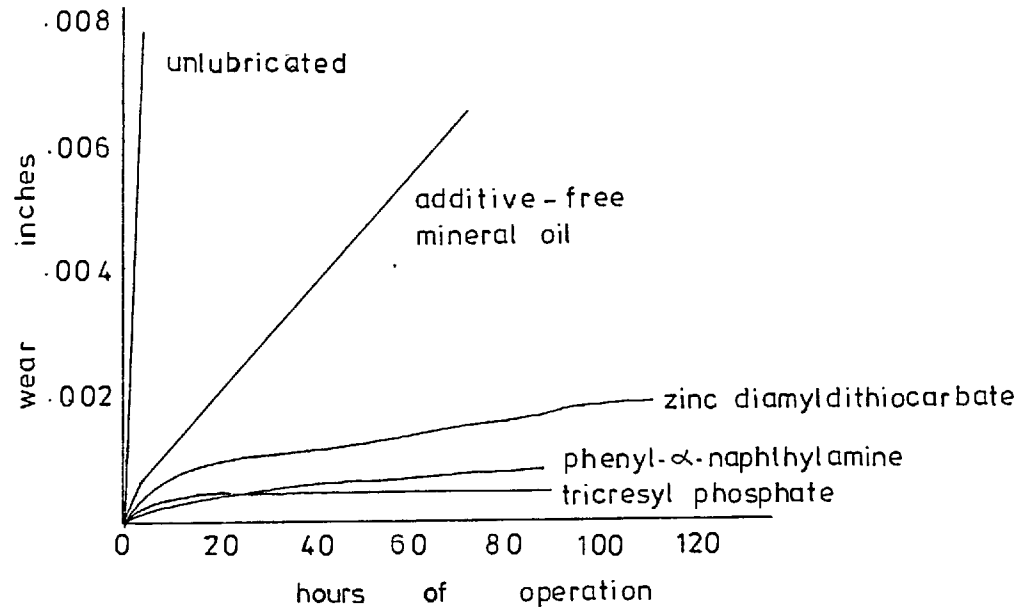

on the wear rate after the induction period except when in combination, i.e. in air, H_2O, had no effect and in moist nitrogen, the presence of oxygen was beneficial. In dry nitrogen adhesion was so severe that fracture occurred at the shank neck although spline wear was low.

In the same paper[12] Weatherford et al. report the results of oil lubricated fretting tests. However, the effect of atmosphere was not tested. The wear rate in an additive-free mineral oil was constant - about one twenty-fifth of the rate of unlubricated wear in air. No induction period was exhibited. Addition of antioxidants to the mineral oil reduced the wear rate to approximately one two-hundredth of unlubricated wear (see fig. 1.6.2). Antioxidants of both the radical inhibitor and peroxide decomposer types seemed effective. An antiwear additive tri cresyl phosphate gave only slightly better protection against fretting than the antioxidants. As a result of the strong correlation between protection from oil oxidation and protection against spline wear it was concluded that "wear involves metal oxidation which proceeds by preferential reaction with hydroperoxides or other hydrocarbon oxidation products rather than with dissolved oxygen".

Peroxides which are known to occur as reactive intermediates in the course of lubricant oxidation[59] are likely candidates. In a further paper[13], Ku et al examine the effects of spline material, surface treatment, spline design and misalignment on wear in fuels. It is shown that reducing the misalignment or crowning of the spline teeth can bring about a significant reduction

in wear.

1.6.2 Interaction Between Metals, Lubricants and Atmosphere - Sliding Wear I

Similar interactions between oxygen, lubricant and metal have been studied in situations where fretting is not involved. Boundary lubrication and wear have been extensively studied in the four-ball apparatus.

Klaus and Bieber(5) have shown that the presence of polar impurities found in hexadecane as a product of oxidation results in a wear scar of half the diameter of that from a test in pure hexadecane. It would appear that some oxidation of a highly refined lubricant is beneficial. In contrast they found that decreasing the oxygen content of the atmosphere above a highly refined oil, hence decreasing the dissolved oxygen content of the oil, also decreased the wear except at very low oxygen concentrations (figs. 1.6.3 and 1.6.4). Note that the slopes of the ester curves are lower and there is no sign of the high wear rate at very low dissolved oxygen concentrations. There is a marked temperature effect due it is said to the thermal instability of the ester. In both oils the result of addition of an antioxidant appears to be masked by the influence of dissolved oxygen.

Fein and Kreuz(58), also working on a four-ball machine showed a decrease of wear with decreased oxygen with the following hydrocarbon lubricants provided seizure did not occur:

Octene
Cyclohexane
Squalane
Dinonyl naphthalene

They suggest that the reduction in wear is due to

Figure 1.6.3 from Klaus and Bieber, ref. 5

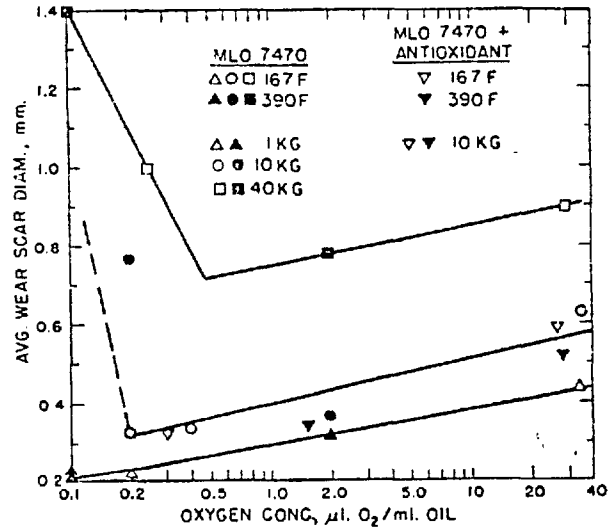

Four ball wear in highly refined paraffinic oil

Figure 1.6.4 from Klaus and Bieber, ref. 6

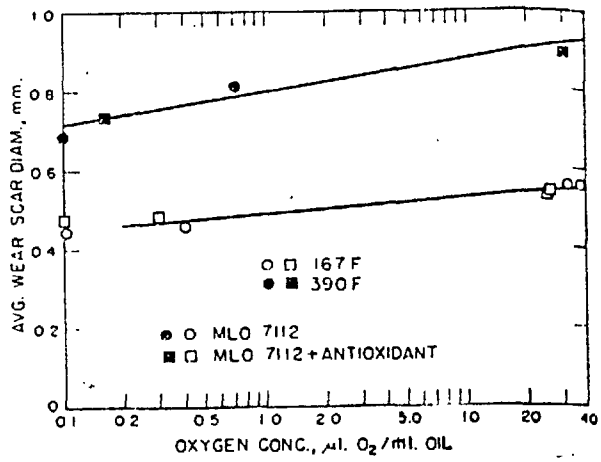

Four ball wear in ester (di-2-ethylhexyl sebacate)

the formation on the nascent metal surfaces of a hydrocarbon "friction polymer" by reactions of the lubricant with the surface. The presence of dissolved oxygen leads to oxide formation in competition to chemisorption of the hydrocarbon and thus a loss of protection. X-ray diffraction studies of the debris showed increasing concentrations of the higher oxides of iron as the dissolved oxygen concentrations increased. Iron carbide and FeO were found in conditions of low wear and low oxygen, Fe_3O_4 in intermediate conditions with an increasing concentration of Fe_2O_3 towards the higher wear regimes.

Appeldoorn, Goldman and Tao[14] investigated wear in the four-ball tester, a ball-on-cylinder rig, a vane pump and the scuffing loads of a micro-Ryder gear rig in the presence of a lubricant and under different atmospheres. The ball-on-cylinder rig (at 25°C) showed that when lubricated with a highly refined oil there was less wear in a dry atmosphere than a humid one. Both gave substantially higher wear than a dry argon atmosphere. On the other hand the presence of oxygen and moisture increased the resistance to scuffing under severe loading (i.e. they were beneficial)[124]. The duration of the tests was probably too short and the test temperature too low to be affected by lubricant deterioration*. The influence of oxygen on the wear rate of the ball-on-cylinder rig is shown in fig. 1.6.5. (This relationship is very similar to that found as a result of the fretting tests described in Chapter 4.) Evidence that the main wear mechanism was

---

*This was observed in some higher temperature tests.

Figure 1.6.5 after Appeldoorn et al. ref. 14

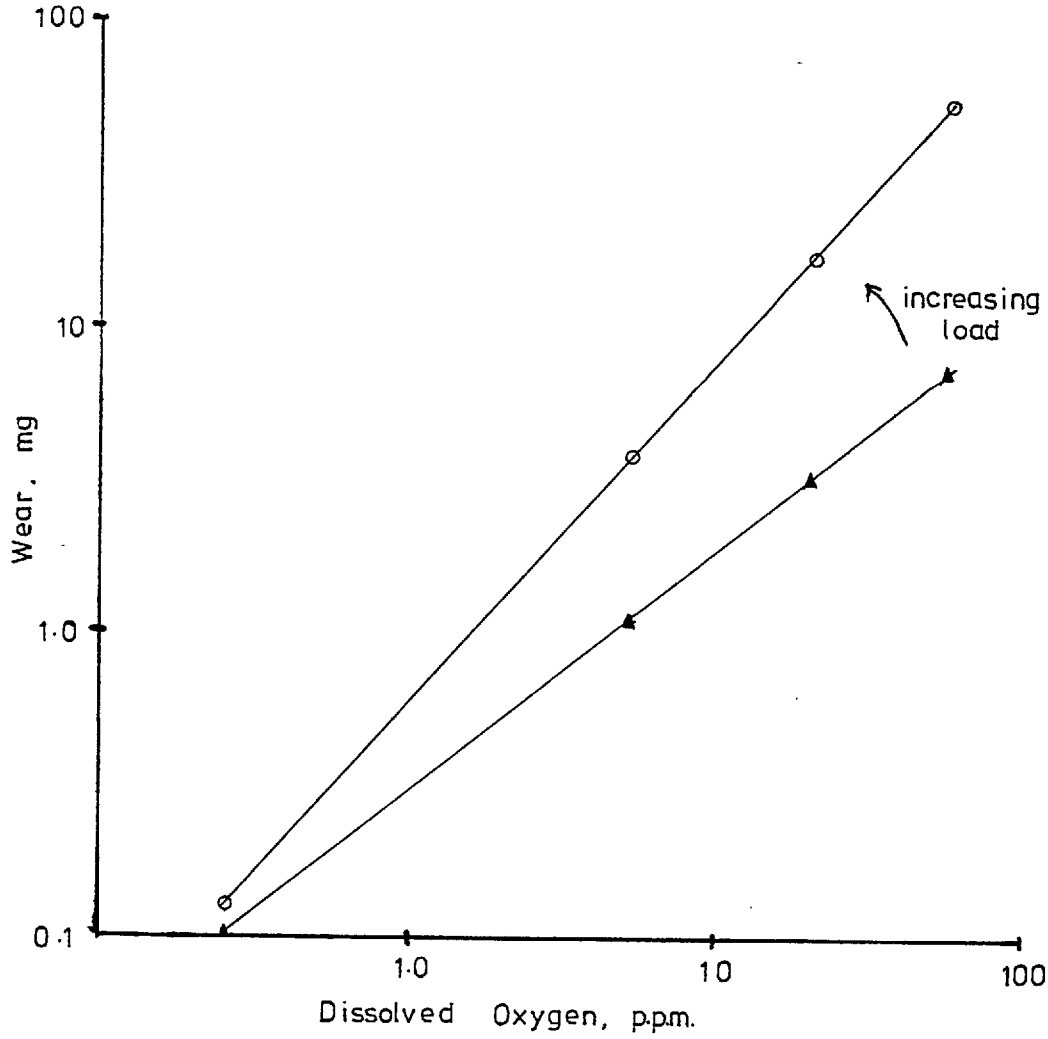

Effect of oxygen concentration on wear rate of a Ball-on-cylinder rig

Lubricant: Bayol 35

Steel-on-steel

25° C

corrosive in nature was provided by the wear rate of "stainless" materials, i.e. those that rely on a passivating oxide film. When tested in the four-ball machine they gave increasing wear with increasing oxygen concentration as above, whilst gold which does not require an oxide film to make it inactive towards oxygen, gave wear results which were independent of the oxygen concentration in the atmosphere. N.B. the tests with gold were run at lower loads to avoid scuffing. Appeldoorn tested a series of lubricants which all, with the exception of methylnaphthalene, gave similar results. Wear in air was found to decrease with increasing viscosity because of the thicker lubricant film in the contact and also because of the reduced oxygen diffusivity in high viscosity oils(60).

In the four-ball tester, 50 p.p.m. of Oleic acid in "Bayol 35" reduced, by a factor of three, the wear scar diameter in a moist air environment. It was the most effective additive; two antiwear additives, zinc dialkyl dithiophosphate and tricresyl phosphate were required in 10 to 100 times larger quantities for the same wear reduction. The effectiveness of Oleic acid is explained by Appeldoorn in terms of its action as a "corrosion inhibitor", but an alternative explanation is that wear reduction was a result of its boundary lubrication. (The tests were conducted at room temperature, at which boundary additives are more effective than anti-wear additives(67).) In a further paper(125) Appeldoorn and Tao show that the addition of Oleic acid reduces abrasive wear by Fe_2O_3 in

the vane pump by forming an adsorbed layer on the debris particles.

The increase of scuffing resistance conveyed by the presence of oxygen in a lubricant was investigated by Bjerk[18]. In nitrogen test rollers were found to scuff at very low loads when lubricated with a plain mineral oil. In oxygen a scuffing resistant layer is developed on the rollers and on the track. Microprobe analysis showed a substantial increase in oxygen in this protective layer. It was found in tests with an ester, however, that an anti-scuffing layer was developed independently of oxygen. It was proposed that the ester decomposed to yield an acid which reacted with the metal surface. Scuffing resistance in ester lubricants will therefore be dependent on the stability of the molecule towards decomposition.

1.6.3 Interaction Between Metals, Lubricants and Atmosphere - Sliding Wear II

The preceding papers have established the effect of oxygen on the different types of wear. The emphasis shifts now towards the interaction between oxygen and the lubricant and the influence of small quantities of lubricating additives on oil impurities on wear in different atmospheres. Rudston and Whitby[6] tested a variety of additives to a purified light paraffinic oil (four-ball tester) in air and nitrogen. Several additives showed good anti-wear properties in air but were ineffective under nitrogen (e.g. long chain alkanes and aromatics attached to hydrocarbon chains) indicating that

oxidation of the additive either in the bulk or at the surface was a prerequisite for boundary action. Only very highly reactive hydrocarbons reduced wear in both air and nitrogen. Non-hydrocarbon compounds that were found to reduce wear in both air and nitrogen i.e. those which did not require preliminary oxidation were organic acids, organic disulphides and nitrogen compounds. Pro-wear compounds in both air and nitrogen were sulphur compounds and organic hydroperoxides. To determine whether hydroperoxides - formed as a result of oil oxidation - were promoting wear a test with 1% of a hindered phenol oxidation inhibitor in the pure oil was run. No reduction in wear was observed. It was suggested that the critical hydrocarbon oxidation was occurring at the wearing surface where the inhibitor could not operate.

The work of Bose, Klaus and Tewksbury(9) was aimed at identifying the products of lubricant/metal/oxygen reactions. As a result of a separation procedure the debris collected from a four-ball test was classified as follows: Oil soluble metal, Pyridine soluble metal (the organometallics) and Pyridine insoluble metal (iron oxide and metallic iron). The organic component of the debris was calculated by subtracting the weight loss of metal from the total weight of debris (usually about 85% by weight). It was shown that the formation of organometallic occurred mainly in the initial stages of the test when the contact geometry of the four-ball rig produces the highest pressures and surface temperatures (the bulk temperature was 75°C). Thereafter the debris was produced as pyridine

insoluble metal and metal oxide. The duration of each test was one hour.

For two highly refined oils replacement of air by a nitrogen atmosphere reduced both metallic wear and the amount of organic debris. The use of 1.0 wt. % of an oxidation inhibitor in air while reducing wear was less effective than removal of oxygen.

Similar experiments were conducted with the ester Di-2-ethyl hexyl sebacate. A test in nitrogen reduced both wear and organic debris slightly, but a test with 0.5 wt. % phenothiazine (an oxidation inhibitor) in air whilst greatly reducing the organic component of the debris gave no reduction in metallic wear. It has been suggested by Klaus[5] that the ineffectiveness of the inhibitor is due to the presence of oxygen in the ester molecule and the lower thermal stability of di-z-ethyl hexyl sebacate compared with the mineral oils used.

It is evident from the above[5, 9, 18] that the stability of esters towards decomposition under the severe conditions imposed by a wearing contact, has a marked effect on wear rate. Lansdown and Hurricks[7] compare the thermal stability of a number of synthetic ester lubricants under service conditions. The thermal stability limit of diesters is about 250°C.

1.6.4 Interaction between Metals, Lubricants and Atmosphere - Fatigue

In many instances, fatigue is the major wear mechanism of fretting. The effect of oil deterioration on fatigue processes is worth considering.

Mould and Silver[10] have studied how oil oxidation

influences the fatigue life of balls in a rolling four-ball machine.

Rapid degradation of the oil was obtained in tests where a small sample of oil was retained in the ball pot. The extent of oil degradation was measured by the acid content. The fatigue lives were much shorter than those obtained with a circulated oil in which there was much slower degradation. Further tests were conducted with different acids[61] added to the circulated oil. Strong acids gave large reductions in life at low acid numbers and fatigue cracks appeared to have propagated by a corrosive mechanism from the rolling track. However, with weak acids such as might result from oil oxidation the concentrations required for similar wear reductions were high, indicating that there is some other degradation product which is more corrosive.

Similar work has been carried out by Koved[62]. Longer fatigue lives of roller bearings were obtained in a paraffinic oil compared with a naphthenic base oil owing to the former's greater oxidation stability. With the naphthenic oil it was found that after a critical degree of oxidation there was a marked decrease in fatigue life (fig. 1.6.6). Inhibition of oxidation of the oil with dibutyl-p-cresol increased the fatigue lives $2\frac{1}{2}$ times.

1.6.5 Summary

Complex interactions between atmosphere, lubricant and metal affect the wear rate in both fretting and sliding wear.

Figure 1.6.6 after Koved, ref. 62

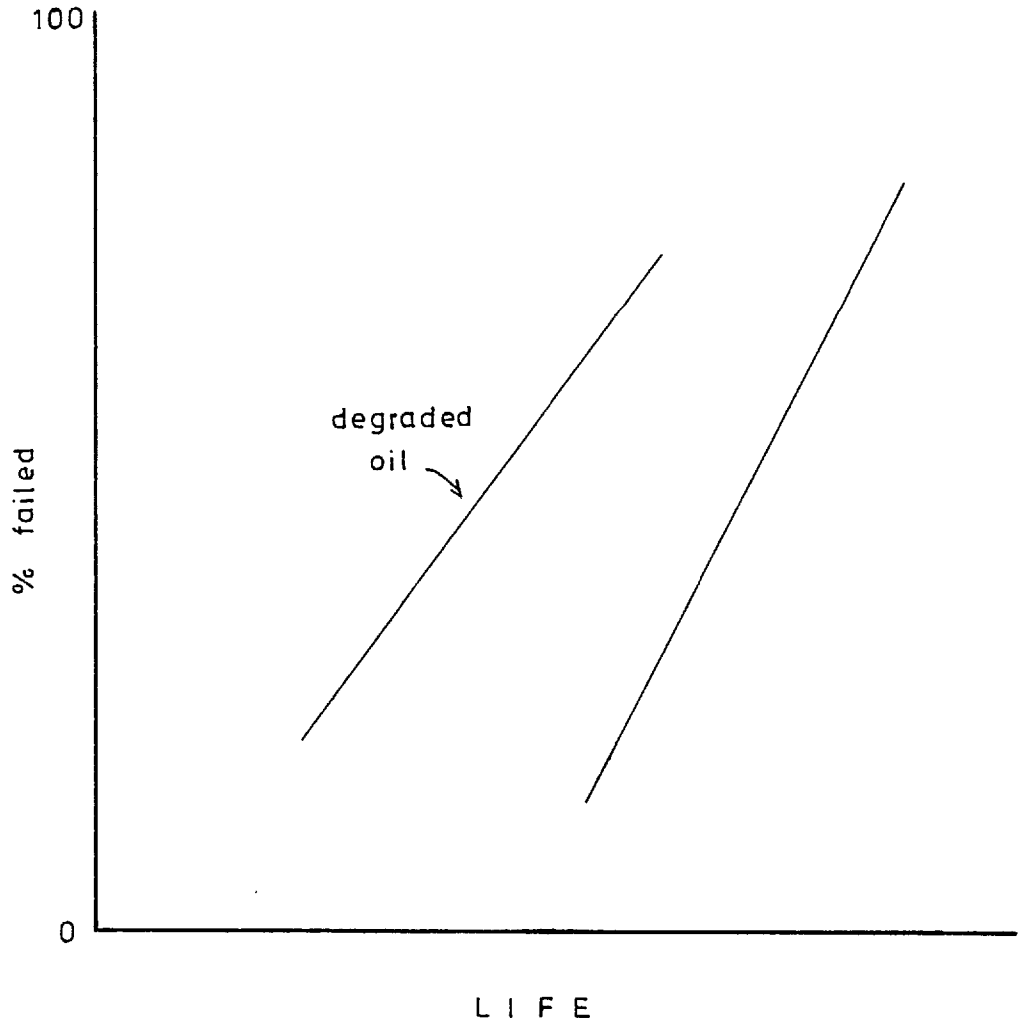

Fatigue life of roller bearings in fresh and oxidised Naphthenic oil.

Scuffing is promoted by the extreme conditions of high load, a highly refined lubricant and an atmosphere whose oxygen content approaches zero. In this situation the presence of oxygen or polar lubricant impurities or even moisture is beneficial[5].

However, when there is no likelihood of scuffing, wear is aggravated by increased oxygen, by highly active surface agents (such as e.p. additives) and by some of the oil oxidation products. Under these conditions, wear may be reduced by operating in an inert environment, or by using oil antioxidant additives to mineral oils in order to cut down lubricant oxidation. The results of Klaus[5, 9] indicate that similar additions to esters will not be as effective. Physically adsorbed polar substances are in general beneficial, e.g. weak acids, alcohols and esters. Oils of high viscosity are beneficial in two ways: they maintain a better film in the contact than oils of lower viscosity and cut down the rate of diffusion of oxygen.

Fatigue crack propagation in the presence of a lubricant is enhanced by oil oxidation. The results of Mould and Silver[10, 61] show that although acid in the oil reduces fatigue life markedly when present in high concentrations, an additional agent must be produced, during oil oxidation, to account for the reduction in fatigue life observed.

1.7 Corrosion by Oxidised Lubricants

In order to gain an understanding of the corrosive processes occurring during wear it is valuable to examine corrosion by lubricants in the absence of wear. A

selection of the published literature is reviewed in this section.

Denison[92] investigated the corrosion of bearing materials* by oxidised mineral oils. He monitored the concentration in the oil of peroxides and acids, which are produced by oxidation, the adsorption of oxygen and the corrosion rate. A typical result is shown in fig. 1.7.1 - the maximum corrosion rate occurs just after the peak peroxide concentration. He noted that the oxide formed on the specimens underwent further reaction and passed into solution as the acidity increased. He proposed the following mechanism of oxidation by peroxides:

$$M + RO_2 \longrightarrow RO + MO$$

$$MO + 2HA \longrightarrow MA_2 + H_2O$$

where RO_2 is a peroxide and HA is an organic acid. However, it was also noted that in two different oils the same rate of corrosion could occur at widely different peroxide concentrations.

A similar series of tests was performed by Wilson and Garner[63] who investigated the corrosion of lead. Specimens were immersed in a white oil which was heated and agitated in the presence of a copper catalyst. Samples of the oil taken at regular intervals were tested for acid and peroxide content. Every half hour the lead specimen was removed and replaced by a fresh lead specimen. The weight loss of the specimen was used to calculate the

---

* Whilst steel would not be expected to corrode at a similar rate to metals such as lead these experiments illustrate the corrosive nature of an oxidising oil.

Figure 1.7.1 after Denison, ref. 92

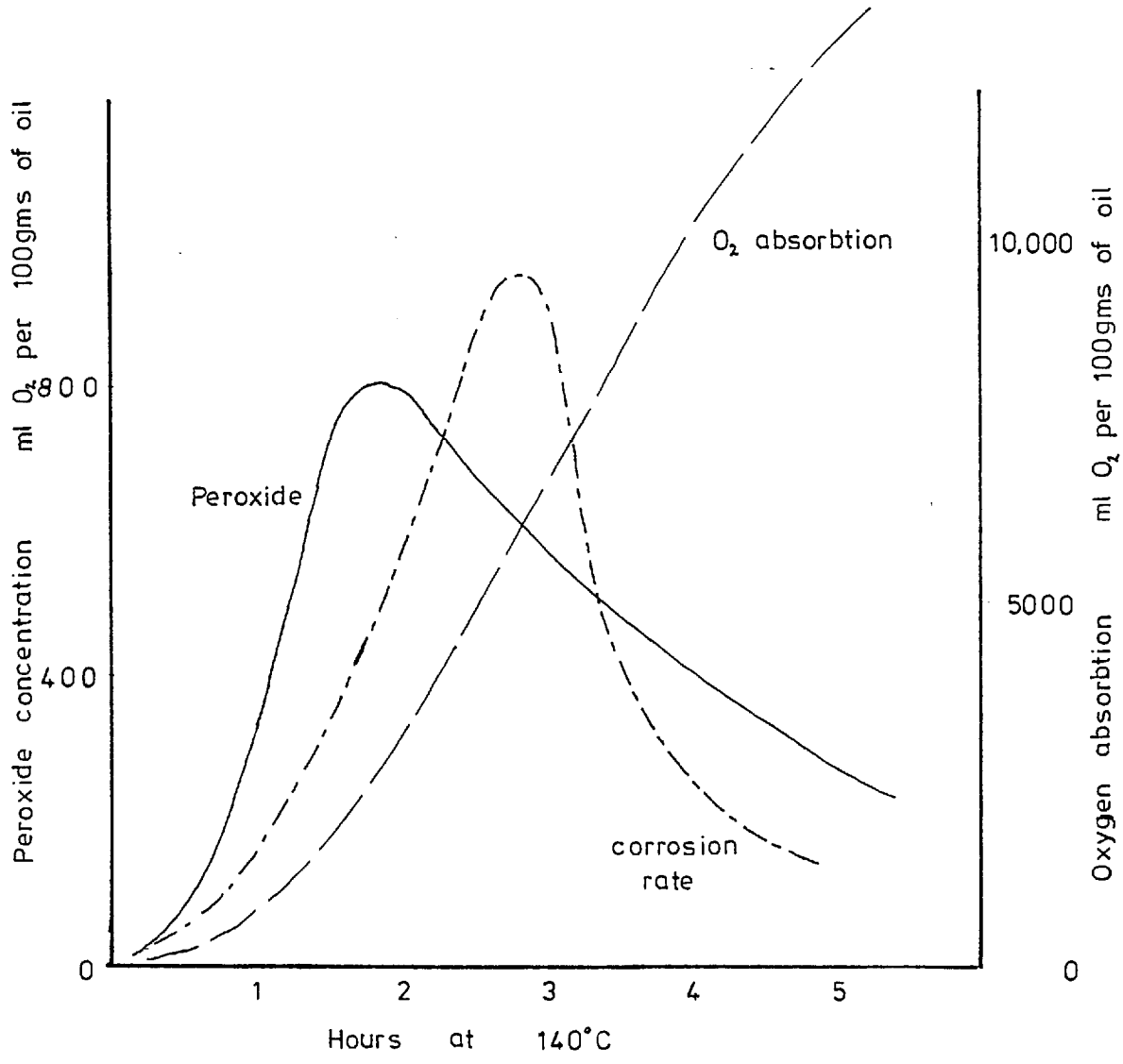

Bearing metal corrosion in an oxidising mineral oil.

corrosion rate. Three different white oils were tested each giving essentially the same behaviour (fig. 1.7.2). When the atmosphere above the oil was nitrogen no corrosion occurred and there were no measurable quantities of peroxides or acids produced. It was observed that the maximum corrosion rate occurred at the maximum rate of fall of the peroxide concentration, indicating that corrosion is associated with peroxide decomposition. A yellow deposit found on the lead was thought to be an organometallic.

Tests on engine oils showed that unlike white oils the peroxide concentration increased logarithmically and did not decay. The oil acidity increased at the same rate observed with white oils.

In so-called interrupted oxidation experiments, samples of the oil were oxidised without the lead test pieces for periods up to 20 hours. These oil samples were initially highly corrosive to lead compared with oils which had been oxidised in the presence of lead for the same period of time, despite having similar measured peroxides and acidities. Either there was a build up of some unknown corrosive agent or it was suggested the corroding of lead leads to a decrease in the oxygen concentration within the oil. In an interrupted test the lead is immersed in an oil that has a high concentration of peroxide and is saturated with oxygen. Unfortunately, oxygen measurements were not made on the oils to confirm this theory.

Chapter 6 describes how the methods of Wilson and

Figure 1.7.2 after Wilson and Garner ref. 63.

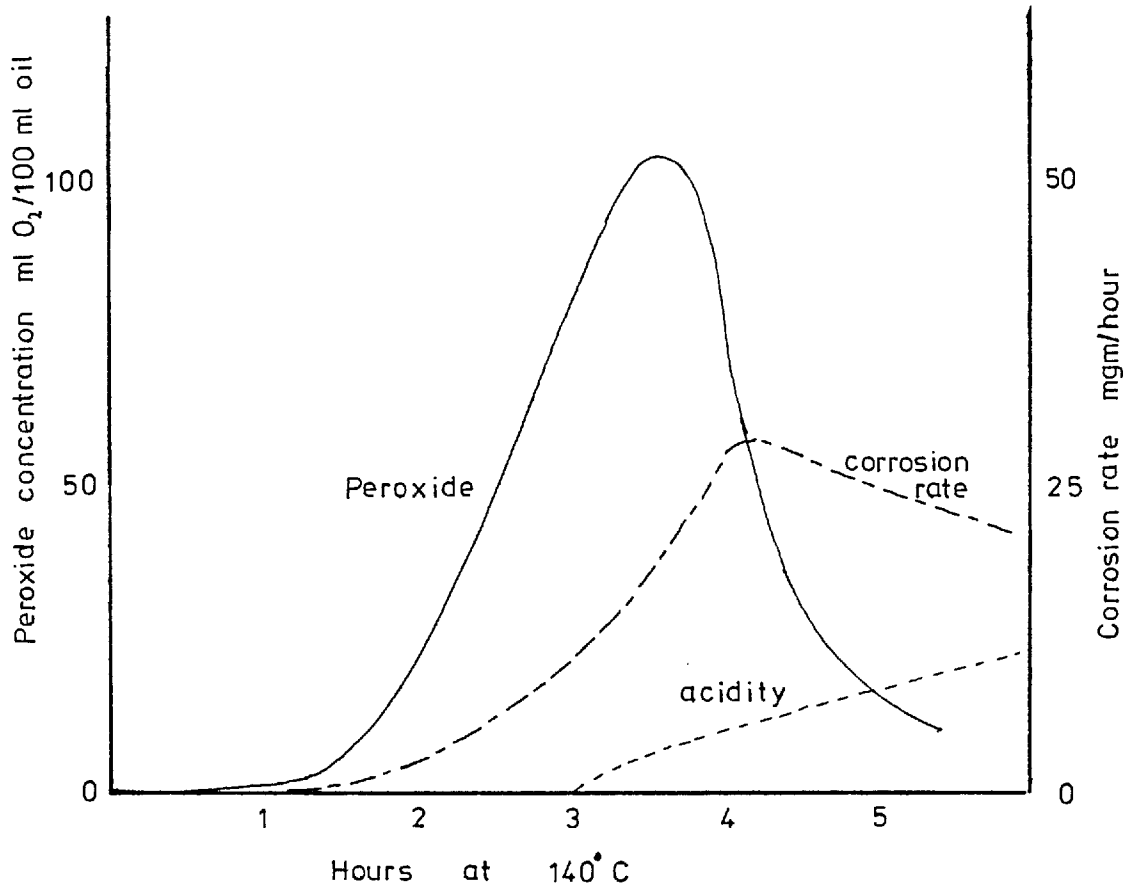

Oxidation and corrosion curves of White oil 'B'.

Garner were used to follow the oxidation in the fretting rig of the ester and hexadecane lubricants. It is not suggested that fretting is a straightforward corrosion process but that corrosion activated fretting could be a significant damage mechanism.

1.8 Summary of Chapter One

Fretting processes have been defined and the four basic mechanisms of surface damage have been described. A survey is given of the incidence of these mechanisms in practice. A longer review is to be found in reference (1).

The effect on fretting wear of a selection of variables has been discussed in the light of published results. The parameters examined are those which may be altered in a controlled way in the spline fretting rig. Of these a change of atmosphere is considered to have one of the largest effects on lubricated wear and to be the most significant.

Since the results of Weatherford, Valtierra and Ku[11, 12] on a similar rig suggest that metal oxidation during fretting occurs by interaction with the lubricant rather than direct reaction with dissolved oxygen the published literature in the field of metal-lubricant-atmosphere interactions has been surveyed in the latter part of the chapter.

Chapter 2
Description of the Spline Wear Tester

2.1 Introduction

The spline wear tester was the same design as that described by Weatherford et al.[11] and was built to a set of drawings kindly supplied by the South West Research Institute of San Antonio, Texas. The spline material was a steel of British specification chosen to be close to the U.S. specification of the steel used by Weatherford. This was done to enable comparison of results to be made.

In the spline wear tester a splined outer specimen is clamped in a fixed position whilst the inner specimen is caused to gyrate without rotating thereby simulating the relative oscillatory motion of angularly misaligned splines rotating at high speed.

The details of the splines and rig design are described in this chapter together with an outline of the procedure for setting up a test.

2.2 The Test Specimens

The details of the spline specimen design are shown in fig. 2.2.1. The spline has 12 involute teeth. The teeth were formed by a broaching process. The spline material was EN36C, the properties of which are listed in Table 2.1. EN36C is an alloy case hardening steel with high tensile strength in the core, due to a fine grain size[65], and good resistance to shock loads. Hence typical uses are high duty gears for aircraft, heavy vehicle transmission components, steering worms, gudgeon pins, etc. Its specification is similar to that of the AMS 626 steel used by Ku. The specimens were supplied in

Figure 2.2.1

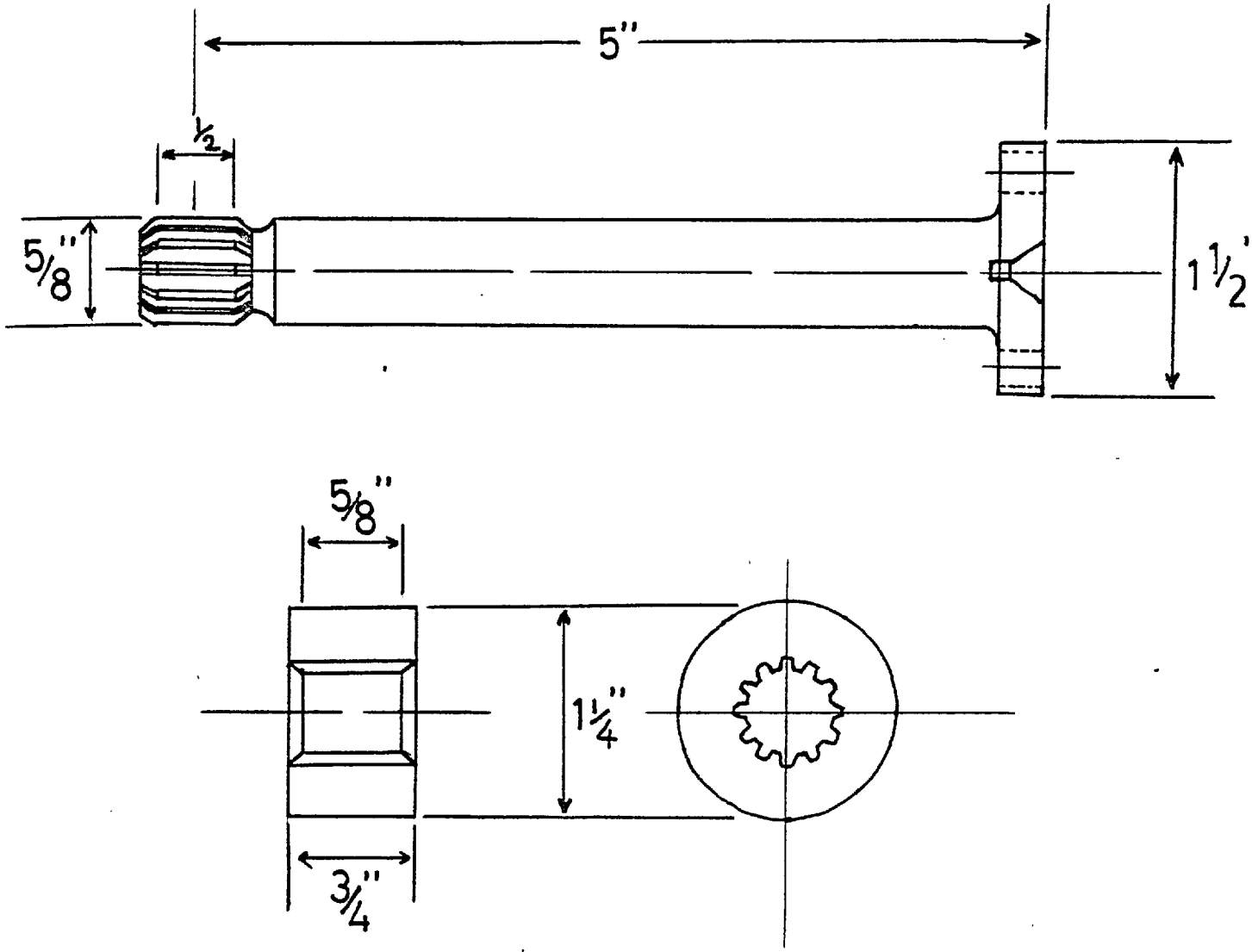

Spline specimen design.

TABLE 2.1

Properties of EN36C steel

Composition :

	C	Si	Mn	S	P	Ni	Cr	Mo	
minimum-	0.12	0.1	0.3	-	-	3.0	0.6	0.1	(%)
maximum-	0.18	0.35	0.6	0.05	0.05	3.75	1.1	0.25	(%)

Mechanical properties :

Tensile strength - 1 GN m^{-2} (65 tons in^{-2})

Elongation - 13%

Izod impact - 41 Nm (30 ft lb)

Specific gravity - 7.87 ($20^{\circ}C$)

Coefficient of thermal expansion- 12×10^{-6} per deg C

Thermal conductivity - 0.09 cal / cm s deg C.

Youngs modulus - 200 GN m^{-2} (12,900 tons in^{-2})

the carburised and uncarburised forms, having measured hardnesses of 735 V.H.N. and 232 V.H.N. respectively.

The splines were manufactured to close tolerances and as far as possible paired to give minimum clearances. When set up in the test rig the circumferential clearance could be measured by measuring the extent to which the male spline could be rotated, using the wear measuring transducer. Clearances were found to be in the range 3 to 10 μm. Accuracy of manufacture was important to ensure that by an early stage in the wear test the applied load was being carried equally by all the 12 teeth. There is no way of telling whether contact is being made between all of the teeth at the start of a test. However, examination of specimens from short runs at low wear showed in almost all cases wear scars on each tooth.

2.3 The Components of the Tester

2.3.1 The Gyrator

The test rig is shown in figures 2.3.1 and 2.3.2. It consists of a gyrator assembly (A) which produces the cyclic motion and below it the specimen housing (B). The gyrator is powered by 1.5 h.p. electric motor (C) which is to the right of the gyrator assembly. Attached to the top of the gyrator assembly can be seen the loading arm arrangement (D). The gyrator, specimen chamber and motor are bolted onto a back plate which is firmly attached to an 'A' frame stand. To the right of the rig can be seen the control box (E) containing the temperature regulator, the L.V.D.T. power supply and safety cut-outs for motor overload, excessive temperature and specimen failure. The L.V.D.T. is attached at (F) and its output displayed

THE SPLINE WEAR TESTER

Figure 2.3.1

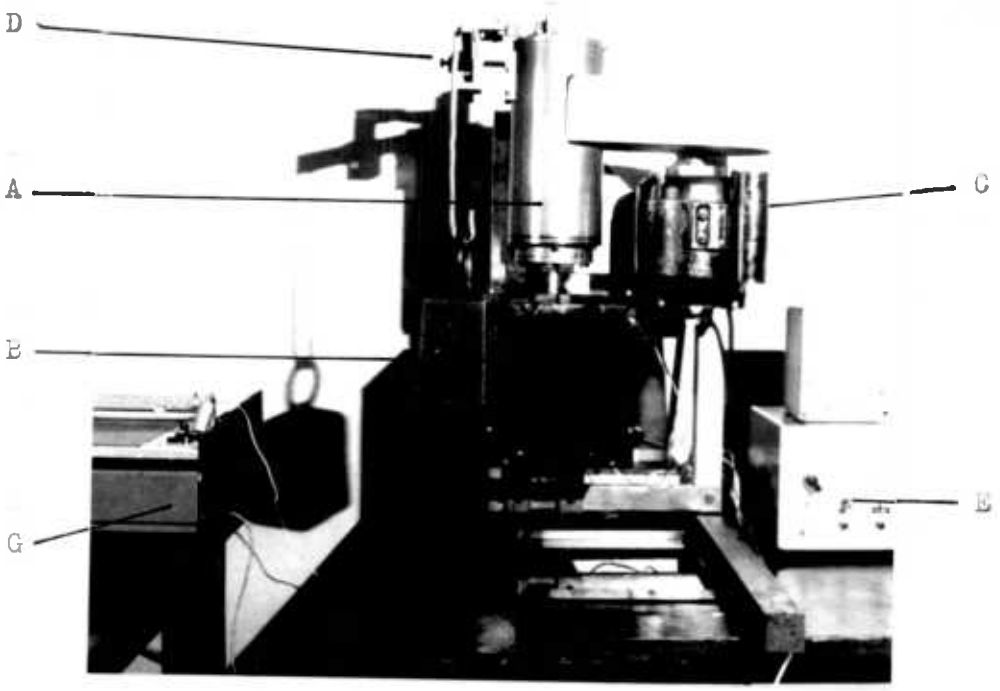

Figure 2.3.2

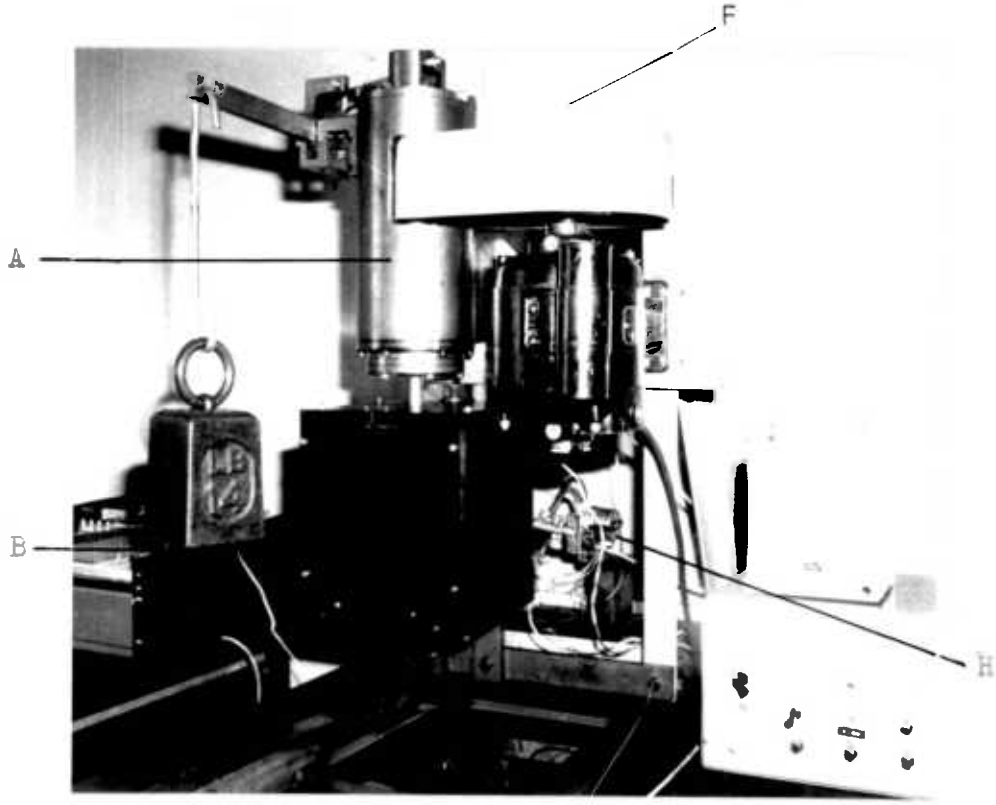

on the chart recorder (G). Temperature was measured by a thermocouple in the specimen chamber and was monitored either on the electronic thermometer or the other channel of the chart recorder. In figure 2.3.2 the peristaltic pump (H) can be seen at the rear of the rig.

The design of the gyrator is shown in fig. 2.3.3. The gyratory motion is produced by placing a non-rotating gyratory shaft (A) eccentrically within a cylindrical drive shaft (B) which rotates at 3250 r.p.m.

The inside of the drive shaft was bored on centres displaced by 0.030"(0.762mm) giving a throw of 0.060" (1.524mm). This motion is transferred to the flanged end of the male spline specimen through a flexible spring steel diaphragm (C). This specimen pivots in the female specimen and the gyrator simulates the motion in a junction between 2 shafts misaligned with respect to each other by 0.344° when rotating at high speed. Assuming that the rig mountings are absolutely rigid and there is no bending of the spline shaft the amplitude of movement between the spline teeth if measured at the pitch diameter would be 90 μm (0.0036") and at the tooth tips 120 μm.

A second cylindrical drive shaft was fabricated to produce a 0.76mm throw (equivalent to an angular misalignment of 0.172°) in order that the effect of slip amplitude on wear might be investigated.

2.3.2 The Specimen Chamber

The arrangement of the specimen chamber is shown in fig. 2.3.4. The chamber is in 2 halves, one half (A) attached to the backplate, the other (B) acting as a

Figure 2.3.3

Diagram illustrating the Gyrator design.

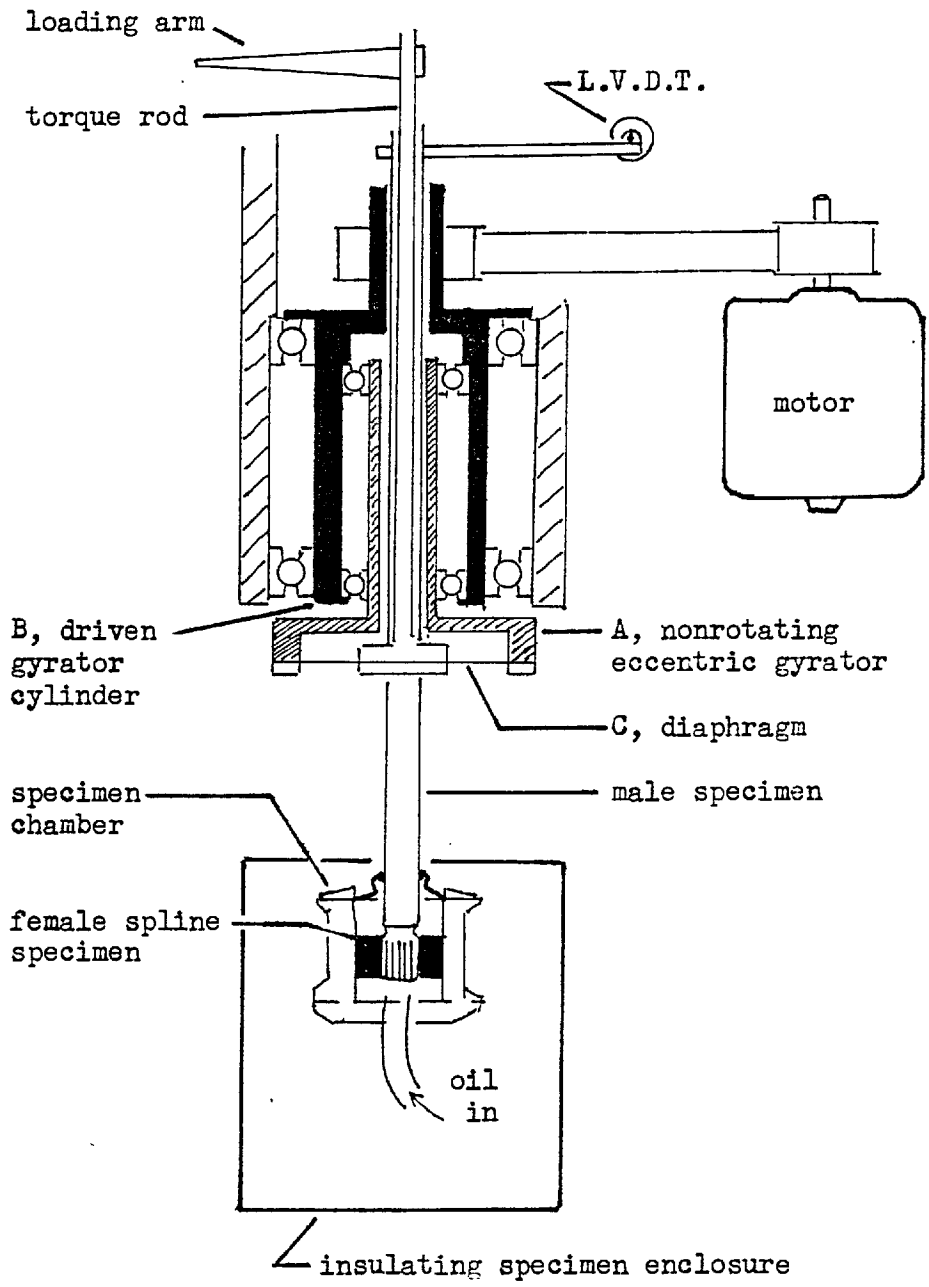

Figure 2.3.4

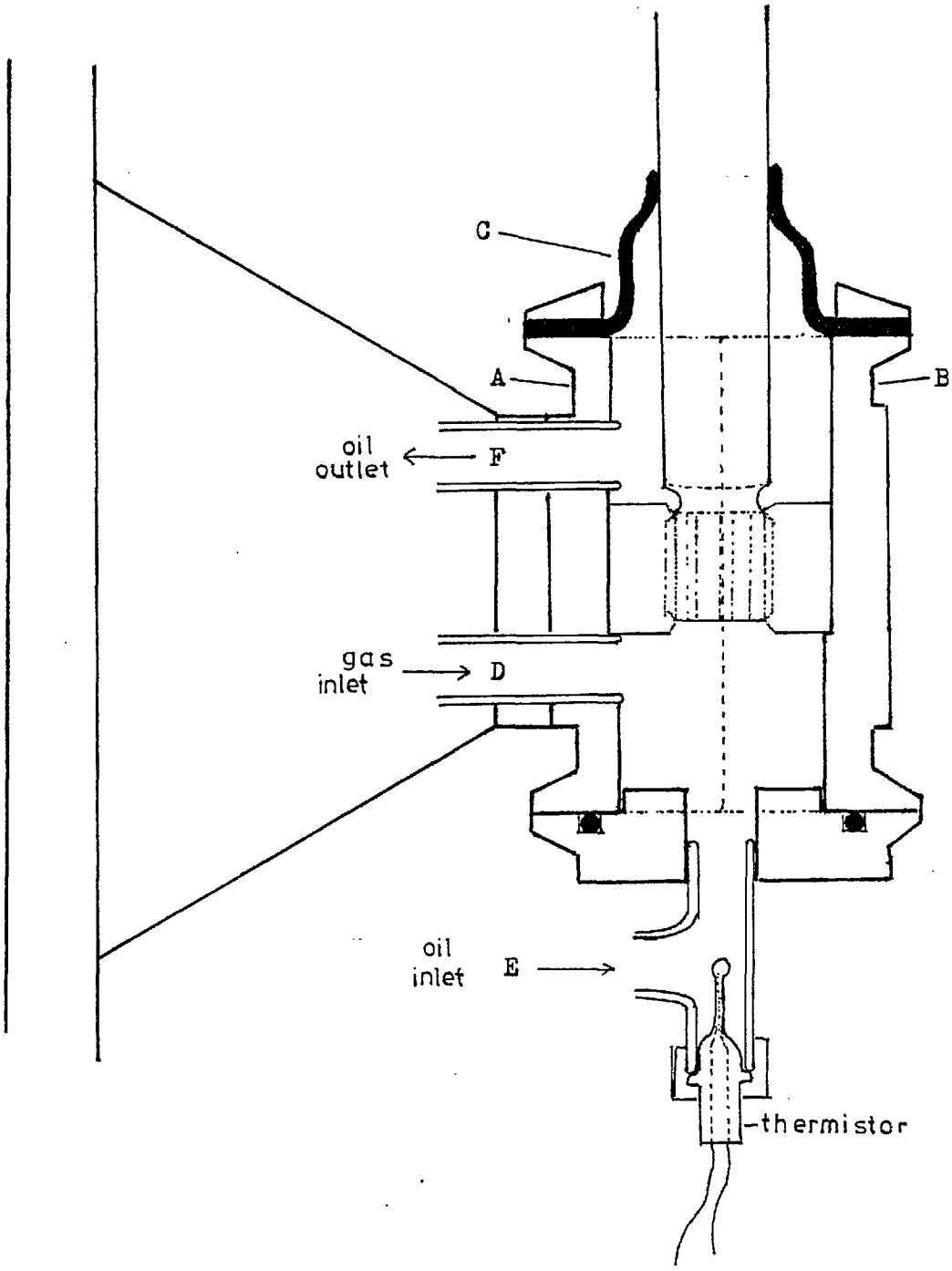

Diagram of the specimen chamber

Figure 2.3.5

Close up of the specimen chamber with the thermal insulation enclosure removed.

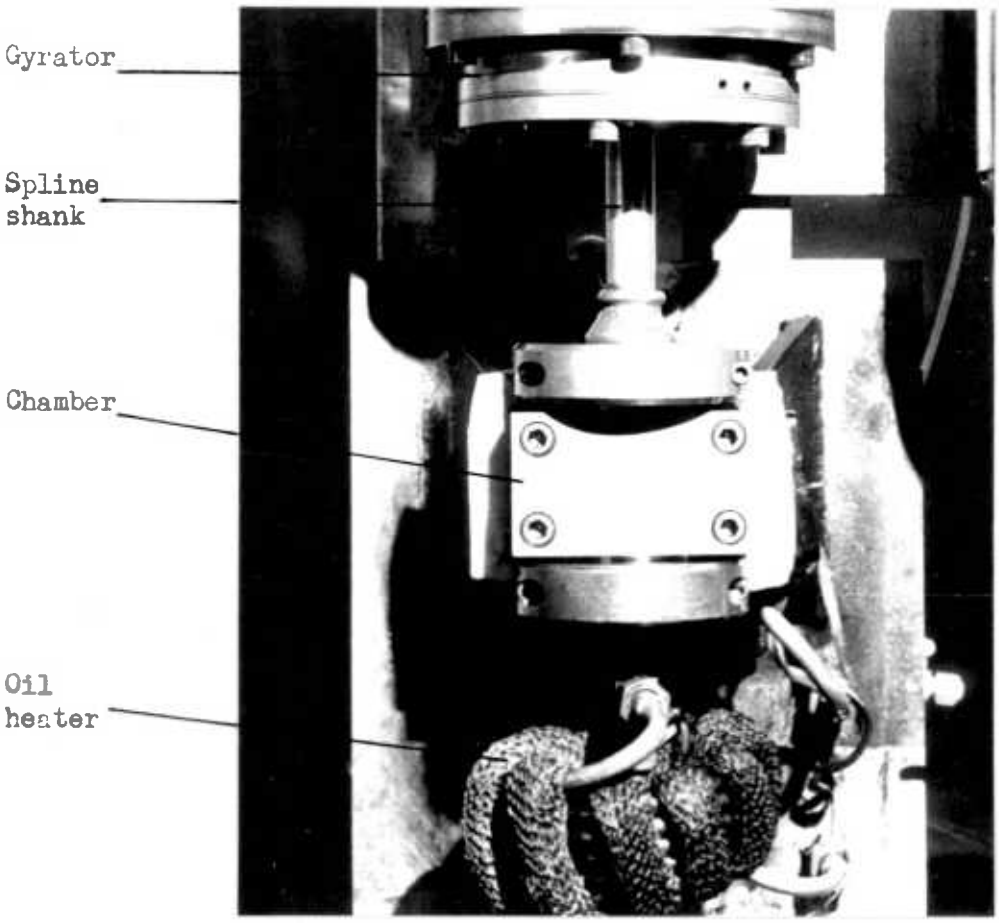

Figure 2.3.6

One side of the specimen chamber has been removed so that the location of the specimens can be seen.

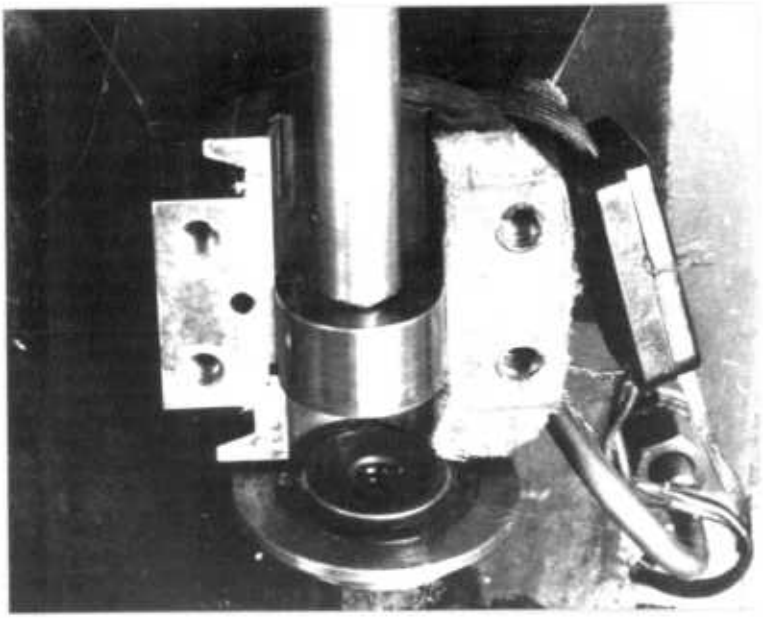

clamp to hold the female spline specimen rigidly in position. When mounting the specimen chamber onto the backplate a careful check was made to ensure that the centre line of the specimen chamber was concentric with the centre line of the gyrator mechanism to within a thousandth of an inch.

The top of the chamber may be sealed with a flexible rubber sleeve (C) which is a close fit around the shaft of the inner spline specimen. For lubricated tests preheated oil is circulated through the oil inlet pipe (E) around the specimen via flutes in the chamber wall, filling the chamber to the level of the oil outlet (F). A controlled atmosphere may be obtained by allowing a steady flow of gas through the inlet (D) and out through a small hole in the rubber sleeve. When a lubricant is present the gas bubbles up through it aiding equilibration between dissolved gases and the atmosphere in the chamber.

2.3.3 Oil Circulation System (Fig. 2.3.7)

The oil is circulated through the specimen chamber (A) by a peristaltic pump (B). The pumping action is provided by squeezing of a flexible rubber pipe. The system has the advantage that the lubricant is isolated from the pump. Pumping speed can be easily varied by changing to a rubber tube of a different diameter. A pumping rate of 20 mls/min. was used in these tests.

Disadvantages of this pump are the susceptibility of the silicone rubber pipe to deterioration in contact with hexadecane and the fact that the low pumping pressure prohibits use of a filter. The pump feeds the oil through

Figure 2.3.7

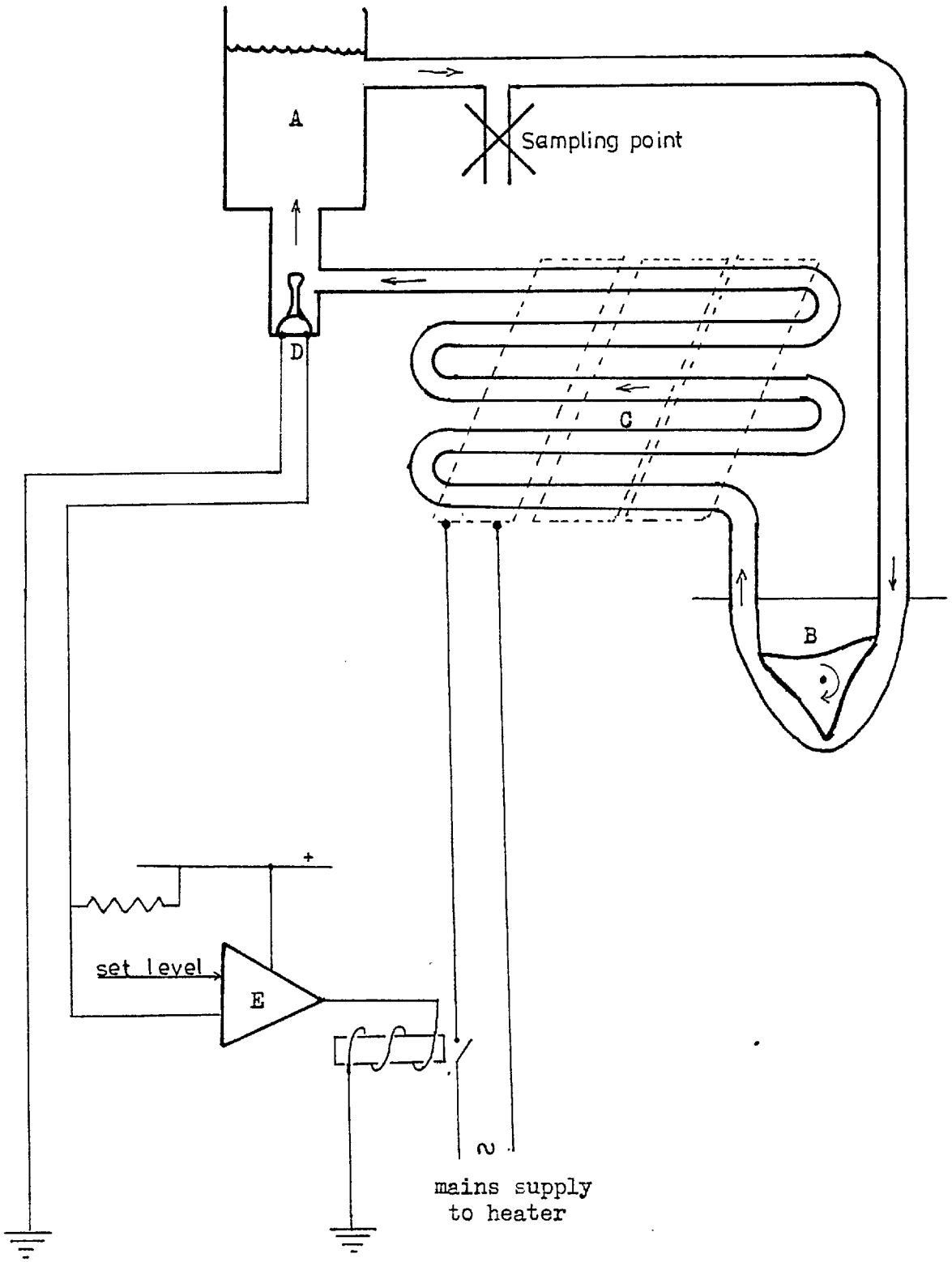

The oil circulation system and temperature regulation circuit.

the heater (C) a spiral copper tube wrapped round with a heating tape. The oil passes up through the spiral tube into the bottom of the specimen chamber. The output of a thermistor (D) projecting into the flow at this point is fed to a voltage comparator (E) the output of which operates a relay in the heater circuit. The oil temperature in the chamber is thus controlled to within 2 degrees of the set level. Connections between the rig and the pump were transparent polythene which was replaced for each series of tests with a new lubricant. The silicone rubber pump tube was replaced after every test.

2.3.4 The Loading System

In order to simulate a load being transmitted by the splines an axial torque is applied to the inner spline by a deadweight through the linkage shown in fig. 2.3.2 and 2.3.8. The male spline is bolted up through the steel diaphragm to the shank of a flexible torque rod (A). Torque is applied to the other end of the rod by the loading arm (B) which is acted on by the lever (C) to which is attached a suitable weight.

Tooth Loading

The mechanical advantage at the position of the weight over the pitch diameter of the spline teeth is 46.7:1. In nearly all the tests a load of 14 lbs. (6.35 kg.) was used giving a torque, T of approximately 22 Nm.

The spline dimensions (see fig. 2.2.1) are such that the area of one tooth side = 12.7 x 1.27 = 16.12 mm^2. Ideally the load should be equally distributed over the

Figure 2.3.8

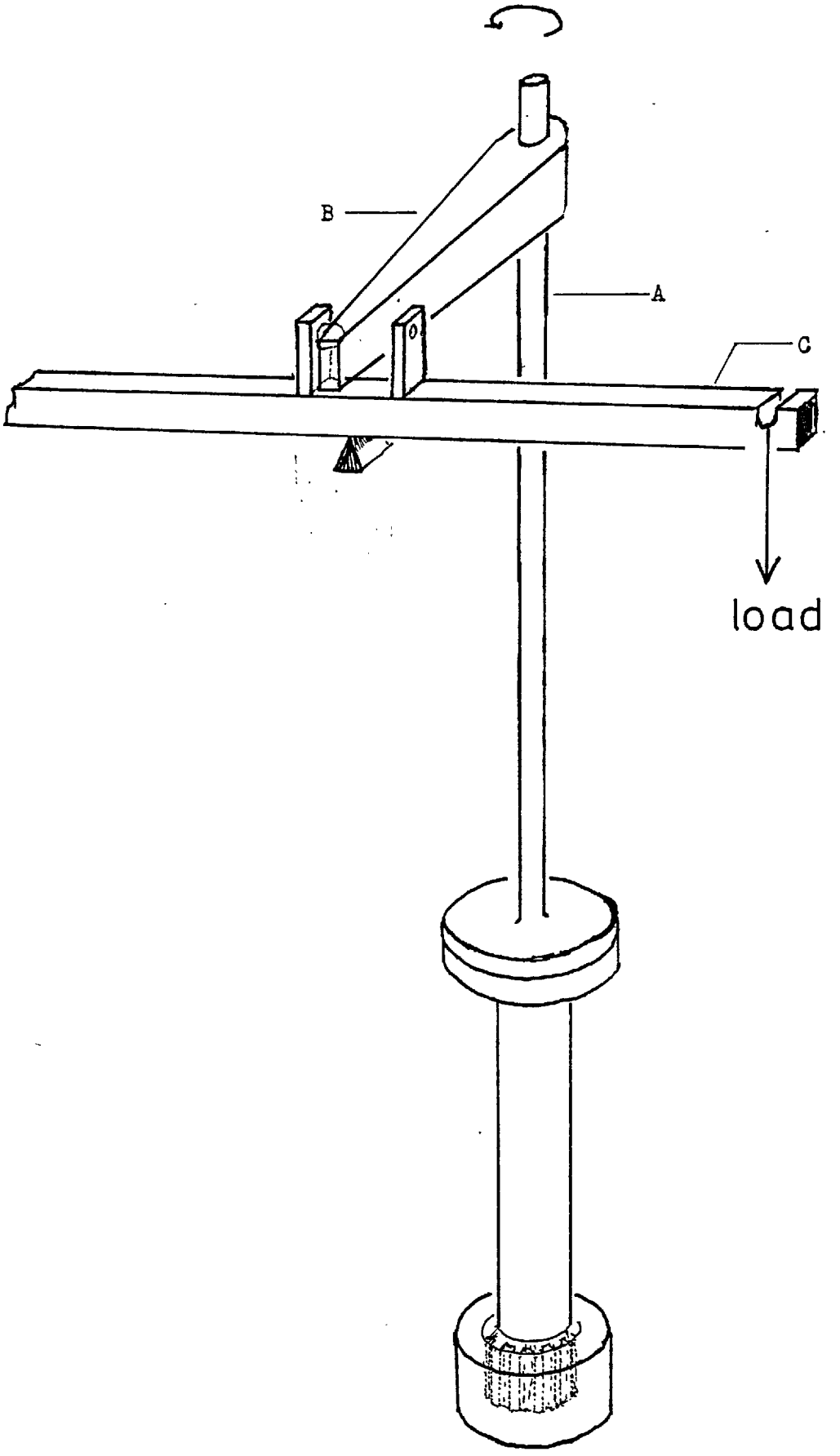

Diagram of the loading linkage.

12 teeth. In practice, provided that the spline specimens are well matched wear will ensure that all 12 are in contact within a few hours - a much shorter time if wear is rapid. The loading at any point in the contact is a function of its distance from the spline axis, the total contact area and the orientation of the surface (the spline teeth have an involute form).

The nominal contact pressure, P may be calculated using the formula :

$$P = \frac{2 \times \text{torque}}{\text{pitch diameter} \times \text{number of teeth} \times \text{tooth contact area}} \quad (113)$$

$$= \frac{2 \times 22}{15.2 \times 12 \times 16.12 \times 10^{-9}} = 15 \text{ MN m}^{-2} = 2200 \text{ psi}^{*}$$

2.3.5 Wear Monitoring

As the contact areas wear away the inner spline rotates under the action of the applied torque and the deadweight drops. In the original design a displacement transducer (L.V.D.T.) measured the movement of the loading lever (C in fig. 2.3.8). The system was later modified so that the rotation of specimen was measured directly eliminating errors caused by stiffness in the linkage and by the torque rod "winding up". A tube concentric with the torque rod was brazed to the flange at the torque rod base. Its top end was supported by a nylon bush enabling the torque rod to rotate and flex within the tube. A lightweight arm was clamped to the tube and linked at its outer end to the L.V.D.T. The mechanical advantage of the position of measurement over the spline pitch

---

* Design loadings for splines are calculated as $K_m P$ where K_m the 'load distribution factor' allows for the increased loading because of spline misalignment. At a misalignment of 0.34° K_m has a value of about 1.25.(126)

diameter was 21.9:1. The L.V.D.T. output was nominally 20 volts per inch. Its output was checked for linearity and calibrated over a large range against a dial displacement indicator. Further calibration checks were carried out periodically - it was found that the calibration did not vary by more than 3%. A full scale deflection on the chart recorder indicated a displacement at the spline pitch diameter of 26.2 microns. A 2000 μF capacitor was wired in parallel with the recorder to remove the high frequency "noise" caused by vibration when the rig was running.

2.4 Cleaning Procedure

2.4.1 The Specimen Cleaning Procedure

The specimens were immersed in toluene and placed in in an ultrasonic cleaner for about 10 minutes. They were then removed from the toluene rinsed in acetone and dried. The female spline specimen was weighed at this stage to an accuracy of two-tenths of a milligram for the purpose of weight-loss determination. The specimens were then assembled in the rig. Other more rigorous cleaning methods available in the laboratory were considered.

(a) Soxhletting - a process by which specimens are immersed in an organic solvent which is continuously refluxed.

(b) Ionic bombardment - surfaces are cleaned under vacuum by bombardment with medium energy ions accelerated by an electric field.

Spikes[67] found that the former process failed to remove all the surface contaminants even after many

hours cleaning. Ionic bombardment proved to be an effective method for flat surfaces. However, the complicated geometry of the spline specimens would impair its efficiency. Whilst it has been shown by Stinton[68] that even the smallest quantity of contaminant will affect the initial friction, it was considered that under the conditions of the test any contaminant layer left after the simple cleaning procedure described above would not affect the wear rate after the first few cycles, as the surface layers are worn away by the rubbing action.

2.4.2 Cleaning of the Rig

Cleaning of the rig between tests was essential as during a test there was a build up of deposit on the specimen chamber and oil-ways. In a test when the oil was subjected to severe oxidation this deposit was visible as a brown lacquer. Wear debris suspended in the oil settled out to the chamber base (whence it was collected for analysis) and in the oil-ways.

At the end of a test the rig was dismantled and all fixtures that could easily be removed were ultrasonically cleaned in toluene. This included most of the pipework, the chamber base and side. Any remaining deposit was easily removed by rubbing. Short lengths of pipe were cleaned with pipe cleaners. These items were then rinsed in acetone and dried in an oven. Those parts remaining on the rig were rubbed with a toluene soaked cloth and thoroughly washed with toluene and acetone. It was not possible to abrade the chamber as this would destroy the close fit necessary to grip the specimen. Cleaning of the

coiled copper pipe heat exchanger was most difficult. It was too long and too tightly coiled to be able to pass a pipe cleaner through. A high pressure airline was used to blow through the pipe following ultrasonic cleaning in toluene. It was then repeatedly washed through with toluene and finally acetone. It was then dried in the oven. The polythene tubing was cleaned with the other items and replaced from time to time.

As a measure of the effectiveness of the above procedures the initial acidity of a sample of oil extracted from the rig before a fretting test was started may be compared with that of the oil before it was input to the rig. This was done when the acidity was to be measured throughout a test and it was shown that although there was a small but detectable increase in acidity indicating possible contamination its influence on subsequent running was short-lived. (Table 2.2.)

2.5 Theoretical Determination of Fretting Conditions Within a Spline Tooth Contact

2.5.1 Calculation of Slip Amplitude

The top of the shank of the male spline is subject to a gyratory motion of 1.525mm (0.060 inches) amplitude. Assuming that the splines pivot about their centre (i.e. instantaneously about A in fig. 2.5.1) an angular misalignment of 0.34° is simulated. Movement between contacting teeth is opposed by the frictional force between the surfaces. Approximately, a bending moment is applied to the spline shank equal to half the applied torque times the coefficient of friction. A simple beam bending calculation (fig. 2.5.1) shows that if μ, the

TABLE 2.2

This table of values demonstrates the extent of contamination of the lubricant after introduction into the Spline wear rig.

Test code	Lubricant	ACIDITY mole equivalents KOH litre^{-1}		
		Before use	In the rig	At end of test
G	Hexadecane	b.d.l.	2.5×10^{-3}	1.5×10^{-3}
J	Hexadecane	b.d.l.	0.55×10^{-3}	0.34×10^{-3}
E	Ester	b.d.l.	0.85×10^{-3}	3.5×10^{-1}
D	Ester	b.d.l.	3.7×10^{-3}	1.75×10^{-1}

b.d.l. : Below the detectable limit (10^{-4})

Figure 2.5.1

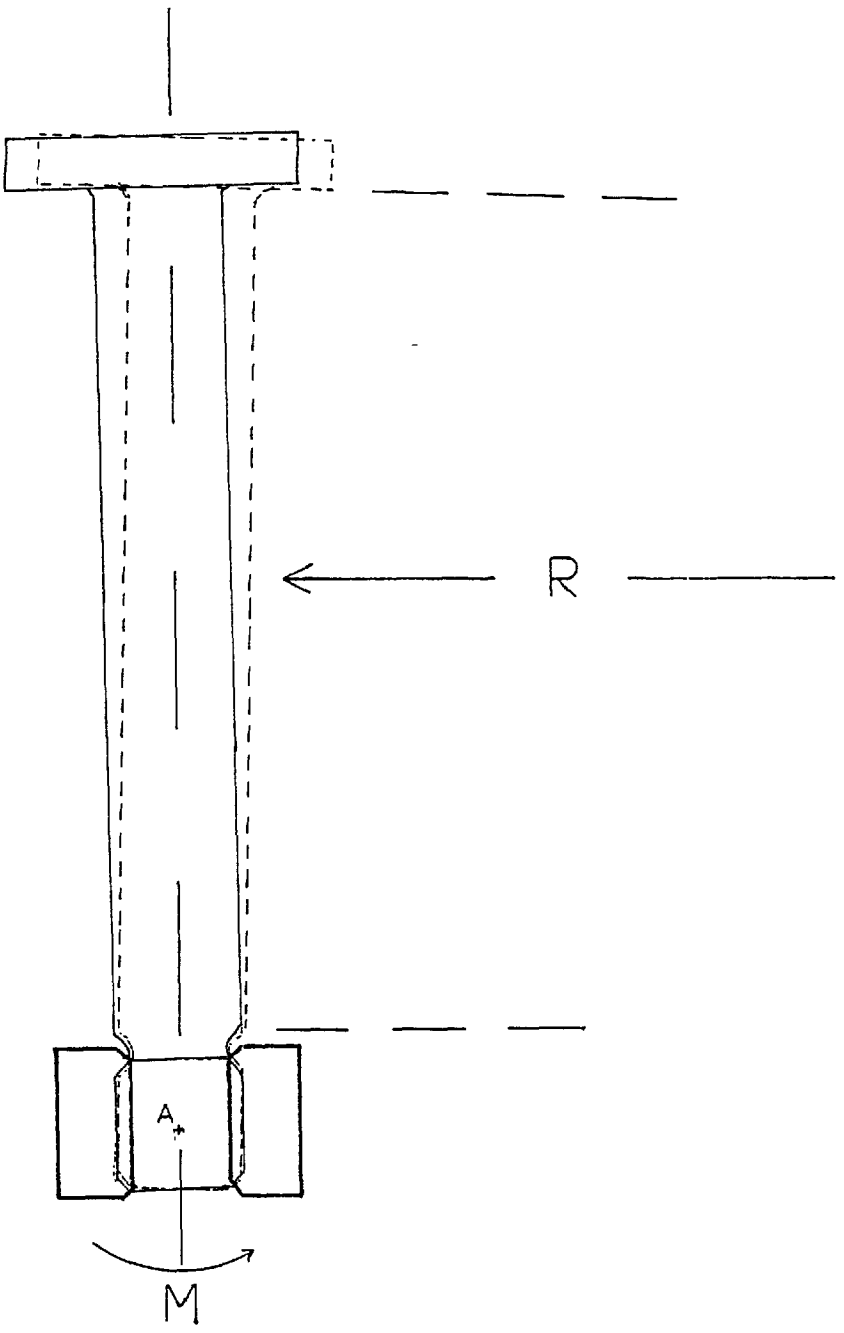

Calculation of magnitude of spline shank bending.

The torque loading generates a bending moment, M, which is given approximately by :

$$M = \mu \times \text{torque} = 6.6 \text{ Nm}$$

assuming that the coefficient of friction μ has a value of 0.3.

The radius of bending of the shank, $R = \frac{E \times I}{M}$

$$= 200 \times 10^9 \times \pi \times (.015)^4 / 64 \times 6.6$$

$$= 23 \text{ metres.}$$

Therefore, the deflection of the shank is approximately

$$= \frac{(\text{length of shank})^2}{\text{radius of bending}} = \frac{0.11^2}{76} = \underline{\underline{1.6 \times 10^{-4}}} \text{ m}$$

coefficient of friction, is in the range 0.1 to 0.3 the shank will bend by 0.05 to 0.16mm when gyrated, hence the relative slip between the teeth will be between 3 and 10% less than the following values calculated assuming the shank to be perfectly rigid.

The points in the tooth contact vary in their distance from the pivot point. At the tooth tips furthest away from the pivot point the slip amplitude will be a maximum given approximately by 0.8 tan 0.344° = 4.8 thousandths of an inch (120 μm). Similarly, the minimum slip amplitude at the centre of the teeth is given by

0.5 tan 0.344 = .003" = 76 μm

At the pitch diameter the amplitude is 90 μm. This range of amplitudes lies towards the upper limit generally agreed for a fretting process (100-150 μm)[1]. Oscillatory slip amplitudes of this magnitude represent an appreciable mid-cycle displacement velocity (of the order of .022 m/sec.). It was considered necessary to check that under these conditions the load was not being supported by a hydrodynamic or elastohydrodynamic film and also that high flash temperatures were not being attained.

2.5.2 Calculation of the Oil Film Thickness

Because of the variation in amplitude of relative slip between the tooth surfaces and the reciprocating motion calculation of accurate film thicknesses would be a complex problem. The situation may be simplified by considering a typical small area of the tooth and showing that any films generated are well within the surface

roughness excursions.

Considering then the configuration shown in fig. 2.5.2. The hydrodynamic film thickness, h is given by the formula for a wedge:[69]

$$h = \left(\frac{6\eta.l.u}{P_a}\ \beta.K_p\right)^{1/2}$$

where η is the oil viscosity (for ester 1.5 x 10^{-6} reyns at 80°C)

u is the relative speed

β is a factor dependent upon $\frac{b}{l}$

Kp is a factor dependent upon the angle of tilt of the wedge.

Pa is the average pressure over the area which under the standard test conditions = 15 MN m^{-2} = 2.2 x 10^3 p.s.i.

The amplitude of motion is approximately 100 μm the frequency 54.2 H_z therefore the average speed is 10^{-4} x 2 x 54 = 1.08 x 10^{-2} m/sec. The maximum speed will be about twice this value i.e. 0.022 m/sec. (0.9 in/sec.).

The factor Kp is fairly insensitive to the angle of tilt (which in this case approaches zero as the maximum speed is attained) so a value of 0.025 is a good approximation[69].

β varies with $\frac{b}{l}$ in the following way:

$\frac{b}{l}$	β
0.25	0.06
0.33	0.09
0.5	0.185
0.67	0.278

Figure 2.5.2

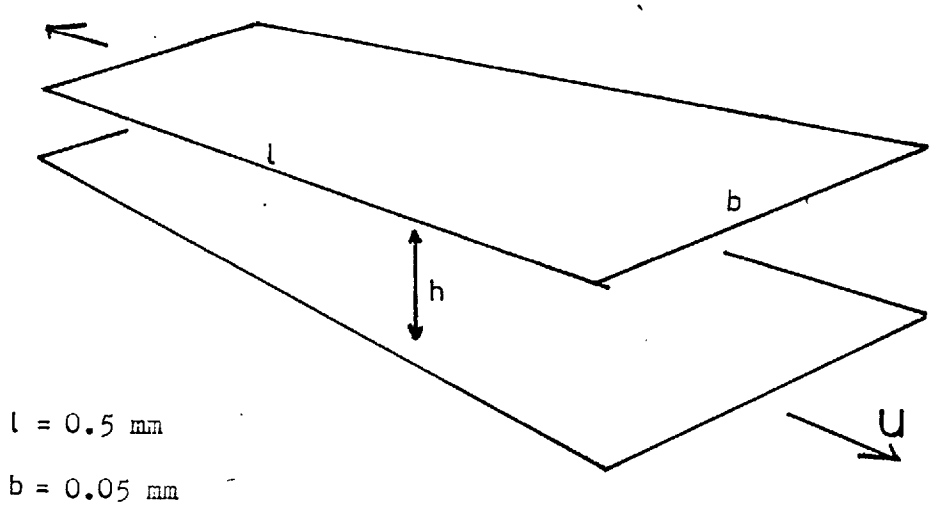

The simplified sliding pad model

β = 0.2 was chosen as a reasonable approximation.

Under these conditions

$h = (1.8 \times 10^{-12})^{\frac{1}{2}}$

$= 1.3 \times 10^{-6}$ inches.

This order of film thicknesses is negligible compared with the surface roughnesses measured (Section 4.10) of about 3 μm cla (10^{-4} inches). However, it has been shown that in reality film thicknesses in this type of situation are much greater than predicted by hydrodynamic theory due to elastohydrodynamic effects[70].

Consideration of the situation in detail* revealed that because of the low contact loads employed in these fretting tests and the high modulus of the spline material the resultant deformation of the surfaces is too small to set up any appreciable elastohydrodynamic film.

2.5.3 Surface Temperatures in the Fretting Contact

The fretting wear results discussed in later chapters indicate that reactions between the lubricant and the metal surface influence the wear rate. The rates of such reactions will be affected by the temperature. It is therefore important to know the surface temperatures attained in the fretting contact.

The temperature of a sliding contact is increased above that of the surroundings by the generation of heat by the dissipation of frictional energy. The theoretical treatment of this problem by Blok[71] enables the calculation of a value for the temperature attained in a

---

*For which I am indebted to Dr. S. Yung

contact, both the mean temperature and the instantaneous peak ("flash") temperatures. Archard[72] considers that the maximum flash temperature attainable is the more important parameter. It is convenient to use the results calculated by Archard for the maximum attainable flash temperatures for sliding contacts of steel.

Using the formulae developed by Blok, Archard has constructed a graph of θ/μ against the factor $W^{\frac{1}{2}}V$ for a low alloy steel of hardness 250 VPN (fig. 2.5.3). The fretting conditions yield a factor value of about 10^3:

Assuming that all the applied load is carried by 2 asperities, W, the load = $\frac{1}{2}$ x 141bs x mechanical advantage = 0.7×10^6gms.

The maximum sliding velocity V $\simeq$ 1.0 cm/sec. (see previous section)

$\Rightarrow$ The factor $W^{\frac{1}{2}}V = 800$

Thus $\theta/\mu \simeq 10^2$. The temperature depends to a great extent on the coefficient of friction. As it is impossible to measure the frictional forces with this type of fretting rig it is necessary to make an estimate of the friction coefficient. A value of 0.3 seems reasonable in view of the results of Halliday[32] who found the friction coefficient in a lubricated fretting contact to vary between 0.2 and 0.4 under similar conditions of loading and slip amplitude. If there is an accumulation of debris within the contact it is probable that the friction coefficient falls to a lower value[1,53].

The above approximate analysis indicates that the maximum attainable flash temperature will be of the order of 30° Centigrade above the bulk. The assumptions made

Figure 2.5.3

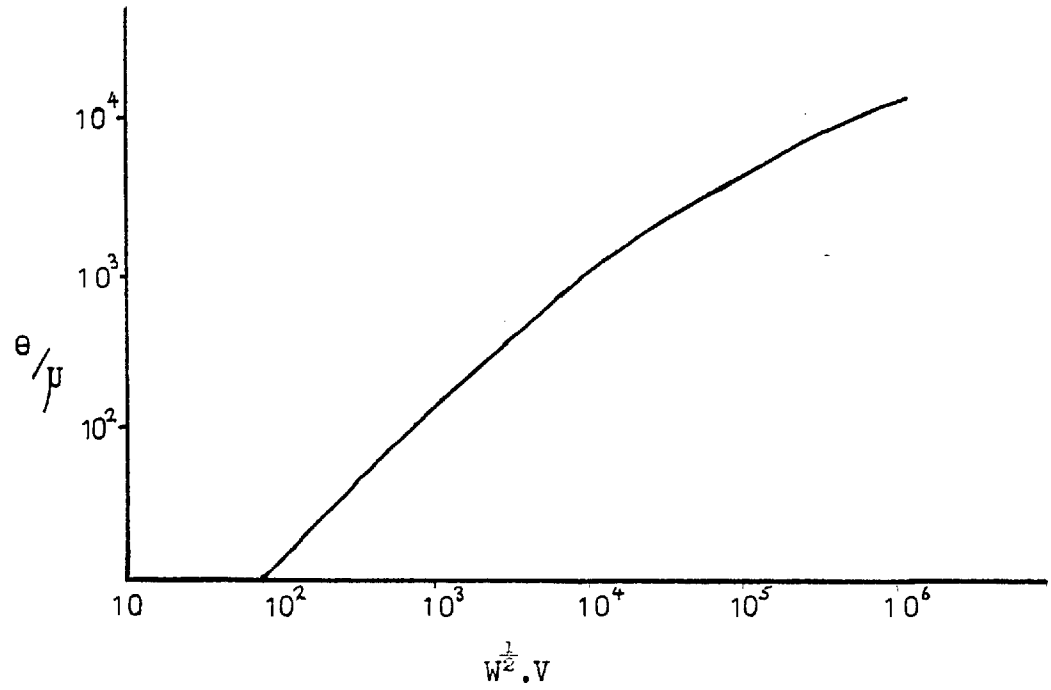

after Archard, ref. 72

Variation of flash temperature with load.

Figure 2.5.4

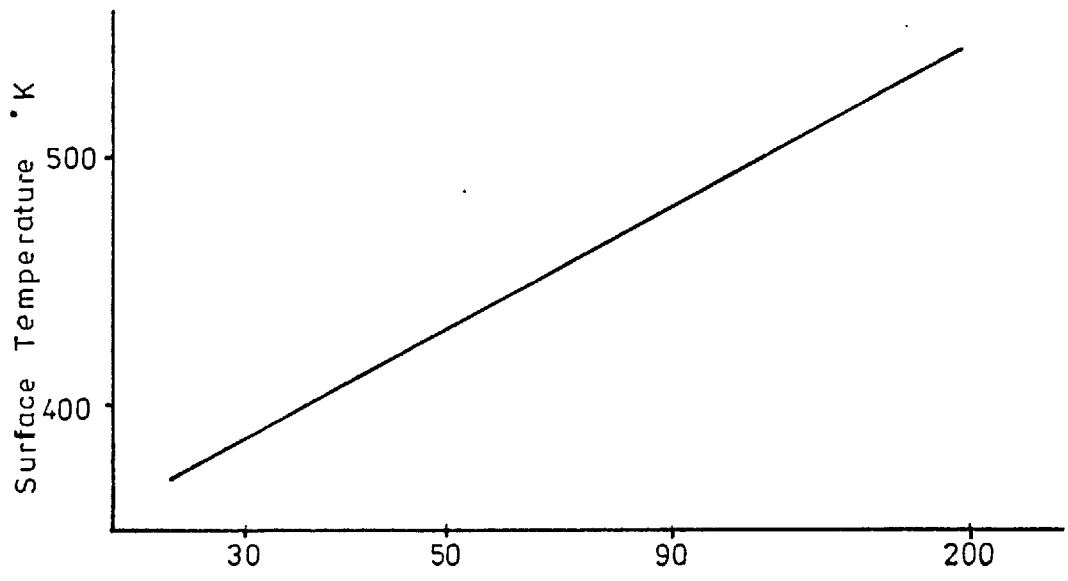

after Alyab'ev et al., ref. 73

ensure that this is likely to be if anything on the high side of the actual temperatures attained. For instance, the velocity varies from zero and the load is likely to be distributed on many more than 2 points.

The temperature generated in a fretting contact has been investigated by Alyab'ev et al[73] who fretted the bead of a thermocouple against a steel surface. The temperature in the contact which may be considered analogous to an asperity contact, was found to increase with load and slip amplitude. The variation with load at an amplitude of 150 μm is shown in fig. 2.5.4. It can be seen that at the load used in the spline tests ($15MNm^{-2}$) very little temperature increase is predicted.

In order to measure the temperature in the contact a thermocouple was embedded into the tooth surface of the female spline so that the junction was in contact with the opposing surface (fig. 2.5.5). The temperature was found to remain constant throughout the test and to be (within the accuracy of the measurement) identical to the bulk oil temperature.

It was therefore concluded that the mean surface temperature was the same as the bulk oil temperature and that any instantaneous temperature rises would not be in excess of 30 C^{o} under the standard conditions of a fretting test.

2.6 Summary

The main features of the design of the spline wear tester and its mode of operation have been described. The experimental procedure of setting up and running a test is dealt with in Chapter 4.

Figure 2.5.5

Diagram showing the location of a thermocouple inserted into a spline specimen to monitor the bulk temperature.

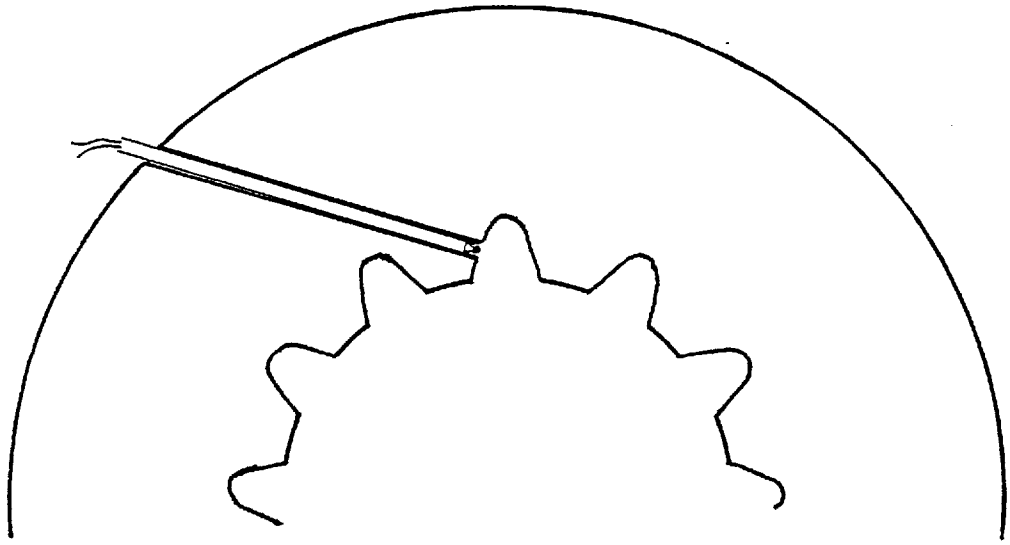

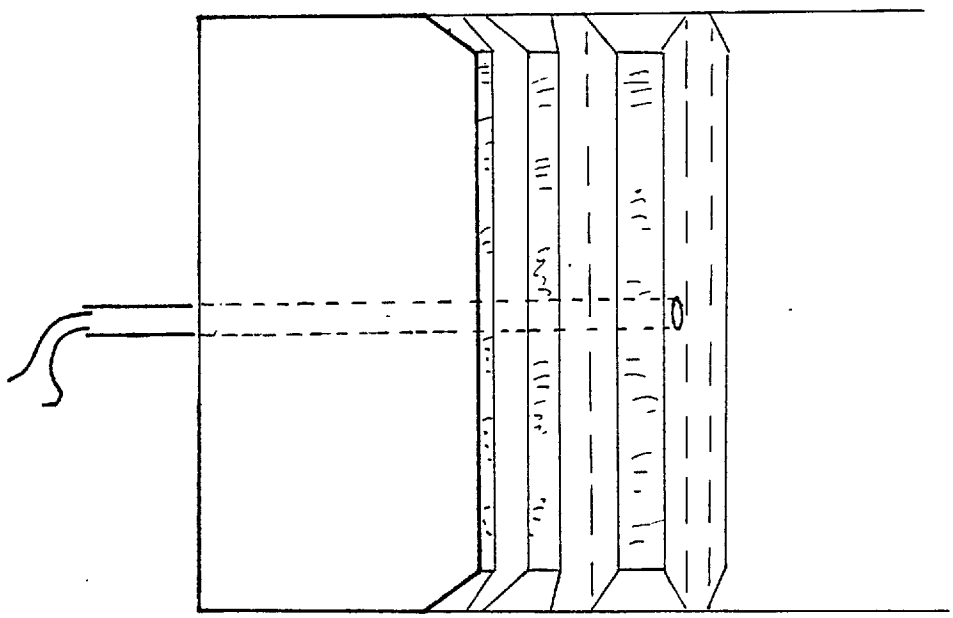

The conditions under which wear takes place in a spline tooth contact have been discussed. In a standard test the following conditions apply.

(i) Slip Amplitude 70 - 120 μm depending on the position on the tooth and the coefficient of friction.

(ii) The Coefficient of Friction - It was not possible to measure the coefficient of friction between the contact surfaces. It is considered that μ will be close to that measured by Halliday for a lubricated fretting contact between steels with a similar loading and slip amplitude[32] i.e. within the range 0.2 to 0.4.

(iii) State of Lubrication - The conditions are such that the spline wear tester operates well within the boundary lubrication regime. Speeds of relative motion are not sufficient to cause a build up of a hydrodynamic film and the contact loads are not high enough in relation to the modulus of the spline material for there to be any elastohydrodynamic effect.

(iv) Surface Temperature - It was concluded from theoretical considerations and actual surface temperature measurements with an embedded thermocouple that the average surface temperature was very close to the bulk oil temperature. It was calculated using the theoretical treatment of Blok that any flash temperatures would not exceed 30 C° above the bulk temperature.

The spline wear tester was designed to allow continuous monitoring of the wear during a test. This is a feature possessed by few fretting wear rigs and, indeed, by few wear testers of any description. The two configura-

tions that have found most general application as sliding wear testers are the "pin-on-disc" machine and the Four-ball machine. Whilst frictional forces can be quite easily measured on these testers, the measurement of wear rates is not so straightforward. On the four ball machine wear rates can only be calculated after a test from the width of the wear scar. Similarly wear can be assessed on a pin-on-disc machine by measuring the scar diameter of a hemispherically ended pin. However, the increase in size of the contact as the result of wear leads to a reduction in loading.

The 2 advantages of the spline wear tester over conventional wear rigs are therefore:

(1) Continuous measurement of wear is possible. (Measurement of wear as a rotation rather than a displacement aids sensitivity). Changes in wear rate are immediately obvious.

(2) The apparent contact area attains a constant value so that parameters such as contact pressure do not change as wear proceeds.

The spline wear tester is therefore suited to the study of changes in the wear rate (for example changes caused by lubricant oxidation) and to the study of the influence on the wear rate of a number of variables.

However, as a first step the mechanism of wear under standard conditions had to be established. To this end the tests with an ester lubricant described in Chapter 4 were conducted. An important feature of these tests was the measurement of the oxygen activity in the lubricant.

The development of a technique for this purpose is described in the following chapter.

Chapter 3 Oxygen Determination

3.1 Introduction

The chapter begins with a review of methods that have been used to determine the solubility of oxygen in lubricating oils. In the past oxygen concentrations in wear rigs have often been assumed to be the concentration that is attained under equilibrium conditions. This may be calculated from published data. In other cases samples of the oil have been analysed on a gas chromatograph. The oxygen electrode is commonly used in the fields of Biochemistry and Biology to measure the solubility of oxygen in water. This instrument was adapted for use with oils. It is a rapid and convenient method for oxygen determination but is less accurate than a gas chromatograph.

The atmosphere in which the fretting tests were run was controlled by maintaining a flow of dried and (in some cases) deoxidised gas through the oil and specimen chamber. The gas purification system is described in section 3.4.

3.2 Methods of Determination of Oxygen Concentration

In order to be able to measure the dissolved oxygen concentration at frequent intervals throughout a fretting test a convenient technique was required. A survey of the literature was undertaken to determine what methods were available. The methods used by previous workers when investigating the effect of atmosphere on wear will be considered first.

Klaus and Bieber (5) used a gas chromatograph with a precolumn attached, devised by Petrocelli and Lichtenfels (74). The precolumn is packed with brick which absorbs the hydrocarbon. The sample of oil is injected through a

self-sealing rubber septum into the precolumn. The gases are not absorbed and pass into the analyser column in the carrier gas stream. The time taken to pass through the analyser column to the detector, the "residence time", is characteristic of the molecule. The quantity of a gaseous component can be determined to $\pm$ 5%.

A similar apparatus designed to measure oxygen concentration in oil is described by Elsey (75) (figure 3.2.1). The oil sample is retained in the sample chamber by fritted discs. The apparatus must be maintained at 75°C to ensure quantitative removal of oxygen. A sample size of 1 to 2ml could detect a minimum concentration of 0.01% by volume of oxygen*. However, this apparatus could not differentiate between oxygen and argon as they had similar residence times. The advantages of a precolumn are that it is much easier to clean and it shortens the analysis time. (Residence time of oxygen was about six minutes.) By nitrogen purging Bieber was able to reduce the oxygen concentration to about 9×10^{-3} millimoles/litre. The solubility of oxygen when a paraffinic mineral oil is in equilibrium with air was found to be 1.43 millimoles/litre (32 µls/ml). The solubility of oxygen in the oil was found to be more or less independent of temperature - a 6% fall over 120°c.

Fein and Kreuz (58) did not monitor the oxygen concentration. This was calculated from reference data (76).

---

* Already there is a confusion over units of oxygen concentration. Systems used in the literature include: µls/ml, vol %, moles/litre, p.p.m. It is proposed in this work to express oxygen measurements in millimoles/litre. The conversion factors are as follows:

1 µl/ml $\equiv 10^{-1}$ vol % $\equiv 4.46 \times 10^{-2}$ millimoles/litre $\equiv$ 1.5 p.p.m. by weight.

Figure 3.2.1

Gas Chromatograph with precolumn for separating out dissolved oxygen from oil. After Elsey, ref. 75.

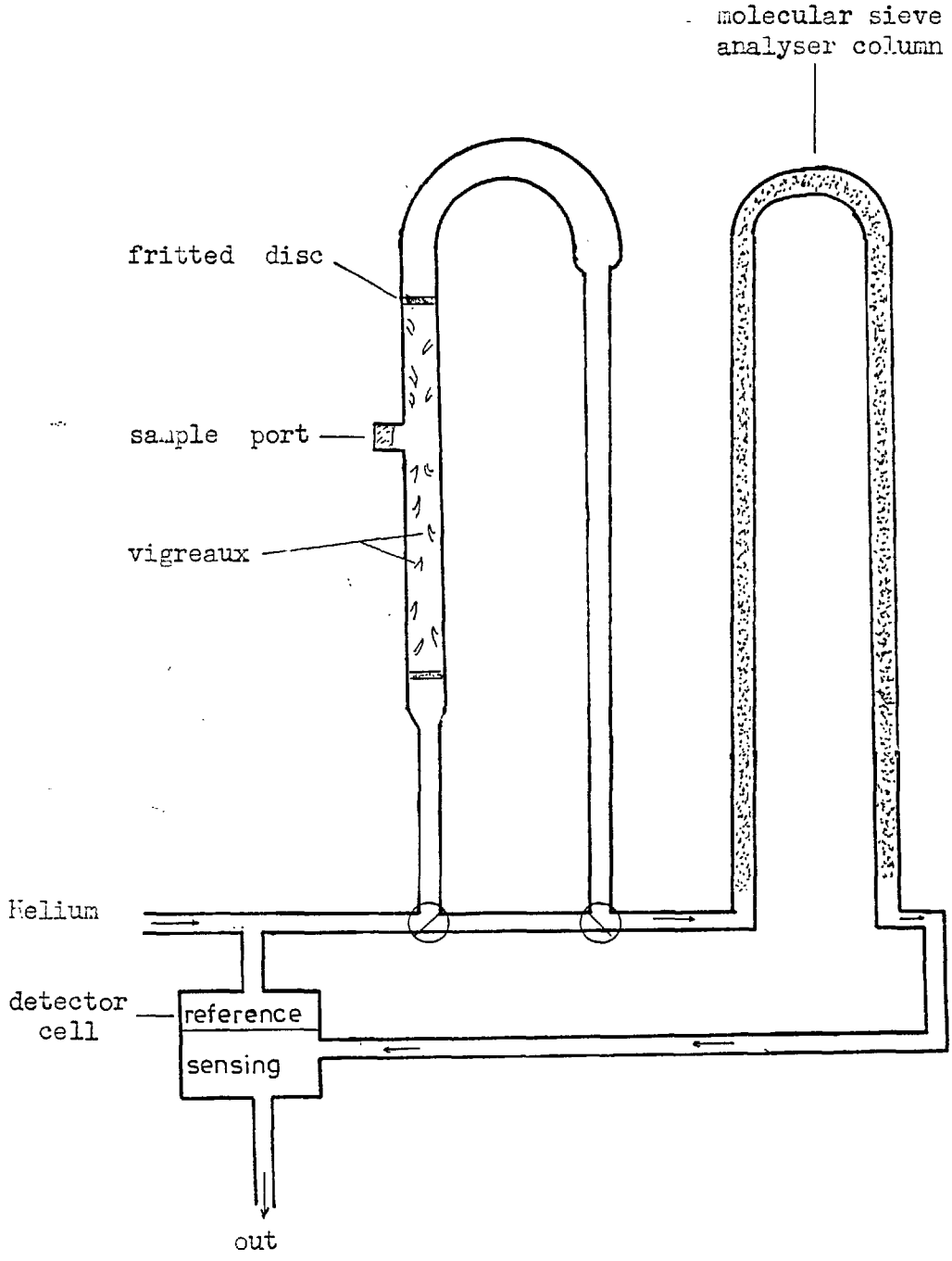

Appeldoorn, Goldman and Tao[14] ran tests in air, argon and nitrogen. The concentration of oxygen was measured by an oxygen analyser calibrated by gas chromatography. Concentrations ranged from 6×10^{-3} millimoles to 2.4 millimoles per litre. The solubility of oxygen in a highly refined hydrocarbon (Bayol 35) when in equilibrium with air was found to be 1.75 millimoles/litre. This illustrates that oxygen solubility differs from oil to oil - it depends on the molecular structure [77]. The effect of oil viscosity is discussed later.

Bose, Klaus and Tewksbury [9] used controlled atmospheres of air, argon and nitrogen. The oxygen concentration one of the test fluids, a super-refined paraffinic mineral oil, was "estimated" as 1.2 millimoles/litre (40 p.p.m.) in equilibrium with air, 0.015 millimoles/litre (0.5 p.p.m.) in equilibrium with nitrogen and less than 0.003 millimoles/litre (0.1 p.p.m.) in equilibrium with argon.

Two other fluids were tested a naphthenic oil and Di-2-ethylhexyl Sebacate ester for which no values are given.

Of the papers on fretting wear in controlled environments in none was the oxygen concentration monitored in any way. The following methods of oxygen determination were found in a wide survey of the literature:

(1) Volumetric or manometric extraction of a gas from the oil under vacuum. There is an Institute of Petroleum standard procedure for this process[78]. A somewhat simpler gas extraction apparatus has been designed by Hayward which is described in detail in section 3.33. Having extracted the gas one is left with the problem of analysing it. Mass spectrographic or gas

chromatographic methods could be employed.

(2) Mass spectrographic methods. It is necessary to transfer the dissolved species into an inert carrier gas for analysis in a similar way to the gas chromatography described above.

(3) Measurement by Fluorescence Quenching.

Fluorescence quenching like mass spectroscopy and gas chromatography is a method for determining the concentration of oxygen in inert gas streams. A fluorescent material is illuminated by monochromatic light. This energises electrons from the ground state S_o to higher levels. Any vibratory energy possessed by the electron is soon lost and it decays quickly to the lowest S_1 state, figure 3.2.2. From this level it drops back to the ground state with the emission of characteristic radiation. A steady state is set up in which the rate of decay equals the rate of activation of the electrons by the incident radiation. Decay may also take place without radiation by processes known as 'inter-system crossing' and 'internal conversion' and also by transfer of energy to a 'quenching' molecule. The ratio of intensities of emitted radiation to absorbed radiation is known as the fluorescence efficiency ϕ_f . For a fluorescent substance ϕ_f is near unity (i.e. the radiationless transitions make little contribution to the decay process). A quenching molecule such as oxygen interacts by collision with the fluorescent substance whilst it is in its activated state and absorbs energy. The rate of collision is proportional to the quencher

Figure 3.2.2

A Diagramatic Representation of Electron Excitation and Decay Processes.

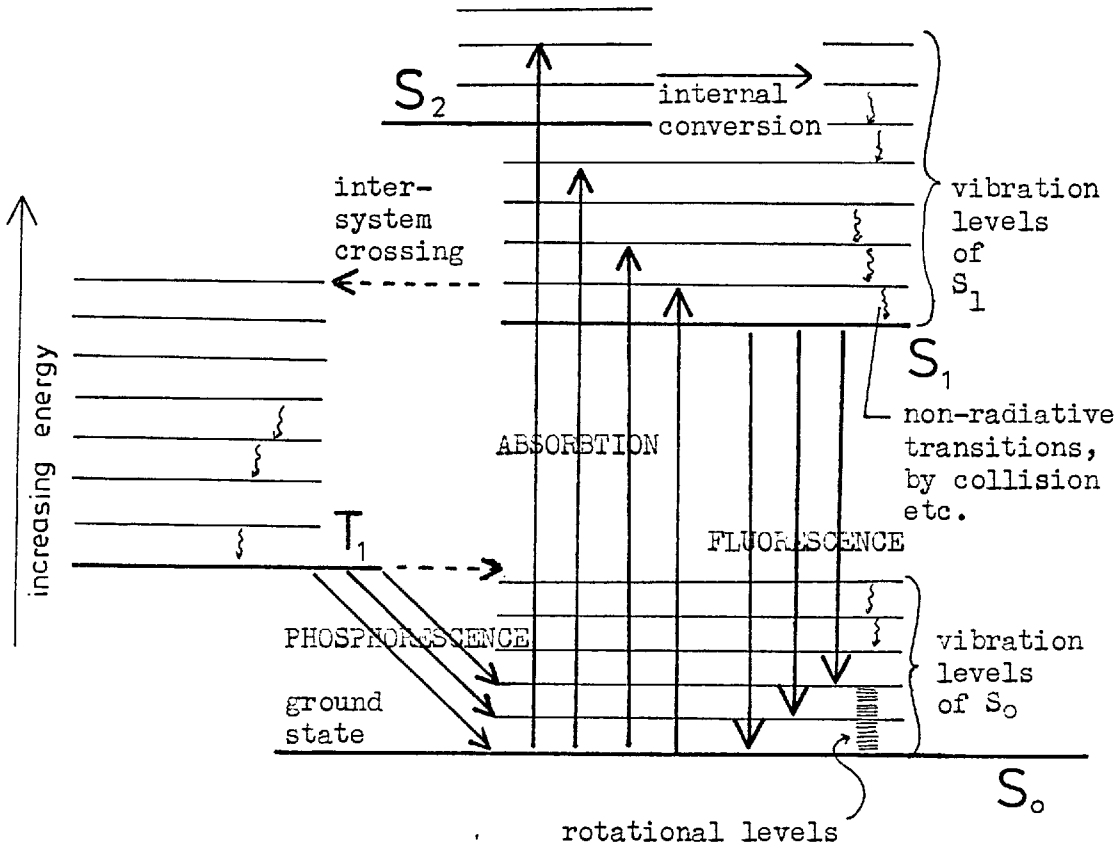

concentration, $[Q]$. As a result in the presence of oxygen ϕ_f is reduced - the reduction being related to $[Q]$ by the Stern-Volmer equation.

$$\frac{\phi_f}{\phi_o} = 1 \quad K[Q]$$

Oxygen is a particularly good quenching agent because it is paramagnetic. The sensitivity of a fluorescer depends on its lifetime in the activated state. Long lifetimes are required to allow plenty of time for collision if the quencher is in low concentrations. A range of oxygen concentrations may be covered by the two substances.

Fluorescein (half-life 10^{-8} sec) for O_2 up to 0.5 atm

Eosin (half-life 10^{-3} sec) for O_2 as low as 1 p.p.m.

(4) Chemical Methods.

Chemical analysis provides one of the main determination methods for oxygen dissolved in water(79). Most commonly employed is the Winkler method(80). Dissolved oxygen oxidises a manganous hydroxide precipitate to manganic hydroxide in the presence of alkali. Addition of acidified potassium iodide liberates a quantity of iodine proportional to the original dissolved oxygen. This is determined by titrating against sodium thiosulphate.

This method was found to be unworkable in non-aqueous solutions as it is essential that the precipitate is formed as this acts as a gathering agent for oxygen. Attempts were made to dissolve oil samples in ethanol and shake with deoxidised water under a nitrogen blanket, but without success.

(5) The Oxygen Electrode. Dissolved oxygen in a sample liquid equilibrates with the electrolyte of an electrochemical cell across a semi-permeable membrane. The activity of dissolved oxygen in the electrolyte affects the electrochemical reaction. In principle, the electrode should be sensitive to oxygen in any fluid, requires only a small sample and is quick and easy to use.

Of the above methods, gas chromatography probably offers the most satisfactory method for oxygen determination. It gives a reasonably quick and accurate result and requires only a small oil sample. However, access to an instrument was limited so it was decided to investigate oxygen electrodes. The next section describes an oxygen electrode which gives satisfactory oxygen determinations with ester oils, with the advantage over other methods that it gives on-the-spot measurements.

3.3 The Oxygen Electrode

3.31 Description

Electrodes are of two types: the probe and the cell which has a sample chamber attached. Were it not for a deterioration in the cell voltage with time, the ideal solution would be to insert a probe electrode at some point in the oil circulation system and monitor the oxygen concentration continuously. A cell type electrode was in fact used and samples of oil extracted from the rig for analysis. It is shown in figure 3.3.1.

The electrode consists of a Pt/ KCl /Ag electrochemical cell separated from a test solution by a membrane permeable to oxygen and other gases. The behaviour of this cell is similar to that described by Mancy[81].

Figure 3.3.1

The Oxygen Electrode

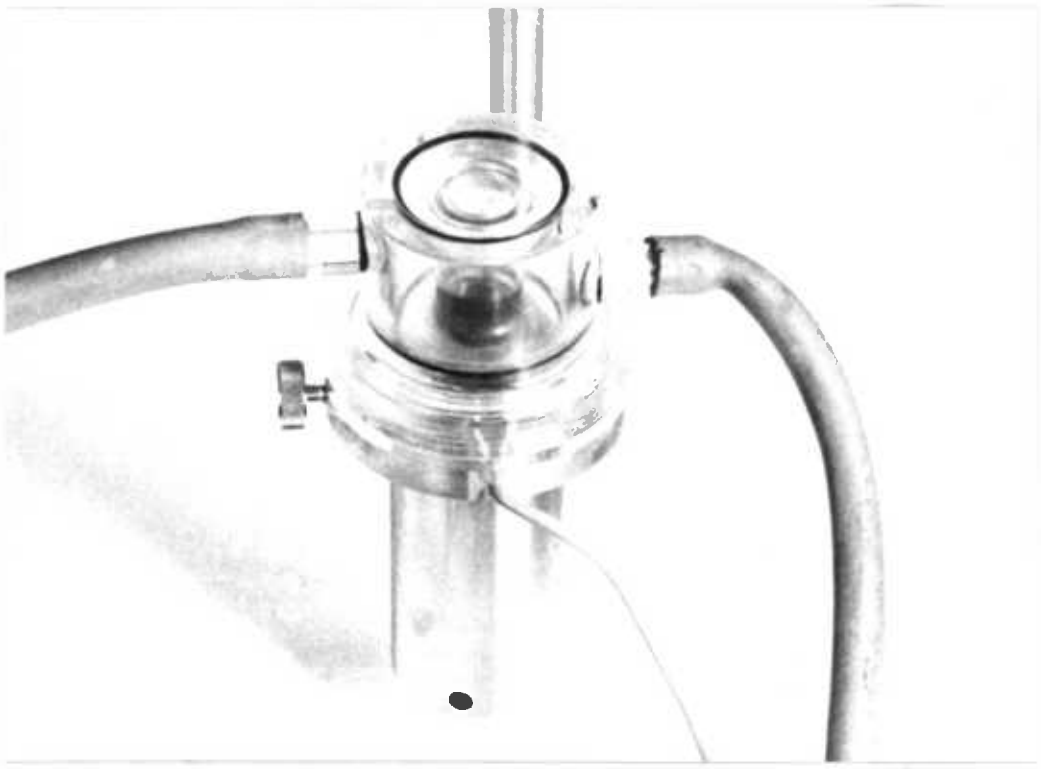

The cell employed is shown diagramatically in fig. 3.3.2. It is made of perspex. The base has two inset electrodes - a central Pt cathode surrounded by an anular Ag anode: A small quantity of saturated aq.KCL solution is pipetted into the recessed well so that it wets both electrodes. A square of teflon which acts as a membrane permeable to oxygen is placed over the well. The cylindrical specimen chamber which is surrounded by a water jacket is screwed down onto the base. The Pt/aqKCL/Ag cell is then separated from whatever liquid is placed in the specimen chamber only by the teflon membrane. Oxygen diffusing through the membrane quickly brings the concentration in electrolyte and test liquid into equilibrium so that the oxygen concentration in the electrolyte reflects the activity of the oxygen in the test solution. A magnetic flea within the test liquid chamber is rotated remotely by a motor beneath the base of the electrode, to stir the liquid to minimise the concentration gradients that are set up. To prevent loss or absorption of oxygen through the meniscus after the chamber is filled, the top is partially sealed by a plunger with a central capillary. In theory it should not matter that the test solution is non-aqueous and indeed this was found to be so - the cell would respond to the oxygen content of air in the specimen chamber. Water may be passed through the cooling jacket so that readings may be taken at constant temperature. Current passed by the cell varies with the applied potential in the way shown in figure 3.3.3(a). Over the range 0.5 V to 0.9 V the current flowing is independent of voltage. If a potential of about 0.65 V

Figure 3.3.2

Diagram of the cell type of oxygen electrode.

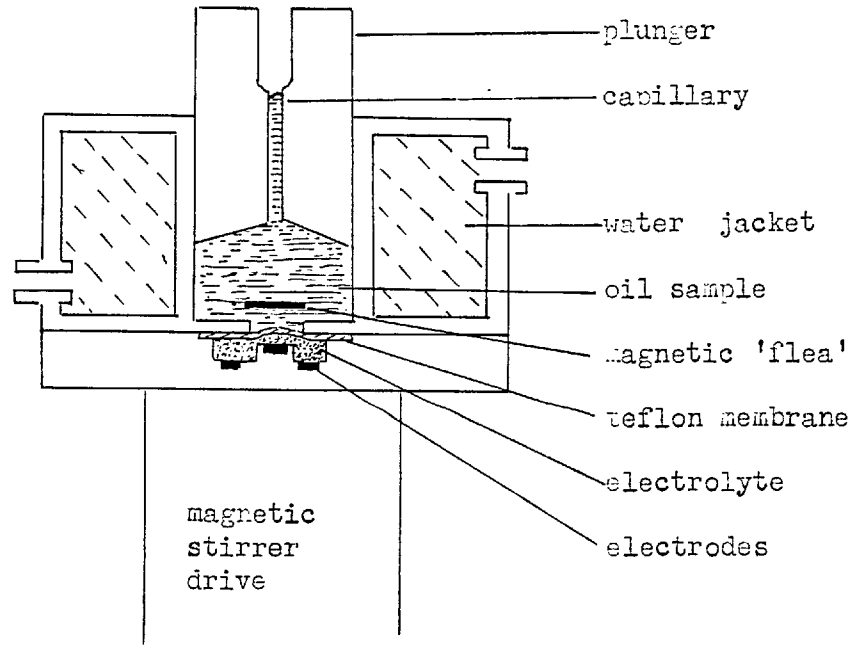

Figure 3.3.3

(a)

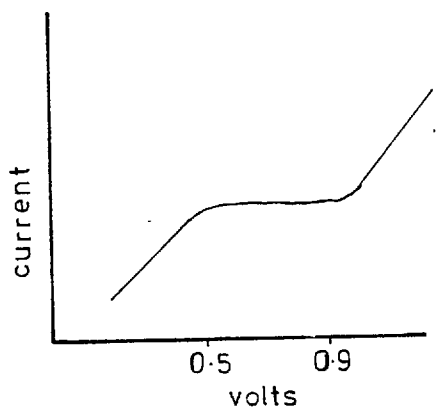

Variation of current with applied voltage

(b)

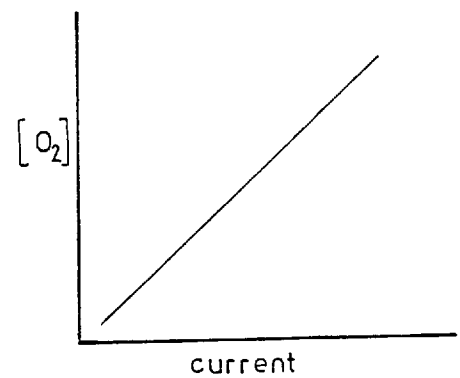

Relationship between cell current and oxygen conc^{n} when Pt electrode is polarised at - 0.6 volts.

is applied to the cell, the current flowing is proportional to the concentration of dissolved oxygen in the electrolyte (fig. 3.3.3(b)). The reason for this is thought to be that at the cathode in addition to the normal reaction

$$2e^- + 2H_3O^+ \longrightarrow \uparrow H_2 + H_2O$$

the reaction

$$4e^- + O_2 + 4H_3O^+ \longrightarrow 6H_2O$$

proceeds at a rate which increases with oxygen concentration. The current flowing is measured as a potential across a variable resistor (fig. 3.3.4).

3.32 Experimental Procedure

The oxygen electrode does in fact give a good measure of the activity of oxygen dissolved in lubricating oils although there are a number of practical limitations. Primarily the oils seem to in some way 'denature' the teflon membrane so that after a minute or so the measured potential drops away. This is shown in figure 3.3.5 - the behaviour is compared with an aqueous test solution. As a result measurements were made of the plateau voltage a few moments after the sample had been added and the oil was then removed.

Secondly since the viscosity of the ester was higher than water a slower stirring speed had to be used to ensure efficient circulation of the test oil. There was therefore presumably some depletion in oxygen in the region of the membrane but provided the same stirring speed is always used, the relative activity measured is meaningful.

Thirdly there was found to be a decrease in the oxygen activity in a sealed specimen over a period of hours which was not shown with water. Presumably oxidation of the oil within the sealed container was

Figure 3.3.4

Electrical circuit for the oxygen electrode.

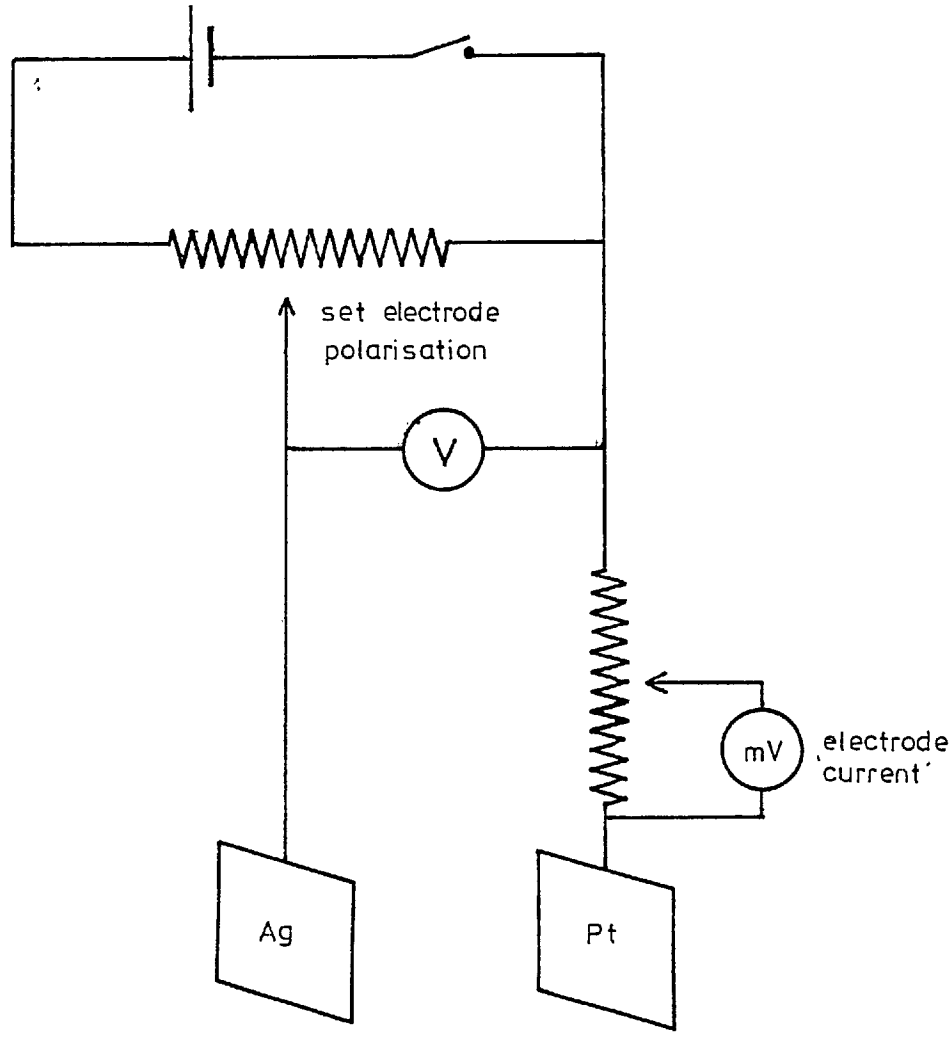

Figure 3.3.5

Oxygen electrode. Variation of measured voltage after addition of an air saturated sample.

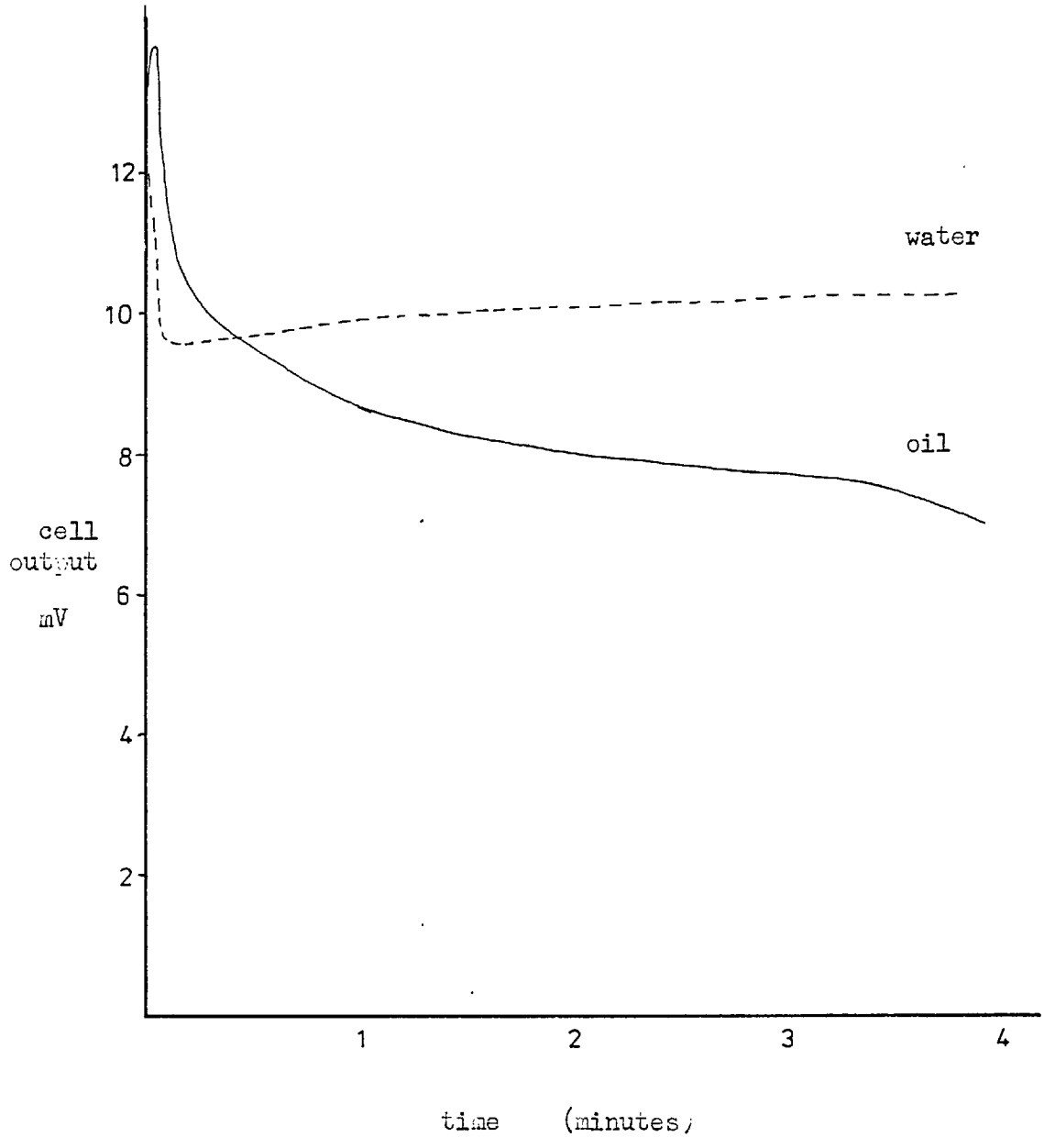

consuming the dissolved oxygen. Oil samples were therefore tested without delay.

Fourthly after a test it was not possible to rinse out the chamber with an oil solvent, e.g. toluene as this attacks the perspex. The chamber could be wiped sufficiently clean, however, with absorbent tissue. Therefore a given cell was never used for more than three determinations (within a ten minute period). Each new cell required recalibration so two standard solutions were used Air Saturated Water (adjusted to give a reading of 10mv) and air saturated ester.

These experimental problems were solved and as a result of experience the following simple routine was adopted. It was found that reasonably accurate results were obtained when it was followed.

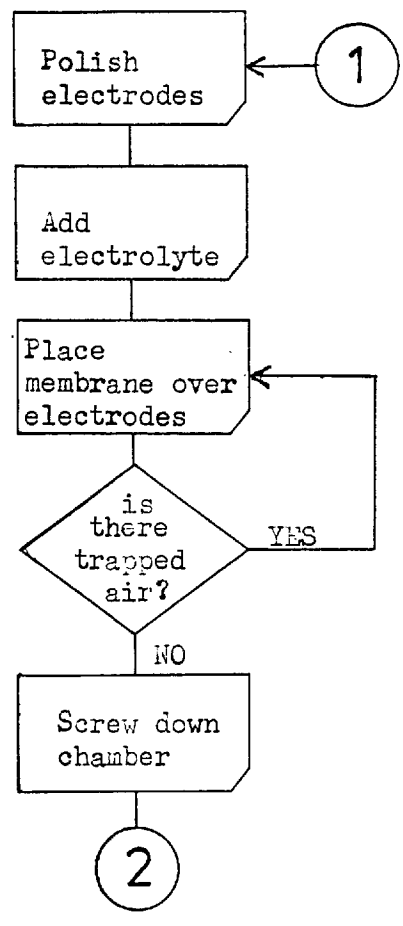

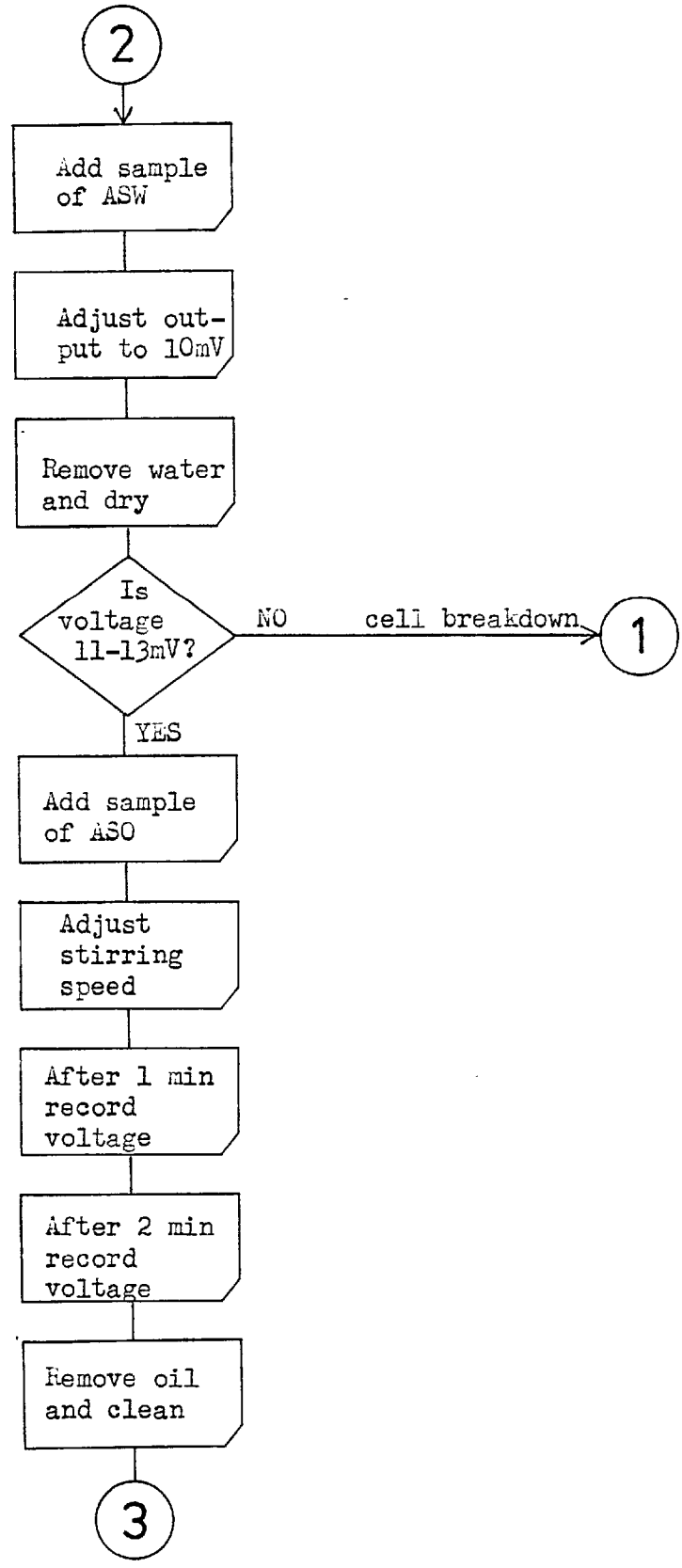

ASW : air saturated water

ASO : air saturated oil

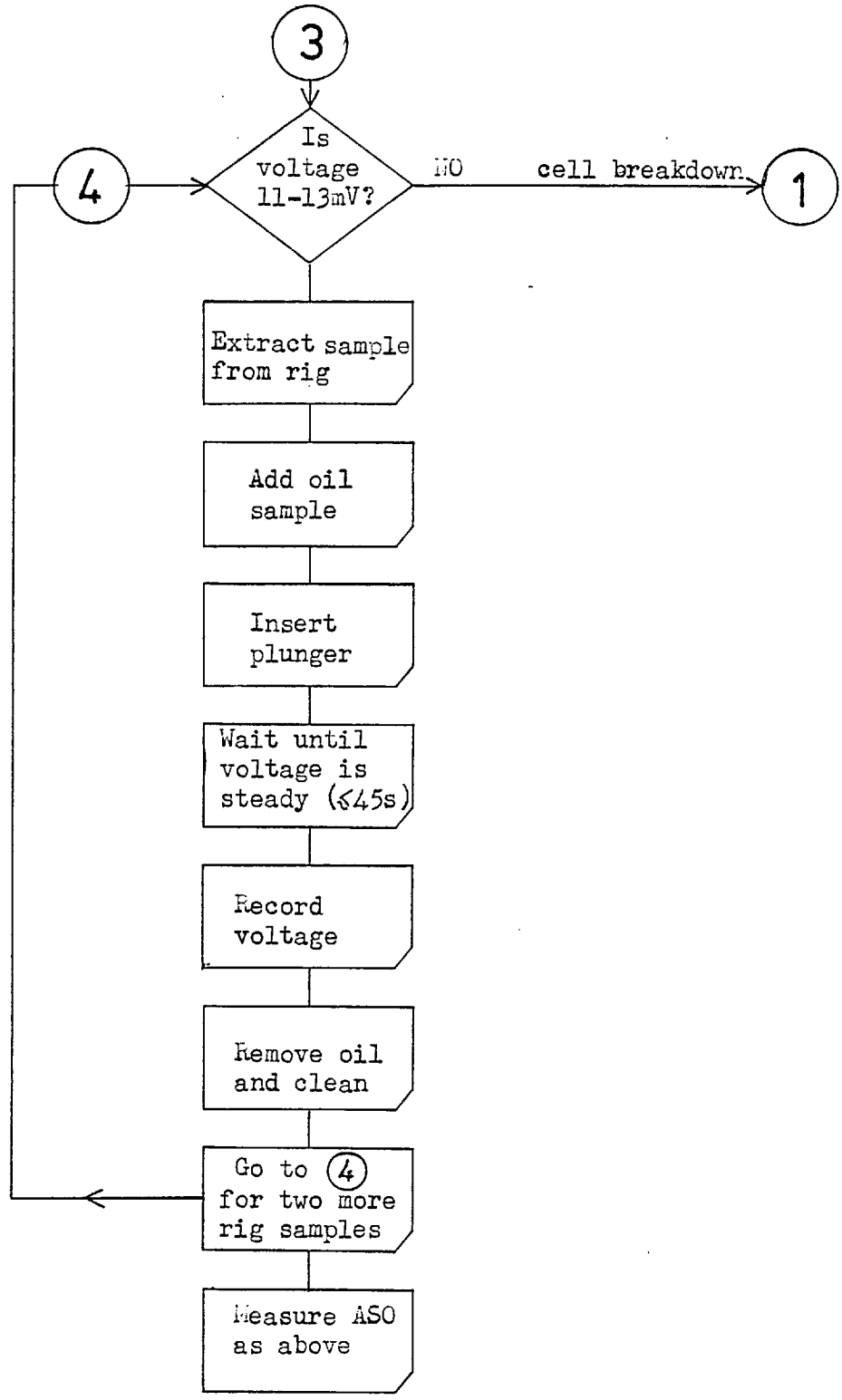
3
Is voltage 11-13mV?
NO
cell breakdown
1
4
Extract sample from rig
Add oil sample
Insert plunger
Wait until voltage is steady (≤45s)
Record voltage
Remove oil and clean
Go to (4) for two more rig samples
Measure ASO as above

The four recorded Air Saturated Oil values are averaged. The three sample values are averaged and expressed as a percentage of the Air Saturated Oil value. Initially only one reading of the Air Saturated Oil oxygen was taken and only two sample readings. A statistical analysis of some results showed that accuracy was poor. This analysis is given below. The value of Air Saturated Oil is assumed to be invariant. In fact the value of Air Saturated Oil was found to drop significantly if the oil was exposed to sunlight (presumably because of oxidation). The Air Saturated Oil was therefore kept away from strong light. The values measured for the oxygen activity in air, in water and in oil are all different because of concentration gradients set up in the cell. The diffusivity of oxygen in the ester must be lower than in water as ideally all the activities should be measured as equal.

Accuracy

Whilst the accuracy of individual readings is not high a set of readings gives a good estimate of the oxygen activity. For instance in the course of tests the activity of oxygen in the air as measured by the cell was noted down. Analysis of these readings of a known fixed quantity enables an estimate to be made of the accuracy of the average of a smaller number of readings. Fifty measurements of the activity of oxygen in air had an average value of 1.5 times the activity in air saturated oil with a standard deviation of 0.12 (8%). The values formed an approximately Normal distribution about the mean.

Assuming that the above distribution of measurements is typical,

the accuracy of a small number of measurements may be estimated using the 't' Probability Distribution Function. By this criterion it is 95 % certain that the actual activity value differs from the mean of THREE measurements by less than :-

$$\frac{8}{\sqrt{3}} \times 4.3 = 20\ \%$$

3.33 Calibration

The oxygen activity values obtained in the manner described above were converted to absolute values by the calibration of the electrode against a gas extraction apparatus. The principle of this device is that if a sample of oil saturated with a gas is introduced into an evacuated chamber nearly all the dissolved gas will come out of solution.

In order to speed the evolution of gas the liquid is agitated in some way. In the ASTM/I.P. procedure(78) the oil is forced repeatedly through a narrow anular orifice. In Hayward's funnel apparatus the oil is agitated by a vibrating paddle(82).

Figure 3.3.6. is a diagram of the funnel apparatus that was used. The instrument has a deaeration chamber in the form of a short wide funnel closed by a lid carrying three tappings. The lid is sealed to the funnel with a rubber 'O' ring in the rim of the funnel. The tappings comprise an attachment for a sample bottle, an outlet to the vacuum pump and an outlet to a vacuum guage. Incorporated in the lid is a phosphorous pentoxide container which removes any water vapour from the chamber.

The bottom of the funnel is sealed by a flexible

Figure 3.3.6

Hayward's Gas Extraction apparatus. Ref. 82.

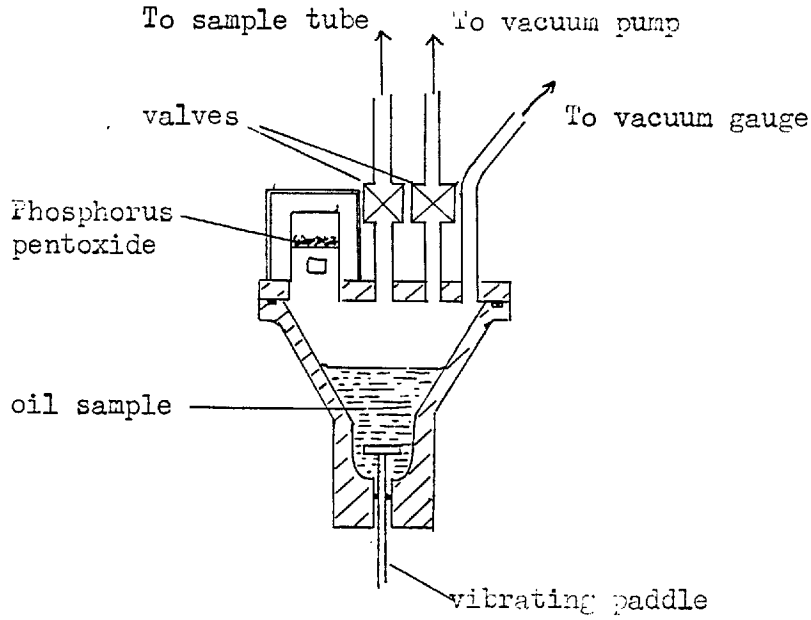

rubber diaphragm penetrated by the shaft of a vibrating stirrer. The experimental procedure is as follows. The sample tube containing the oil is connected to the apparatus. The sample tube is a cylindrical container with a valve at either end which is filled with oil. The Chamber is evacuated down to a pressure of 0.01 to 0.02 mm Hg. The valve to the pump is then closed and the pressure P_1 is recorded. The sample tube valve is opened to admit the oil into the chamber. Immediately the oil starts bubbling. Gas evolution is assisted by turning on the vibrator. After about a minute a stable pressure is reached and the pressure P_2 is recorded after two minutes.

Then the air content expressed as a volume at standard temperature and pressure ($T_s = 273^\circ$; $P_s = 760$ mm Hg) is given by

$$\text{Air Content} = 100 \times \frac{T_s}{P_s} \times \frac{V_c}{V_t} \times \frac{P_2 - P_1}{T} \quad \text{percent by volume.}$$

Where T is the ambient temperature

Vc is the volume of the chamber.

Vt is the volume of the sample bottle.

On the apparatus used the factor $\left(\frac{T_s}{P_s} \times \frac{V_c}{V_t}\right)$ had been accurately calibrated for each sample tube. Three oil samples were tested to obtain a calibration curve. The oil was the ester used in the fretting study.

(1) The oil was degassed under vacuum for an hour ($\lesssim$0.01 mm Hg). A small quantity of oxygen was then bubbled through. The oil was poured into the sample tube (which had previously been evacuated) under this low pressure of oxygen. Samples of oil were also removed and the oxygen content was measured with the electrode.

(2) The oil was degassed as (1). Oxygen was then bubbled through for rather longer than in (1). Under this atmosphere the oil was poured into a previously evacuated sample tube. Oxygen electrode measurements were made.

(3) A sample tube was filled with air saturated oil.

Table 3.1 lists the results of the calibration tests. These are graphed in figure 3.3.7. The origin should ideally be a point on the calibration line. Hayward(82) estimates that the error in the gas extraction procedure to be less than $\pm$ 3%. The error due to the small quantity of gas that remains dissolved in the oil at the P_2 pressure is less than 1% at the pressures P_2 recorded in this test.

According to Henry's Law, the solubility of a gas in a liquid should be directly proportional to the absolute partial pressure of the gas. A dissolved gas will attain equilibrium with the atmosphere above the liquid such that the activity of the gas in both media is equal. The activity of dissolved oxygen (which is what is measured by the electrode) is related to the concentration in solution by the activity constant.

i.e. the activity of oxygen $a_{O_2} = K_a [O_2]$

When considering the reactions of oxygen in solution in lubricants it is activity rather than concentration which is the important parameter.

3.34 Sampling from the Rig

Oil samples were removed from the rig by syringe which was inserted into a nozzle. A tap was opened enabling oil to be drawn into the syringe through the nozzle without being exposed to air. The sampling tap was in the

TABLE 3.1

Results of Oxygen Electrode calibration.

ELECTRODE MEASUREMENTS			GAS EXTRACTION MEASUREMENTS			
Number of determinⁿs.	Oxygen concⁿ % ASO	Standard deviation	Tube factor	Pressures (mm of Hg) P	P	Oxygen concⁿ millimoles per litre
6	24.5	1.8	678	.015	.24	0.23
4	225	5	790	.015	1.45	1.7
air saturated	100		790	.018	3.3	0.82

Concentration was determined at temperature, T 295° K.

concentration % by volume of gas = T.f. x $(P_2 - P_1)$/ T , at S.T.P.

concentration moles per litre = T.f. x $(P_2 - P_1)$/(T x 2240) ,

where T.f. is the Tube factor.

(ASO : Air Saturated Oil)

Figure 3.3.7

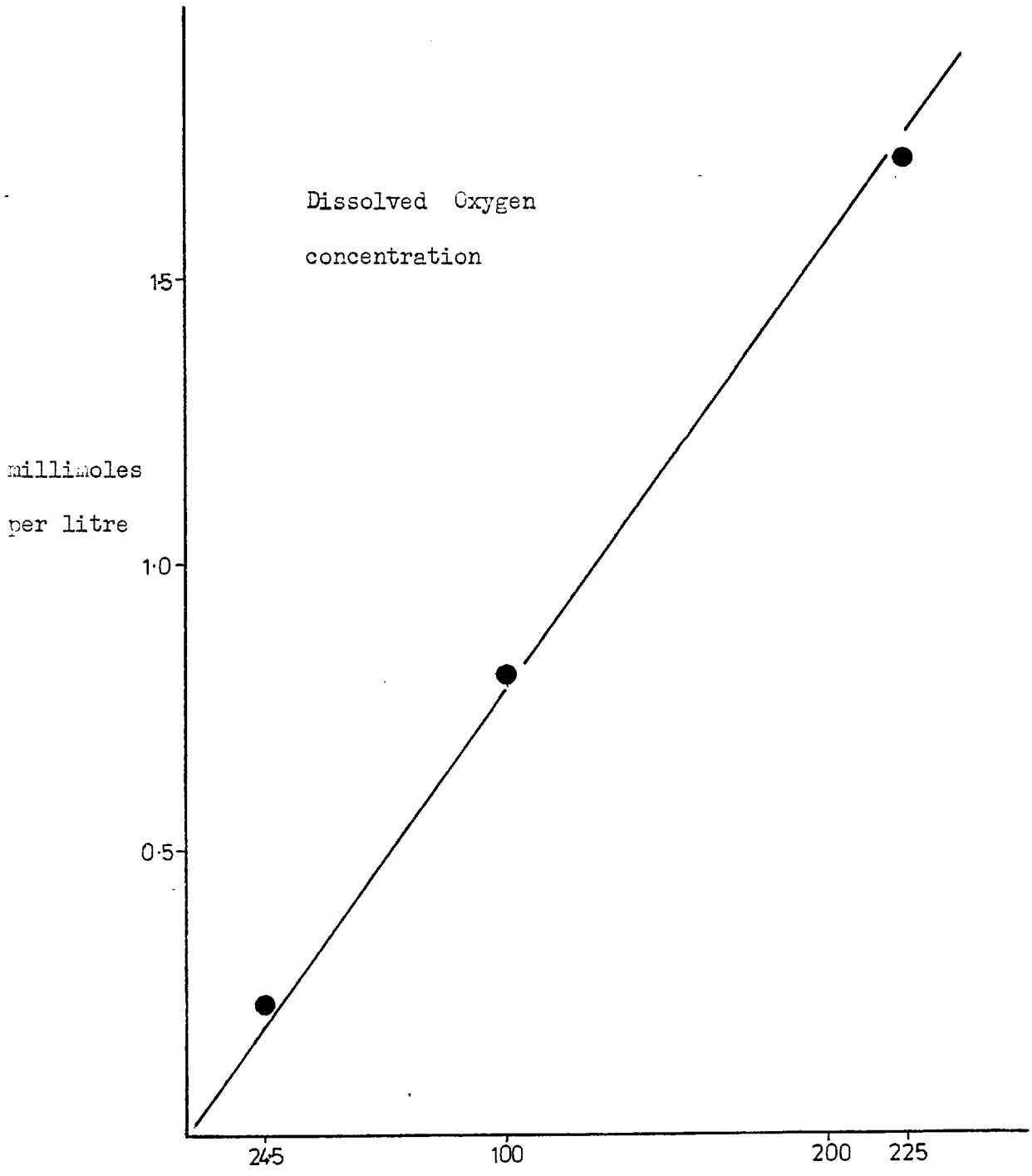

The calibration graph of the oxygen electrode against a gas extraction apparatus.

outlet pipe from the test chamber (figure 2.3.7). The oil was quickly injected into the oxygen electrode sample chamber and a reading taken of the voltage (ignoring the initial transient). No attempt was made to maintain the oil at the test temperature whilst in the oxygen cell. Having made a series of measurements the oil used could be returned to the rig or used for acid or peroxide determinations.

The temperature of the oil in the oxygen cell could affect the reading in two ways. The solubility of gases in liquids varies with temperature. Secondly, the sensitivity of the cell to oxygen increases with increasing temperature. This has been shown by Mancy (figure 3.3.8). Since the cell was not being maintained at constant temperature it was decided to monitor the variation in temperature after injection of the oil sample. Figure 3.3.9 shows the temperatures and oxygen concentrations measured following injection of an oil sample. Samples were taken from the rig at two different temperatures, 60° and 80°C. It can be seen that the oil temperature falls rapidly to about 35°C (within 15 seconds). The temperature recorded after 5 seconds is low due to the slow response of the thermocouple. Over the next five minutes the oil cools slowly a further ten degrees. The measured oxygen concentration also decreases over five minutes. However, the rate of decrease is not very different from that observed with air saturated oil at a constant 23°C. A lower oxygen value was measured for the oil removed from the rig at 60°C because air was being bubbled through the rig at a slower rate.

Typically the oxygen concentration of a sample was

Figure 3.3.8

Variation of Oxygen Electrode sensitivity with temperature. After Mancy et al. ref 81.

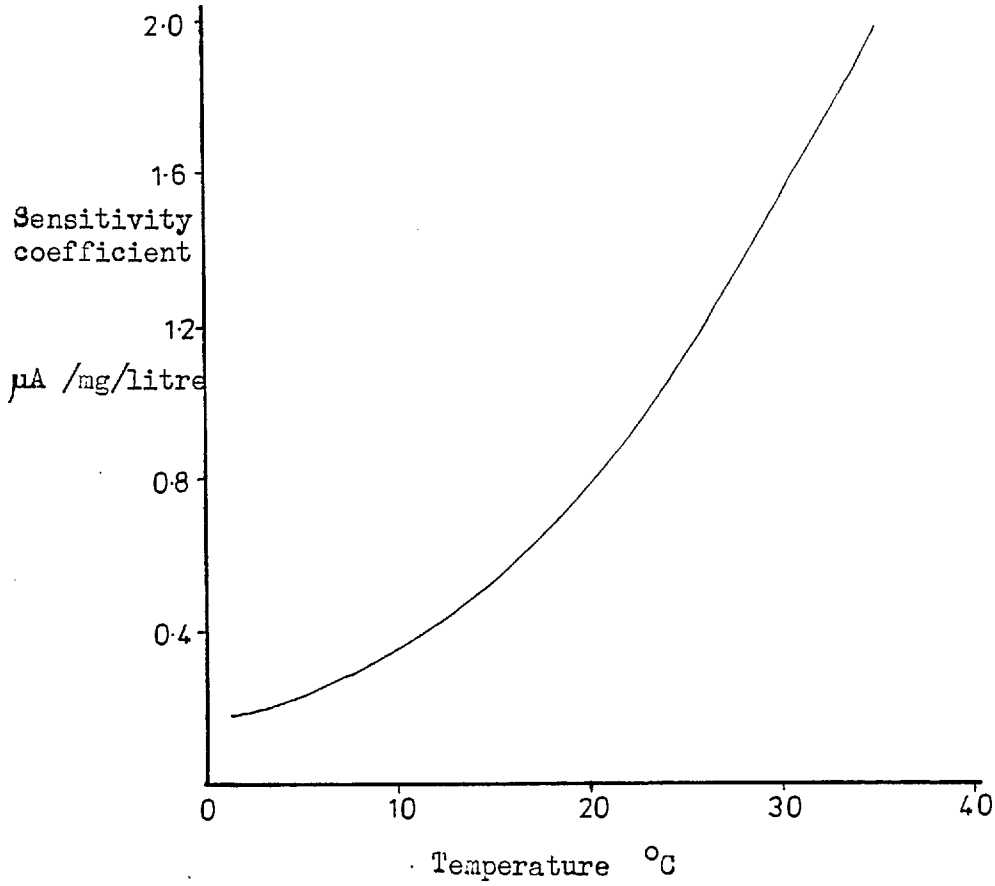

Figure 3.3.9

Variation of measured voltage (cell current) and oil sample temperature after addition of sample.

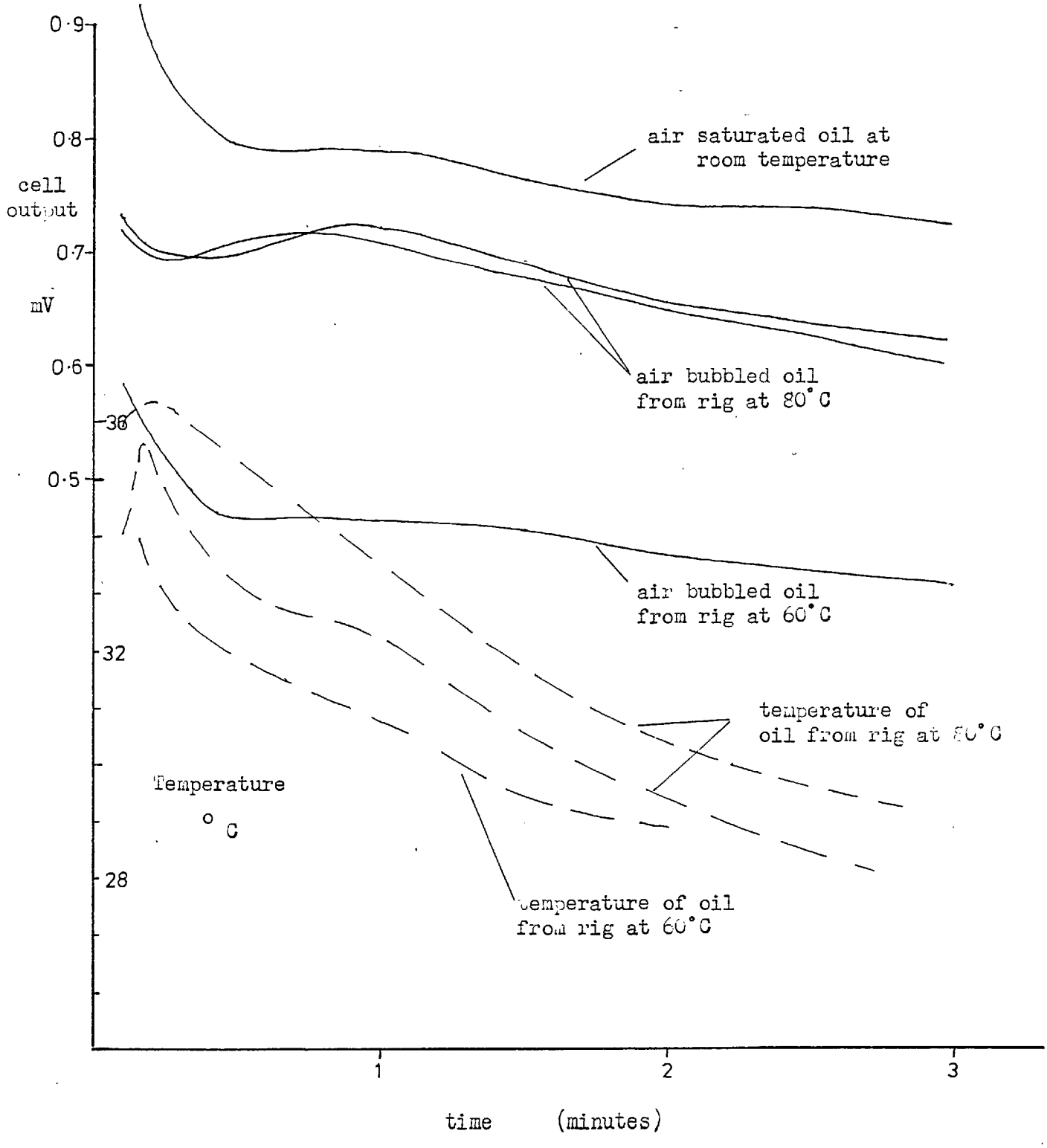

recorded after the initial transient, i.e. 30 to 45 seconds after injection. The temperature of the sample at this time is likely to be in the range 30 - 35°C so the variation in sensitivity of the cell is small enough to be ignored. For all of the tests in which the oxygen concentration was measured the rig oil temperature was controlled at 80°C. Any difference in solubility of oxygen in oil at 80 and at 32.5°C will introduce a systematic rather than random error into the results but because solubility is nearly independent of temperature[5] the error will be small.

3.35 Summary

In the past measurement of dissolved oxygen concentration in lubricants has required sophisticated equipment. The oxygen electrode provides a simple means of measuring the oxygen activity - a more useful parameter than concentration when considering interaction of dissolved oxygen with lubricants and metal surfaces.

3.4 Atmosphere Control

Having developed a means of measuring the oxygen content a means of controlling the composition of the gas passed through the specimen chamber was required. For inert atmosphere tests, nitrogen gas was used. This gas was then bubbled through a solution of pyrogallol in water and then through concentrated H_2SO_4 in gas bubblers to remove oxygen and water vapour contaminants.

The flow of gas from the cylinders was controlled by a sensitive pressure regulator. Flow rates of between 1 and 5 litres per hour were used. The gas input system is shown in figure 3.4.1. The system was essentially the same for air and oxygen atmospheres minus the

Figure 3.4.1

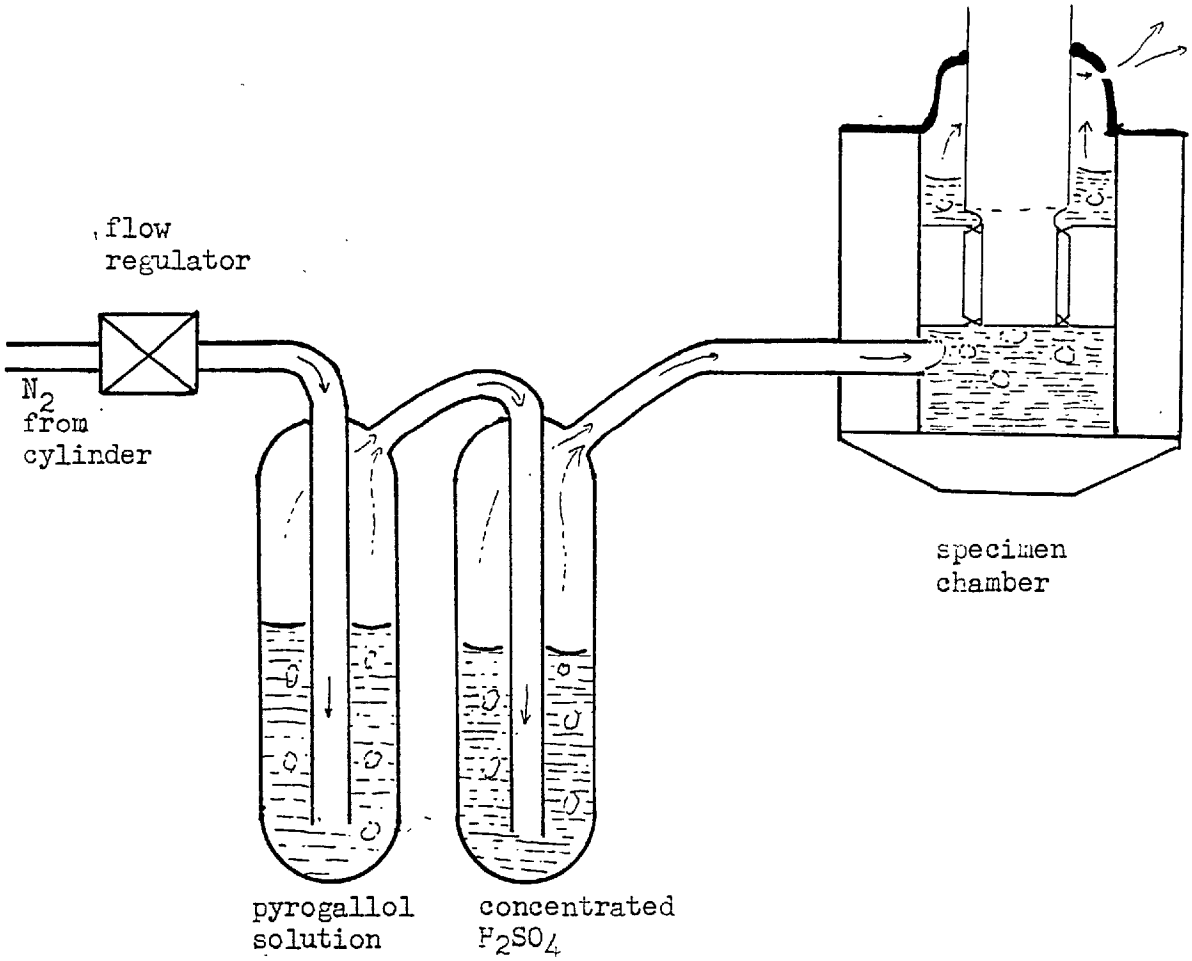

Gas flow system for low dissolved oxygen concentrations.

pyrogallol bubbler. Air was supplied from an air line. After purification the gas passed into the specimen chamber at the bottom and bubbled up through the oil. It exited from the chamber through a small hole in the rubber diaphragm. Because there was some back diffusion of air through this hole the atmosphere in the chamber was to some extent varied by the flow rate of gas. It was considered that leakage of water vapour into the chamber was negligible.

It was important to exclude water vapour from the tests as its effect on fretting wear is somewhat uncertain. In different situations it has been observed to have a pro-wear effect[4,12], an anti-wear effect[12] and in some lubricated tests very little effect[42].

Fretting tests indicated that oil acidity was responsible for reduced wear. In order to ensure that acid vapour was not being carried into the oil in significant quantities a few tests were repeated using activated $CaCl_2$ granules as a drying agent. This substance was activated by heating over a bunsen for about $1\frac{1}{2}$ hours and then packed immediately in a tube. The tube was inserted into the gas line in place of the H_2SO_4 bubbler. No differences in wear rates were observed that exceeded the normal experimental variation. It was concluded, therefore, that there was no significant carry-over of acid vapour in the gas stream.

Chapter 4. Fretting tests in Ester.

4.1 Introduction

This chapter presents the results of fretting wear tests performed with the spline wear tester using an ester base stock as the lubricant. Tests were performed under atmospheres of nitrogen, air and oxygen with the result that the concentration of oxygen in solution in the oil varied from 1/25th to 1 atmosphere partial pressure. It was found that there was a clear relationship between the fretting wear rate and the dissolved oxygen activity.

Before presentation of the results the composition of the ester and its lubricating properties are described and discussed. Under an oxygen atmosphere it was noted that there was a rapid degradation of the oil which affected the wear rate. For this reason a section on lubricant oxidation processes has been included.

At the end of the chapter a section is devoted to the results of photomicroscopic and other studies of the worn surfaces, from tests in both ester and hexadecane lubricants. The results are presented at this stage because the photographs illustrate the type of wear damage that occurs in the fretting contact under different rates of wear.

A preliminary step in this investigation was to compare the results of the ester lubricant with those obtained by Ku [12,13] using mineral oil and jet fuel lubricants. The test results are compared in the following section.

4.2 A Comparison of the Results with those of P.M. Ku

Several tests were performed initially to compare the wear behaviour in ester with Ku's results for a mineral oil. No attempt was made to reproduce the conditions of Ku's tests exactly with a mineral oil since it was considered that the fretting wear rate would be sensitive to small differences in mineral oil base stocks.

However, wear tests conducted with a mineral oil and the ester base stock showed a similar wear behaviour to that observed by Ku. In particular tests run with a spline misalignment of 0.34° gave a linear increase of wear with time whereas a misalignment of 0.17° resulted in a non-linear relationship between wear and time (fig. 4.2.1).

The lower wear in ester compared with Ku's mineral oil may be explained partly by the lower loading used and partly by a difference in lubricating properties. Having demonstrated the similarity in wear behaviour the lubricating properties of the ester were investigated in more detail.

4.3 Properties of the Ester Base Stock

4.3.1 Composition of the Ester

The ester used in this test programme was a base stock supplied by the Mobil Oil Company. While not prepared to reveal the composition of the oil the Company provided some data on its physical properties (Table 4.1). It is a dibasic acid ester with complex ester thickeners to bring the viscosity up to 7.4 cS at 100° C.

Esters based on dibasic rather than monobasic acids have many advantages in that compounds of high molecular weight can be prepared from low molecular weight starting

Figure 4.2.1 A comparison of wear results with those of P. M. Ku et al. ref. 12,13,

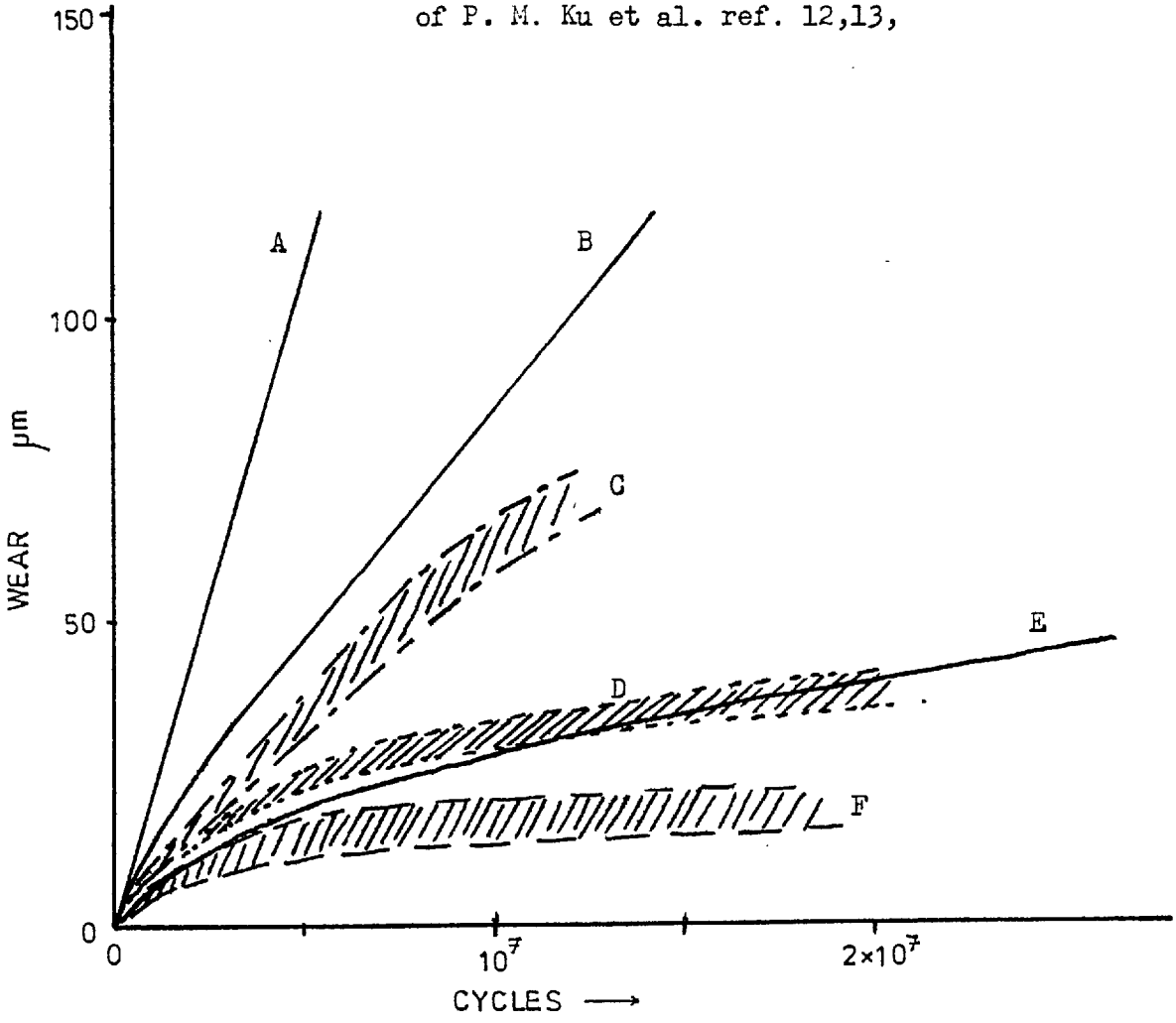

Key	Worker	Lubricant	Viscosity at 100°F	Load p.s.i	Temperature °C	Misalignment	Frequency Hz
A	Ku	Jet fuel	-	1950	121	0·34	4400
B	Ku	Mineral	300 SUS	3850	121	0·34	4400
C	Newley	Ester	44 cS	2180	80	0·34	3250
D	Newley	Ester	44 cS	2180	140	0·17	3250
E	Ku	Jet fuel	-	1950	121	0·17	4400
F	Newley	Mineral		2180	80	0·17	3250

(shaded area represents observed variation in the wear rate in different tests)

Table 4.1

Physical properties of the Ester base stock.

Kinematic viscosity at 38° C :	44 cS
Kinematic viscosity at 100° C:	7·4 cS
Specific gravity at 15·6° C :	0·912
Viscosity index :	146

materials:

(1) Long chain dicarboxylic acids

e.g. Sebacic Acid (x = 9)

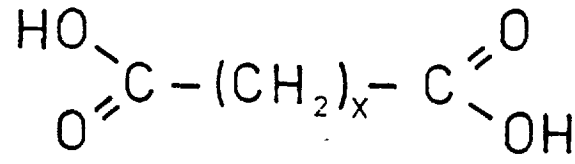

(2) Long chain branched primary alcohols

e.g. 2 - ethyl - 1 - hexanol

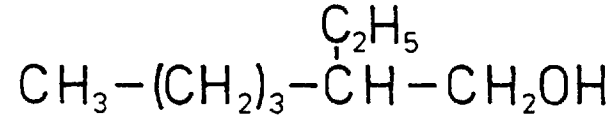

In the esterification process the reactants are introduced into the reaction vessel roughly in proportion (normally a 10% excess of alcohol is used). Five per cent of benzene is added as a water entrainer. Pressurised steam raises the temperature to 150°C. The reaction requires several hours to go to completion:

The physical properties of the ester are determined by configuration of the starting materials[83]. In order to lower the viscosity at low temperatures short branches from the main chain are desirable. This is most often achieved by using branched primary alcohols.

For a typical ester, physical properties are affected in the following way:

(1) Increasing the length of the main chain increases viscosity, Viscosity Index (V.I.) and freezing point.

(2) Addition of side chains increases viscosity lowers V.I. and pour point.

(3) The position of branches influences viscosity, V.I. and temperature stability.

(4) Addition of cyclic groups causes larger increases in viscosity and reduction in V.I. than aliphatic groups owing to their rigid structure.

Viscosity index improvers are frequently added to ester lubricants. Long chain polymers such as methacrylates are good in this respect and can also act as sludge dispersants. However, they tend to break up into small fragments under severe stress. More modest viscosity improvement is obtained with complex esters. These are polyesters of di-acids and polyalkylene glycols. They are not subject to shear breakdown and act as good load carrying additives.

4.3.2 Lubricant Performance

Diesters are found to be more effective boundary lubricants than mineral oils of the same viscosity. R. L. Johnson et al[84] tested several esters, measuring the sliding velocity at which effective lubrication broke down. The failure of di(2 ethyl hexyl)esters occurred at a sliding speed of 7,000 to 8,000 feet/min. which may be compared with the values obtained for a mineral oil (MIL 06081a) of 2,400 to 3,000 f.p.m. By this criterion silicone diesters were found to be the best boundary lubricants. The superior lubricating properties of esters results from their better absorption and orientation at

the metal-lubricant interface.

4.4 Oxidation of the Ester

4.4.1 Oxidation Mechanisms

The oxidation of ester lubricants occurs by a free radical chain reaction process in a similar way to the mechanism of oxidation of long chain hydrocarbons and mineral oils[85]. The reactions of the chain process may be classified as follows[85]:

Initiation by the action of light, heat or metal catalysis:

(1) Initiation $RH \longrightarrow R^{*} H$ an activated state

(2) $R^{*} H + O_2 \longrightarrow$ P an activated complex involving oxygen

Initial propagation:

(3) $P + RH \longrightarrow ROOH + R^{*} H$

(4) termination $P \longrightarrow$ Inert products

There is some disagreement about the initiation reaction (1), there being two other possibilities[59].

a) $RH \longrightarrow R\cdot + H\cdot$

b) $RH + O_2 \longrightarrow R\cdot + HOO\cdot$ i.e. direct reaction with oxygen. However, this question does not affect the overall reaction.

After a period of time decomposition of the hydroperoxide (chain branching) is the major source of radicals:

Branching:

(5) $ROOH \longrightarrow RO\cdot + HO\cdot$

(6) $RO\cdot \longrightarrow R\cdot$ + carbonyl compounds

Propagation:

(7) $R\cdot + O_2 \longrightarrow ROO\cdot$

(8) $ROO\cdot + RH \longrightarrow ROOH + R\cdot$

Termination:

(9) $R\cdot + R\cdot \longrightarrow$ Stable products, i.e. any combination of two radicals is a termination step. Such products are acids, ketones and alcohols.

In the above reaction sequence the symbols stand for:

RH = Ester molecule

ROOH = Hydroperoxide of the ester

RO· and R· = free radicals

ROO· = Peroxide free radical

R in these cases refers not solely to an alkyl group but also contains the main ester functional group.

The chain reaction propagation mechanism is illustrated diagrammatically in Figure 4.4.1.

The bulk of oxidation occurs by the propagation reaction shown by the small circular cycle in the figure - reactions (7) and (8). The peroxy radical is able to abstract a hydrogen atom from a hydrocarbon chain to form the hydroperoxide ROOH* and a new radical which reacts directly with oxygen. The rate of this process is very high, limited by the availability of dissolved oxygen and

---

*Also referred to as a "peroxide".

Figure 4.4.1

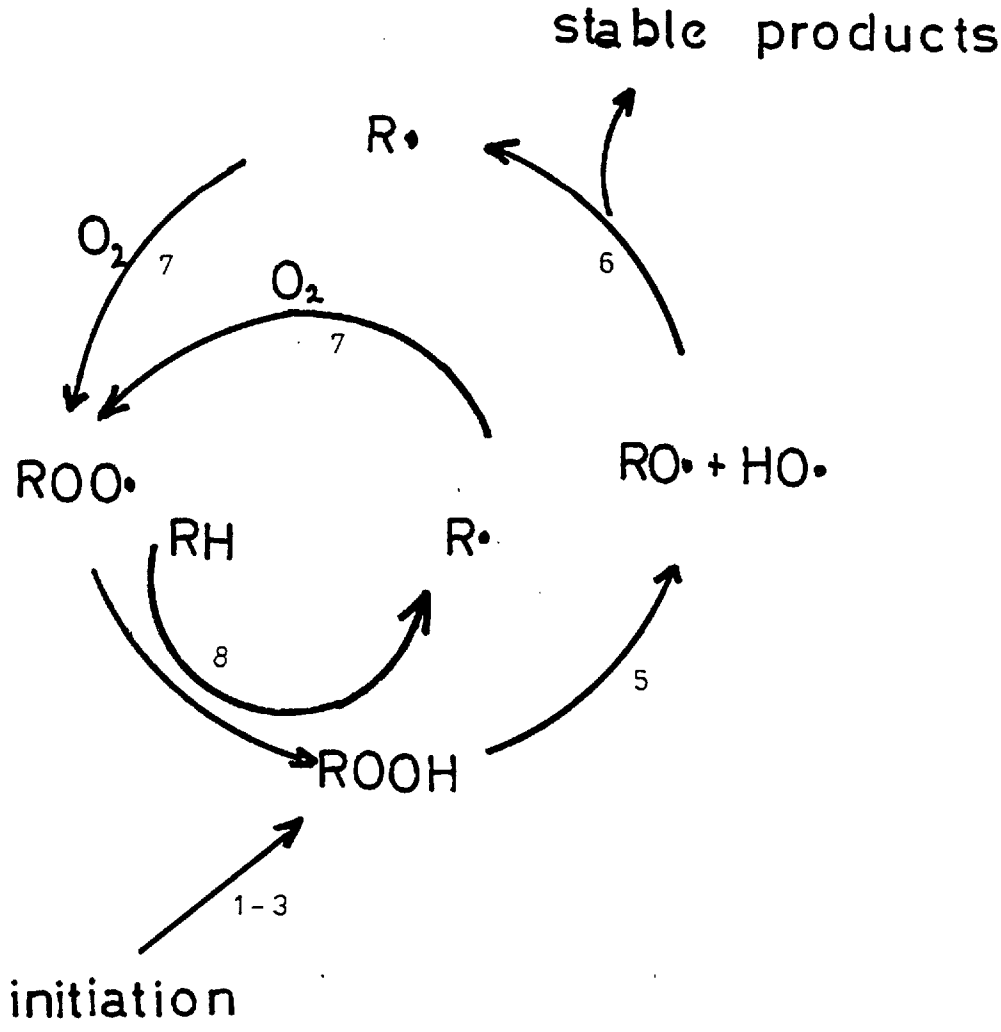

A diagram illustrating the reaction sequence during the steady state propagation stage of hydrocarbon oxidation.

the readiness of the hydrogen to be displaced from the hydrocarbon chain. However, before this rapid oxidation can take place sufficient radicals must be formed by the initiation processes producing hydroperoxide which subsequently decomposes to form radicals. An initial period of low oxidation of hydrocarbons, termed an "induction period", is therefore often observed.

The above mechanism has been proposed for both ester[85] and mineral oils[59]. However, the position of initial attack on the carbon chain is influenced by the position of ester linkages. Oxidation of hydrocarbons takes place preferentially at sites where one carbon is bonded to more than two carbons i.e. attack is in the order tertiary, secondary then primary carbons[86]. This is because the C· radical is better stabilised if bonded to alkyl groups rather than hydrogen.

This trend has been confirmed by Rigg and Gisser[85] studying the oxidation of adipatic diesters. They also examined the effect on the rate of oxidation of the position of the side branches on the primary alcohols. The overriding effect was that the rate of reaction increased as the distance from the ester group increased. This is because of the electron withdrawing effect of the ester group - the unshared electrons of the linking oxygen are delocalised over the group leaving the oxygen slightly positively charged as shown below:

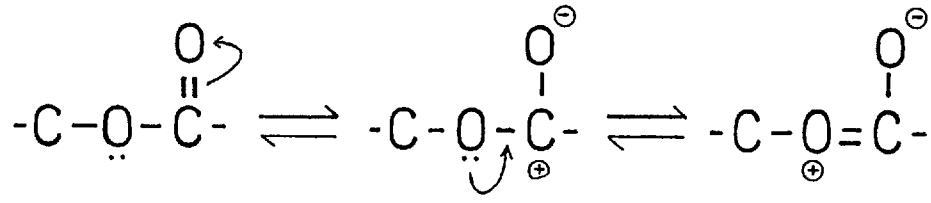

A recent study of the oxidation of Neopentyl Hexanoate[87] yielded the relative rates of attack at each carbon position. The results are shown in Table 4.2. They show that oxidation of the carbons adjacent to the ester group is inhibited.

Under severe oxidation it is possible that the acid group will be split in the middle. Ermolaeva and Freidin[88] studied the oxidation of dimethyl sebacate and found 40% of the product had split in this way.

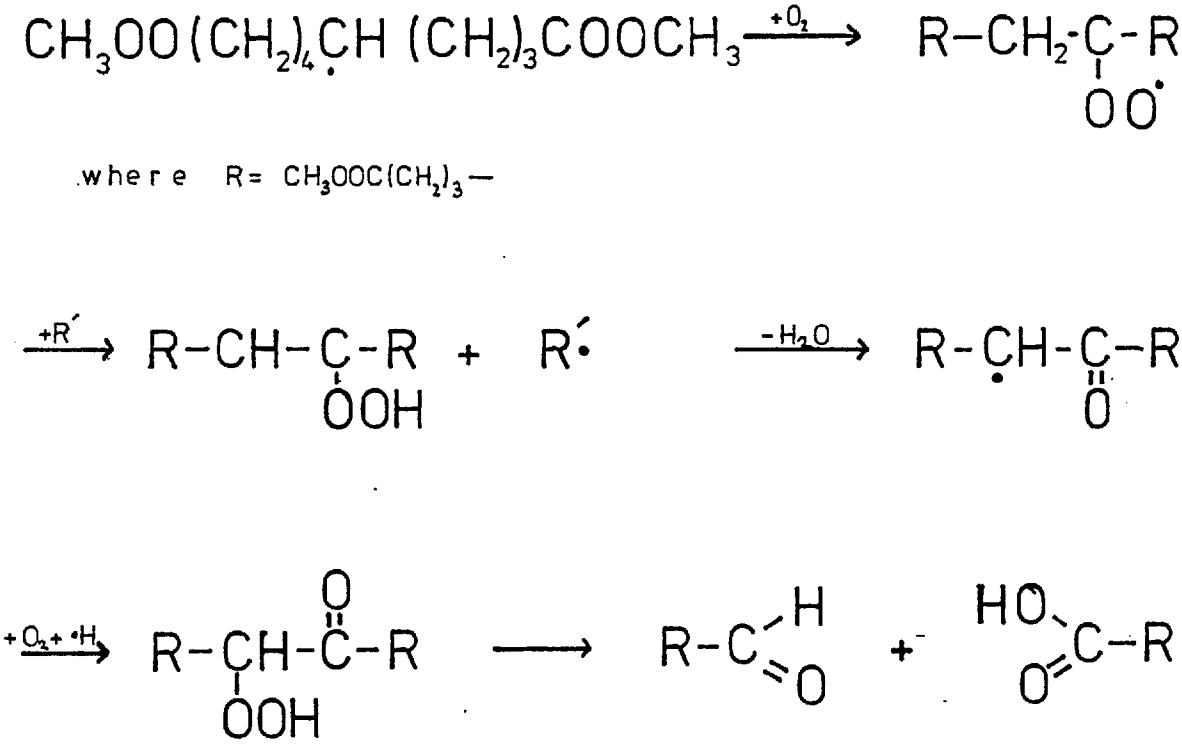

where R= $CH_3OOC(CH_2)_3-$

4.4.2 Oxidation of the Ester - Reaction Rate

Rigg and Gisser monitored oxidation of esters in two ways.

(1) Measuring consumption of oxygen.

Table 4.2

The relative rates of attack by Oxygen at each type of C-H bond during oxidation of an ester.

Neopentyl hexanoate

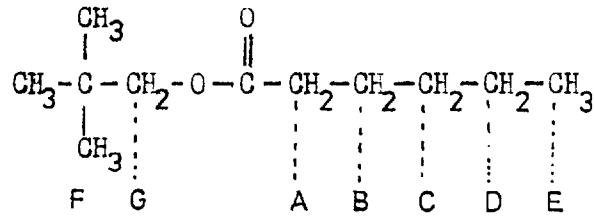

Type of C-H bond	Sites	Relative rate of attack
Primary	E,F	1·0
'Normal' secondary	B,C,D	15·2
alpha-acyl secondary	A	1.8
alpha-alcohol secondary	G	4·2

from 'Selectivity of the Oxidative attack on a model ester lubricant' P. J. Sniegowski, ref. 87.

(2) Determination of the acidity and peroxide concentrations by the method of Wagner and Smith[89].

When an ester was oxidised in air it was found that the concentration of peroxide increased uniformly and then decreased (probably towards a steady value) due to an increasing rate of peroxide decomposition. The concentration of acid built up slowly at first, then quite rapidly when the peroxide concentration began to level off. The oxygen consumption measurements showed a similar increase at this time (ref 85). By performing the following experiment Rigg and Gisser demonstrated that over the initial period the reaction is dependent on thermal activation whilst in the steady state the reaction is propagated by decomposition of the peroxide.

They oxidised di(3 methyl butyl)adipate in solution in diethyl adipate and determined the effect on the rate of reaction of the solute concentration. Since the rate of oxidation of diethyl adipate is very much lower, they were able to neglect the effect on oxygen uptake of oxidation of the solvent. They found that the rate of oxygen uptake was dependent on the concentration of dissolved ester to the power 2 during the initial period and to the power $\frac{1}{2}$ in the steady state. The relationships are predicted by the mechanism outlined above.

4.5 Experimental Conditions

In order to study the effect of oxygen on fretting wear rate a standard set of conditions was employed for all tests in this series in so far as the various parameters could be controlled.

(1) Bulk oil temperature. This was controlled at

80°C - a thermocouple inserted into the chamber showed that regulation was to within ± 3 degrees. This temperature was chosen because it was the highest temperature that could readily be maintained by the heating system. It was noted that at higher temperatures degradation of the lubricant was fairly rapid. A temperature of 80°C also means e.p. action (as opposed to anti-wear action) of substances in the oil can be discounted as e.p. action (chemical combination of additives with the surface) has been shown not to become effective until temperatures greater than 120°C[67]. Any boundary action of the lubricant will be a thin film adsorption effect.

(2) Load. This was chosen for convenience as 14lbs. wgt. The corresponding contact load of 2180 psi falls within the range of loads used by Ku - 3850 psi, 2530 psi and 1790 psi[11,12,13]. The effect of different loads is discussed in chapter 10.

(3) Misalignment. A misalignment of 0.34° was used as this has been shown to give linear wear initially.

(4) Frequency. The frequency used 54.2 Hz was determined by the speed of the motor and the pulley ratios giving the gyrator shaft a rotational speed of 3250 rpm. Gyration frequency may be varied by altering the pulley ratios but the effect of different frequencies has not been investigated. The frequency used by P. M. Ku was 73.3 Hz. The effect of frequency on wear has been discussed in section 1.51.

(5) The splines. The spline specimens were fabricated from EN36C steel as described above (section 2.1). They were used in their unhardened state for ease of metallographic sectioning and examination. The case

hardened specimens were found to have a much finer microstructure in the hardened layer so that any subsequent changes as a result of fretting would be hard to detect. The hardness of the untreated specimens was 232VHN.

(6) Controlled atmosphere. Most tests were performed under a controlled atmosphere as described in the previous chapter. A few tests were performed with the top of the chamber unsealed and the lubricant exposed to atmosphere. The resultant wear rates were not significantly different to those obtained later in dry air. However, because of the reported affects of moisture on wear rates (often conflicting) it was excluded from subsequent tests.

4.6 Experimental Procedure

Setting up. Before each test the rig was cleaned in the way that has been described above. The specimens were assembled in the rig in such a way that the loading lever on which the weight is hung was approximately horizontal otherwise the moment of the weight would be reduced. For instance, a 10° tilt of the loading lever decreased the moment of the load by a factor of $\cos 10^{\circ} = 0.985$.

The lubricant was then poured into the specimen chamber from which it was circulated by the pump. About 70 mls of oil was sufficient to fill the system. When the chamber was full the rubber seal was clamped in position and the requisite gas was bubbled through. Before the test was started the oil was circulated for about an hour to allow its temperature to rise to the test temperature - generally $80^{\circ}C$ and allow the dissolved gases to attain equilibrium with the atmosphere at the test

temperature.

When a low concentration of oxygen was required, the oil was first degassed under vacuum and then saturated with Nitrogen in the apparatus shown in figure 4.6.1. The sintered glass through which the gas was passed ensured that it was dispersed in fine bubbles throughout the oil. Any dissolved oxygen remaining tends to condense out on these bubbles. The rig was purged with N_2 and the oil pumped directly into the rig to minimise the exposure to air.

In all cases each lubricant was purged by the appropriate gas at the correct temperature for at least $\frac{1}{2}$ an hour. Once the test was started the oxygen activity was measured regularly by extracting samples of oil for analysis in the oxygen electrode (as described in Chapter 3). In the course of some of the fretting tests leakage of the oil caused the level in the specimen chamber to drop below the outlet and gas was drawn into the circulation system. When using hexadecane evaporation caused a similar problem. This led to a drop in circulation of the oil so fresh oil was added through the stopcock using a syringe.

At the end of a test the specimens were removed and cleaned. The wear scars were examined and the female splines reweighed and its weight loss calculated. The weight loss results provided a useful check on the wear displacement measurements.

4.7 Experimental Results

From the chart recorder traces, plots of wear displacement against time were obtained from which wear rates were measured. The latter were then correlated with oxygen data.

Figure 4.6.1

The Nitrogen purging system.

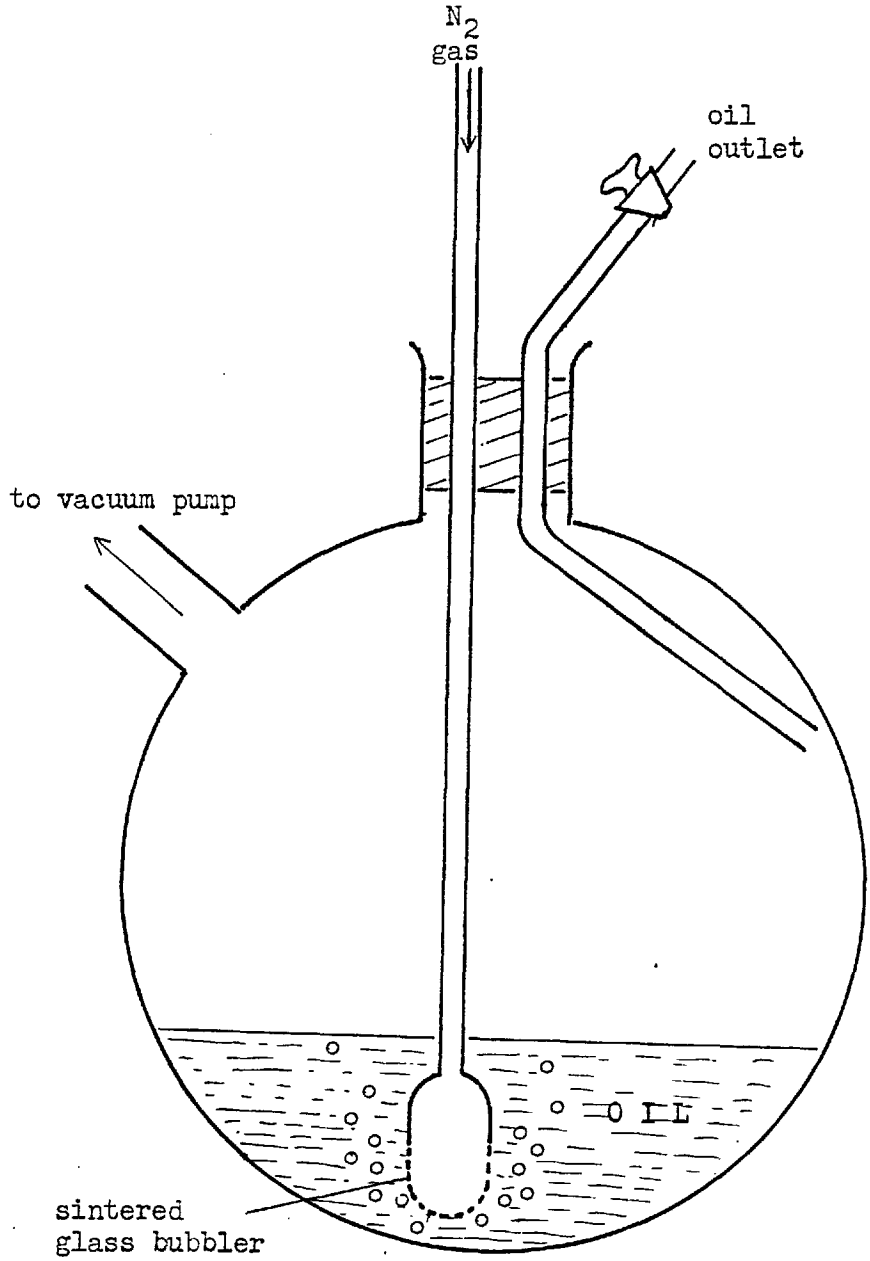

Figure 4.7.1 shows typical wear curves at low, intermediate and high oxygen concentrations. Precise control of the oxygen concentration proved to be difficult so that in many tests a wide range of oxygen concentrations were observed. These fluctuations arose from three possible causes:

(a) Variations in the gas supply pressure. To remedy this a more sensitive pressure control valve was fitted.

(b) A deterioration in the pumping efficiency, as a result of a drop in oil level, led to the sampled oil having a different oxygen content to that within the chamber.

(c) Oxygen uptake during a period of high wear being greater than the rate of absorption into the oil leading to a reduction in concentration.

Because of these fluctuations in the oxygen concentration the wear rate also varied. Figure 4.7.2 is a graph of the results of nine fretting tests obtained by calculating the rate of wear over periods in which the oxygen concentration was approximately constant and plotting this value against the oxygen concentration. These results are tabulated in table 4.3. Those points on fig. 4.7.2 which are shaded were obtained at test times in excess of twenty hours. It was noted that especially under high oxygen conditions these points tend to lie at low wear rates. A fall in the wear rate in the later stages of a test proved to be a characteristic of the fretting tests in both ester and hexadecane lubricants, although it was not observed by Weatherford and Ku[12]. There are two possible explanations for this effect:

(a) The spline teeth were being worn to a shape where

Figure 4.7.1 Fretting wear curves at high, intermediate and low oxygen concentrations.

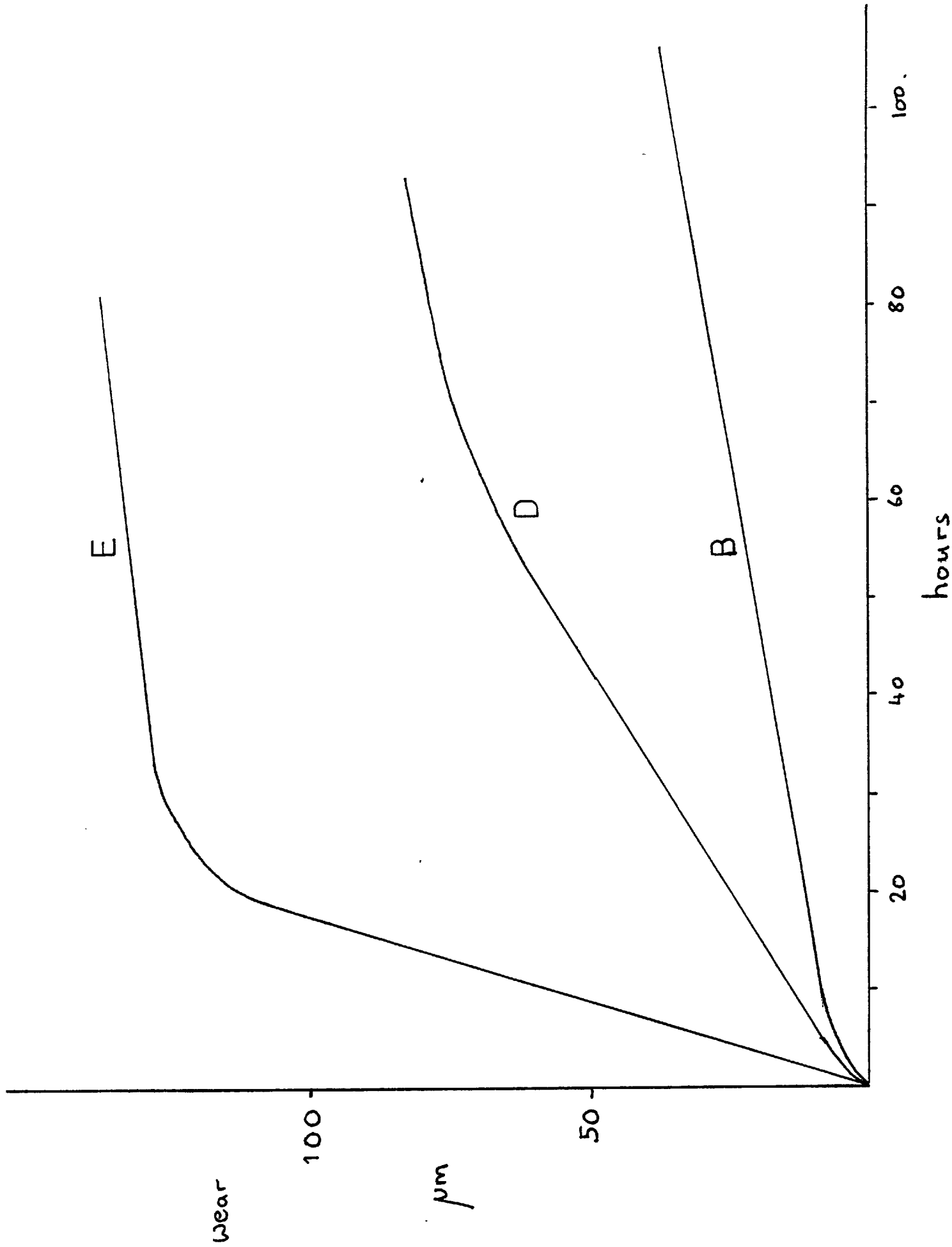

Figure 4.7.2

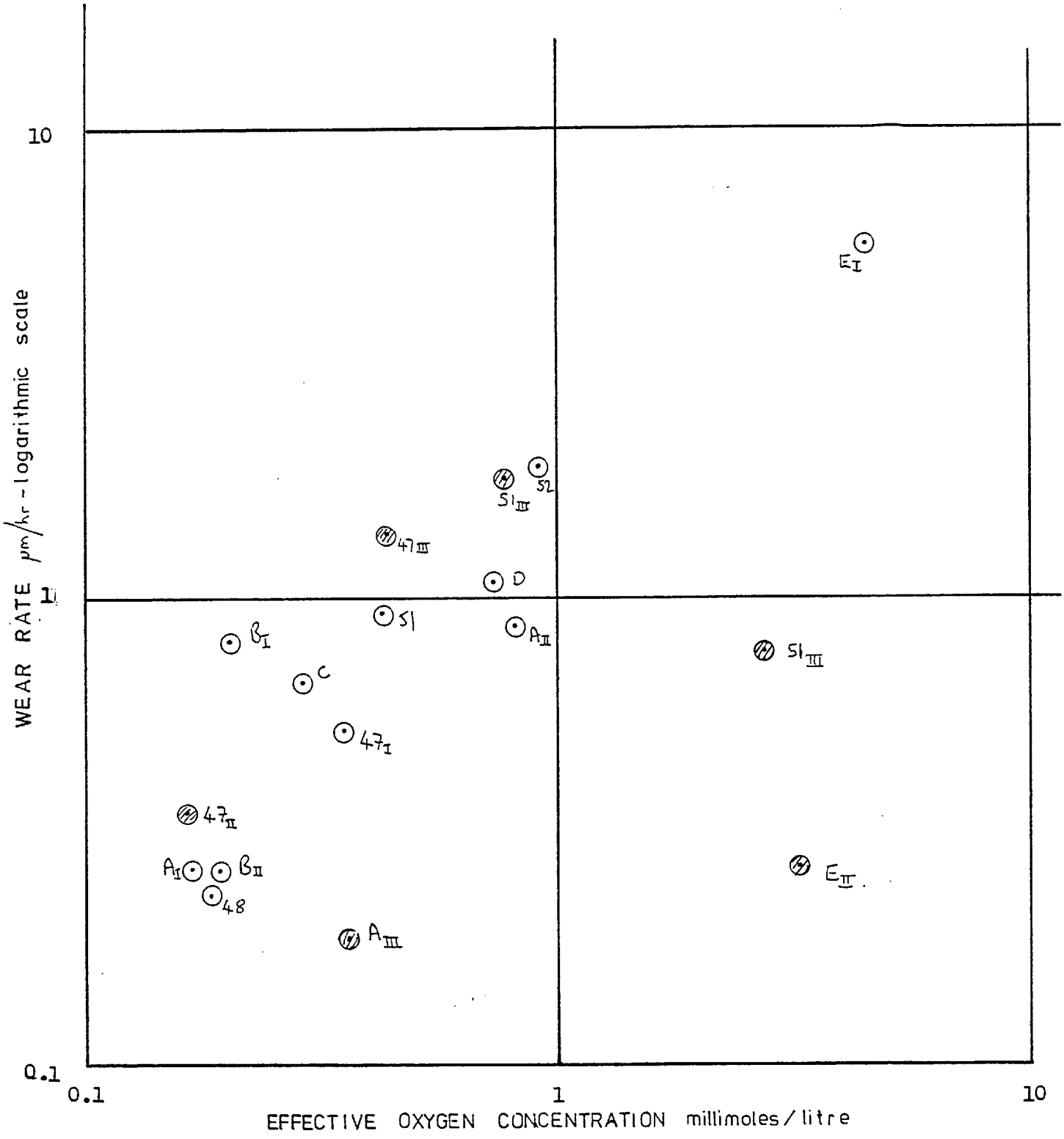

Fretting wear rate plotted against dissolved oxygen activity.

(the letters adjacent to the points identify the test.

The shaded points are the wear rates observed at long times.)

TABLE 4.3

Measurements of Fretting Wear Rate
and Dissolved Oxygen Concentration

Lubricant - ester

Test No.	Code Letter	Test Time (Hours)	Oxygen Conc'n.		Number of (O_2) Determin'n.	Wear Rate μm/hr.	Oxygen Conc'n. σ m.moles /litre
			% ASO	m.moles /litre			
1	47	20-95	45	0.35	1	0.52	
		100-135	21	0.165	2	0.35	0.012
		135-160	55	0.43	1	1.38	
2	48	0-25	23	0.18	5	0.23	0.04
3	51	8-45	54	0.42	2	0.93	0.11
		45-67	100	0.78	3	1.8	0.04
		67-100	350	2.73	4	0.76	* 0.66
4	52	0-10	118	0.92	1	1.88	
5	A	0-40	21	0.165	9	0.265	0.01
		45-65	102	0.80	4	0.86	0.08
		70-90	47	0.36	8	0.19	* 0.06
6	B	4-16	26	0.20	3	0.81	0.06
		26-46	24	0.19	5	0.26	0.05
7	C	1-7	37	0.29	8	0.67	0.03
8	D	0-55	95	0.74	45	1.08 decreasing	0.09 *
		55-100	95	0.74			
9	E	0-20	580	4.5	27	5.65	0.2
		20-35	415	3.23	21	decreasing	* 0.4
		35-70	415	3.23		2.62	*

* N.B. Decrease in wear rate at long test times.

further wear only occurs at a much lower rate.

(b) Changes in the composition of the oil during the test lead to it having better anti-wear properties.

These alternatives are discussed in section 4.9 whilst the initial wear rates are now considered. The results of table 4.3 (excluding those marked with an asterisk which are considered to have been influenced by this secondary wear effect) were subjected to a least squares regression analysis of the wear rate on the oxygen concentration. These points and the best straight line through them given by the analysis are shown in fig. 4.7.3. Also calculated were the following:

Upper and lower bounds, one standard deviation either side of the "best" line which are shown in 4.7.3.

The gradient of the best line = 0.9

The correlation coefficient of the results, R = 0.91

A value of R of 0.91 indicates good correlation - R = 1 denotes perfect correlation. The position and slope of the best line is determined to a large extent by the position of point E. However, this point was closely defined by no less than 27 oxygen activity measurements. Further evidence for the position of the line at high oxygen concentrations is provided by the secondary wear rates observed during fretting tests with an antioxidant additive (shown as XII and YII in fig. 4.7.3). In these tests a low initial wear rate was observed while the additive was active followed by a higher wear rate characteristic, it is believed, of the additive-free oil under the same conditions.

The scatter in the results arises both from errors in

Figure 4.7.3

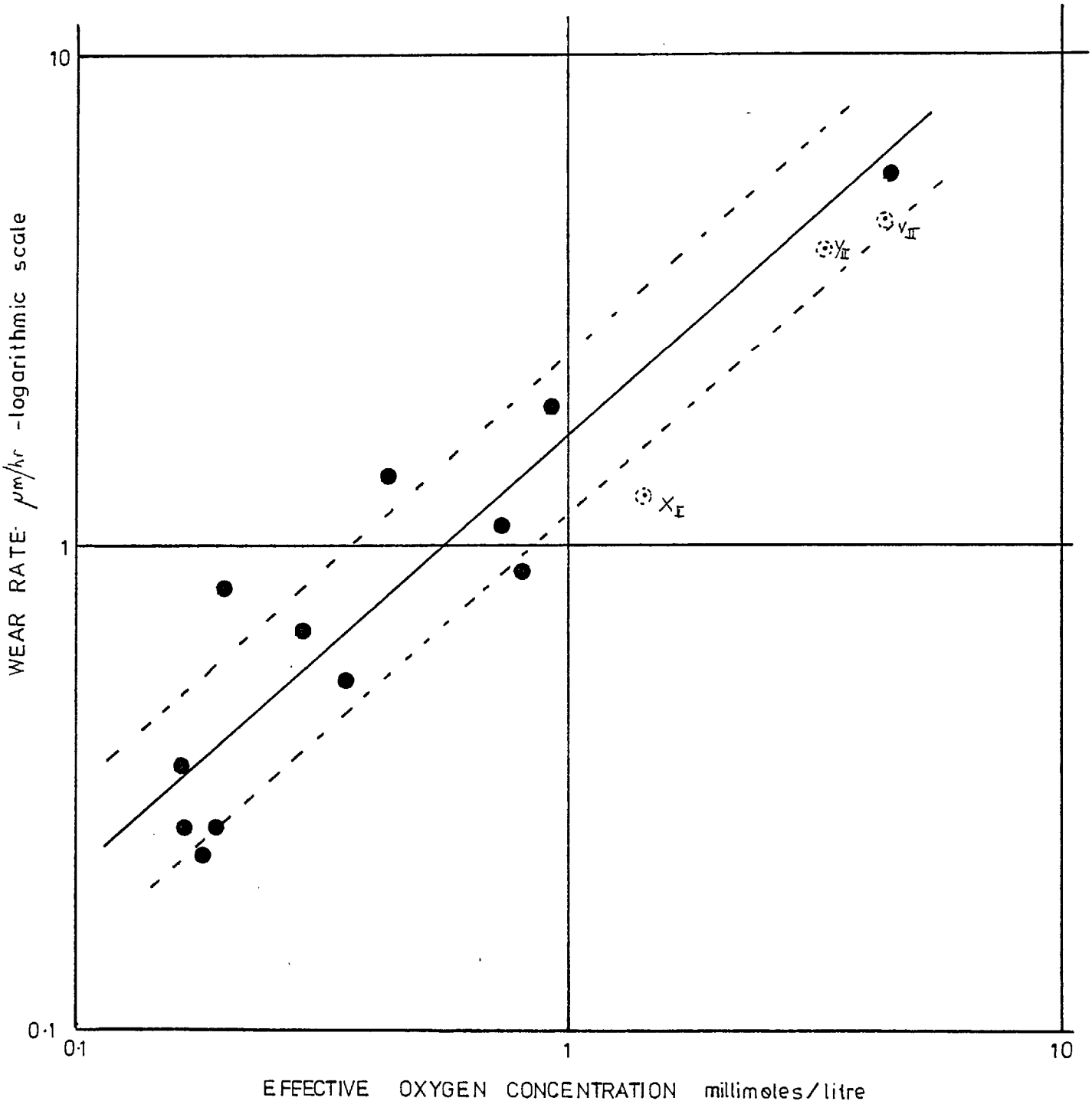

Results of regression analysis of the ester results.

● Points used in regression

⊙ Secondary wear rates observed with ester + antioxidant

oxygen determination and variations in the wear rate under similar conditions. It was observed that the wear rate was to some extent dependent on the previous history of the test. In subsequent test series (e.g. those with lubricant additives) the accuracy of oxygen determinations was much improved by analysing a greater number of samples, and the atmosphere was more tightly controlled. Thus it was found that a small number of tests was sufficient to define the relationship between wear rate and oxygen concentration. In all analysis, however, a scatter band similar to that indicated on fig. 4.7.3 is assumed.

4.8 Discussion

The observed wear rates vary from 0.25 μm/hour at oxygen concentrations of 0.17 millimoles/litre to 6 μm/hour at 5 millimoles/litre of oxygen. These values represent a rate of removal of a thickness of metal equal to 1.3×10^{-3} nm and 3×10^{-2} nm per cycle respectively. These are purely artificial figures as the size of wear particles generated in fretting processes has been reported to be in the range 0.1 - 10 μm.* The size of the wear particles from these tests was not determined (see chapter 9). It is considered that a few thousand cycles are required for the generation of a wear particle. The wear process is discussed in detail in section 4.10.6.

The gradient of the best line through the experimental points (fig. 4.7.3) is approximately 0.9. It follows therefore that the rate of wear is proportional to the oxygen concentration raised to the power 0.9.

---

* Reference 1 p. 82

$$\text{Rate of wear} \propto (O_2)^{0.9}$$

The value of the exponent might vary by ± 10% from this value. Such an equation is similar to a rate equation for a chemical reaction. If the value of the exponent is unity then the wear process could be said to be of "first order" with respect to oxygen.

Of the fretting mechanisms discussed in chapter 1 a first order dependence on oxygen concentration is compatible with

i A corrosive mechanism

ii A mechanism in which wear results from the removal of surface oxide layers by abrasion.

A first order mechanism is not compatible with a mechanism of fatigue alone and it conflicts directly with an adhesive mechanism.

Whilst the accuracy of the results is not sufficient as to be able to discriminate a gradient of 0.9 from 1.0 the observation of the lower value for the exponent may be explained in the following way.

If, as has been proposed, the metal is oxidised not by direct reaction with oxygen but with an oil oxidation intermediate (e.g. a peroxide) then the wear rate will depend not only on the oxygen concentration but also on the concentration of peroxide formers the R· radical.* These radicals are produced by two mechanisms:

i As a product of the oil oxidation propagation reaction - an oxygen dependent process.

---

* See section 4.4

ii From various initiation reactions which occur independently of oxygen.

Thus at low oxygen concentrations the peroxide forming radicals will be relatively more abundant and so the wear rate correspondingly higher than predicted from a linear extrapolation from the high oxygen wear rate back towards zero (fig. 4.8.1).

4.9 Wear Rates at Long Times

It was considered that there were two possible explanations for the drop in the wear rate after an initial period during which the wear increased linearly with time.

(a) The spline teeth were being worn to a shape where further wear occurred at a much lower rate. In other words, some form of running-in process takes place.

(b) Changes in the composition of the oil during the test led to it having better antiwear properties. Such changes could be the result of oil oxidation.

Both of these explanations are consistent with the observed characteristics of the drop in wear rate shown by a large number of tests. Namely that the drop occurred much earlier and was more marked in tests in an oxygen saturated oil (when wear was most rapid) than in air and in nitrogen.

On the basis of further tests the first explanation was discounted for the following reasons;

(1) The length of the initial wear period could not be correlated even very roughly with a critical value of wear. For instance under the high oxygen conditions of test E wear of 110 μm was recorded during the initial wear period (20 hours) whereas in test D under air-saturated conditions wear of only 65 μm occurred in the initial

Figure 4.8.1

Linear plot of wear rate against Oxygen activity.

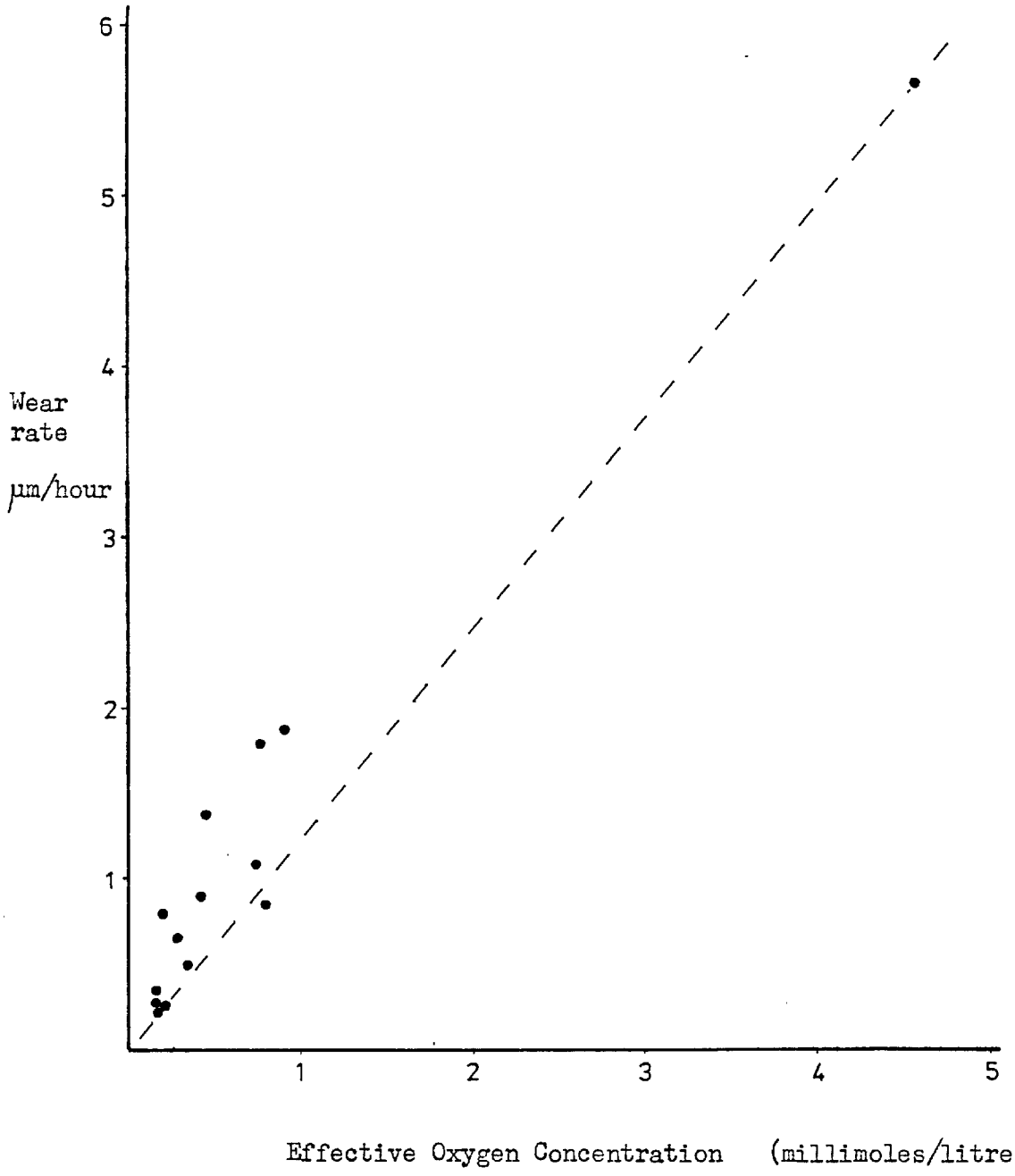

wear period of 57 hours.

(2) A test in the absence of a lubricant showed no decrease in wear rate even after wear in excess of 200 μm (fig. 4.9.1).

(3) A test was run in air until the secondary wear rate had been established. The rig was then disassembled, all components including the specimen cleaned and then reassembled. A fresh quantity of oil was used and the rig was restarted under an air atmosphere. For the first five hours there was little wear but thereafter wear occurred at a rate compatible with the measured oxygen activity (see fig. 4.9.2). This result indicates that the limiting wear observed in the previous test was due to a factor other than the attainment of a critical wear value.

The observation that oxidation of the oil as indicated by its discolouration was related to the length of the initial wear period lent credence to the second alternative. In air first signs of discolouration were observed after about ten hours. After twenty to forty hours the wear rates were observed to fall. It is known that organic acids such as might be formed as a result of oil oxidation are readily absorbed onto metal and oxide surfaces[90] and it was considered that they might have an antiwear action[6].

Accordingly an investigation of the oxidation of the lubricant in the fretting rig was undertaken. This work is described in chapters six and seven.

Figure 4.9.1

Wear graph of test run without lubricant.

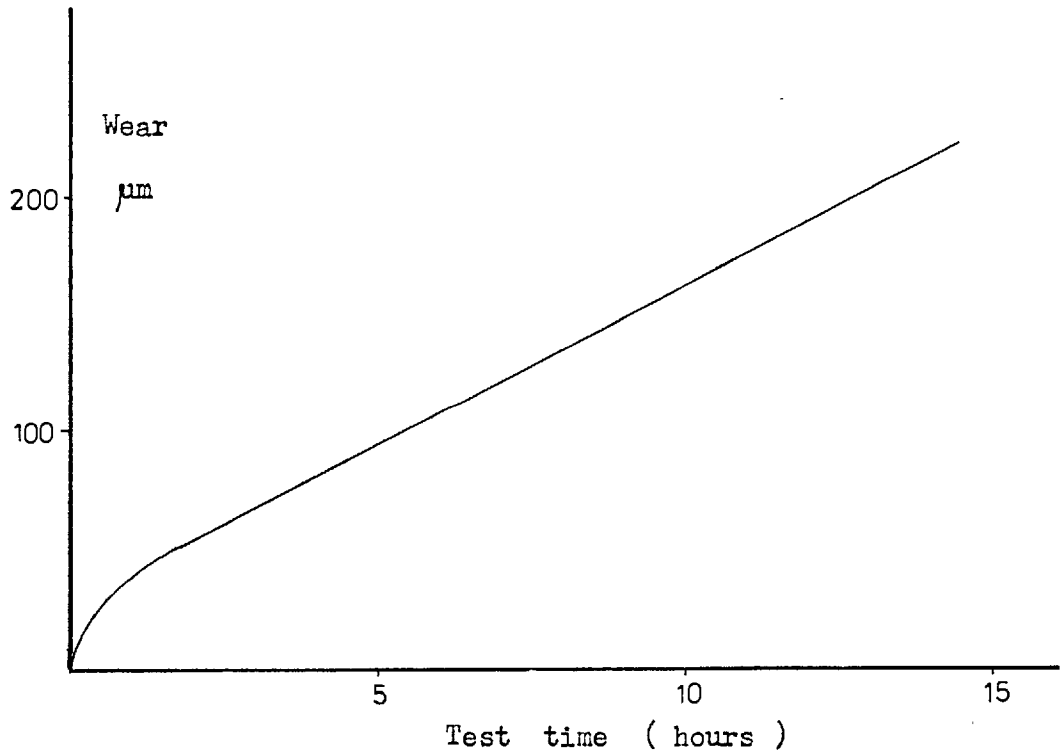

Figure 4.9.2

Results of successive tests with the same spline specimens but with a fresh quantity of lubricant.

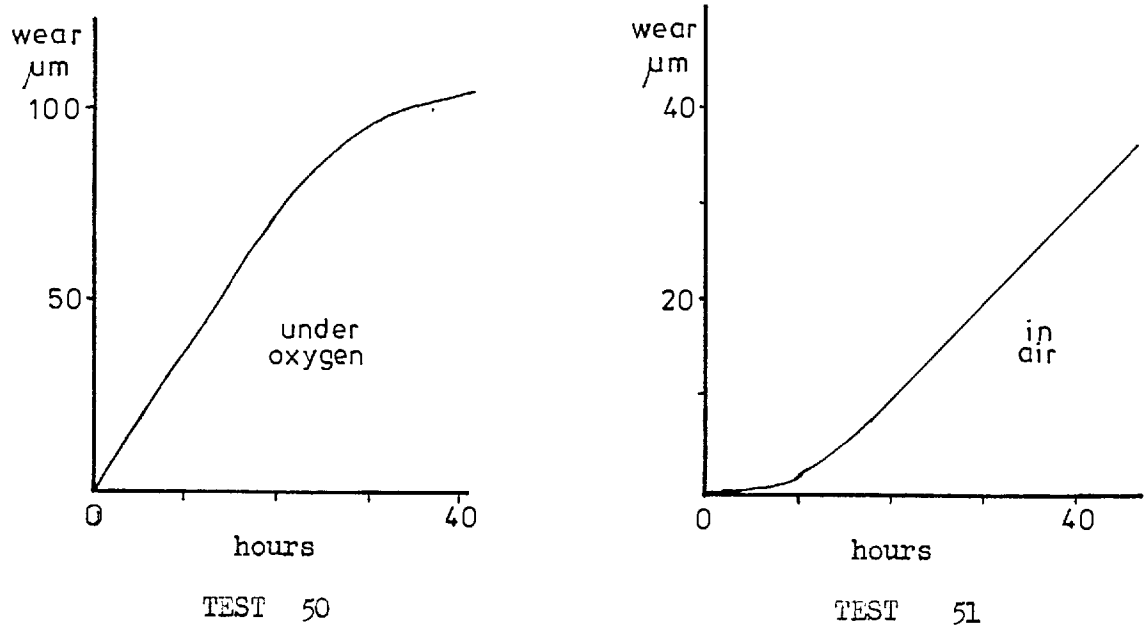

4.10 Examination of the Worn Surfaces

4.10.1 Introduction

The topography of the worn surface of the spline teeth tells a great deal about the mechanism of removal of material during fretting. The spline specimens used in each test were examined after removal from the rig under a binocular microscope. The appearance of the tooth surface shown in Plate 4.1 is typical. There are, however, obvious differences between an unworn, slightly worn and a severely worn surface. The spline teeth were formed by a broaching process which left characteristic markings running down the length of the tooth. Specimens which had suffered only slight wear had a burnished appearance in the central area, with roughened areas appearing at the tooth tips. Specimens which had worn at a high rate looked very rough but the broach marks appeared to be enhanced. This latter effect was also noted by Ku[12]. Specimens from tests in which the initially high wear rate had reduced by the end of the test to a low value still showed a rough surface.

Three other methods of surface examination were employed:

Scanning Electron Microscopy (S.E.M.)

Surface profile traces (Talysurf)

Sectioning and metallographic examination.

The talysurf traces were used to measure the peak to valley roughness of the wear scars. The centre-line average (c.l.a.) roughness output by the talysurf instrument is not considered meaningful because of the

Plate 4.1

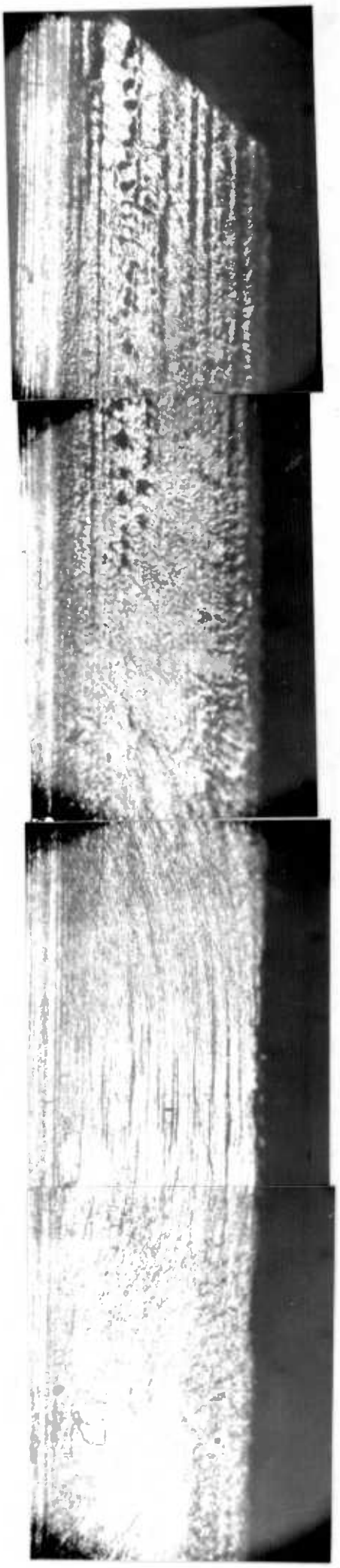

The worn surface
of a spline tooth
(photomicrograph)
Specimen 95, test G

anisotropy of the surface texture. Measurements could only be made along the length of the tooth. Metallographic examination of polished and etched sections of the spline teeth was undertaken in order to gauge the degree of work hardening of the surface layers.

The fine microstructure of EN36C made investigations of the subsurface region very difficult. To protect the surface during sectioning and polishing the splines were nickel plated. This appears in the photomicrographs as a white layer. Surface work hardening may be identified by a darker etching finer microstructure.

The development of fretting damage is illustrated in the following sections by specimens from tests in which wear was low (less than 10 mgms. weight loss), mild (less than 50 mgms. weight loss) and severe (greater than 50 mgms. weight loss). Table 4.4 is a key to the plates and figures in this section.

4.10.2 The Unworn Surface

Plate 4.2 is a S.E.M. picture of the surface of an unworn spline tooth. The horizontal lines are formed by the broaching tool. It is also evident that the broaching action causes transverse cracking shown in plate 4.3 and the formation of large surface pits. The splines were used as supplied, i.e. no surface treatment was performed after the broaching action. As a consequence a small degree of fretting damage is hard to differentiate from the broaching process.

Plate 4.4 is a transverse section through an unworn

Table 4.4 A Key to the Figures and Plates of Section 4.10

Specimen Number	Test Code	Lubricant	Additive	Average O_2 Concentration Mmoles/litre	Weight loss (female spline) mgms.	Method of Examination			Remarks
						S.E.M.	Talysurf	Sectioning	
77	-	H	-	0.35	1.4			Plate 8	
96	W	E	ZDDC	1.1	4	Plates 4,5,6	4.10.2		LOW WEAR
53	B	E	-	0.2	9		4.10.2		
75	C	E	-	0.29	12	Plates 9,10, 11			Plate 1 MILD WEAR
95	G	H	-	1.55	44		4.10.4		
54	-	E	-	0.78	59		4.10.6		

Table 4.4 A Key to the Figures and Plates of Section 4.10 (continued)

Specimen Number	Test Code	Lubricant	Additive	Average O_2 Concentration Mmoles/litre	Weight loss (female spline) mgms.	Method of Examination			Remarks
						S.E.M.	Talysurf	Sectioning	
67	U	E	P∝N	2.7 4.4	77	Plates 12, 13			
76	X	E	ZDDC	4.6	128	Plate 14		Plate 15	SEVERE WEAR
63	-	E	-		246		4.10.6		
93	N	H	L.A.	5.0	270		4.10.6		

E = Ester
H = Hexadecane
ZDDC = Zinc di-ethyl-dithiocarbanate
P∝N = Phenyl∝naphthylamine
L.A. = Lauric Acid

Plate 4.2

x 410

S.E.M. view showing surface flaws left by broaching.

Plate 4.3

x 1500

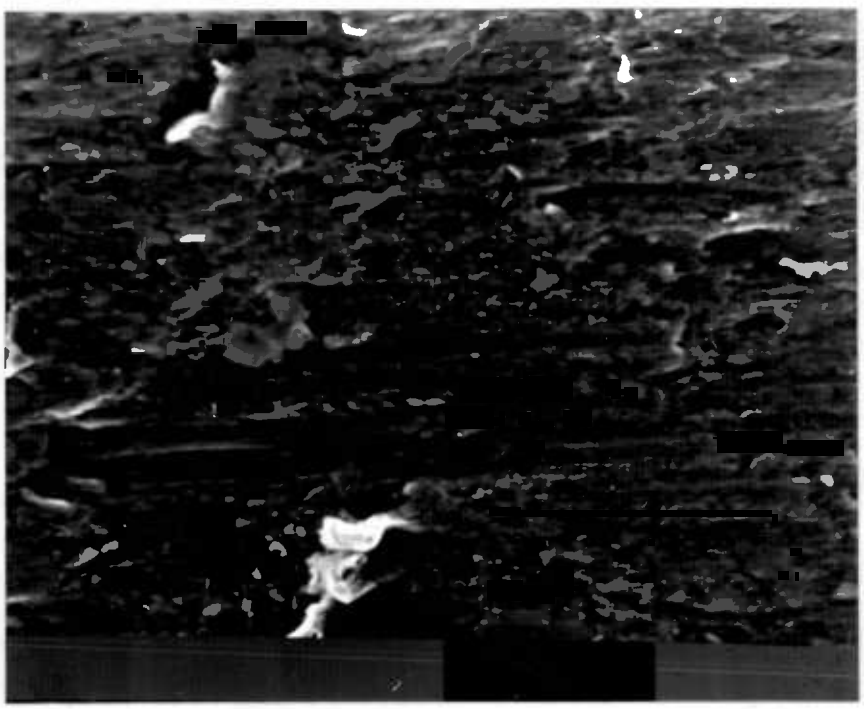

A higher magnification S.E.M. view.

THE UNWORN SURFACE

Plate 4.4

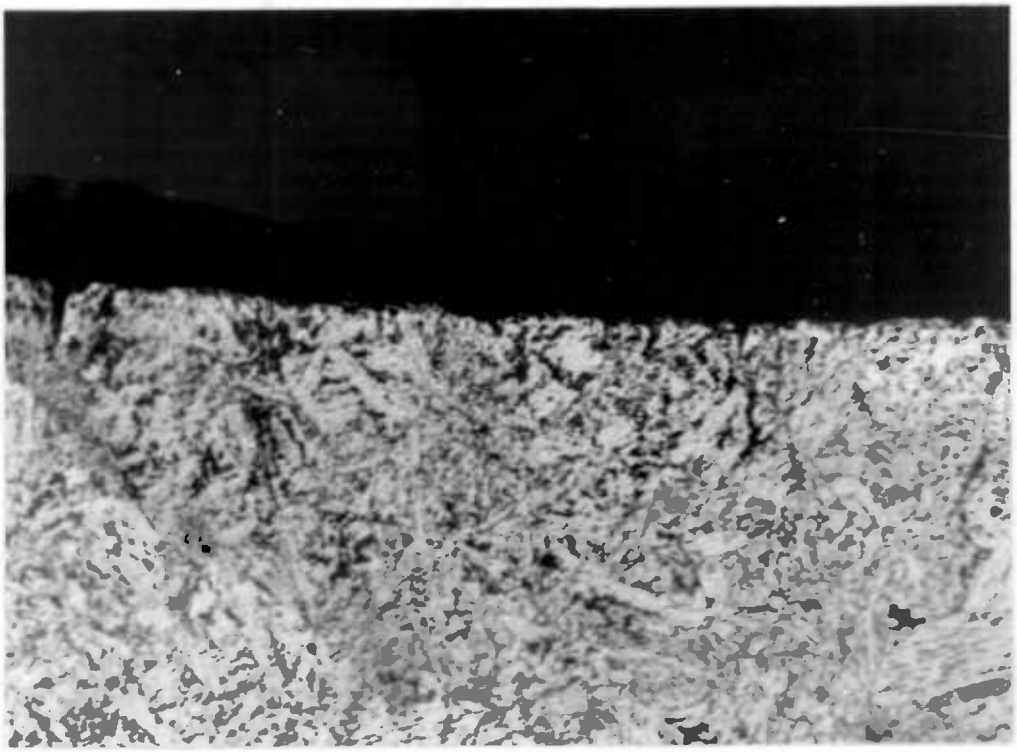

Transverse section through an unworn surface.(x 235)

Figure 4.10.1

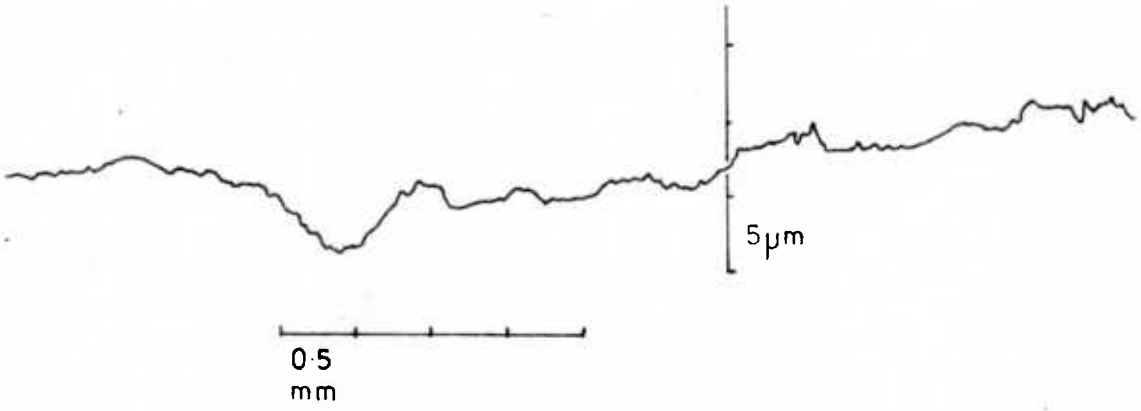

Talysurf trace from an unworn tooth.

spline tooth, showing that there is no change in microstructure of the surface layers.

The talysurf trace shown in fig. 4.10.1 illustrates that there is very little high frequency roughness on an unworn tooth.

4.10.3 Low Wear

In contrast, in the talysurf traces of low wear specimens a high frequency component is present (fig. 4.10.2). Wear in these specimens was restricted to the tips and the top edge of the spline teeth (of the male specimen) as shown in fig. 4.10.3. Wear starts in these regions because they are the areas on which the contact load is carried initially. The gyratory motion of the spline transfers the load cyclically from one end of the tooth to the other.

Plate 4.5 shows that fretting wear is just beginning to obliterate the broaching marks. The damage appears to be caused by adhesive smearing of the surface layers. However, on another tooth of the same specimen, wear is more advanced (plate 4.6). Embedded debris particles can be seen to have gouged out the surface. Plate 4.7 taken near the centre of the tooth (see fig. 4.10.3) shows a likely source of debris particles - the shear lips left by the broaching.

Plate 4.8 is a longitudinal taper section which magnifies the surface roughness about five times. The microstructure of the surface layers is slightly finer than the bulk indicating work hardening at the surface.

4.10.4 Mild Wear

Plate 4.9 is a S.E.M. picture of a tooth that has

LOW WEAR

Figure 4.10.2

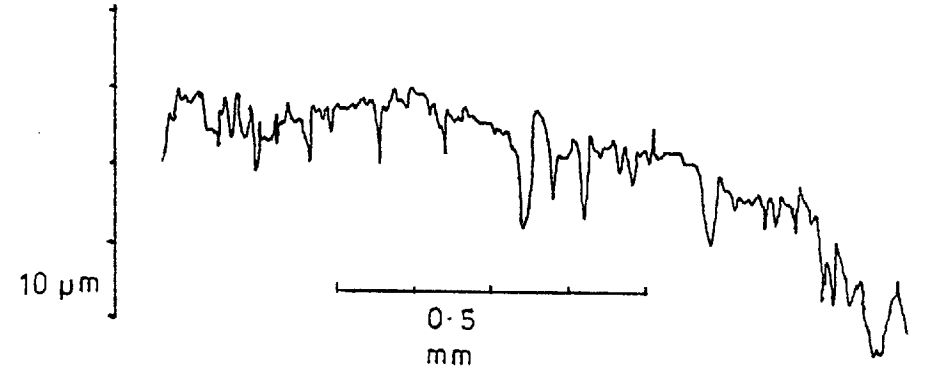

(a) Test B

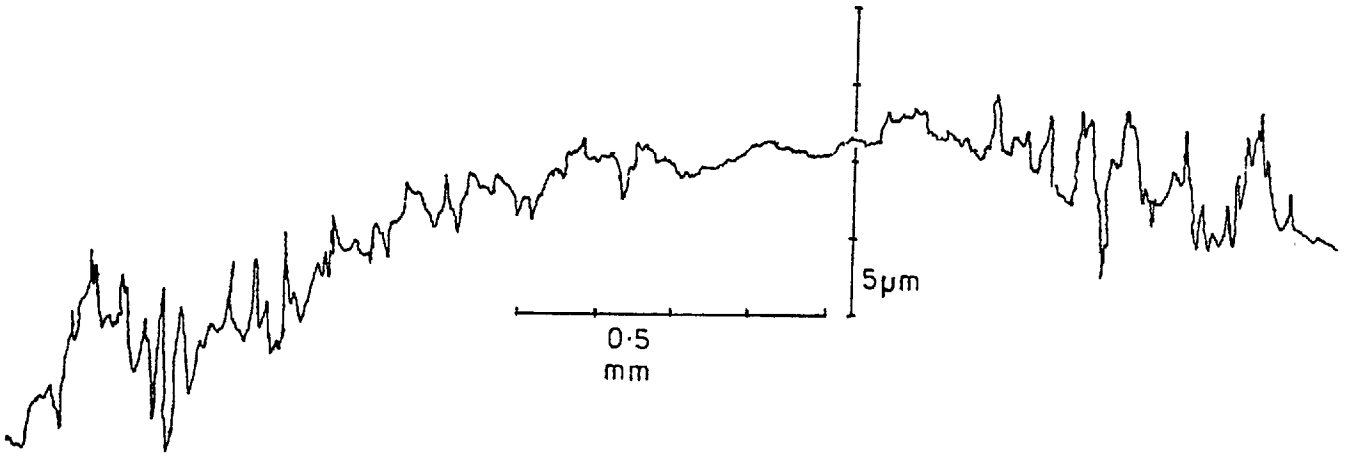

(b) Test W

Talysurf traces from low wear specimens.

Figure 4.10.3

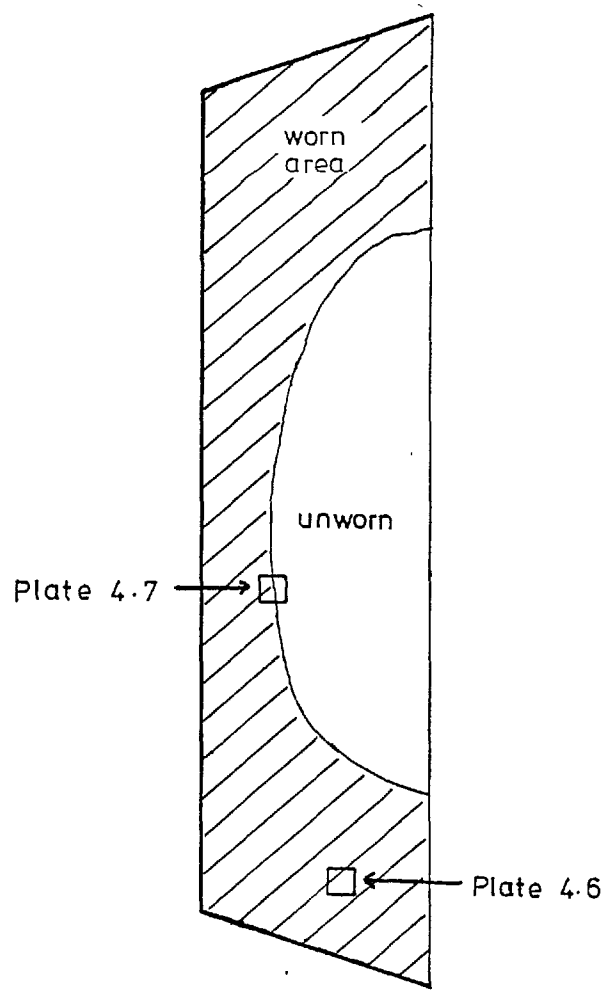

Diagram (not to scale) of a low wear specimen.

Plate 4.5

x 390

S.E.M. view. The early stages of wear.

Plate 4.6

x 75

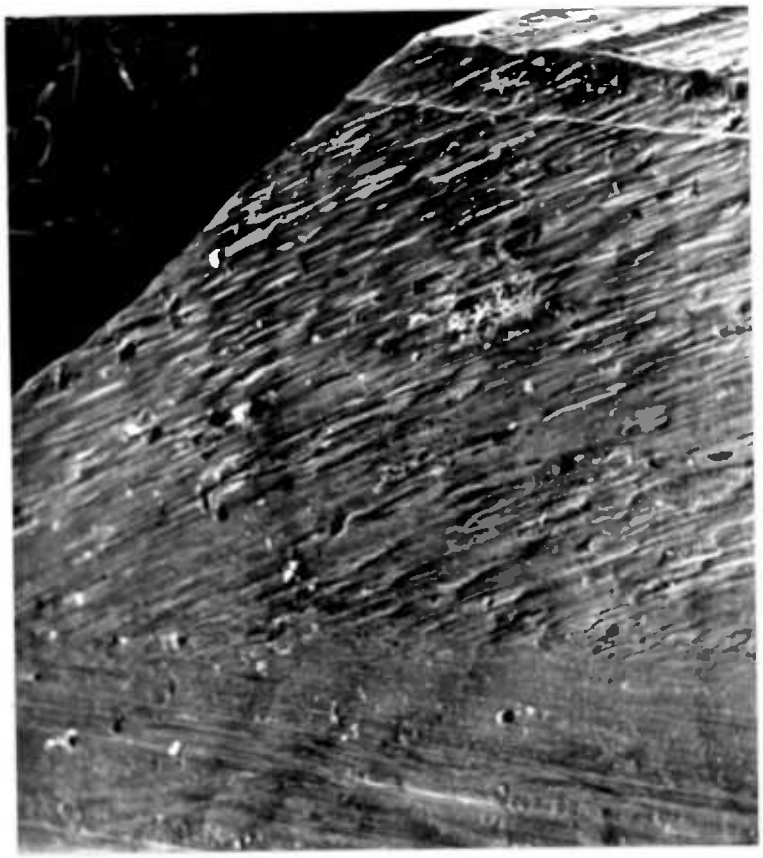

S.E.M. view of spline tooth tip.

Plate 4.7

x 178

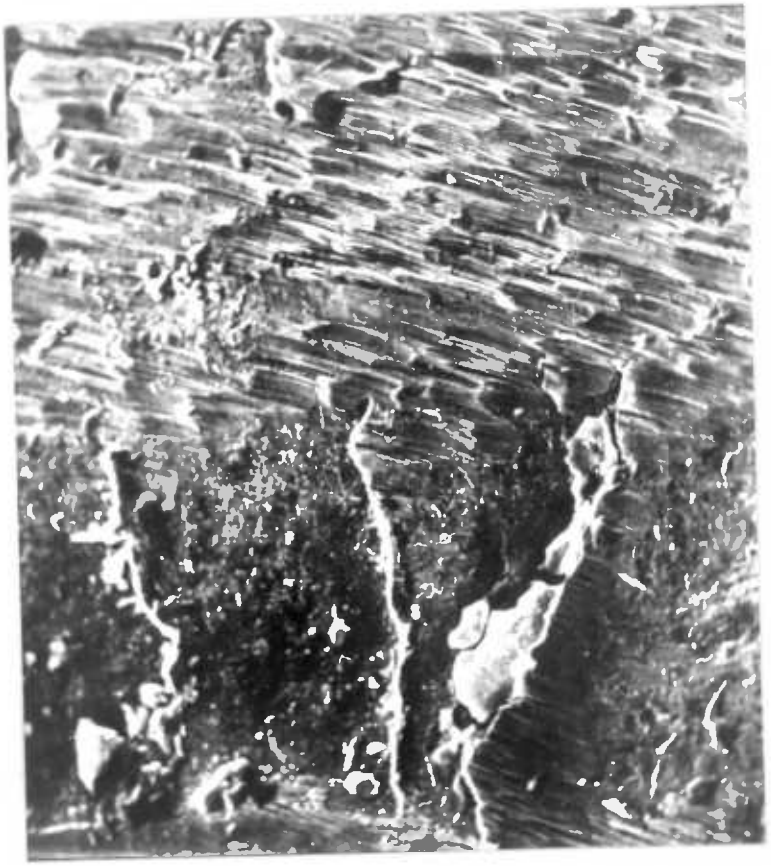

S.E.M. The border between worn and unworn area.

Plate 4.8

x 940

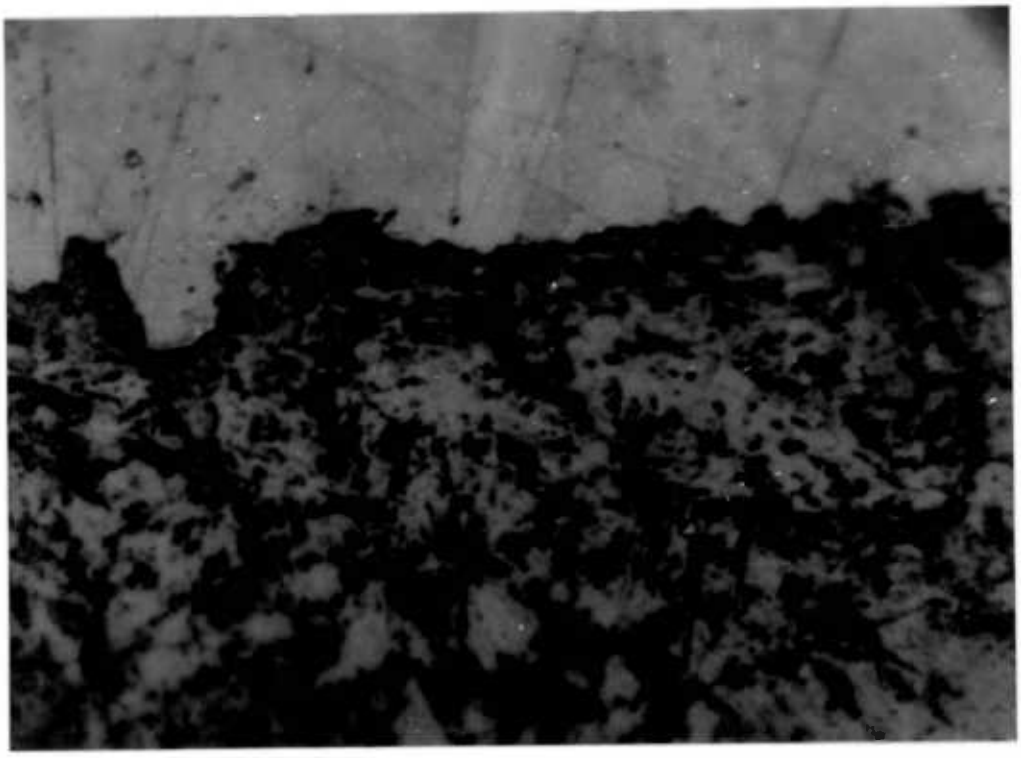

A longitudinal taper section near the tooth tip. Angle of taper : 12°

undergone mild wear. The scoring of the surface has spread over the whole surface of the tooth. In plate 4.10 the fretted surface is shown enlarged 600 times. Wear was greatest at the tooth tips as the broaching marks here are obliterated while in the centre of the tooth the surface cracking caused by the broaching is still evident (Plate 4.11). It is fairly certain that these cracks arise from the broaching process (rather than as a result of fretting) since the "lip" was always found to point towards the spline shank.

Fig. 4.10.4, a Talysurf trace from a mild wear specimen, shows that the tooth tips have worn more than the centre. The roughness is of a longer "wavelength" in the middle of the tooth because the Talysurf stylus is tracking parallel to the grooving marks in this region whereas at the tips the stylus is tracing across the "grain" of the roughness.

4.10.5 Severe Wear

Under conditions of severe wear a characteristic surface structure is developed as shown in Plate 4.12 which covers the whole contact surface. This scale-like structure is shown in more detail in Plate 4.13 and viewed at an oblique angle in Plate 4.14. Each "scale" is a shallow depression with smooth scoring marks running in the direction of oscillatory motion.

Abrasion by debris trapped in the contact is thought to give rise to this structure in the manner proposed by Feng and Rightmire[45] (fig. 4.10.5). Hollows are formed packed with debris which eventually escapes into adjacent

MILD WEAR

Plate 4.9

x 60

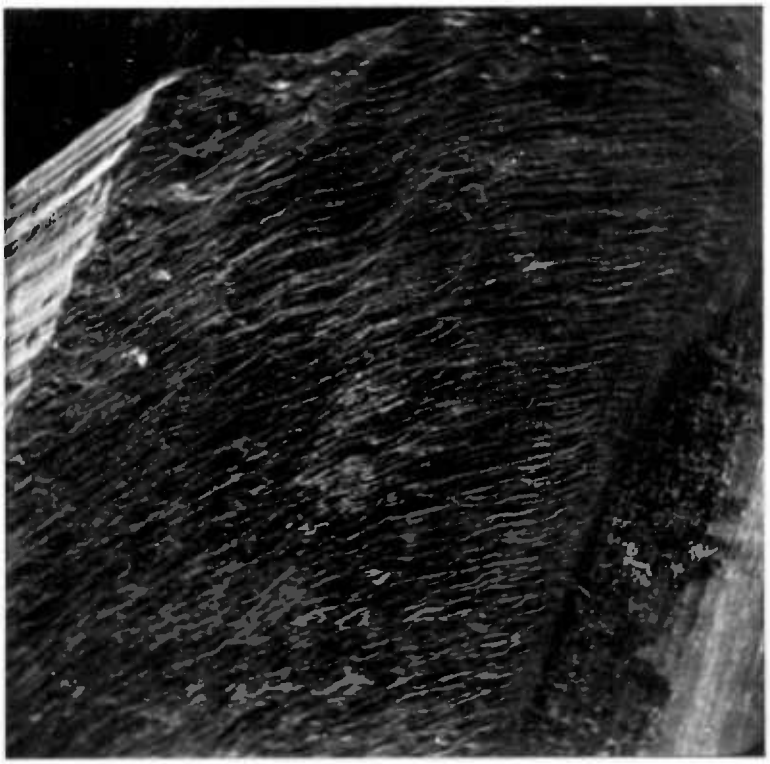

S.E.M. view of spline tooth tip.

Plate 4.10

x 600

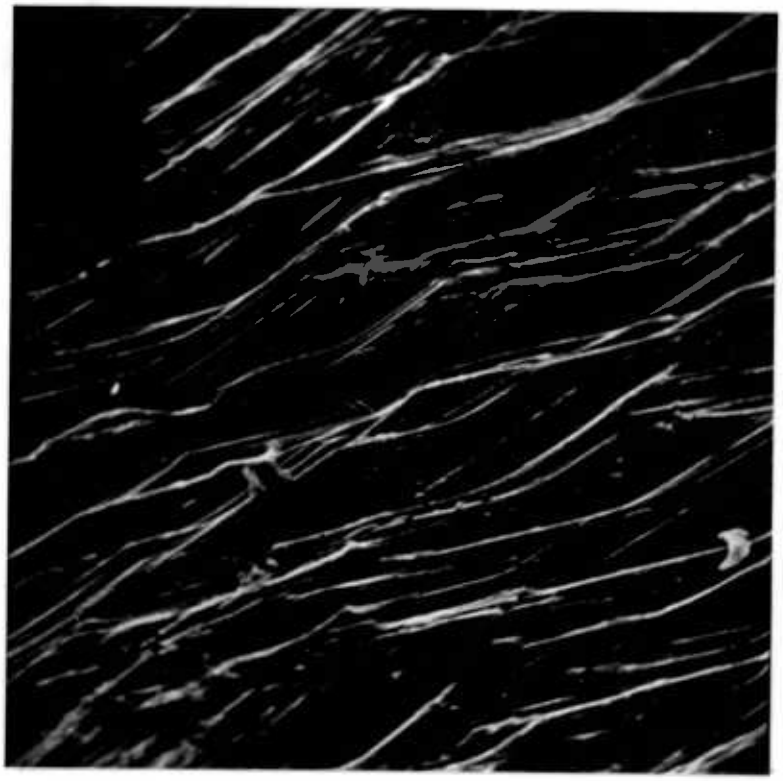

A higher magnification of the area shown in 4.9.

Plate 4.11

x 330

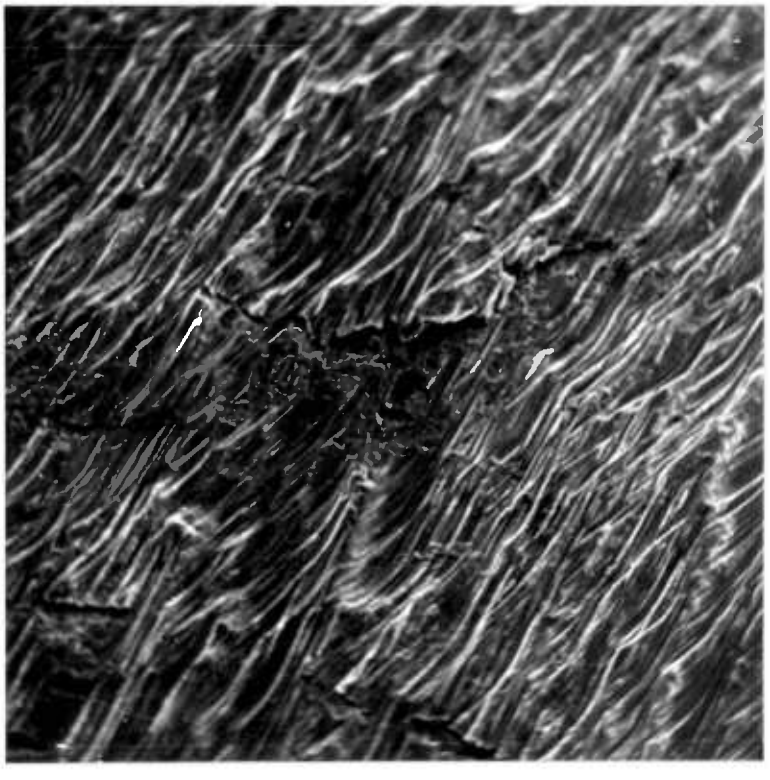

S.E.M. view of the worn surface in the central region of the tooth. Note that the broaching flaws are still evident.

MILD WEAR

Figure 4.10.4

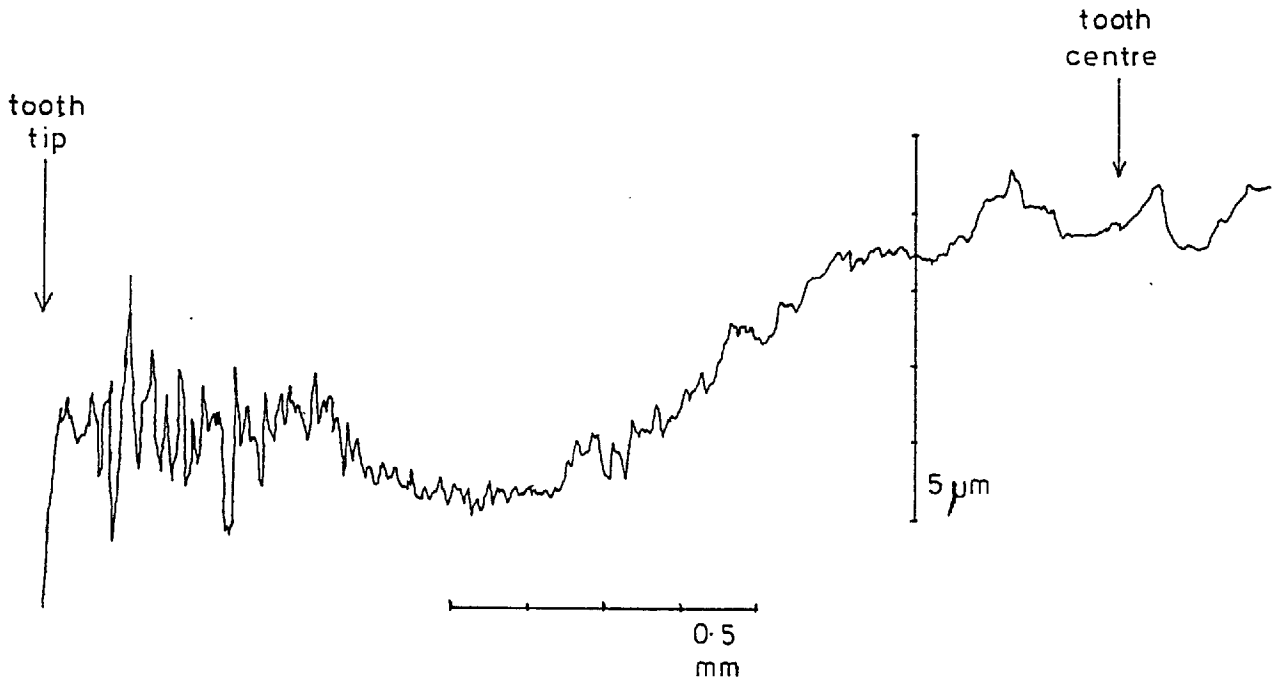

Talysurf trace of spline from test G.

Plate 4.12

x 70

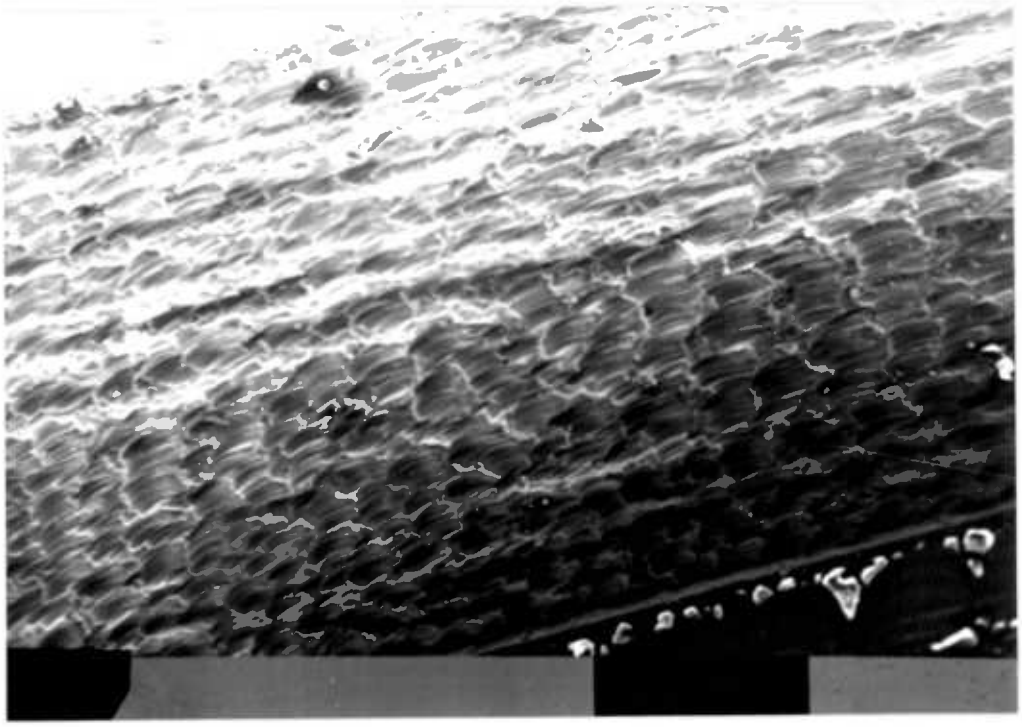

The characteristic appearance of a severely worn specimen.

Plate 4.13

x 300

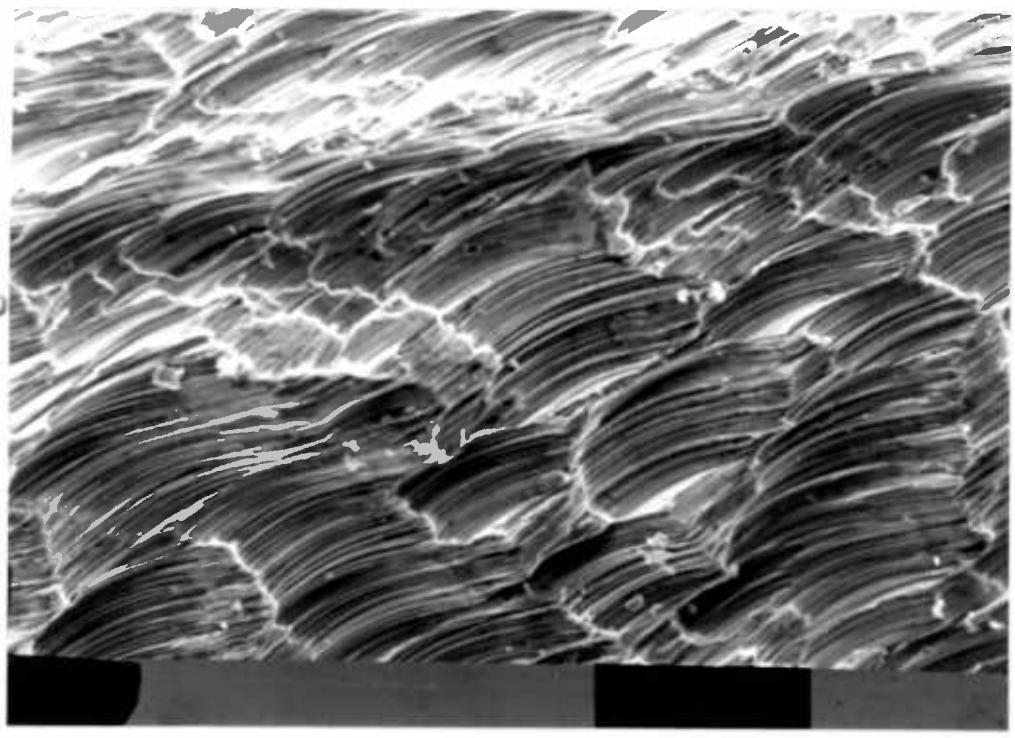

Detail of the surface structure. Note the longitudinal trough at the top of the frame.

SEVERE WEAR

Plate 4.14

x 600

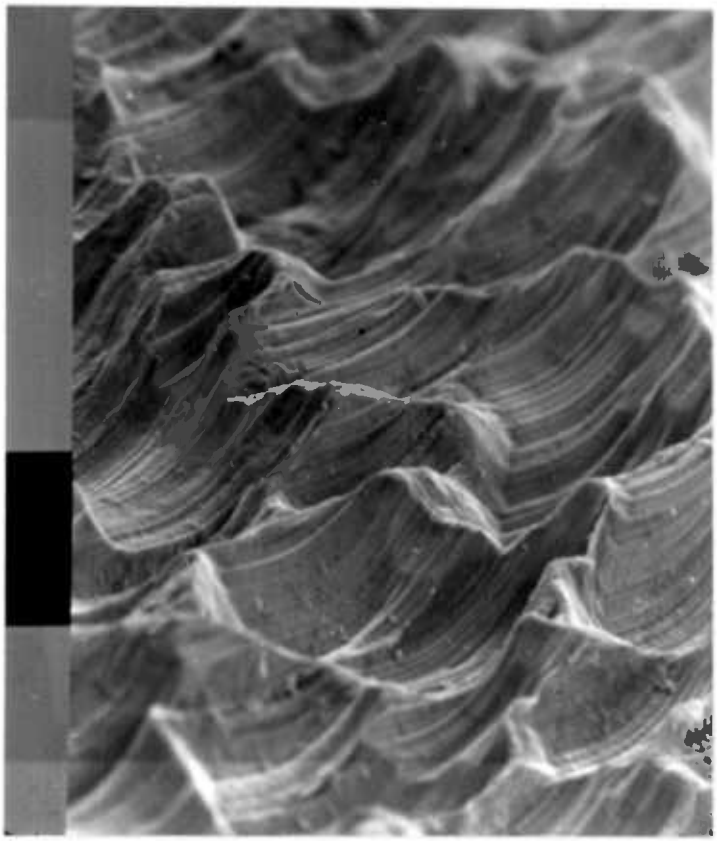

An oblique view of the surface near the tooth tip.

Plate 4.15

x 235

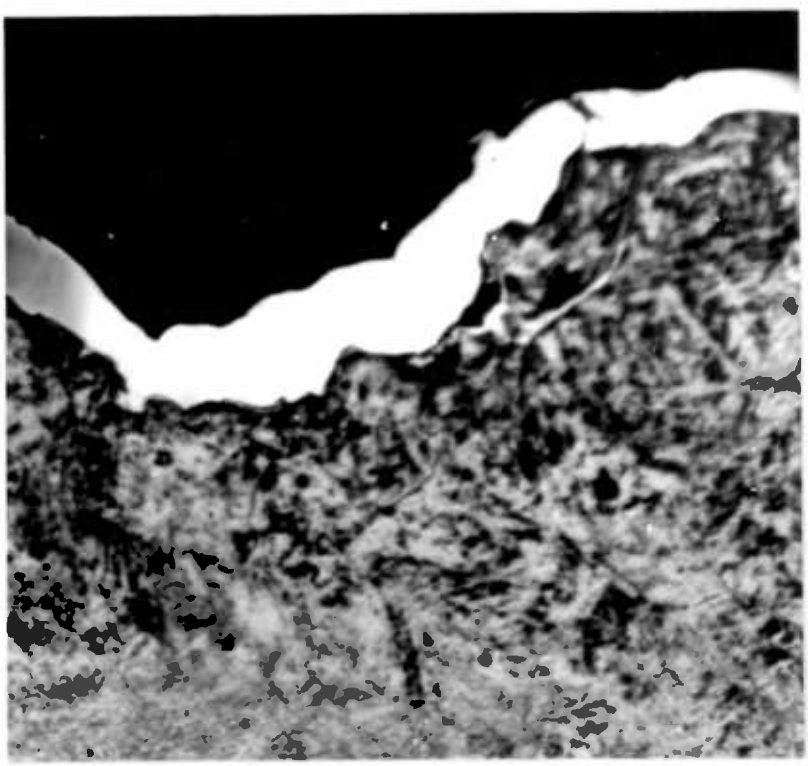

Transverse section through worn surface.

Figure 4.10.5 after Feng and Rightmire, ref. 45.

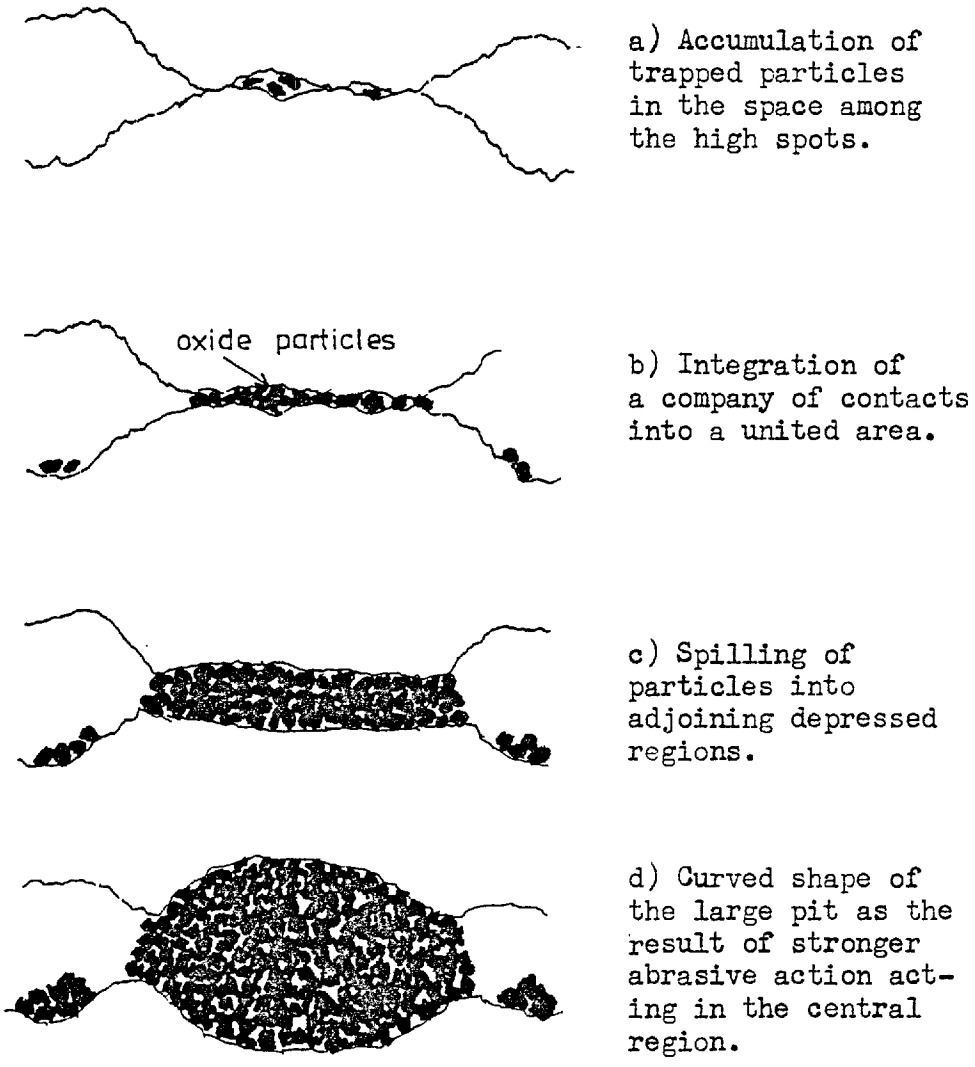

Schematic representation of initiation and spreading of fretting damage.

hollows. Debris generated within the contact will be forced towards the edges of the contact (from right to left in Plate 4.14). It is interesting to note that the "wavelength" of the scale pattern is approximately 100 μm i.e. about the same magnitude as the amplitude of the fretting motion.

The Talysurf traces are illustrated in fig. 4.10.6. Trace(b) shows that the centre of the tooth has again worn to a lesser extent than the tooth tips. This trace was of a tooth on the male spline specimen. However, a trace of the corresponding female spline tooth shows greater wear in the central region and the surfaces conform to each other (fig. 4.10.7).

Plate 4.15 is a transverse section through a spline tooth. The section was not cut on a taper so that the roughness is not accentuated. It can be seen that although the surface has been severely worn the microstructure at the surface is not different from the bulk, indicating that little work hardening has taken place.

4.10.6 Conclusions from Surface Studies

It is considered that the surface topography generated during severe fretting can only arise from a mechanism of abrasion by the debris - the scale-like structure being developed as a result of the reciprocating motion. The debris produced in these tests was composed mainly of haemetite (Fe_2O_3) which is hard and abrasive (see Chapter 9). Wear should be greatest in areas where the debris accumulates. This is thought to be the reason for the accentuation of the original broaching marks as is seen near the tooth tips in Plate 4.1 and also very

SEVERE WEAR

Figure 4.10.6

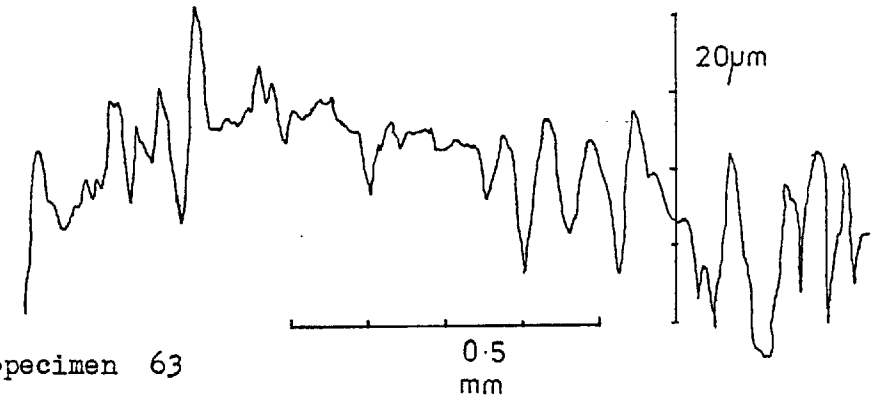

(a) Specimen 63

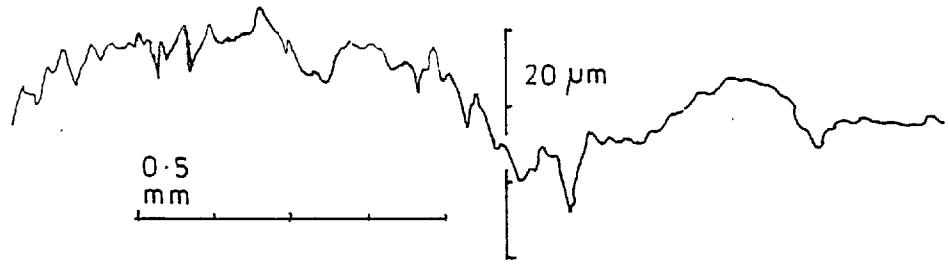

(b) Specimen 93

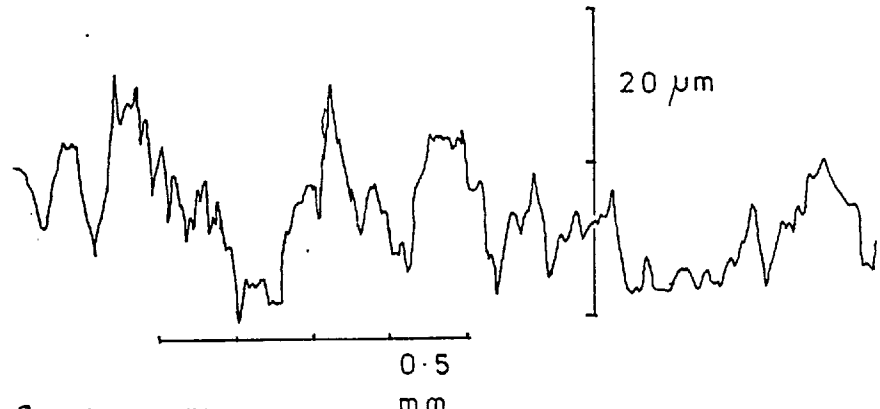

(c) Specimen 54

Talysurf traces of high wear spline specimens.

Figure 4.10.7

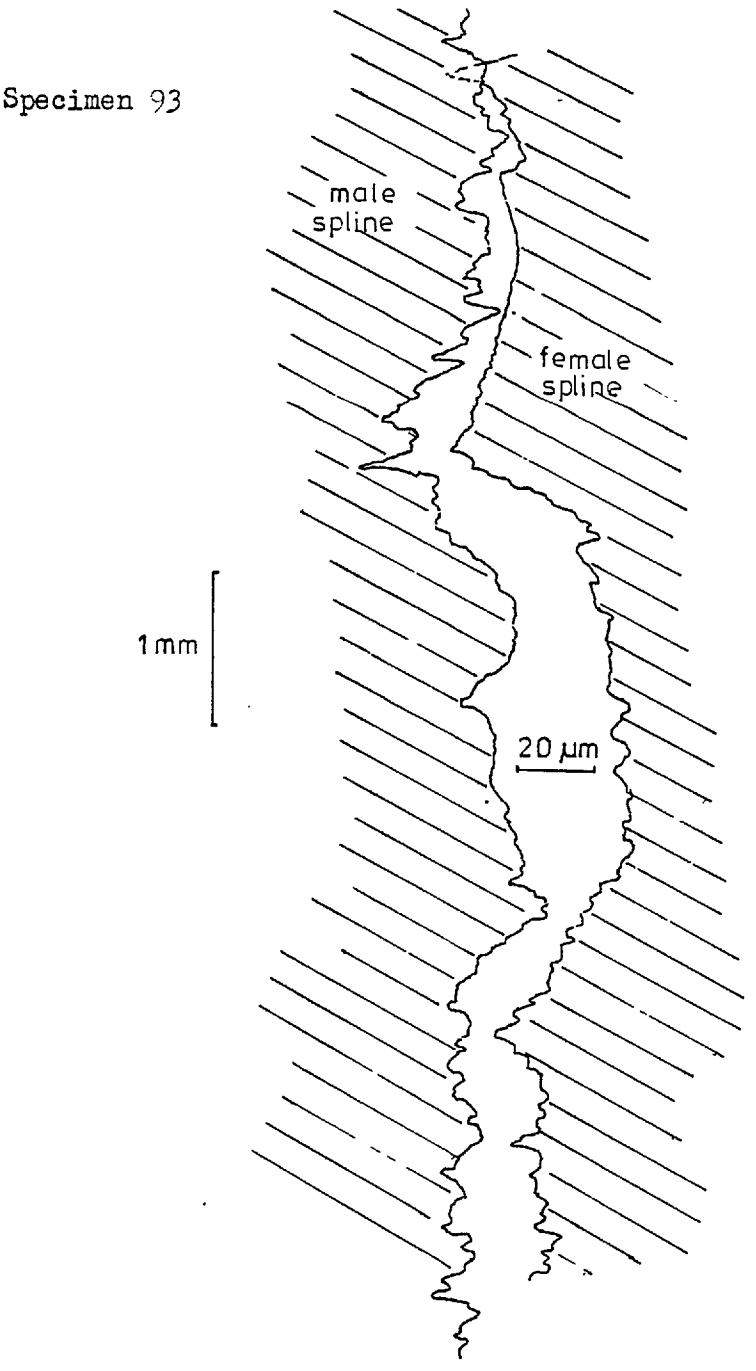

Two Talysurf traces illustrating the degree of conformation of the contacting surfaces.

N.B. The magnification across the page is 25x that vertically.

clearly in Plate 4.12. It is proposed that the debris, escaping from the contact, flows along these shallow grooves towards the tooth tips (fig. 4.10.8). In the course of its passage the debris wears away the channel - greatest wear occurring in the bottom of the channel.

The beginnings of this scale-like structure were evident on specimens which had undergone mild wear. In the low wear specimens there was little sign of wear mechanisms other than abrasion. Metallographic examination did not reveal any subsurface cracking - as evidence of abrasive or delamination wear.

It is therefore concluded that in the early stages the wear mechanism is one of mutual abrasion by the opposing surfaces. One of the initial sources of wear debris are the flaws left by the broaching process (Plate 4.7). The debris passes out of the contact along the grooves left by the broaching process. There is therefore an increasing accumulation of debris towards the tips of the teeth. A "three body" abrasive process (i.e. abrasion of the tooth surfaces by the debris trapped between them) will predominate where there is a large accumulation of debris giving rise to severe wear. There is therefore a transition from two body abrasion at the tooth centre to three body abrasion at the periphery. This is shown clearly in Plate 4.1. This situation is analogous to that modelled by Godet[91] with chalk on glass (reviewed in section 1.3.5) where a transition was observed when a critical quantity of debris had accumulated.

It is proposed that as conditions are made

Figure 4.10.8

Illustration of the direction of flow of debris from the contact.

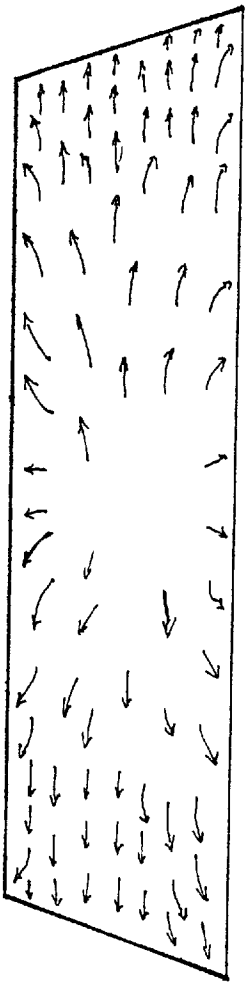

increasingly arduous (e.g. the activity of oxygen in the oil is increased) a greater quantity of debris is produced so that the boundary between the two regimes moves inwards. Under the severest conditions the whole of the surface is being worn by debris abrasion.

4.11 Conclusions

The spline fretting tests with an ester base stock gave similar results to those obtained by Ku et al. using a mineral oil. The test conditions employed by Ku were not duplicated in detail but a comparison of results indicates that wear is reduced in the ester lubricant.

The spline fretting rig was used to study the effect of atmosphere on lubricated fretting wear - the oxygen content of the oil being regularly monitored. This novel technique showed that the initial wear rate was related to the activity of the dissolved oxygen. It is concluded that under a normal air atmosphere oxidative wear is the major factor in fretting.

It was observed that wear rates at long test times fell to values below the initial wear rate. It was considered that this fall in rate was the result of the appearance in the lubricant of oil oxidation products.

Studies of the fretted surfaces of specimens from a variety of tests have been described.

It is concluded from these studies that wear is by mutual abrasion of the contacting surfaces, resulting in a low rate of wear, or by abrasion by the debris. At intermediate wear rates the two regimes coexist - the overall wear rate being the combined material removal of the two mechanisms.

Chapter 5. Fretting tests in Hexadecane

5.1 Introduction

The previous chapter described fretting wear tests that were performed in an ester lubricant. This chapter presents the results from a similar series of tests in which hexadecane was used as the lubricant.

Hexadecane has frequently been used as a model lubricant in tribology. As a "simple" lubricant for the fretting wear tester it had a number of advantages over the ester base stock:

(1) It was an advantage to use a lubricant of known composition.

(2) Much research had been undertaken in the Lubrication Laboratory of Imperial College into the lubricating properties of hexadecane, notably the work of Spikes[67] and Stinton[68]. Hence techniques for purification of the lubricant were well established.

(3) Purified hexadecane does not act as a boundary lubricant as it is non-polar.

(4) The effect of oxidation of hexadecane on sliding wear had been investigated by Stinton.

(5) In theory identification of oxidation products in hexadecane should be easier than in the ester.

The series of tests with hexadecane was undertaken to clarify the effect on fretting of lubricant oxidation. The results presented in this chapter show that the wear varies with test time in a similar way to the ester. In a following chapter (chapter 7) the results of oxidation studies of both lubricants are presented. They show that the behaviour of the two lubricants in detail is different.

5.2 The Oxidation of Hexadecane

n-Hexadecane ($C_{16}H_{34}$) is an unbranched straight chain alkane. Stinton[68] has shown that purified hexadecane is resistant to oxidation. A sample heated for three days showed little increase in impurities. However, when used to lubricate wearing metals these latter catalyse oxidation with the generation of the following types of product of varying molecular weights:

Carboxylic acids

Alcohols

Esters

Ketones

Di-acids and di-alcohols

Stinton found that the oxidised hexadecane produced lower friction in the 4-ball machine but higher rates of wear, indicating attack of the wearing surfaces. By adding small concentrations of pure compounds of each of the above types (choosing those chemicals likely to be formed by hexadecane degradation) he tested the effect of each active group in isolation. The order of activity (i.e. effectiveness in reducing friction) was found to be acid > alcohol > ketone > ester - those molecules with two functional groups were found to be more active than those with a single group.

Initially, hexadecane is quite stable to oxidation. In common with many aliphatics such as the ester described in the previous chapter oxidation proceeds by a free-radical reaction which once initiated continues at an appreciable rate. The reaction scheme is shown in figure 4.4.1. In the rig the hexadecane is exposed to a variety of metals which act as catalysts for these reactions,

notably copper (in the piping) and nascent steel at the wearing surface. The presence of these metals increases the chance of free radical generation and so tends to shorten the "induction period". However, the metals are unlikely to have affected the oxidation products formed.

5.3 Purification Procedure for Hexadecane

Puriss grade hexadecane was obtained from Koch-Light Laboratories Ltd. Spikes[67] has shown that in this condition there are still significant quantities of impurities present. There is a marked difference in surface tension (with respect to water) between this grade and the literature value for pure hexadecane. In order to avoid the possible effects of such impurities the hexadecane was purified by the technique, due to Spikes, described below. Any further purification (such as recrystallisation [68]) was considered unnecessary as contamination by impurities from the rig was a more significant problem than any residual impurities.

The hexadecane was shaken with activated alumina and activated silica gel in a brown glass bottle for 48 hours, by which time any odour had disappeared. The mixture was left to stand for at least two weeks before use. When required the hexadecane was filtered through an activated silica gel column and then pumped through a sintered glass filter to remove solids.

The glassware used in this filtration procedure had been previously cleaned with concentrated nitric acid and ethyl alcohol to give a hydrophilic surface. It was then washed in distilled water and dried. The efficiency of this purification procedure was demonstrated by Spikes who made measurements of the surface tension of hexadecane and obtained a value in close agreement with previous determinations.

5.4 Experimental

A series of tests was performed over a range of oxygen activities. The rig was set up and when required

deaeration of the lubricant was carried out as previously described in chapter four. Two problems were experienced when using hexadecane. Firstly, it caused the silicon rubber tube in the peristaltic pump to swell and become fragile. Since the pump requires that this pipe be stretched fairly tightly round a 3-pointed rotor there was a decrease in pumping efficiency of a new tube as it swelled and lengthened. It was found that shortening the tube by about $^1/_4$" restored pumping to the correct rate.

Secondly, the lower viscosity and higher volatility of hexadecane resulted in a greater lubricant loss through leakage and evaporation during the course of a test. Small quantities of hexadecane were therefore added from time to time to maintain the level.

5.5 Results and Discussion - General Remarks

Before the results of the fretting tests with hexadecane are presented a remark will be made concerning the lubricant viscosity. A factor which has to be considered when comparing results of tests using hexadecane with those of the ester, is the lower viscosity of hexadecane at the test temperature. For instance in hexadecane a higher wear than in ester was obtained under the same atmospheric conditions. The explanation for this is unlikely to be due to a thinner lubricant film separating the teeth as calculations show that any hydrodynamic component is very small and operation of the rig is well within the boundary regime (see section 2.5.2). It was also noted that under similar conditions of bubbling the measured oxygen content was always greater for hexadecane than for ester. This was due either to greater

absorption of oxygen from the bubbled gas leading to a higher activity of oxygen in solution or it was because the lower viscosity of the hexadecane gave a higher measured activity for the same actual activity by reducing the concentration gradient at the oxygen cell membrane as was discussed in section 3.32. A measurement of the gas content using a gas extraction apparatus would resolve these alternatives although the observation that nitrogen bubbling of hexadecane failed to produce as low oxygen activities as those measured for ester indicates that it is an anomaly due to measurement. In any event the important point is that the supply of oxygen to any interface, be it the membrane in the oxygen cell or the wearing area of fretting splines is greater in hexadecane than in ester. This would explain the higher wear rates observed.

Another observed difference between lubrication of hexadecane and the dibasic ester was the nature of the debris produced. A test run with ester at a high oxygen concentration produced little solid debris compared to a hexadecane test. There was very little debris carried round in suspension in the oil. The ester was found to discolour more rapidly than the hexadecane. Any debris that was deposited was black and proved difficult to prepare for x-ray diffraction analysis as it was tarry. On the other hand, debris produced in the hexadecane tests could be observed in suspension in the oil. It was reddy-brown in colour - the colour of rust. When prepared for XRD analysis by washing in toluene and acetone the solvent would evaporate to leave a dry fine brown powder.

It would appear that the debris produced is strongly combined by the ester and held in solution in the oil whilst the debris remains insoluble in hexadecane. It will be shown in Chapter 7 that the suspended debris plays an important role in reducing the acid content of the oil exposed to oxidising conditions.

5.6 Results and Discussion - Initial Wear Rates

Wear tests in hexadecane were performed under the same standard conditions as tests in ester. These were:

Bulk oil temperature 80°C

Load 14lbs wgt. applied ≡ 15 MN m^{-2}

Misalignment 0.34° ≡ maximum displacement of 150 μm

Frequency 54.2 Hz

Material EN 36C untreated V.H.N. = 232

Gas supply H_2SO_4 dried

Tests were performed under different atmospheres: nitrogen, air and oxygen to give a range of oxygen partial pressures. The results of these tests are tabulated in table 5·1 The trend was similar to the ester tests in that the wear increased linearly with time initially. Again the departure from linearity occurred earlier for tests at high oxygen concentrations. Figure 5.6.1 shows a log-log plot of the initial wear rate against the measured oxygen activity. The dashed line shows the relation obtained for the ester lubricant (replotted from fig. 4.7.3). The wear graphs of these tests are shown in figure 5.6.2. As with results for ester a 'good' straight line may be drawn through these points. The gradient of this line (1.25) is significantly different to that for the ester and that of a linear relationship between wear and oxygen concentration (gradient = 1). This suggests

TABLE 5.1

Test code	Test time Hours	Oxygen conc^{n}. mmoles/litre	Number of determin^{ns}.	Wear rate μm / hour
F	0 - 10	0.48	7	1.0
	10- 40	1.2	7	1.7
G	0 - 6	1.55	12	2.95
	6 - 30	1.63	12	decreasing
	30 - 80	1.5	21	0.55
H	0 - 6	decreasing	2	decreasing
	8 - 23	0.4	4	0.55
I	0 - 6	3.2	9	14.4
	6 - 8	4.3	2	1.6
J	0 - 13	6.0	17	14
	13 - 20		-	decreasing
	20 - 27	5.6	9	1.7

A summary of the results of fretting tests in Hexadecane.

Figure 5.6.1

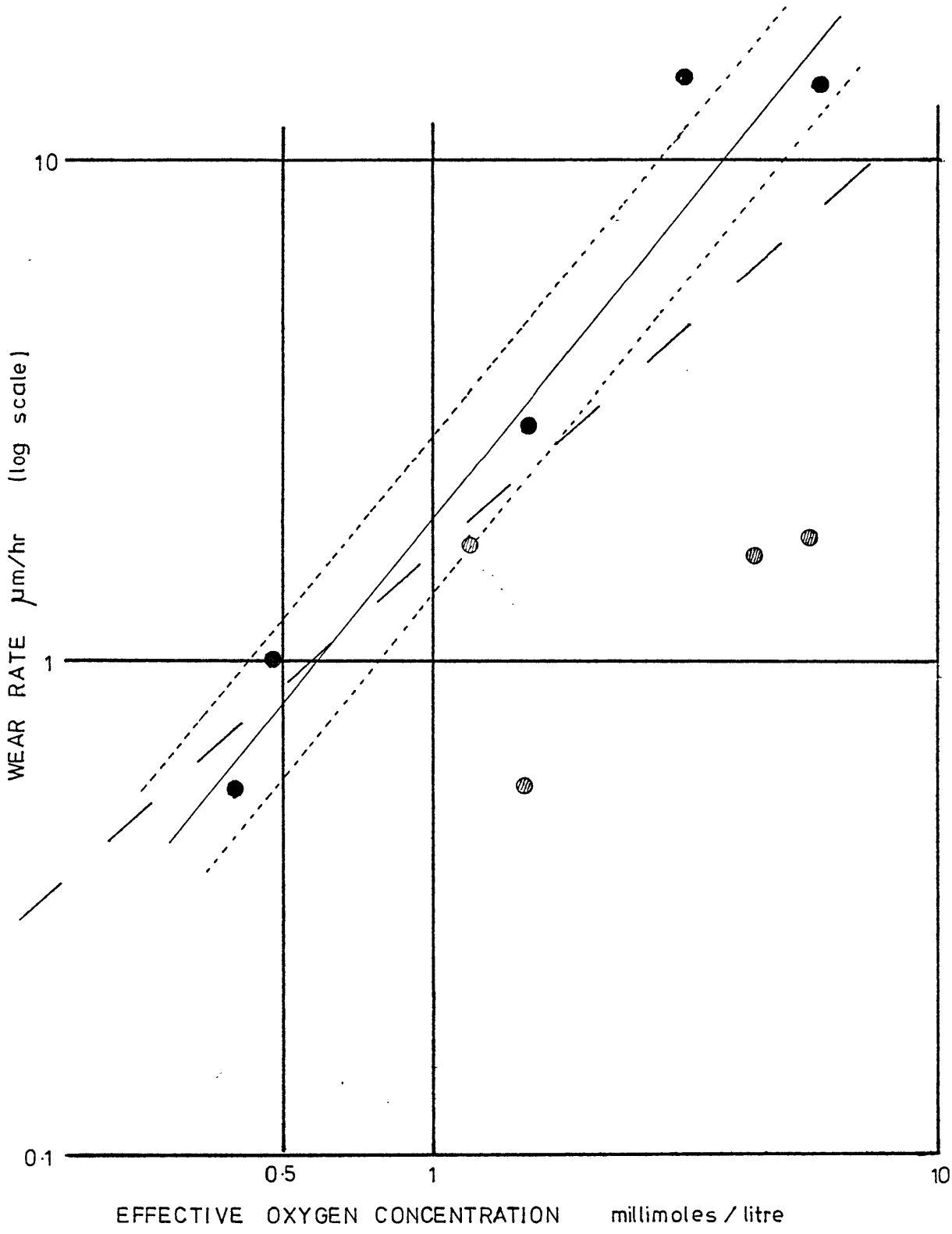

Wear rates in Hexadecane

● Initial wear rate. Points used in regression analysis.

◍ Secondary wear rates.

— — Broken line shows the relationship established with Ester

——— Line of best fit to Hexadecane results.

Figure 5.6.2

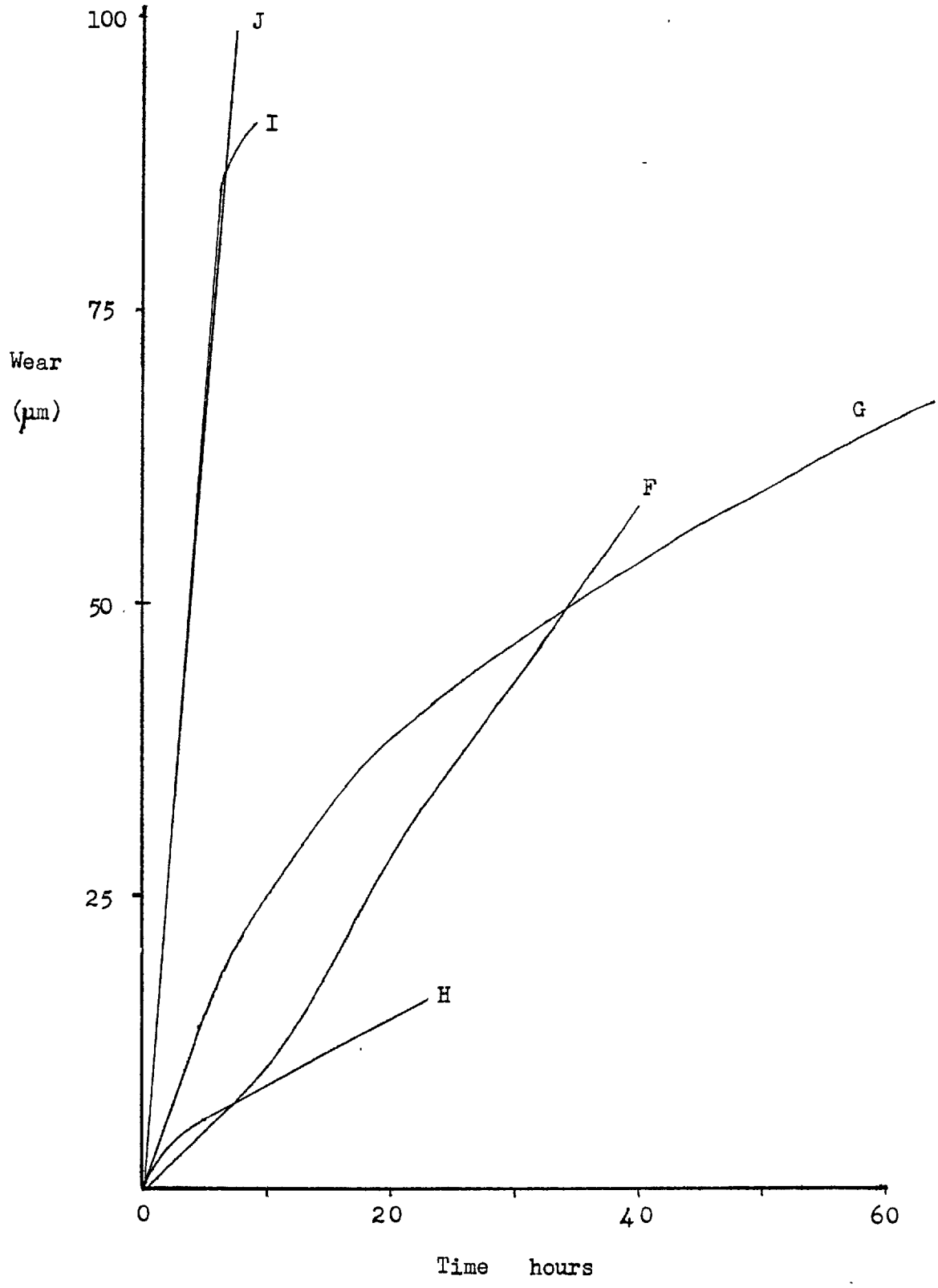

Results of wear tests in Hexadecane.

that the oxidative wear may be occurring in a two stage process only one stage of which in the ester is rate determining whilst in hexadecane the rate of the second step becomes significant. However, in a complex system such as the fretting process investigated here it is inadvisable to attempt to draw too many conclusions from such a relationship. It will be shown in Chapter 8 that the results obtained from the addition of antioxidant additives give evidence of a higher order reaction mechanism.

5.7 Results and Discussion - Wear Rates at Long Times

The tests performed with hexadecane were not run for as long periods as the ester. Where the oxygen concentration was maintained at less than 150% air saturated (1.1 millimoles/litre) there is no evidence of a drop off in the wear rate. For instance the wear rate observed in test F at 30 - 40 hours falls in line with the initial wear rates. At high oxygen concentrations, however, the fall off in wear rate is quite rapid after about five hours for tests G , I and J . It had been thought that the drop off in wear rate observed both with ester and hexadecane was caused by a similar factor, namely the build up of oil acidity as a result of oxidation of the oil. However, the results presented in Chapter Seven show no build up in acidity in hexadecane.

5.8 Summary

Wear tests in hexadecane give results not radically different from those obtained using the ester. The wear rates for hexadecane are generally higher under the same experimental conditions. This can be explained in two ways. Either

(1) It is a result of the lower viscosity of hexadecane.

Or

(2) Oxygen is more readily absorbed from the bubbled gas by hexadecane giving a higher oxygen activity.

As with the ester the wear rate at high oxygen quickly falls from an initially high value - in the case of hexadecane after about five hours.

A clear relationship was established between the initial wear rate of the splines and the oxygen concentration in the lubricant.

Introduction to Part II

Part II describes the experiments which were undertaken to elucidate the chemical nature of the wear process. The results presented in the previous chapters have established that the major fretting wear mechanism in misaligned splines is abrasion. Severe wear is caused by the abrasive action of debris particles. The rate of wear (and therefore the rate of debris production) was found to be governed in both base lubricants tested, by the oxygen content of the atmosphere above the lubricant and also by the state of oxidation of the lubricant. These observations imply that some chemical process is an important factor in wear. Little has been published about the chemistry of fretting wear in lubricated contact apart from Ku's demonstration that oil antioxidant additives reduced wear. The results of tests with the base lubricants showed that at low oxygen partial pressures wear was reduced, but in apparent conflict with this it was observed that oxidation of the lubricant led to a reduction in wear.

Investigation of the chemistry of the wear process was pursued on three fronts:

(1) Studies of the changes in the chemical composition of the base lubricants throughout fretting tests. This work is described in Chapters 6 and 7.

(2) An investigation into the effect of two antioxidant additives in the ester base stock upon fretting wear and also upon the changes in chemical composition observed in (1) above. (Chapter 8.)

(3) An examination of the worn surfaces and analysis of the wear debris composition to determine the state of oxidation of the surfaces at the end of a variety of fretting tests (Chapter 9).

A summary of the main conclusions drawn from these experiments is to be found in the final chapter.

Chapter 6. Methods of monitoring oil oxidation.

6.1 Introduction

The results of the previous 2 chapters indicate that lubricant oxidation leads to a reduction of fretting wear. In this chapter methods by which the oxidation of lubricants may be monitored are discussed. A survey of the literature established the following as practicable methods:

1. Acid titration
2. Interfacial tension
3. Viscosity
4. Oil insoluble product determination
5. Chemical analysis
6. Thin layer chromatography
7. Infra-red spectroscopy
8. Mass spectroscopy
9. Redox titration

Of these methods, 1, 6, 7, 8 and 9 were experimented with - 1 and 9 being used extensively. The techniques are outlined in the following sections, to which table 6.1 provides a guide.

6.2 Methods Which Were Considered But Not Used

6.2.1 Interfacial Tension

As oxidation of a pure lubricant proceeds its surface tension is reduced as a result of the accumulation of oxidised products. Spikes[67] has described a method of determining the surface tension of an oil with respect to water. However, such measurements give only a quantitative estimate of the degree of oxidation.

TABLE 6.1

Summary of Techniques for Monitoring Oil Oxidation

METHOD	REFERENCES	USED IN THIS THESIS?	RESULTS	METHOD USED	OUTLINE OF METHOD	PRESENTATION OF RESULTS
1. Acid Titration	Koved[62], Mould[10], Rigg[85], Wilson[63], Chakravarty[93], Denison[92]	Yes	Quantitative measurement of acidity in solution	A modification of IP.139 was used	Section 6.4	Chapter 7
2. Interfacial tension	Koved[62]	No	Quantitative assessment of degree of oxidation	-	-	-
3. Viscosity	Koved[62], Mould[10]	No	"	-	-	-
4. Oil insoluble product determination	Koved[62]	No	Gives no quantitative information on state of lubricant	-	-	-

continued . . .

TABLE 6.1 (continued)

METHOD	REFERENCES	USED IN THIS THESIS?	RESULTS	METHOD USED	OUTLINE OF METHOD	PRESENTATION OF RESULTS
5. Chemical Analysis	Freidin[88], Fenshe[94]	No	Quantitative detailed	-	-	-
6. Chromatography	Hiley[96]	Yes	Reveals presence of small impurity concentrations	T.L.C. due to Hiley	Section 6.3.2	-
7. Infra red spectroscopy	Hirano[95]	Yes	Reveals presence of C = O bonding Results difficult to interpret	-	Section 6.3.3	Section 6.3.3
8. Mass spectroscopy	Radston[6], Stinton[68]	Yes	Reveals relative proportions of a number of substances	Stinton	Section 6.3.4	Section 6.3.4
9. Redox Titration (Peroxide Determination)	Wilson & Garner[63], Denison[92], Chakravarty[93]	Yes	Quantitative measure of peroxides	A modification of Wheeler's method	Section 6.5	Chapter 7

6.2.2 Viscosity

The change in viscosity of a lubricant may be used as an indicator of the degree of oxidation. Accumulation of oxidation products (which act as thickeners) results in a progressive increase in viscosity.

6.2.3 Oil Insoluble Product Determination

Again the course of oil oxidation may be followed by studying the accumulation of "sludge" in the oil - the products formed as a result of oxidation which, because of their high molecular weight, are insoluble in the oil.

The above three methods yield only quantitative information on the degree of oxidation. The concentration of chemical species within the oil cannot be inferred directly. These methods were considered inappropriate for studying changes in the chemical composition of the lubricant.

6.2.4 Chemical Analysis

Analysis of oxidised oil to determine its composition by chemical techniques can be used to monitor oil oxidation. Such work has been carried out by Freidin (88) who studied the oxidation of Dimethyl Sebacate and Fenske(94) who studied n-hexadecane. However, whilst analysis provides a great deal of data such a procedure is of necessity time-consuming and was not attempted.

6.3 Methods Which Were Tested

6.3.1 Introduction

In this section 3 methods of monitoring oil oxidation are described. The methods were given a trial to determine their sensitivity of detection of oxidation but were not used extensively.

6.3.2 Chromatography

Small concentrations of dissolved substances may be separated out from the pure solvent and identified either by their position on the chromatogram or by subsequent chemical analysis. Of the number of different chromatographic techniques, Thin Layer Chromatography (T.L.C.) was chosen as its use as a tool for separating and identifying additives in an oil had been developed at Imperial College by Hiley[96].

This technique provides a means of separating small quantities of polar substances from a non-polar solvent. It therefore promised to be a good way of studying the oxidation of hexadecane (which is non-polar), since most products formed are polar. For the same reason it is likely to be less effective for the ester oil. The details of the technique are now described.

A 20cm square glass plate was coated with a uniform film of silica gel in the form of a slurry. The silica gel contains a calcium sulphate binder and a phosphor which is activated by 2.54 μm wavelength ultra-violet light. When dried in an oven a dry adherent coating is formed.

Samples of hexadecane extracted at various times from the rig were spotted onto the plate at intervals 1cm from one edge, see fig. 6.3.1. The amount of hexadecane was carefully measured with a micropipette graduated in tenths of a microlitre. Samples of pure hexadecane and pure hexadecane to which known quantities of acid and ester had been added were also put on the plate for comparison (the spot size was 3 μl). Each of the dots at

this stage was a mixture of hexadecane and any impurities present. The hexadecane was first removed by eluting the plate with a 50:50 mixture of petroleum ether and toluene in a chromatographic tank. The following procedure was used:

The plate is stood on edge in 0.5cms depth of the solvent within the tank in which the air is saturated with solvent vapour. The solvent is drawn up through the gel by capillary action. The saturation of the vapour ensures that evaporation of the solvent from the plate does not take place. When the solvent front has reached the top of the plate it is removed and dried. The non-polar solvent carries the hexadecane to the top of the plate leaving the polar substances behind.

The procedure was then repeated using a polar solvent (toluene + 5% by volume of acetone) which carried the polar impurities up the plate. In order to prevent the polar substances being mixed with the hexadecane a "solvent stop" line was scored through the gel about two-thirds the way up the plate. When the solvent reached this line the plate was removed and dried.

The distance of migration of polar substances up the plate under the action of the polar solvent depends on the size of molecule and its polarity. The ratio of the distance moved by a particular species over the solvent movement is known as its r.f. value.

$$\text{r.f.} = \frac{\text{distance of spot from application point}}{\text{distance of solvent front from application point}}$$

Figure 6.3.1

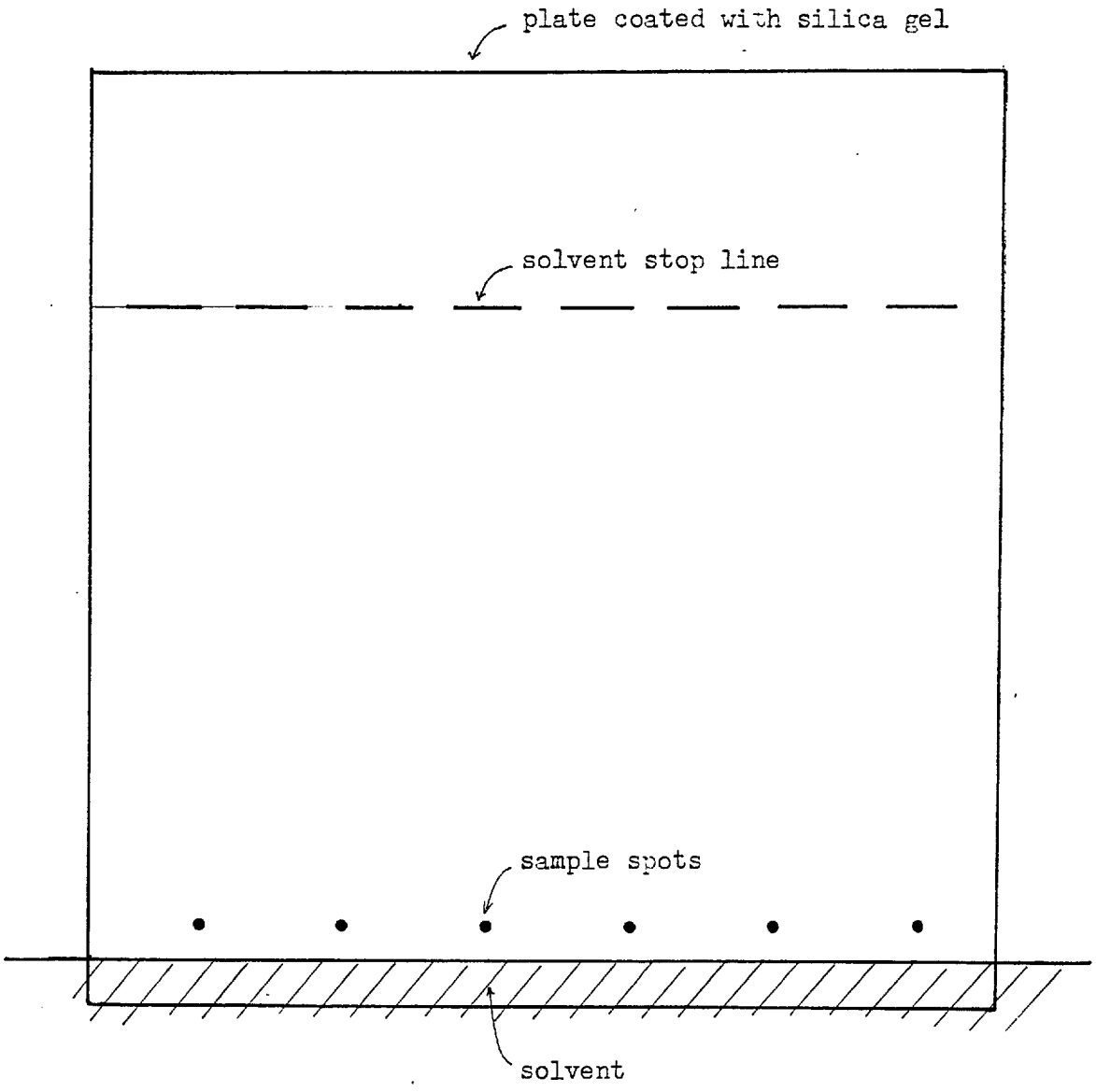
plate coated with silica gel
solvent stop line
sample spots
solvent

The r.f. values of spots on the plate provides an indication of the substance making up the spot. However, comparison with known substances on the same plate is generally the best method of identification. The displacement of substances was not visible under white light. Some spots were visible under ultra-violet illumination as they quenched the phosphor incorporated in the gel. However, the spots could be made visible by spraying the plate with a 5% solution of dodeca-molybdophosphoric acid in isopropanol and "developing" the plate in an oven for half an hour. The spots appeared blue-green on a yellow background. Permanent records of plates must be made by photographing them or by sketching the position and intensity of the spots, as they fade in daylight. Xeroxing the plates was not very effective.

In practice only one or two spots were observed for each hexadecane sample. These were observed at positions corresponding to an r.f. value similar to the literature values for esters (0.7). Fig. 6.3.2 shows the results of T.L.C. on oil from test 'H'. In this test the wear rate was 16 μm/hour for the first 6 hours, followed by a rapid fall off in wear to less than 0.5 μm/hour by the eighth hour. The plate shows an increase in intensity of the impurity spot with test time.

Fig. 6.3.3 shows the results of T.L.C. on hexadecane from tests 'O' and 'P' in which lauric acid had been added to the pure hexadecane to determine the effect of acidity on wear. These tests were run at reduced oxygen concentrations. Spots of increasing intensity were again

Figure 6.3.2

Representation of the result of chromatography of samples from test H.

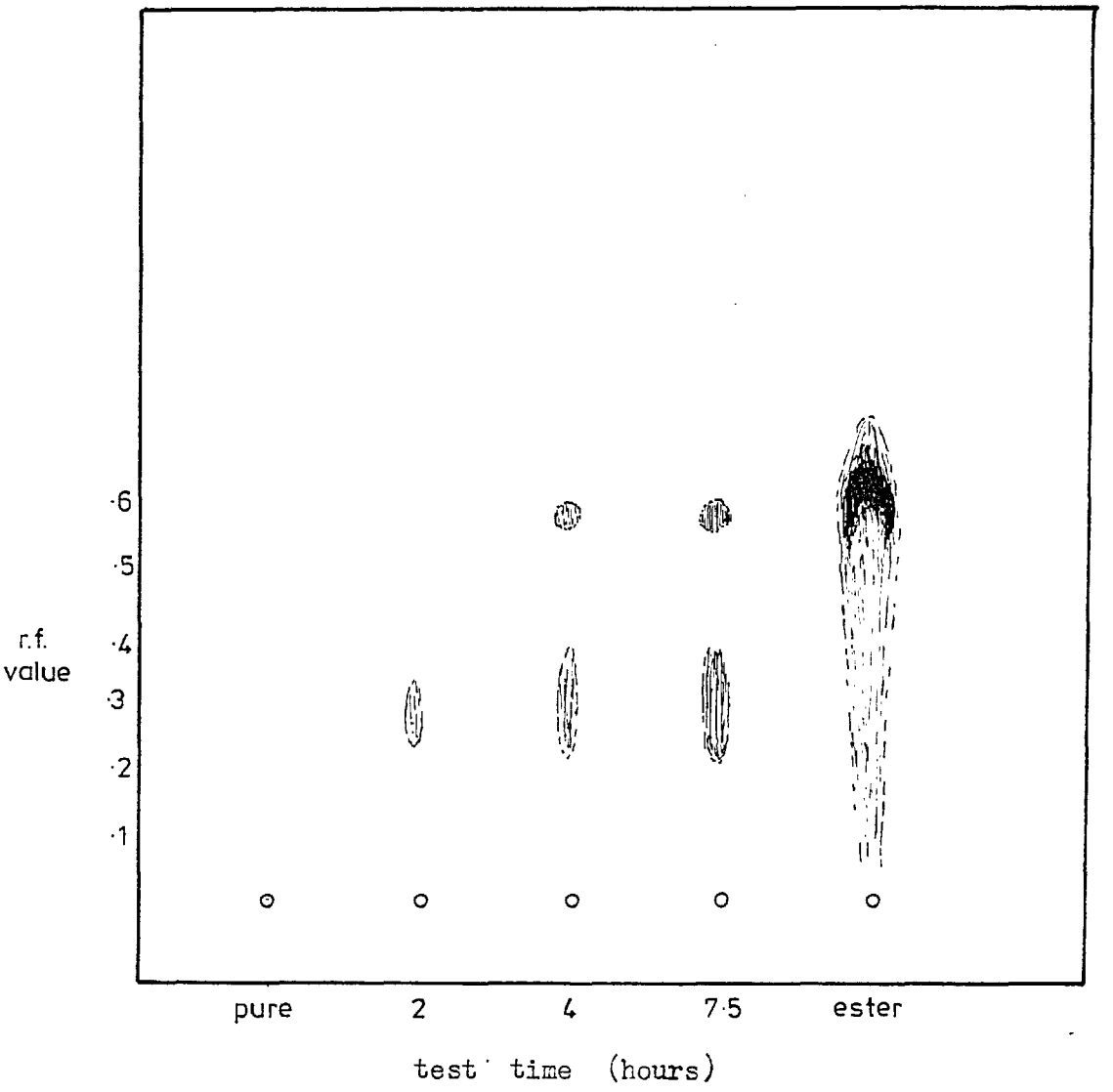

Samples of Hexadecane were extracted from the rig at the times indicated. (Spot size : 4 µls.) For comparison, 4 µls of pure Hexadecane and 1 µl of a pure ester were also chromatographed.

Figure 6.3.3

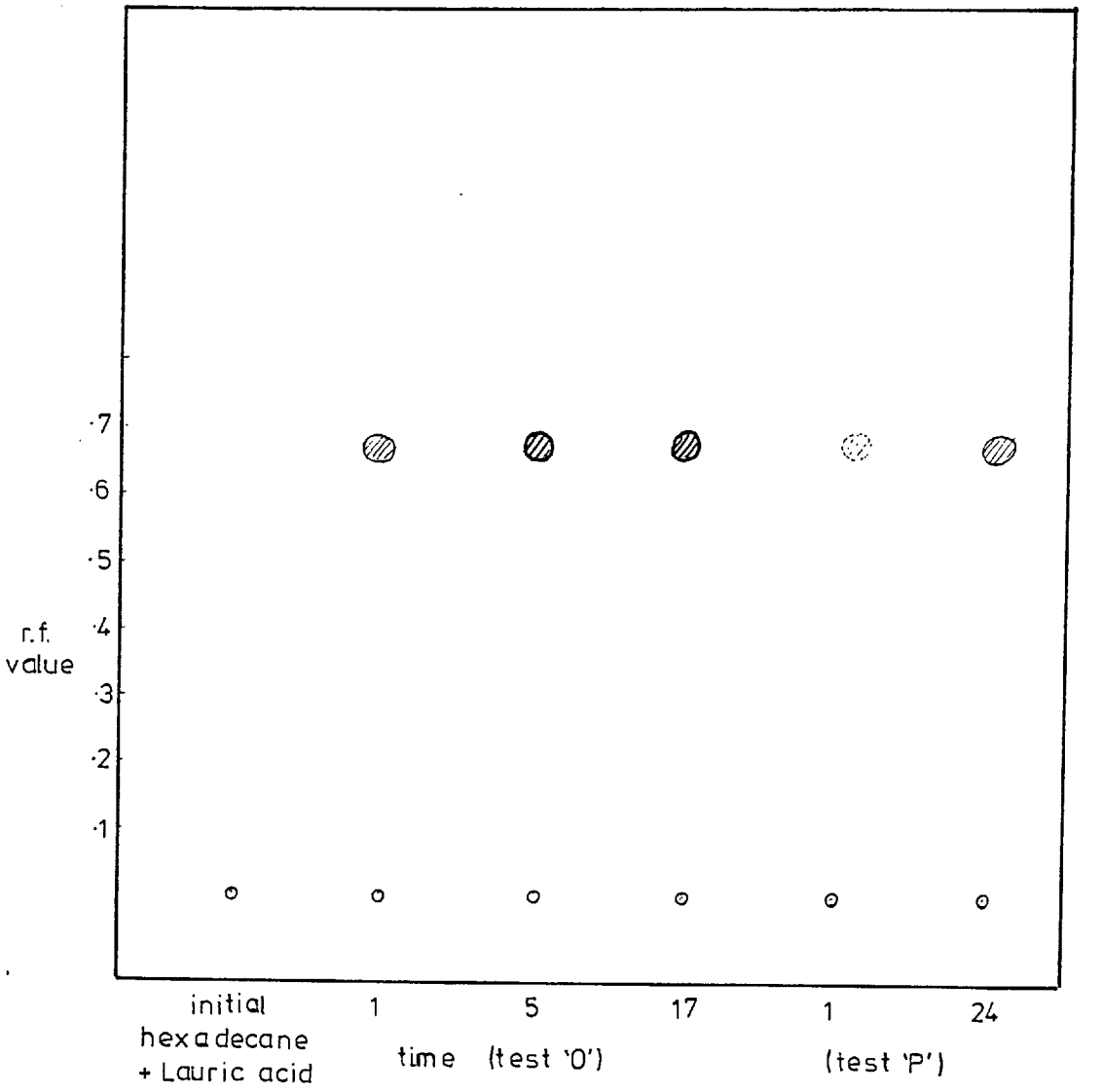

A representation of the results of chromatography of samples from tests O and P. The samples were extracted at the times indicated (hours). Sample size : 5 µls. Note that the high concentration of added acid was not detected. The position of the spots suggests that the used lubricant contains ester impurities.

observed at r.f. = 0.65. However, no spots due to the added acid were detected - these should have been more or less constant in intensity throughout the test.

Because the method was found to be unable to detect acid in hexadecane and gave at best only an estimate of impurity concentration it was abandoned in favour of acid titration methods. However, the method could be pursued if a method for developing the acid could be found. It is also possible to remove the spot area and take a mass spectra of the substances contained in the spot in order to identify them. This technique is discussed by Hiley[96].

6.3.3 Infra-red Spectroscopy

The oxidation of hydrocarbons may be studied by observing changes in the infra-red spectrum. Hirano[95] used i-r. spectroscopy to monitor oxidation of a mineral oil. The spectrum of a hydrocarbon in this region is fairly simple, fig. 6.3.4. The prominent peaks are:

3,000 cm^{-1}	C-H bond stretching
1,480 cm^{-1}	C-H bond bending
1,390 cm^{-1}	CH_3 symmetrical deformation
730 cm^{-1}	CH_2 rocking

The introduction of oxygen into the molecule causes the appearance of a peak at 1,710 cm^{-1}.

The relative intensity of this peak could be correlated with acid concentration. Like T.L.C. this method is likely to be more sensitive in studies of hexadecane than ester (since the spectrum of the unoxidised ester has a 1,710 cm^{-1} peak).

However, measurements of acidity by a titration method showed that there is little or no increase in

Figure 6.3.4

The Infra-red spectrum of Hexadecane.

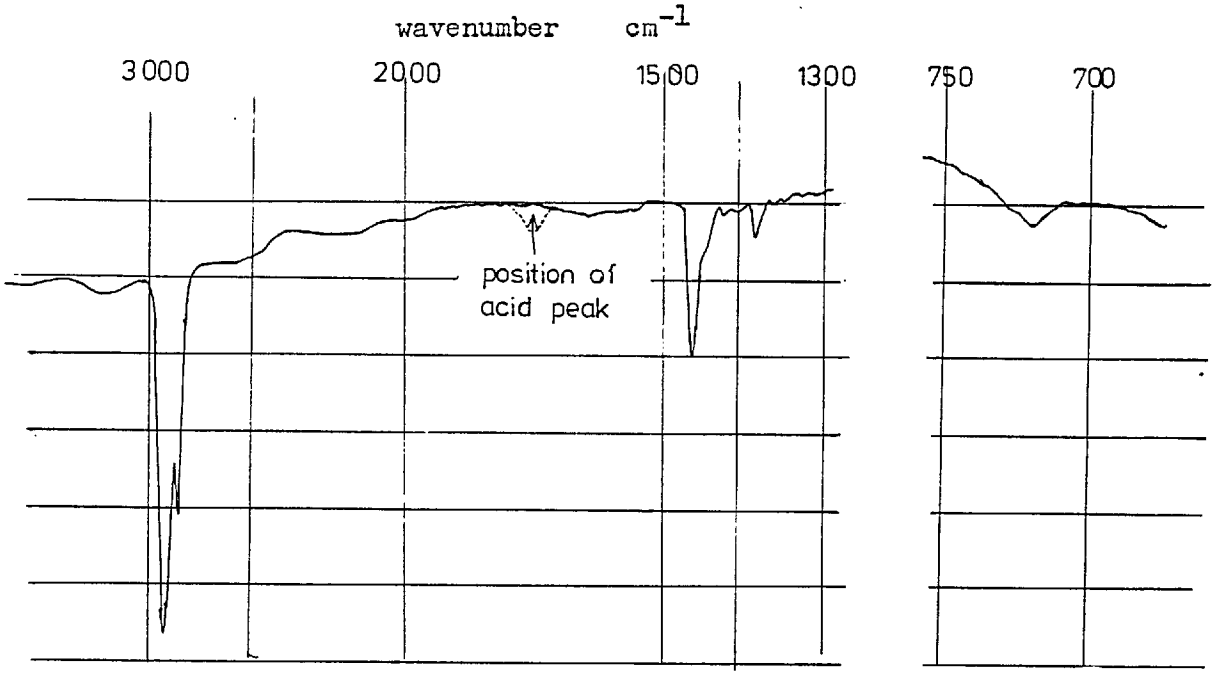

acidity in the fretting tests and i.r. spectra of samples of hexadecane from a test did not discriminate oil oxidation. After a couple of trials the method was rejected.

6.3.4 Mass Spectroscopy

The technique of mass spectroscopy has previously been used by Stinton[68] to study the build up of oxidation products in hexadecane. Compounds containing oxygen in a number of configurations can be distinguished:

alcohols
acids
esters
di-alcohols
di-acids

Polymerisation of the hexadecane may also be detected. In the mass spectrometer, ions are produced from a sample, separated according to their mass to charge ratios and recorded. As a result of the ionisation process the molecules of the sample break into fragments. For hexadecane, a long chain hydrocarbon, cleavage may take place at any point of the chain so a series of peaks is observed at m/e ratios corresponding to $C_n H_{2n-1}$ and $C_n H_{2n+1}$ up to a value of n = 16, the number of carbons in the chain. The commonest ions are those with n = 3, 4 or 5 - as n is increased the ions become less abundant. The spectrum is complicated by the naturally occuring isotopes of different mass numbers. This is more pronounced in the higher molecular weight fragments where there is a greater chance that the molecule will include one or more of these isotopes.

In a similar way fragmentation of the oxidation products of hexadecane gives rise to an additional series

of peaks at intervals of 14 $^{m}/e$ units but a position determined by the mass of the oxygen containing group.

Thus alcohols give rise to the series $^{m}/e = 31 + 14_n$ due to ions with the structure:

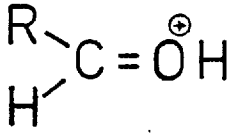

and carboxylic acids to the series
$^{m}/e = 46 + 14_n$ due to ions with the structure:

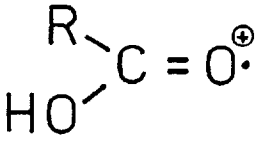

Where the oxygen is incorporated within the chain, as with esters, chain breaking tends to occur at the oxygen bond to the α-carbon because of the stability of the ion so formed,

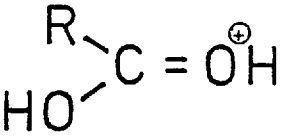

which results from a rearrangement mechanism. Esters are therefore characterised in the mass spectrometer by a series of peaks at $^{m}/e = 47 + 14n$.

The combination of the spectra of the oxidation products and of hexadecane results in a complex and confusing spectrum from a sample of oxidised hexadecane. A useful simplification in studying hexadecane oxidation is to consider the spectrum above $^{m}/e = 227$. In this range any observed peaks must arise from oxidation products. Below 226 the spectra is mainly valuable for identifying the functional groups. For instance, carboxylic acids give a strong peak at $^{m}/e = 60$.

The oxidation of hexadecane during test 'G' was studied using the 3 methods of acid and peroxide determinations and mass spectroscopy. The results are discussed in the context of other tests in section 7.7. The chemical analyses revealed that the acidity decreased to a low value within about 10 hours and that the peroxide concentration at first increased to a value about a tenth of that attained in the ester, and after about 25 hours, when the wear rate was lower, decreased to a low value (see fig. 6.3.5).

The 3 samples sent for spectroscopic analysis were extracted from the rig after the following run times:

five minutes

seven hours

twenty-six hours.

In addition the spectra of a sample of hexadecane purified as described in chapter 5 from the same batch that was used in the rig was recorded. On this spectra there were no peaks detectable above the background variation beyond $^{m}/e = 228$. The spectra of the 3 samples from the wear test are reproduced in fig. 6.3.6. Table 6.2 lists the peak heights recorded and identifies the series to which a peak belongs. Interpretation of the spectra was undertaken with the aid of tables of characteristic fragmentation patterns[97] and possible structures[98,99]. The results clearly show an increase in polymerisation of hexadecane as the test proceeds, and an increase of most species. However, in the last sample there is a marked drop in the relative abundance of the species giving rise to series D - identified tentatively

Figure 6.3.5

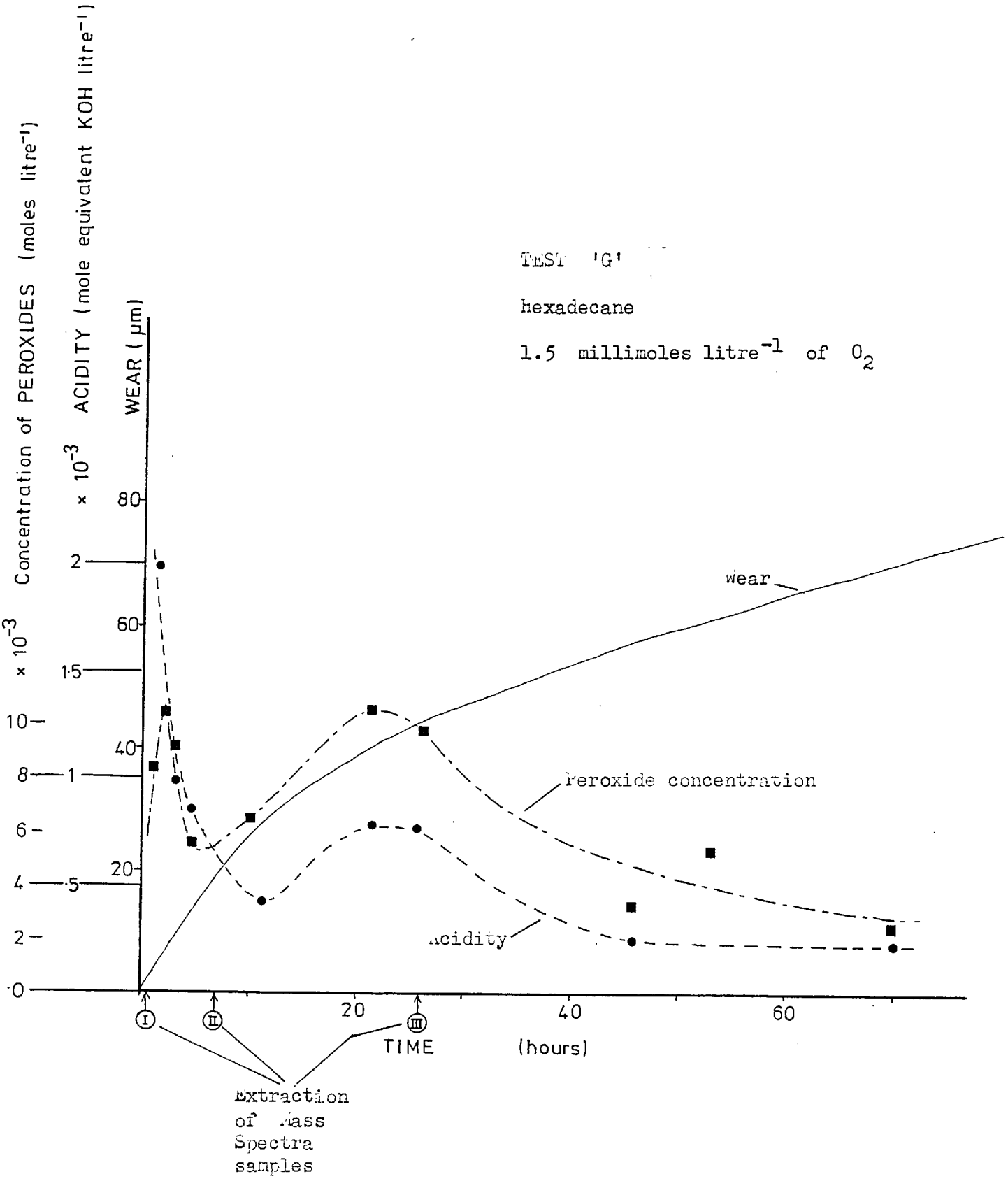

The figure shows the variation in concentration during a fretting test of acid and peroxides as determined by titration methods. Also shown are the times of extraction of samples for spectroscopy.

Figure 6.3.6 Mass Spectroscopy Results

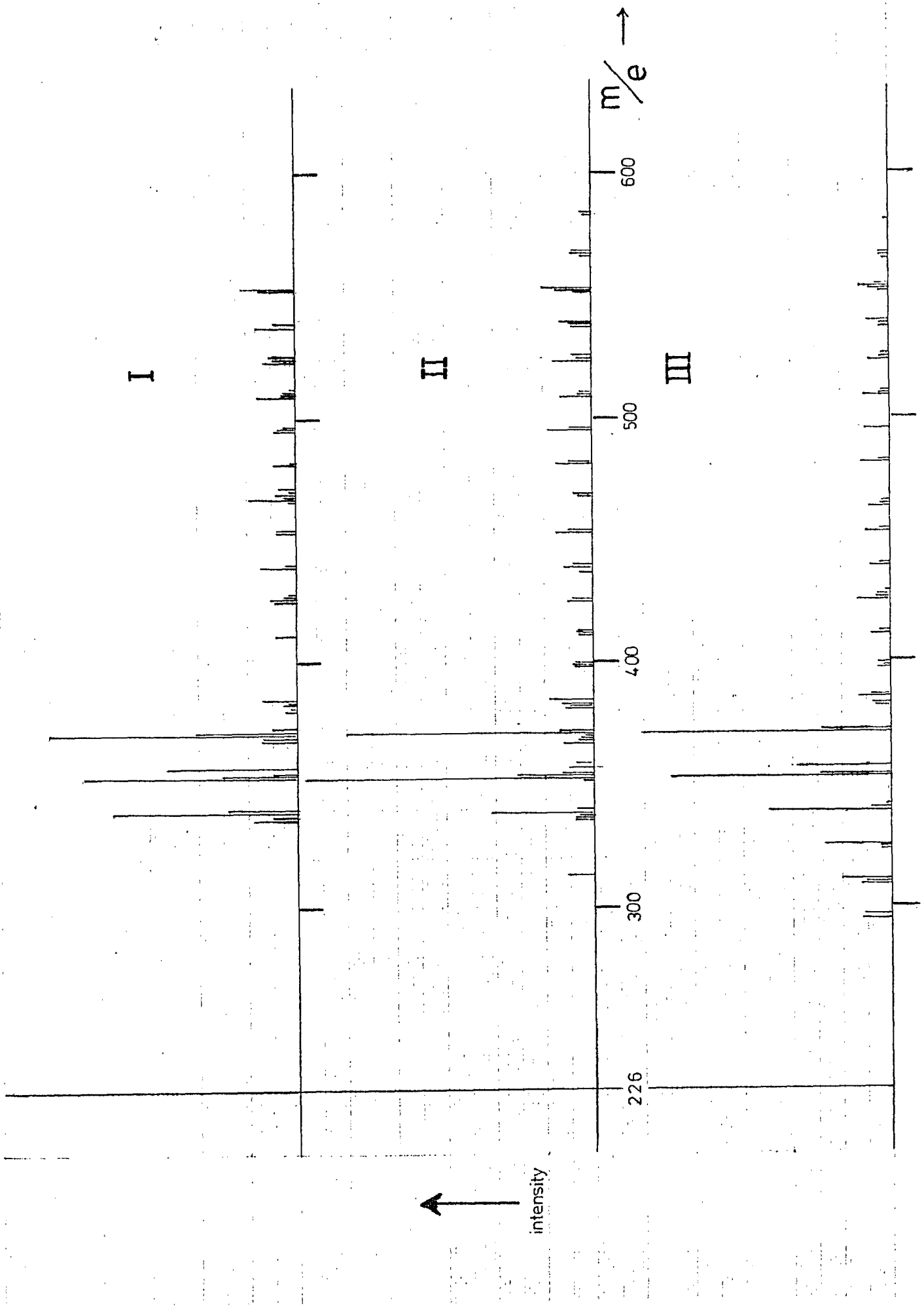

TABLE 6.2

Identification of the peaks in the mass spectra.

SERIES					SAMPLES		
A	B	C	D	E	I	II	III
mass / charge ratios					relative intensities		
311							4.5
325							6.2
339					3.7	3.84	11.2
353					4.2	10.8	19.0
	357				2.6	1.2	8.1
367					-	1.2	-
		369			0.7	0.4	-
	371				4.8	9.0	22.5
381					0.1	1.1	1.3
		383			0.3	1.2	2.8
	385				0.7	3.85	3.0
		397			-	-	1.3
			398		-	0.7	0.9
	399				-	0.8	1.0
		411			0.4	0.6	1.9
			412		-	0.6	0.9
	413				-	0.6	-
		425			0.4	1.0	3.2
			426		0.5	0.8	1.3
		439			0.7	1.0	2.0
		453			0.4	1.2	2.3
			454		0.4	0.9	0.9
				463	-	-	1.8
		467			0.9	0.6	-
			468		0.2	0.7	-
	469				0.4	0.6	-
		481			0.5	1.4	2.7
		495			0.4	1.7	2.3
		509			0.8	1.2	2.5
		523			0.6	1.4	2.0
		537			0.8	0.7	1.2
	539				0.5	1.2	2.1
			552		0.7	1.3	1.7
	553				1.0	1.8	2.7
	567					0.8	0.5
	581						0.4

Series		Functional group
A	31 + 14n	alcohol or ether
B	91 + 14n	di-acid of di-ester ?
C	47 + 14n	acid of ester
D	62 + 14n	cleavage of ROO-C_2H_4-H and rearrangement
E	29 + 14n	saturated aliphatic hydrocarbon

Sample I extracted from rig after 5 minutes
II " " " " 7 hours
III " " " " 26 hours

as peroxides. Series B (91 + 14n) could not be identified from the tables. Possibly it arises from dibasic acids or esters.

Carboxylic acids characterised by the series of peaks (46 + 14n) and by a large peak at $^{m}/e = 60$ were not observed. This is borne out by the acidity measurements which detected very little acid. The significance of this result is discussed in the next chapter.

6.4 Acid Titration

6.4.1 The Method

A number of workers have studied the deterioration of oils by acidity measurements by a titration method. Their results are reviewed in section 7.2. There is an ASTM/I.P. standard test for acidity which has commonly been used - the Institute of Petroleum Test number IP139(100).

A sample of the oil is dissolved in a 50:50 mixture of toluene and isopropyl alcohol containing 0.5% water (the "titration solvent").

The solution is then titrated against potassium hydroxide in alcohol solution at room temperature. The indicator is p-naphtholbenzein which changes from orange to green-brown. The I.P. test procedure recommends a sample size of 20 grams for light-coloured oils.

Clearly, samples of this size could not be repeatedly extracted for analysis from the fretting rig during a fretting test since the total volume of oil in the rig is 70mls. A sample size of 1 to 2mls was considered desirable. However, for samples of this size taken

during the initial stages of oxidation the additions of KOH for neutralisation were so small that a very dilute solution was used. As a result the end point was difficult to detect. The answer to this problem was to use a spectrophotometric method to determine the end point. The experimental procedure follows that of the I.P. test excepting only that the oil sample was not agitated to incorporate sediment as specified in paragraph 6(b) of the standard procedure. Any sediment in the oil samples was mainly wear debris and the aim of the test was to measure the oil acidity only.

6.4.2 Experimental

Samples of oil that had been extracted from the fretting tester for oxygen analysis were sealed in specimen tubes and kept in a cool dark cupboard until tested for acidity. About 1 to 1.5mls of oil was transferred in a graduated syringe to the spectrophotometer cell. Three drops of p-naphtholbenzein solution (10gms/litre) were added and then 10mls of titration solvent. This quantity was found to be sufficient in all cases to dissolve the oil and eliminate interference in end point determination by the darkest oils. The solution was stirred by a magnetic flea when mounted in the spectrophotometer. KOH solution was added through a microburette. The apparatus is shown in fig. 6.4.1. Light shining through the solution falls on a photocell. A filter of complimentary colour to that of the solution after the end point is reached is slotted in front of the photocell. An orange filter giving peak transmission at 660nm was used. The output of the photocell is

Figure 6.4.1

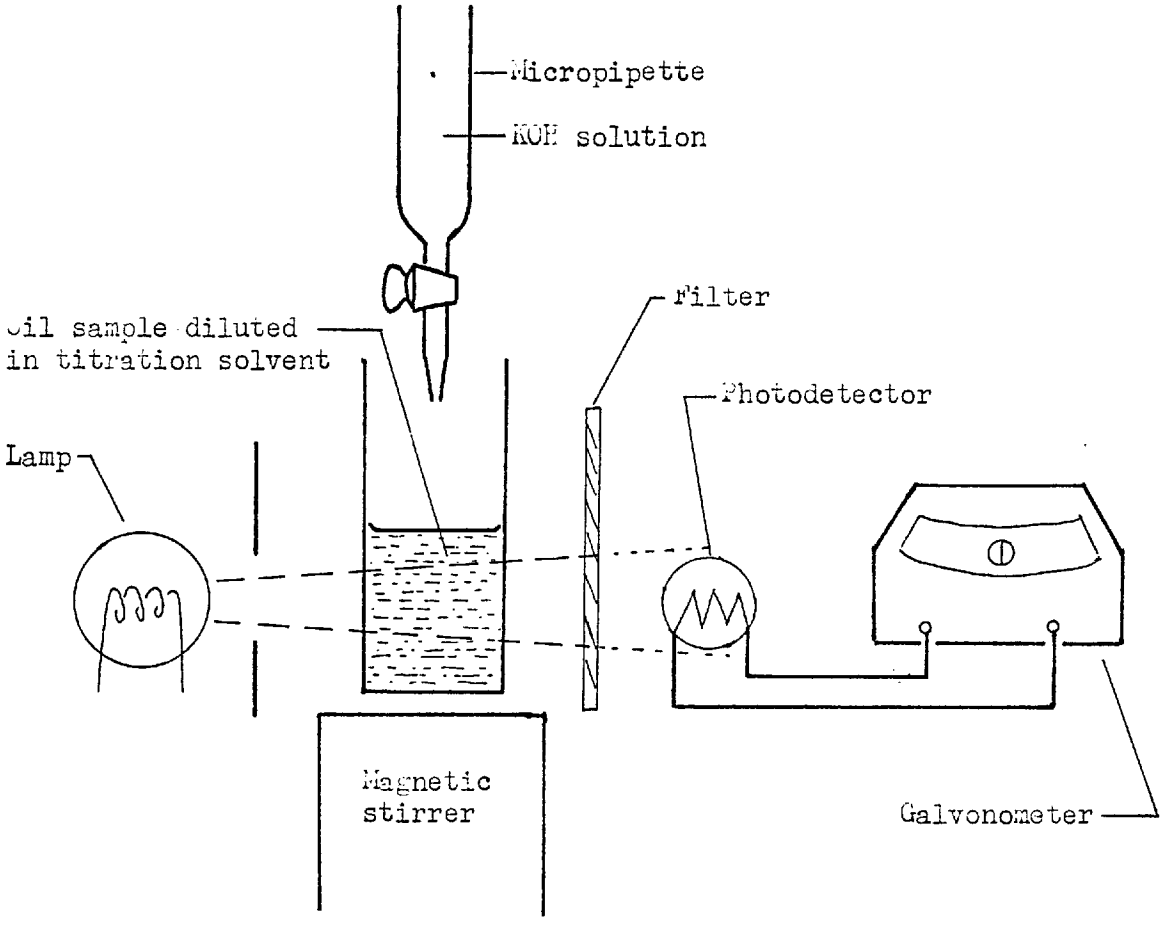

Spectrophotometric Titration Apparatus

connected to a galvanometer calibrated on a logarithmic scale of absorbancy. As the end point is reached the spot moves across the scale most rapidly. KOH solution was added in 0.2 to 1.0ml quantities and after each addition the spot position was recorded after it had stabilised (20 to 30 seconds later). Base was added until well beyond the end point. The readings are then plotted on a linear scale. Figure 6.4.2 shows a typical result. The intersection of the linear portions of the curve defines the end point. From this value must be subtracted the acidity determined for the titration solvent alone. End points could be determined to $\mp$ 0.05mls. For end points in the range 1 to 5mls this represents an error of less than 5% which is comparable to the accuracy of the Institute of Petroleum test method.

The KOH solution was standardised against 0.01 M aqueous potassium hydrogen pthalate in 5 determinations. It was diluted 10 and 100 times to give 3 standard solutions:

6.7×10^{-2} M ($\pm$ 0.5×10^{-2} M)

6.7×10^{-3} M

6.7×10^{-4} M

The acidity of the titration solvent was measured in 4 determinations to be 0.08 $\pm$ 0.04mls KOH soln./10mls solvent at a KOH solution concentration of 6.7×10^{-4} M. The accuracy of determination of a sample obviously improves with increasing acidity.

The results of the acidity tests are conveniently quoted in mls KOH soln. per ml of sample or moles KOH equivalent/litre. However, acidities of oils are

Figure 6.4.2

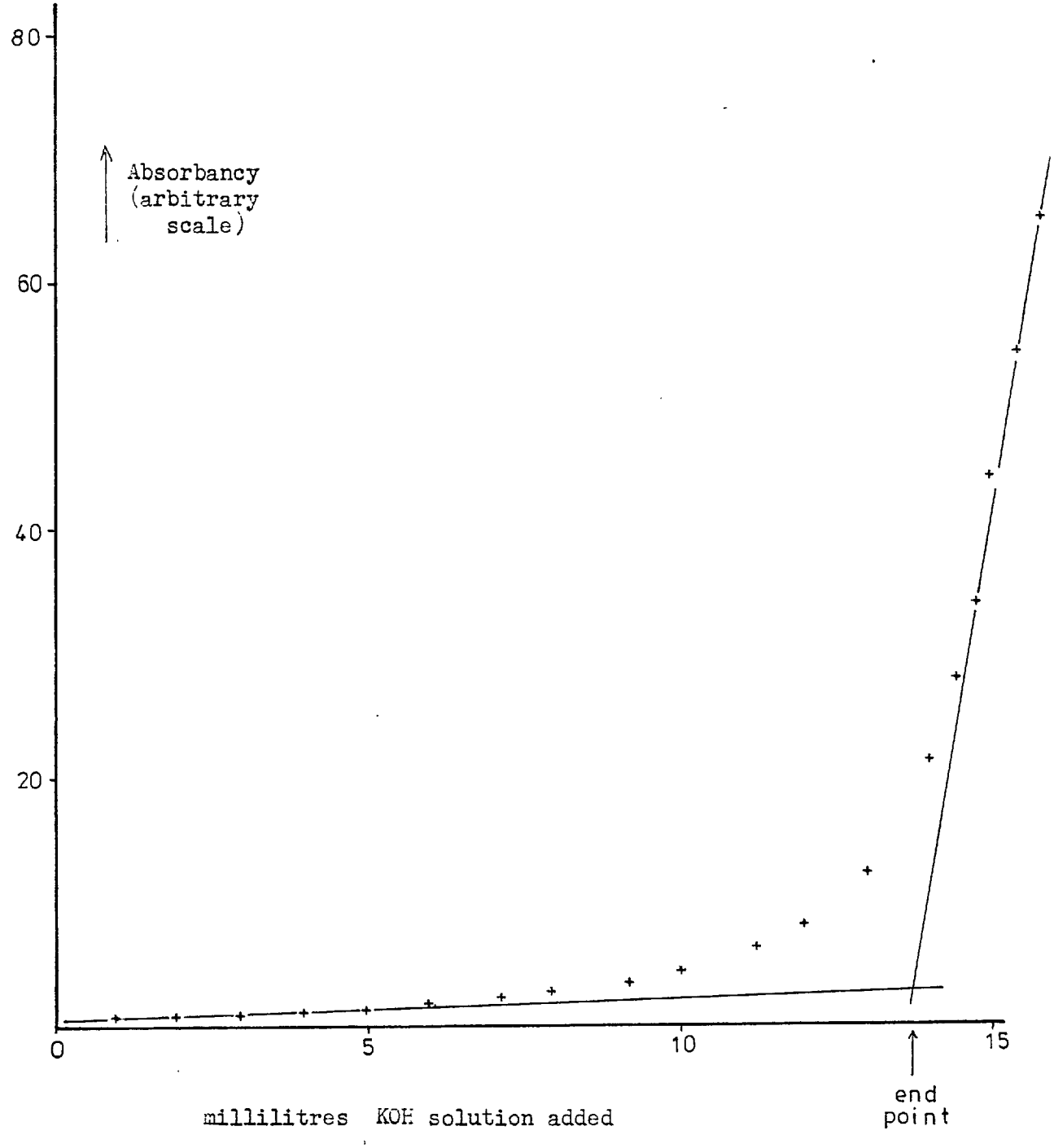

Spectrophotometric determination of the end point of a titration to find the acidity of an oil sample.

generally quoted in terms of the Total Acid Number (T.A.N.). This is the weight of potassium hydroxide (in milligrammes) that is required to neutralise one gramme of the oil. T.A.N. values may be obtained from the moles/litre value by multiplying by the molecular weight of KOH (56.1) and dividing by the density of the oil.

6.5 Redox Titration - Peroxide Determination

6.5.1 Introduction

Wilson and Garner[63] in studying the effect of peroxides on the corrosion of lead by lubricating oils used two methods for determination. These methods detect the stable hydroperoxide groups present in solution in the oil. For tests on engine oils they used a method similar to that described by Wheeler[101]:

50mls of a 50:50 mixture of glacial acetic acid and chloroform were placed in a 250ml flask and a 5ml sample of the oil added. Four g. of sodium iodine were added, the flask attached to a condenser and heated over a small flame at gentle reflux for 2 minutes. The flame was then extinguished and as soon as reflux ceased 50mls of distilled water was poured down through the condenser into the flask. It was then disconnected and shaken vigorously and 0.05 M sodium thiosulphate solution was run in until the end point was approached. A few drops of starch solution were added and titration continued until the blue colour of the aqueous layer disappeared. Chloroform helps to dissolve the sample.

During reflux the peroxides are reduced by the iodide ion in acetic acid solution.

$$R\text{-}OOH + 2HI \longrightarrow I_2 + ROH + H_2O$$

The iodine so released is titrated against aqueous iodium thiosulphate.

$$I_2 + 2\,S_2O_3^{2-} \longrightarrow 2I^- + S_4O_6^{2-}$$

The addition of water speeds up this reaction.

For tests on white oils Wilson and Garner used a method described by Wagner et al[89] using isopropyl alcohol as a solvent in conjunction with a small quantity of acetic acid. The advantages of this method are that atmospheric oxygen has less effect on results and less dilution with water is necessary - water affects the results obtained with diolefinic peroxides. A disadvantage is that a longer reflux time is required.

Forty mls of dry isopropyl alcohol, 2mls of acetic acid and 5mls of the sample oil are placed in a flask. The flask has a gas inlet and CO_2 is passed over the solution for 3 minutes. The solution is then refluxed for 15 minutes. The gas flow is reconnected during titration against sodium thiosulphate.

Experiments conducted by Wagner[89] demonstrated that provided an excess of iodide ion was present there was little or no addition of liberated iodine to unsaturated hydrocarbon bonds (as it combines to form the stable tri-iodide ion) which had been thought to be a disadvantage with iodometric methods. It is also pointed out that use of sodium iodide is preferable to potassium iodide as the former is more soluble in isopropyl alcohol.

When testing oils where unsaturated bonds are not present however there is little to choose between the 2 methods. Because of the shorter reflux time and hence

less likelihood of thermal decomposition (although Wagner showed that 4 out of the 5 peroxides he tested were stable towards heat) the former method was pursued.

In order to continuously sample both peroxide concentration and acidity during a long test without depleting the volume of oil in the rig it was necessary to take a small sample only for analysis. This was replaced in the rig by an equal quantity of fresh oil.

Since the capacity of the rig is about 70mls a sample size of 2mls was chosen to avoid affecting the composition of the oil in the rig significantly. Therefore analysis of peroxides was based on a one ml. sample size.

6.5.2 Experimental

The procedure was similar to that described above but the quantities of reagents reduced. A smaller flask was used to reduce the effect of incorporation of atmospheric oxygen when shaking the flask.

Twenty mls of a 50:50 mixture of glacial acetic acid and chloroform were placed in a 100ml flask. A one ml sample of the oil was added followed by one gramme NaI. The flask was heated in gentle reflux for 2 minutes. Twenty mls of distilled water was then poured down the column carrying with it the condensed liquid. On addition of water the colour of the organic phase changed from dark brown to yellow, but did not mix with the aqueous phase. The flask was then vigorously shaken for about one minute and it was noted that the yellow colouration moved from the acetic acid fraction to the aqueous

layer. For low peroxide concentrations the acetic acid layer completely cleared. Sodium thiosulphate was run in until the end point was approached. A few drops of starch solution were added and the titration continued until the colour of the aqueous layer (a dark purple) disappeared. Because of the small sample and very low initial peroxide contents 0.05 M $Na_2S_2O_3$ as used by Wilson and Garner was found to be too concentrated so 1.5×10^{-3} M and 5×10^{-3}M solutions were employed. Additions of titrate were generally in the range 5mls to 20mls - the end point was distinct and could be determined to ± 0.3mls. It was considered unnecessary therefore to use spectrophotometric method to identify the end point more accurately.

The reaction in reflux is

$$R\text{-}OOH + 2HI \longrightarrow H_2O + R\text{-}OH + I_2$$

on titration $I_2 + 2S_2O_3^{2-} \longrightarrow 2I^- + S_4O_6^{2-}$

It follows that for every mole of peroxide 2 moles of thiosulphate are required in the titration.

6.6 Summary

A number of different tests to monitor the oxidation of the lubricant during a fretting test have been considered.

Of these, 2 titration methods were adopted to measure the oil acidity and hydroperoxide content. Some modification of the standard methods was necessary in order to be able to make determinations from one ml samples of oil without loss of accuracy.

In addition the techniques of mass spectroscopy, infra red spectroscopy and thin layer chromatography

were used in an attempt to identify the oxidation products of hexadecane. Infra red spectroscopy is a convenient method for detecting acidity but was not very useful in this instance since it was shown that there is no build up of acid in this "lubricant" during fretting tests. Mass spectroscopy and T.L.C. indicated the presence of polymeric substances. However, the degree of oxidation was difficult to quantify.

The results of acid and peroxide determinations made during fretting tests are presented in the following chapter.

Chapter 7 - The Effect of Some Oil Oxidation Products on Fretting Wear

7.1 Introduction

In this chapter the results of a study to determine the acid and hydroperoxide content of oils throughout fretting tests, are presented. The interrelation of these quantities with the dissolved oxygen concentration and wear rate is discussed. The results obtained with the 2 test lubricants - ester base stock and hexadecane - showed different behaviour. For this reason the results for each lubricant are presented and discussed separately. Following a review of previous work (section 7.2) the chapter is divided into two parts: Part A deals with the ester; Part B with hexadecane.

7.2 A Survey of the Results of Previous Investigations of Acidity and Peroxide Content of Oxidised Oils

The results of investigations by Denison[92] and Wilson and Garner[63] are concerned with the corrosion of white metals in a lubricating oil by peroxides and acids produced during oil oxidation. They used special rigs which oxidised the oil under quite severe conditions, but it will be shown that the results they obtained are comparable with the values for acid and peroxide measured in the fretting tests. Both Denison and Wilson showed that the maximum rate of corrosion coincided with the maximum rate of disappearance of peroxides from the oil (i.e. the maximum corrosion rate occurred just after the maximum peroxide concentration was attained. (Fig. 7.2.1).

Figure 7.2.1

The relationship between peroxide concentration and corrosion rate.

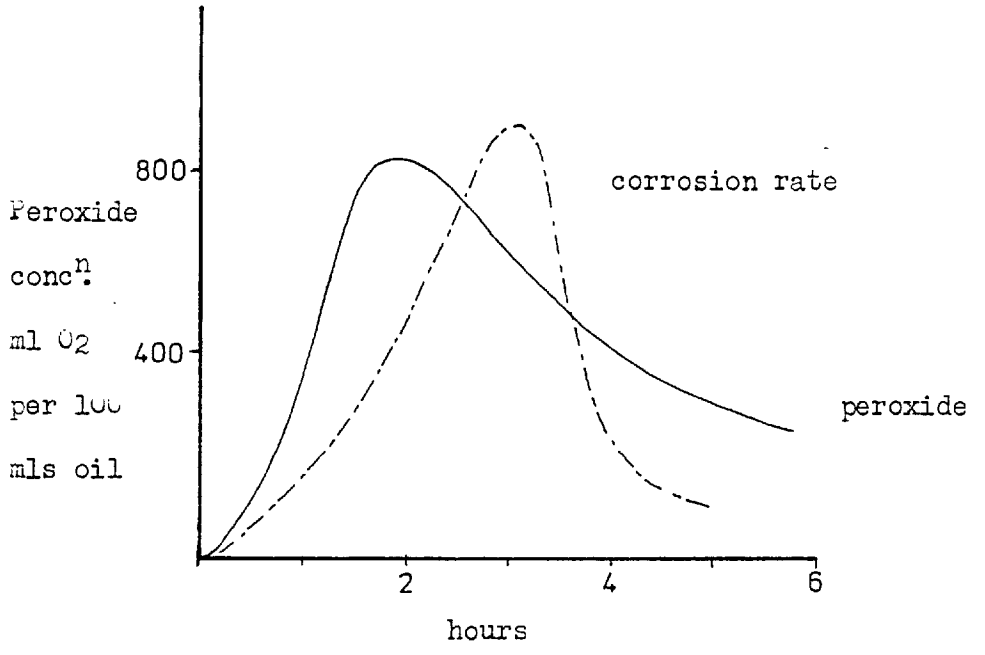

(a) Denison's results. Ref. 92

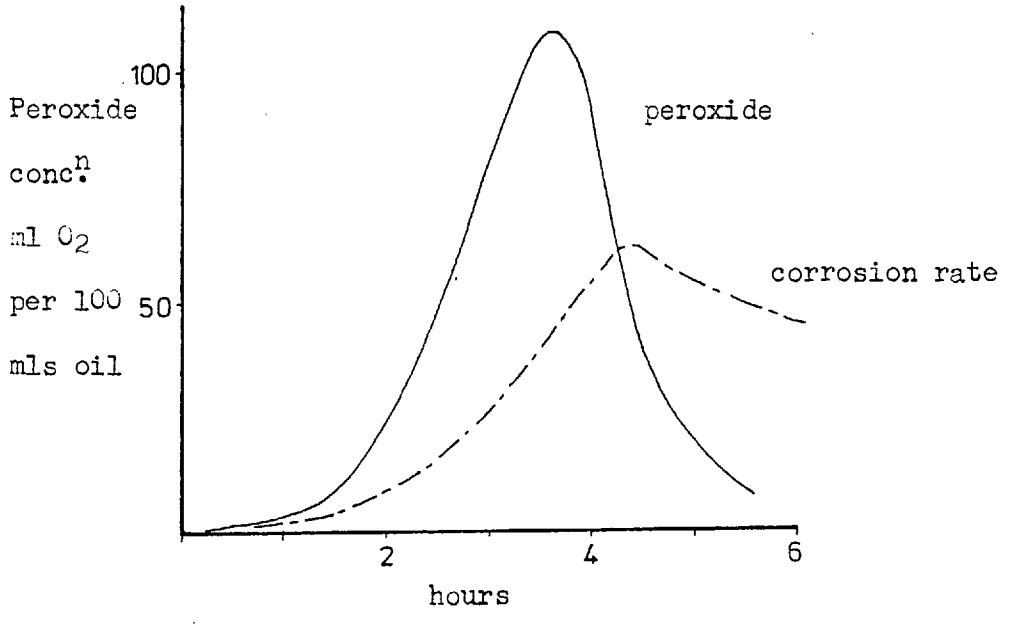

(b) Wilson and Garner's results. White oil. Ref. 63

A comparison of the results of Chakravarty[93] and Wilson and Garner is instructive as their oxidation tests were performed on similar rigs. A quantity of oil was maintained at a constant temperature (140°C or 160°C) and agitated in the presence of a catalyst. Wilson and Garner used a copper catalyst and investigated the corrosion by the oil of lead samples. Increases in acidity and peroxide concentration of white oils were similar to those observed by Denison (fig. 7.2.1). With engine oils the peak peroxide concentration was much lower (fig. 7.2.2) due to the inhibitory affect of sulphur in the oil.

Chakravarty investigated the effect of different metals as catalysts; copper, tin, lead and iron. The results obtained were similar to those of Wilson and Garner[63] except that the maximum value of the peroxide concentration was much lower. This may well be due to a difference in the composition of the white oil. Denison demonstrated large differences in peroxide content in two different oils.

It is interesting that with a copper (or lead) catalyst the peroxide concentration peaks and then falls but with an iron catalyst the peroxide concentration increases to an equilibrium value (fig. 7.2.3). The reason for this difference is probably due to the activity of the catalyst. Chakravarty suggests that the higher activity of copper is a result of the ease with which organometallics formed during oxidation pass into solution, and that the fall off in peroxide concentration

Figure 7.2.2

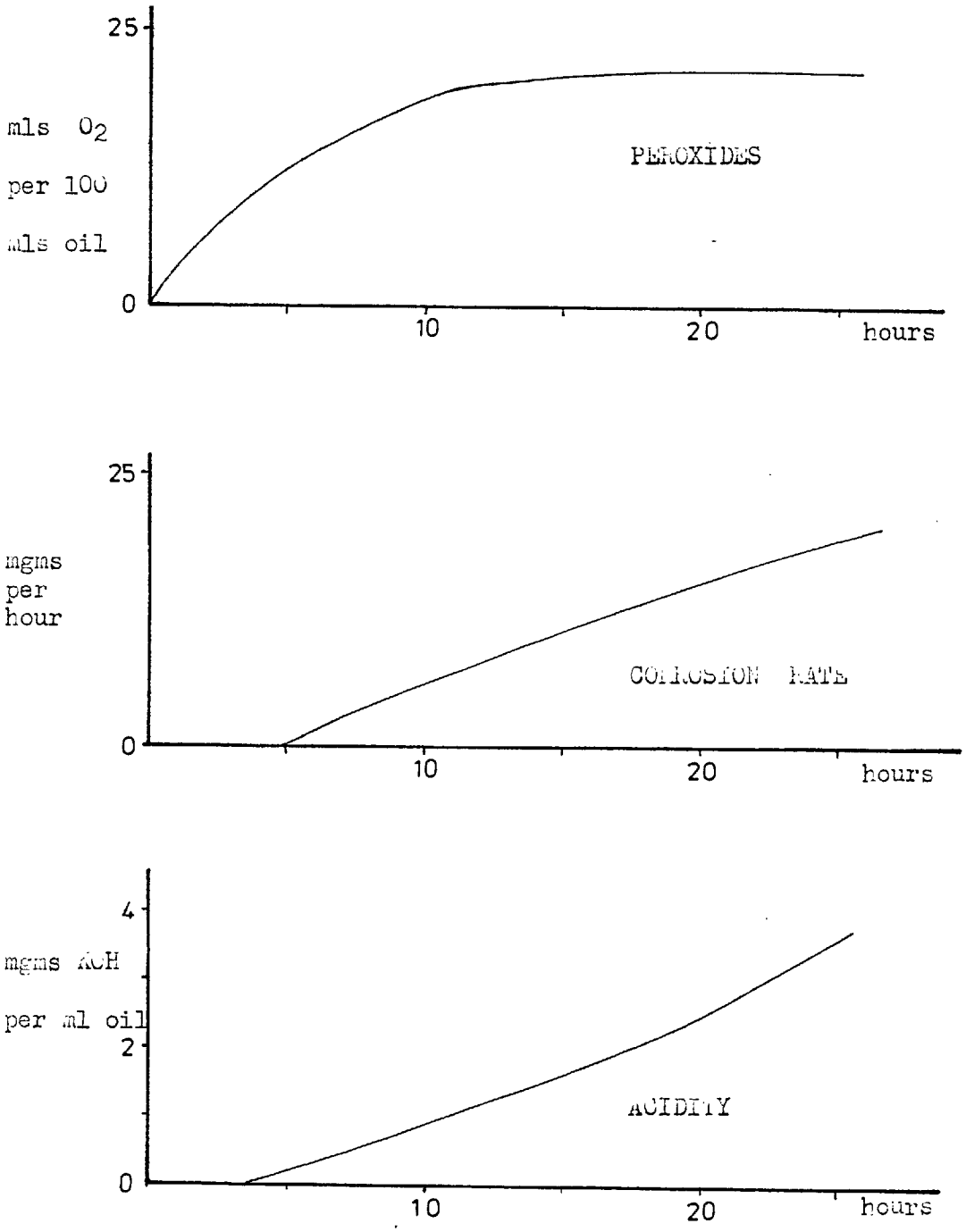

Wilson and Garner's oxidation and corrosion results of tests with engine oils. ref 63.

Figure 7.2.3 after Chakravarty, ref. 93.

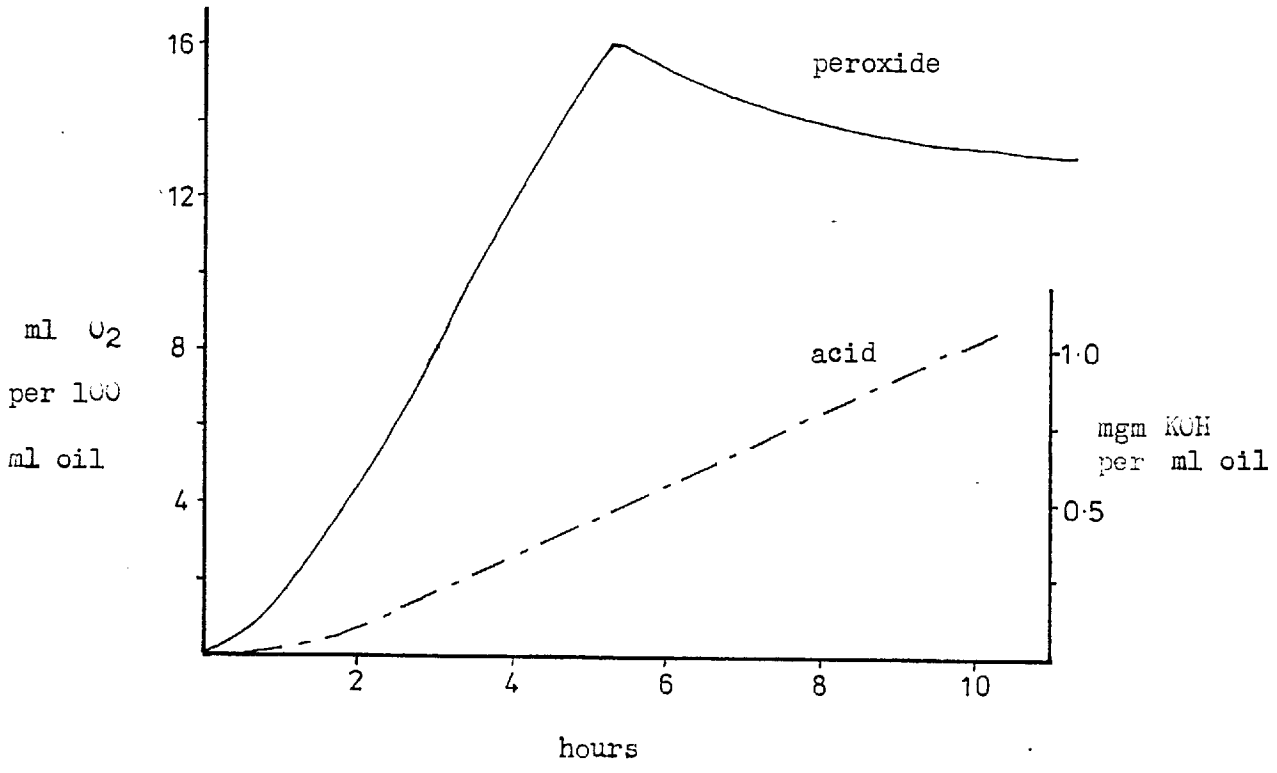

(a) Oxidation of White oil. Copper catalyst.

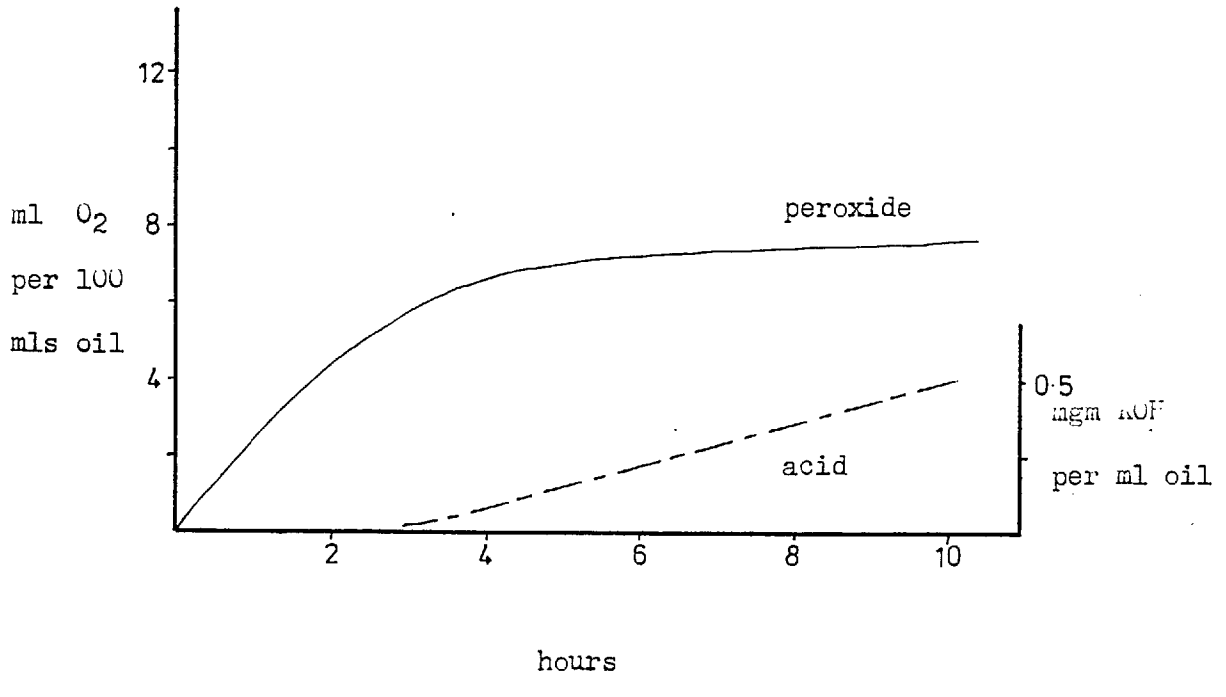

(b) Oxidation of White oil. Iron catalyst.

is due to the inhibitory effect of the accumulating acids.

Denison[92] suggested that the acids take part in a secondary corrosive process reacting with the oxidised metal to form organometallics.

The above results demonstrate that both acids and peroxides produced as a result of oil oxidation are corrosive and therefore might be thought to have a detrimental effect on a metal contact. However, this is not always found to be the case.

Yamamoto and Hirano[95] have demonstrated that in the temperature range 20-150°C a used white oil gave consistently lower friction than an unused oil. It was said that this was because the peroxides present in the used oil reacted with the metal surface to form oxide films with a resultant decrease in friction. An alternative explanation might be the adsorption of acids (shown to be present in the used oils) onto the surface.

Rudston[6] who investigated the effect of a number of different chemicals on the wear in a four-ball rig found long chain organic acids such as might result from oil oxidation to be one of the most potent anti-wear agents.

Conversely, Mould and Silver[10] found that acids produced as a result of oil oxidation had a detrimental effect on the fatigue lives of balls in a rolling four-ball rig. In cases where fretting wear has a fatigue component such behaviour will counteract the advantages of an adsorbed layer.

The conditions of oxidation imposed by Mould and Silver were severe. In one series of tests 15mls of oil was used in the ball pot and was not circulated. An ester showed a linear increase in acidity over a 2 hour test to a T.A.N. of 0.4. However, when 1.2 litres of the oil was circulated through the pot, after a succession of tests, they observed only a small increase in acidity (less than 0.05 T.A.N.) (fig. 7.2.4). The rate of oxidation of an oil is therefore related to the degree of exposure to the severe conditions of a contact.

Figure 7.2.4

The results of Mould and Silver [10] showing the increase in acidity of oil in a rolling Four-ball rig.

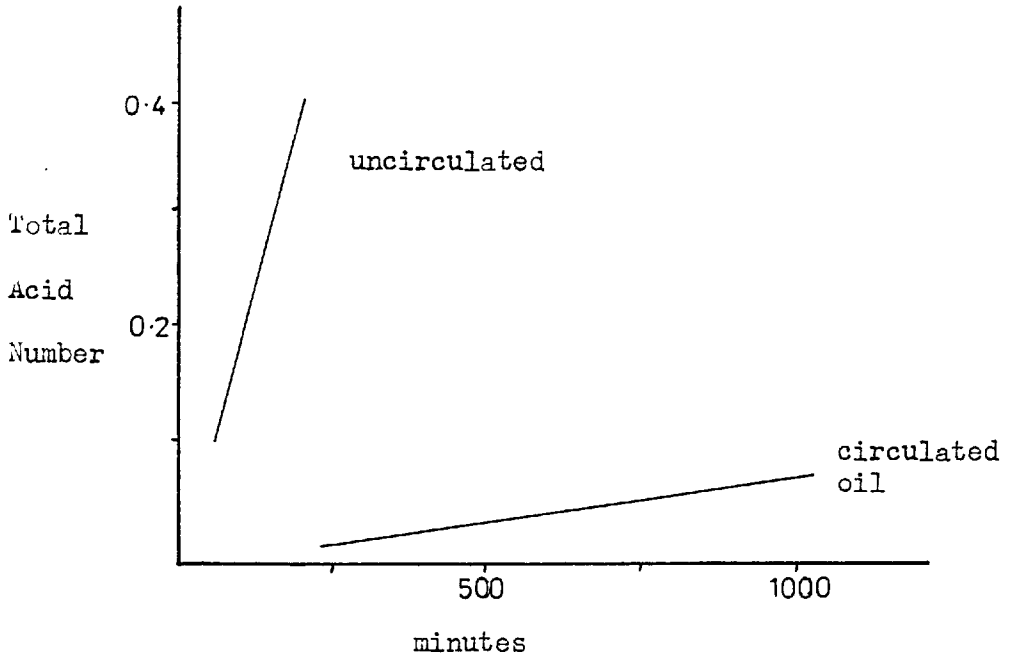

RESULTS AND DISCUSSION

PART A

7.3 Results of tests with Ester Base Stock

The deterioration of the ester lubricant during fretting was studied in detail under two different atmospheres - a test in dry air (test D) and a test under dry oxygen (test E). Samples of oil were extracted from the rig at frequent intervals for analysis for acid and peroxides and for measurement of the oxygen activity. Figures 7.3.1, 7.3.2 and 7.3.3 compare the wear, oil acidity and peroxide content of the two tests. Figs. 7.3.2 and 7.3.3 also show the results of a control experiment (K) in which there was no fretting motion. During the fretting tests D and E the oxygen concentration in the oil was maintained at 0.8 and 4 millimoles/litre respectively. Both tests show an initial period during which wear increases linearly with time.

The rates of increase of peroxides and increase in acidity appears to be related to both the oxygen concentration and the wear rate. The peroxide concentration was found to increase rapidly at first but after about 50 hours it remained approximately constant. On the other hand, a fairly slow increase in acidity was observed initially, with a transition to rapid increase at about the time the peroxide concentration and the wear first began to level off.

The length of the initial wear period had been observed (Chapter 4) to depend on the oxygen concentration.

Figure 7.3.1

Fretting wear with Ester lubricant.

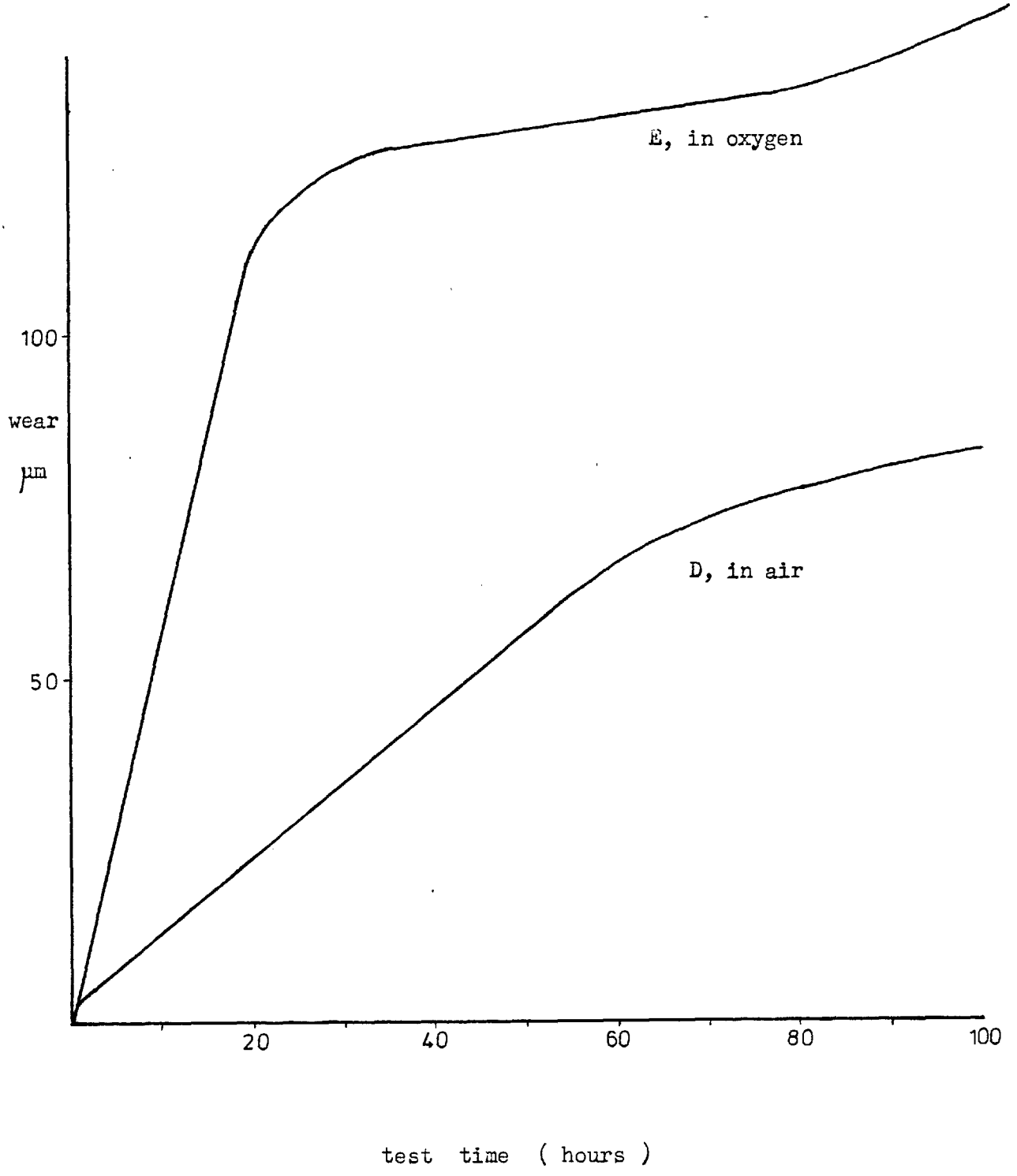

Figure 7.3.2

The increase in acidity during fretting tests in Ester

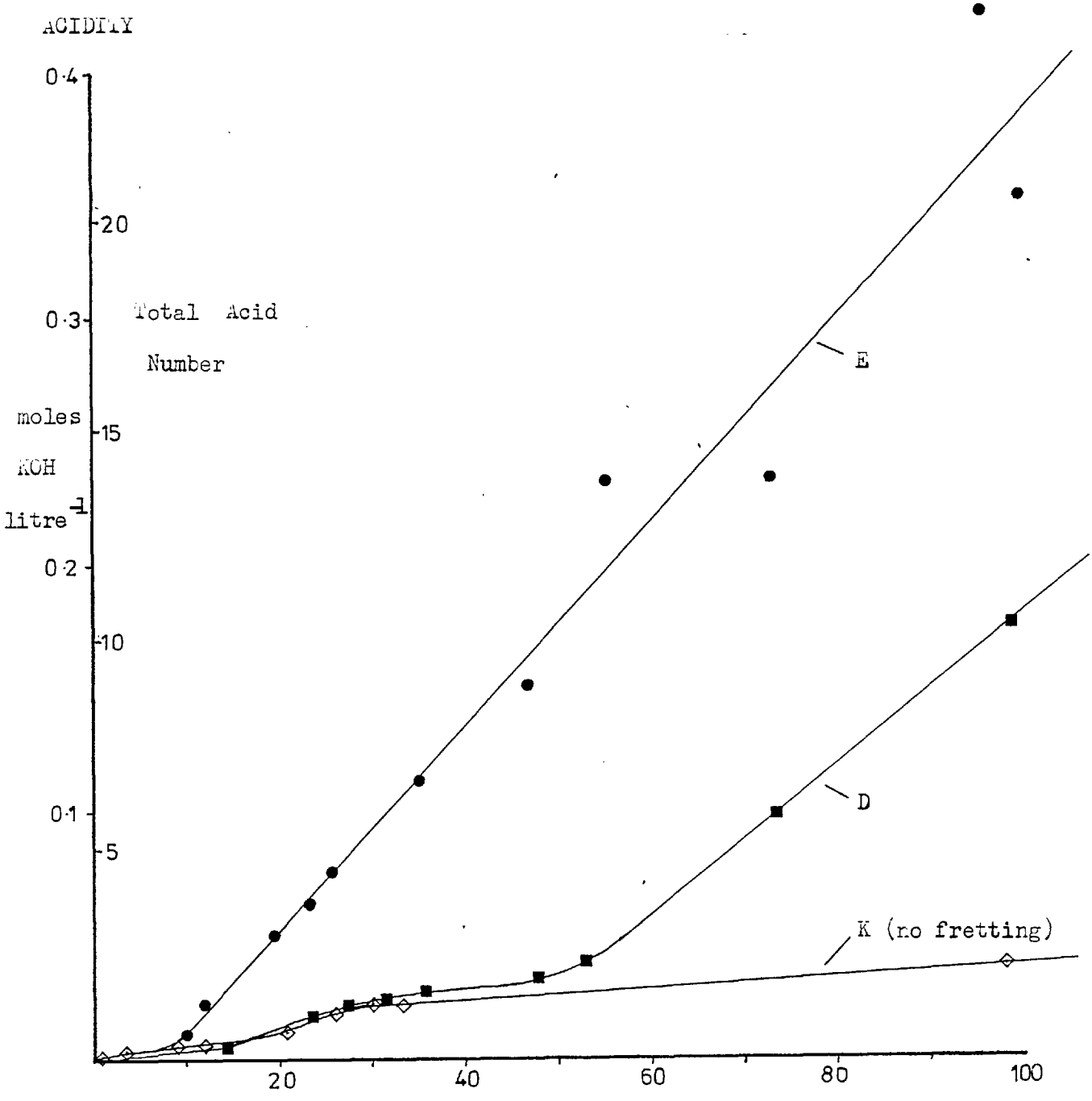

Figure 7.3.3

The increase in Peroxide concentration during fretting tests with Ester

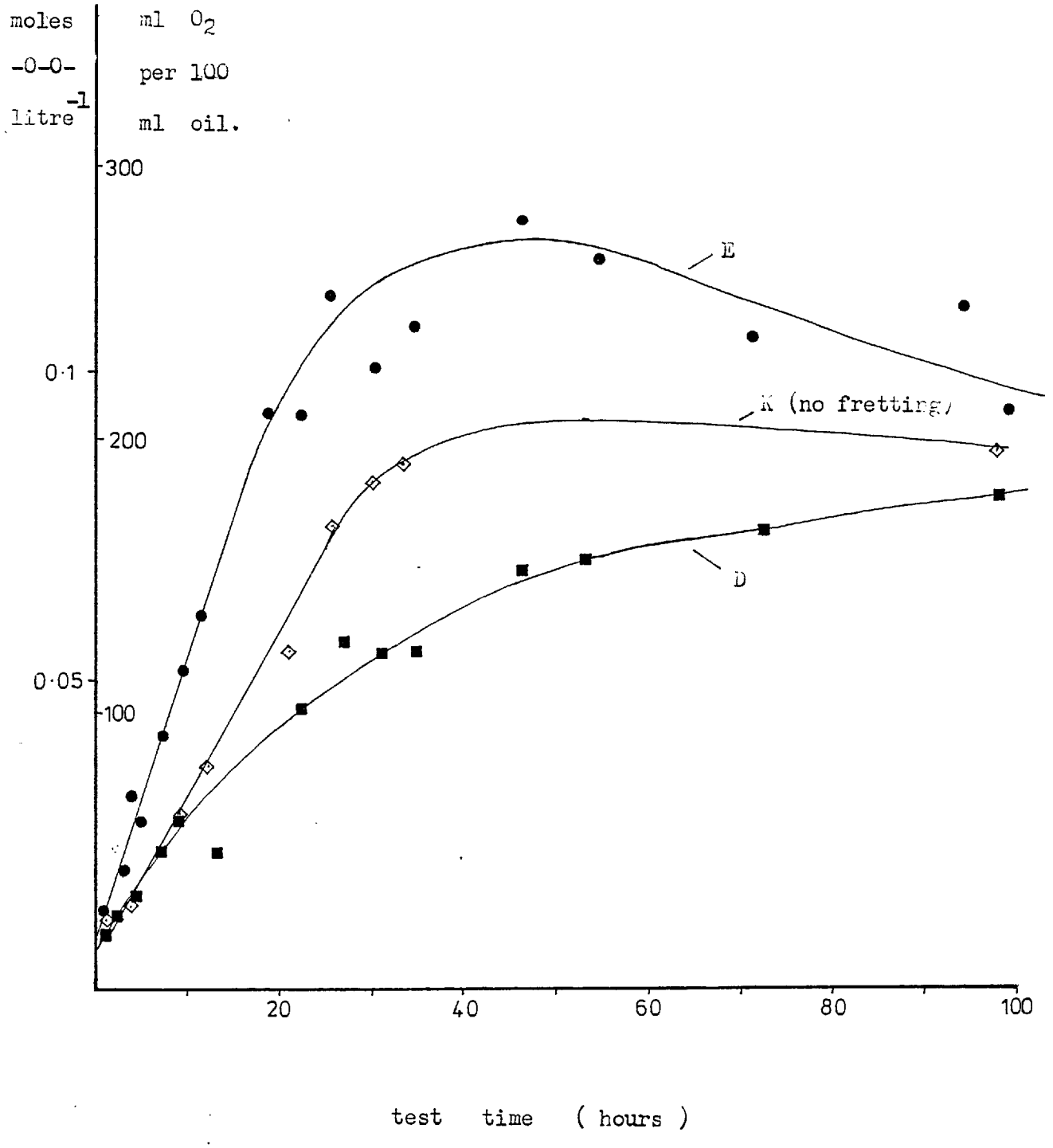

At the end of the initial wear period the following measurements were made.

Test	Oxygen Activity	Wear During Initial Period	Length of Initial Period	Acidity M	Peroxide Moles Litre $^{-1}$ OOH
E	3.9 - 4.7	113 μm	20 hr	5×10^{-2}	10^{-1}
D	0.7 - 0.85	63 μm	55 hr	4.6×10^{-2}	7×10^{-2}

These results show that the limit of the initial wear period is marked not by a certain amount of spline wear but by the attainment of a critical acidity and peroxide concentration. The build up of acidity and peroxides to critical concentrations is more rapid under conditions of high oxygen activity and therefore the initial wear period is shorter.

Metal Catalysis of Oil Oxidation

Oxidation of oil in the fretting rig is complicated by the presence in the circulation system of a variety of metals which might act as catalysts - steel, copper and brass. In addition, the fretting process is constantly exposing areas of highly active nascent metal at flash temperatures of up to 110°C (see section 2.5.3). The control test enables the effect of the fretting on the oil oxidation to be distinguished. A sample of the ester was oxidised in the rig at the standard test temperature (80°C) in the presence of a spline specimen pair and under a high oxygen atmosphere which resulted in a dissolved oxygen activity equivalent to 3.4 m moles litre^{-1}. In this test the specimens were not fretted. Acid and peroxide measurements were made in the usual way and the

results have been plotted in figs. 7.3.2 and 7.3.3. As with the fretting tests, the peroxide concentration increased asymptotically to a value in the region of 10^{-1} moles litre^{-1} of peroxide. The acidity shows a different behaviour - no transition to rapid increase being shown even after 200 hours. What is more, the acidity at any given time was similar to that of the low oxygen fretting test and well below the high oxygen test.

7.4 Discussion of Ester Results

7.4.1 Summary of Results

The main results of acid and peroxide measurements have been summarised in table 7.1. From these tests the following conclusions may be drawn.

1. Whilst the rate of build up of peroxides within the oil is dependent on the oxygen concentration and rubbing, the equilibrium concentration attained in all 3 tests was similar - in the region of 0.1 moles litre^{-1} of peroxide.
2. The acidity of the lubricant increases slowly until, at about the same time that the fretting wear rate drops, it increases rapidly.
3. A higher concentration of oxygen in the lubricant increases the initial fretting wear rate.
4. High oxygen concentrations reduce the time for attainment of reduced fretting wear/increased acidity.

In the following discussion it will be shown that these observations are consistent with an oxidative mechanism for wear - the oxidant species being peroxy radicals formed as a result of oil oxidation.

7.4.2 Metal Catalysis of Oil Oxidation

The mechanism of oil oxidation has been outlined in

Table 7.1

Summary of the Behaviour of the Measured Quantities in the Fretting Tests

Test:	High (O_2) & Fretting	Low (O_2) & Fretting	High (O_2) No Fretting
Peroxide Conc'n.	Fast build-up and levels off at 0.1 moles -00-/ litre	Slower build-up and levels off at 0.08 moles -00-/litre	Intermediate rate of build-up to same level
Acidity	Slow build-up followed by fast after short time	Longer period of slow build-up followed by fast build-up	Slow build-up NO fast build-up
Fretting Wear	High wear rate. Suddenly drops	Slower wear rate - drops more gradually	-

section 4.4 in which the scheme shown in fig. 7.4.1 was introduced. To put it simply, oxidation is initiated by various activated processes after which the oxidation chains multiply by the breakdown of hydroperoxide reactions (5) and (6) leading to rapid oxidation (reactions (7) and (8)).

Metals catalyse both the initiation step and the breakdown of hydroperoxide:

In the initiation stage the metal accepts an electron[59]

$$RH + M^{2+} \longrightarrow R\cdot + H^{+} + M^{+} \qquad (a)$$

Hydroperoxide breakdown is catalysed by the donation of an electron[59]

$$ROOH + M^{+} \longrightarrow RO\cdot + {}^{-}OH + M^{2+} \qquad (b)$$

The activity of the steel as a catalyst will be affected by fretting. It was noted that the difference in the shapes of the peroxide curves at high oxygen, with and without fretting (fig. 7.3.3) is similar to the difference observed by Chakravarty between copper and iron as catalysts of oil oxidation, although the peak peroxide concentrations observed in the latter case were much lower (see fig. 7.2.3). The more active metal (Cu) produces a peak in the peroxide curve from which the concentration descends to an equilibrium value whereas the same value is approached from below when catalysed by iron. This similarity indicates that the catalytic activity of the steel is enhanced by the action of

Figure 7.4.1

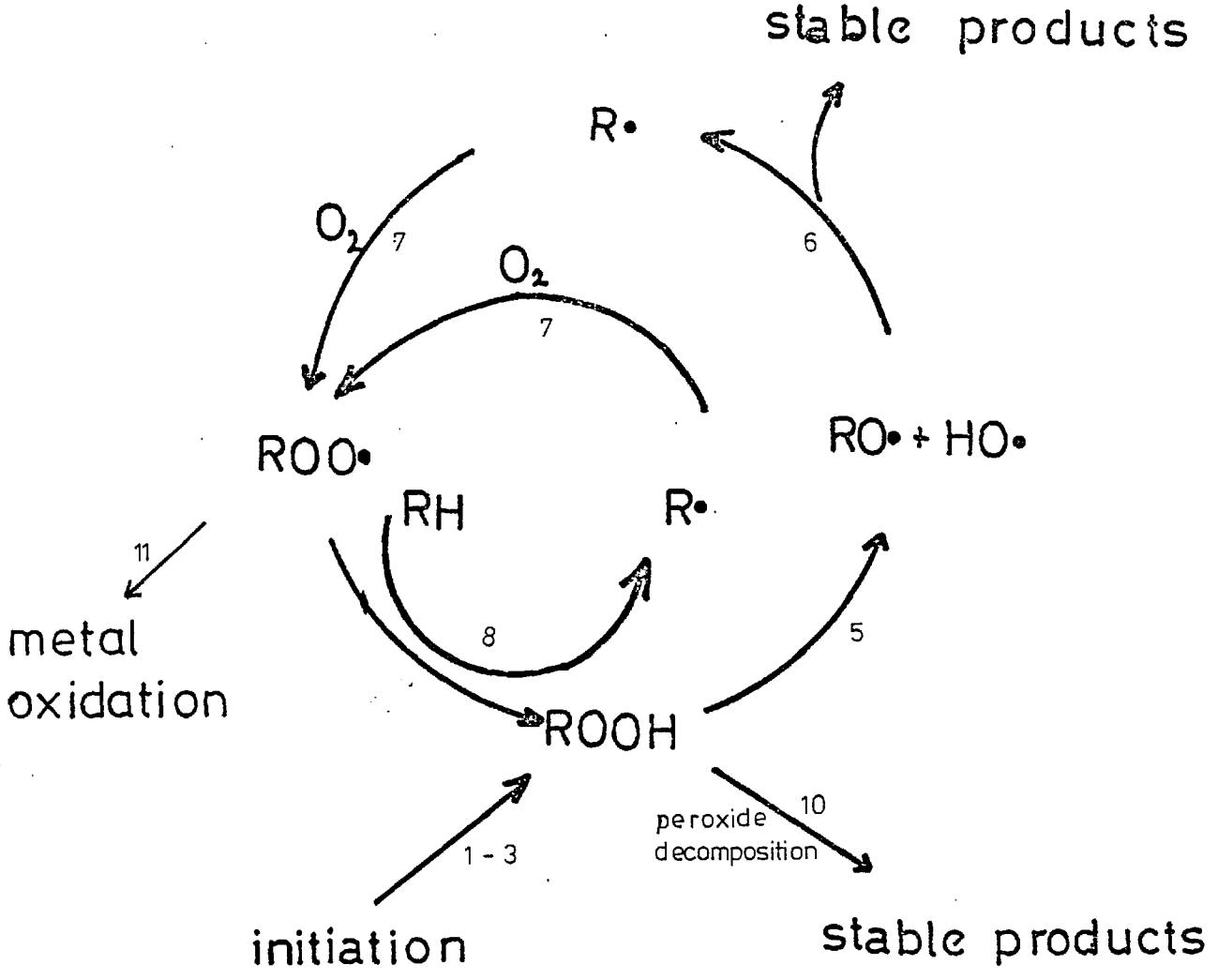

A diagram illustrating the reaction sequence during the steady state propagation stage of hydrocarbon oxidation.

fretting.

Waterhouse[47] has shown that in an electrolyte, fretting leads to an increase in electro-negativity of the metal surface. Kostetskii[36] has suggested that disruption of the surface layers results in a decrease in the activation energy for electron emission. Thus the effect of fretting is to increase the ease of donation of an electron by the metal (reaction (b) above); consequently a higher concentration of radicals and a more rapid rate of oxidation results.

7.4.3 Adsorption of Acid by Debris

The slow rate of acid concentration increase in the early stages of the test is due in part to the slow rate of oil oxidation at this time but also to the adsorption of dissolved acid onto the fretting debris. It is well known that organic acids readily adsorb onto metallic and oxide surfaces and in doing so generally reduce the friction between surfaces by forming a boundary layer. Oleic acid for instance acts as a boundary lubricant in this way.

The observation that the increase in acidity with time was more rapid once the wear rate had dropped suggests that the wear debris was acting as an adsorbent for the majority of the acid produced. A rough calculation may be made using the acid data to show whether such a hypothesis is reasonable. The rate of accumulation of acid is known at the initial and the secondary wear rates. The volume of debris produced is also known and thus it is possible to calculate an approximate size for the particles of debris.

The rate of accumulation of acid in test E after the induction period was an increase in molarity of 4.25×10^{-3} per litre per hour. The initial wear rate was 5.65 μm/hour. For the purposes of this calculation the wear rate after the induction period and the acid build up within the induction period are neglected. If it is assumed that within the induction period the acid is being produced by oxidation at the same rate as that measured after the induction period then the debris generated must be sufficient to eliminate the acid from solution during the induction period.

If the molecules adsorb onto the surface as shown in fig. 7.4.2 each molecule will occupy about 0.21 nm^2 [102,103].

There are 70 mls. of oil. It therefore follows that

The number of molecules generated in one hour =

$$4.25 \times 10^{-3} \times 70 \times 10^{-3} \times 6 \times 10^{23}$$

$$= 18 \times 10^{19}$$

Area covered by this number = $18 \times 10^{19} \times 0.21 \times 10^{-18}$

$$= 38 \text{ metres}^2$$

In test E the whole of each tooth surface was wearing.

The combined contact area = 12 x tooth area

$$= 12 \times 3.2 \times 10^{-5}$$

$$= 3.84 \times 10^{-4} m^2$$

The wear volume is therefore = $3.84 \times 10^{-4} \times 5.65 \times 10^{-6}$

$$= 2.2 \times 10^{-9} m^3 \text{ hour}^{-1}$$

Partial oxidation of the debris would increase its volume by about half as much again, i.e. $3.3 \times 10^{-9} m^3$. [112]

Assuming that the debris is in the form of N spherical particles of radius r

Figure 7.4.2

The Adsorption of Acid molecules onto a surface.

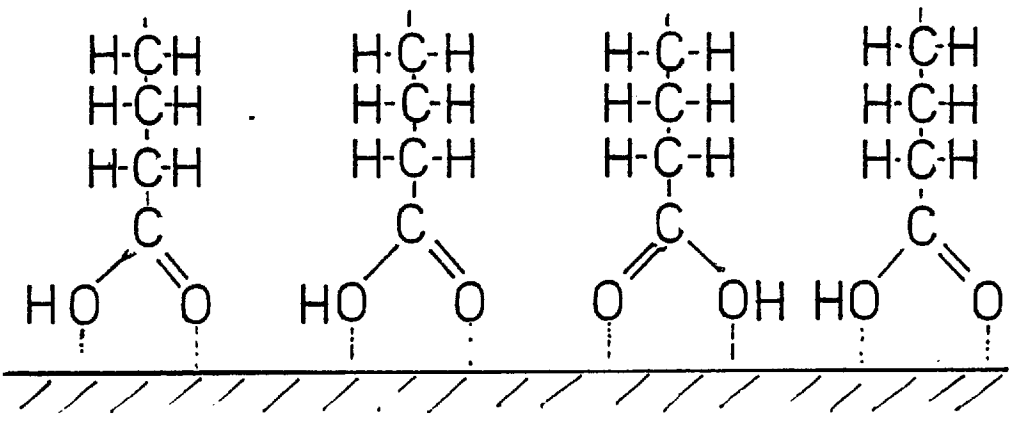

Then r is given by

$$r = 3 \times \frac{\text{Wear volume}}{\text{adsorbing area}}$$

$$= \frac{3 \times 3.3 \times 10^{-9}}{38}$$

$$= 0.26\text{nm}^{*}$$

The production of wear particles of such a size is most unlikely considering that reported observations of debris size from fretted steel have been in the range 0.1 - 1μm[†]. It is possible that comminution in between the spline surfaces would lead to a reduction in size of the debris but it is most unlikely that such a small size would be reached. It would be useful to measure the debris size but unfortunately scanning electron microscope studies of the debris could not resolve the particle size. Another factor is that the occupation of the sites on the debris surface by the ester molecules has been ignored - if this were to be included it would further reduce the value of r. On balance it seems likely that the rate of acid production in the early stages of the test is close to that observed and the concentration of acid is not greatly affected by adsorption onto the debris.

7.4.4 The Role of Hydroperoxides as Pro-wear Agents

As a result of fretting tests in mineral oils P. M. Ku speculated that hydroperoxides might be responsible for spline wear[12]. Rudston[6] observed that additions of cumene hydroperoxide to the lubricant of a four-ball

---

* A calculation based on the results of test D gives a similar result.

† Waterhouse[1] Chapter 6

wear rig promoted sliding wear.

However, the results presented in figs. 7.3.1 and 7.3.3 show conclusively that the wear rate is independent of the hydroperoxide concentration. On the other hand the graphs do show that the rate of hydroperoxide accumulation is closely related to the wear rate. There are two possible explanations for this relationship. Either hydroperoxides are produced as a result of wear, or the precursors of hydroperoxides and the species responsible for wear are one and the same. The first alternative can immediately be rejected because the similar peroxide results of the control test show that fretting does not govern the hydroperoxide accumulation. Peroxy radicals (designated ROO·), the precursors of hydroperoxides are therefore proposed as the attaching species in this form of fretting wear. The oil oxidation scheme can be modified to include this process, fig. 7.4.1 reaction (11). Now such a scheme can be used to explain the observed relations of wear, acidity and peroxide concentration, as shown in table 7.2.

In the absence of wear the hydroperoxide concentration builds up until the rate of decomposition by reactions (5) and (10):

$$ROOH \longrightarrow RO\cdot + HO\cdot \qquad (5)$$

$$ROOH \xrightarrow{\text{rearrangement}} R' = O + R''OH \qquad (10)$$

equals the rate of hydroperoxide production by initiation processes: $RH \longrightarrow R\ast H \xrightarrow{+\,O_2} ROOH$

and reaction (8): $ROO\cdot + RH \longrightarrow ROOH + R\cdot$

TABLE 7.2

A summary of oxidation processes occurring during a typical fretting test.

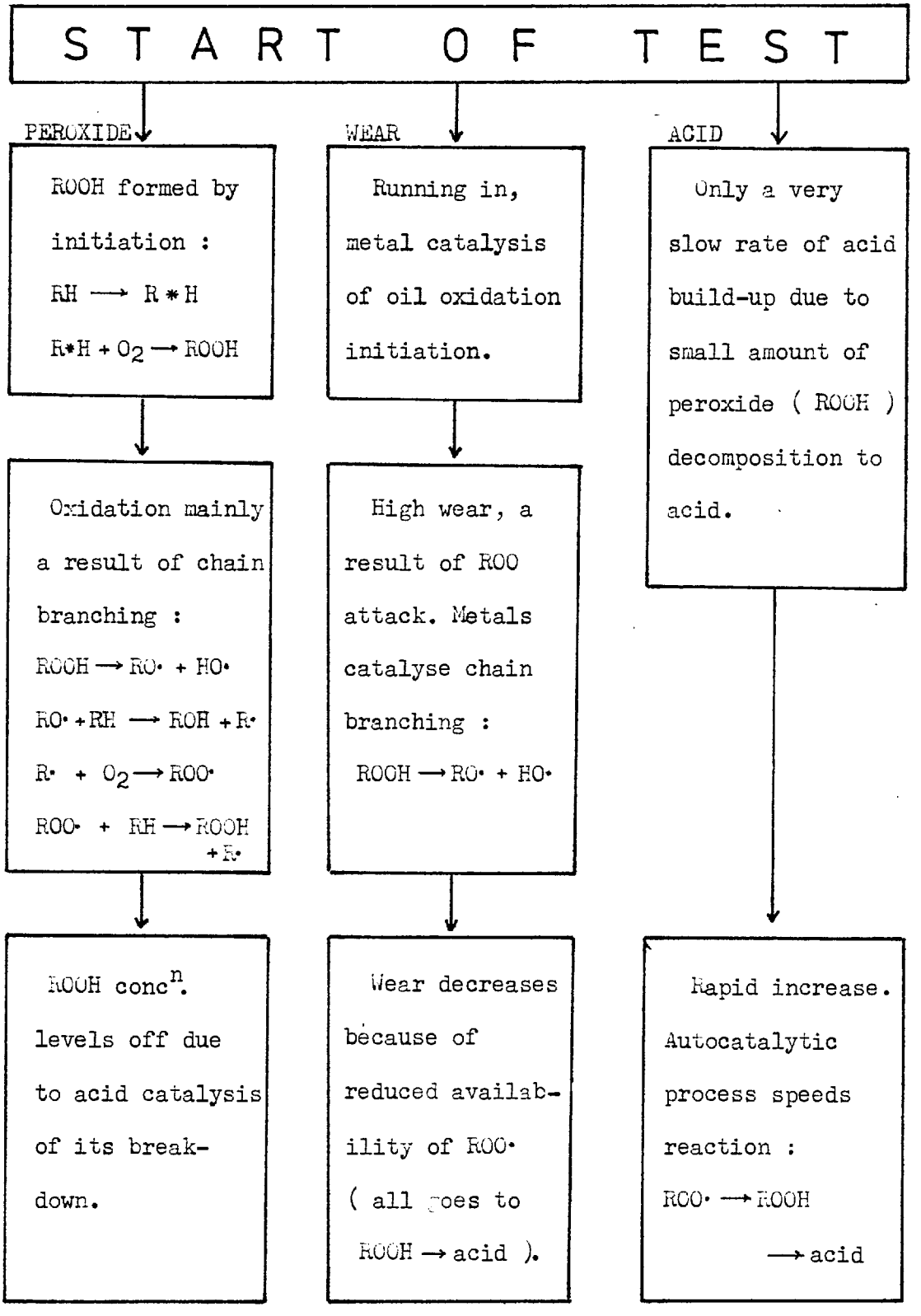

After equilibrium is reached there is a steady accummulation of acids and other carboxyl products via reactions (6), (9) and (10) (fig. 7.4.1).

Hydrocarbon oxidation in acidic solution tends to proceed beyond the ketone alcohol stage to yield carboxylic acids and the formation of small amounts of acid serves to promote the formation of more acid by enhancing decomposition of ROOH via reaction (10)[93]. In addition in the presence of acid there is a tendency for the ROO• radical to accept hydrogen from the acid group. The acid is in competition with the hydrocarbon (RH) to donate a proton to the radical. As the acidity increases this competition has two results. Firstly, the lifetime of the ROO· radical in solution will be reduced and secondly there will be a decrease in the production of fresh R· radicals by reaction (8), leading to a reduced rate of production of peroxy radicals. The effect of fretting is to speed up the whole process by catalysis in both the initiation stage and the propagation cycle as was discussed in section 7.4.2. Thus fretting test 'E' showed a more rapid increase in the peroxide concentration than the control test 'K'. However, the wear reaction introduces further competition for the ROO• radicals. Whilst the acidity is low at the beginning of the test, it is likely that many of the radicals generated within the contact will react with the metal surface. However, as the acidity increases in the course of a test decreasing quantities of ROO· will be available

for reaction with the metal leading to a decrease in wear rate.

In other words it is postulated that at a critical concentration the acid products of ester oxidation become effective peroxide decomposers controlling both the hydroperoxide concentration and the fretting wear rate - in so far that it is an oxidative process.

7.4.5 The Nature of the Wear Reaction

It has been shown that in the ester lubricant the initial wear rate is linearly dependent upon the activity of the oxygen dissolved in the oil. The major wear mechanism at high wear rates appears from surface studies to be one of abrasion. The results of X-ray diffraction analysis indicated that the majority of the debris was oxidised. It appears that the rate of abrasion depends on the degree of oxidation of the debris (see chapter 9). The results discussed above indicate that the peroxy radicals are responsible for oxidising the metal. There are a number of possible reactions:

The radical may combine with the metal to form an organometallic.

The radical may donate some of its oxygen to the metal.

$$M + ROO\cdot \longrightarrow MO_2 + R\cdot$$

or

$$\longrightarrow MO + RO\cdot$$

The radical may catalyse metal oxidation by accepting an electron:

$$M + ROO\cdot \longrightarrow M^{+} + ROO^{-}$$

These possibilities will be discussed further in light of the results of tests with antioxidant additives presented in the next chapters.

7.5 Conclusions - Part A - Ester Lubricant

The results of chapter 4 showing a dependence of wear rate on dissolved oxygen activity indicates an oxidative mechanism for fretting wear of the splines in an ester lubricant.

Lubricant oxidation leads to a reduction in fretting wear. Observations of the hydroperoxide concentration show that the wear rate is dependent on the rate of increase of the hydroperoxide concentration which in turn is dependent on the dissolved oxygen concentration. The hydroperoxide concentration eventually attains an equilibrium value which is independent of the wear rate (as shown by the control experiment). However, the rate of increase in concentration of acidic oxidation products in the oil was shown to be inversely related to the wear rate.

It appears that the build up of acid in the oil inhibits wear either because it adsorbs onto the metal and debris to form a boundary lubricating layer or because it enhances the decomposition rate of the peroxy radicals and the hydroperoxides.

These conclusions are summarised in table 7.2 which illustrates the sequence of interactions between the lubricant and the wearing metal during a fretting test.

RESULTS AND DISCUSSION

PART B

7.6 Results of Tests with Hexadecane - Introduction

The wear results obtained with hexadecane were broadly similar to the ester (see Chapter 5) in respect of the variation of the 'initial wear rate' with oxygen concentration and the fall in wear rate at long test times in air and oxygen. It was assumed therefore that similar relationships between acidity peroxides and time would be observed. Furthermore it was hoped to use hexadecane as a model for the ester lubricant because of its chemical simplicity and its ease of purification.

The results obtained show however that the oxidation products which accumulate during a fretting test are different from those observed in the ester. The results presented fall into two sections:

(i) the results of acidity and peroxide determinations of tests using purified hexadecane

(ii) the results of tests run using hexadecane with an added organic acid.

7.7 Tests Using Purified Hexadecane

The acidity and peroxide content of the lubricant was measured at intervals throughout a test as previously described in chapter 6. The hexadecane was purified by the method described in chapter 5. The purified hexadecane contained no detectable acid or peroxide (i.e. less than 5×10^{-4} moles litre^{-1}). However, due to the difficulty experienced in cleaning the rig some acidity

was detected once the hexadecane had been circulated through the rig before starting the test.

The monitoring procedure was carried out for two tests - one in air (test G) and one in oxygen (test J). The wear results have been presented in Chapter 5. The results of acid and peroxide determinations are given in table 7.3. Figures 7.7.1 and 7.7.2 show the variation of these quantities with time.

The small acidity resulting from contamination is quickly reduced to a low value once fretting is started and remains at a low value throughout the test in contrast to the ester results. Also in contrast are the peroxide determinations (fig. 7.7.2). The concentration of peroxide observed was much lower than that in ester - so low in fact that the accuracy of estimation by the technique described in section 6.4 was poor. In both air and oxygen atmospheres the peroxide concentration increased to a maximum and then fell to a low level. The peroxide concentration in oxygen bubbled hexadecane was at all times lower than in air bubbled hexadecane and reached a peak earlier in the test. It is clear that the rate of peroxide accumulation does not have the correlation with the wear rate that was shown for the pure ester results.

It is thought that there are two reasons for this different behaviour.

(i) The wear rate in hexadecane was higher than that in ester under the same conditions and atmosphere. There is little adsorption of

TABLE 7.3

Fretting tests in Hexadecane. Results of Acid and Peroxide concentration determinations.

Test code	Test time hrs.	Peroxide moles/litre x 10^{-3}	Acidity	
			moles KOH/litre x 10^{-3}	T.A.N. x 10^{-2}
G	0	2.25	2.7	19
	1.25	8.5	1.8	13
	2	10.5		
	3	9.5	1.0	7
	4	9.5		
	5	5.5	0.9	6.3
	11	6.5	0.4	3
	21.25	10.8	0.8	5.7
	25.9	10.0	0.8	5.7
	32.3	2.0		
	45.4	3.25	0.25	1.8
	52.9	5.5		
	69.5	2.75	0.24	1.7
	81.7	3.25		
J	2	0.15	0.57	4.1
	3.25	0.34	0.62	4.4
	4.25	0.3	0.37	2.6
	6.7	0.15	0.33	2.3
	8.75	0.46	0.14	1
	9.5	0.4	0.37	2.6

Figure 7.7.1 Hexadecane - Acidity measurements.

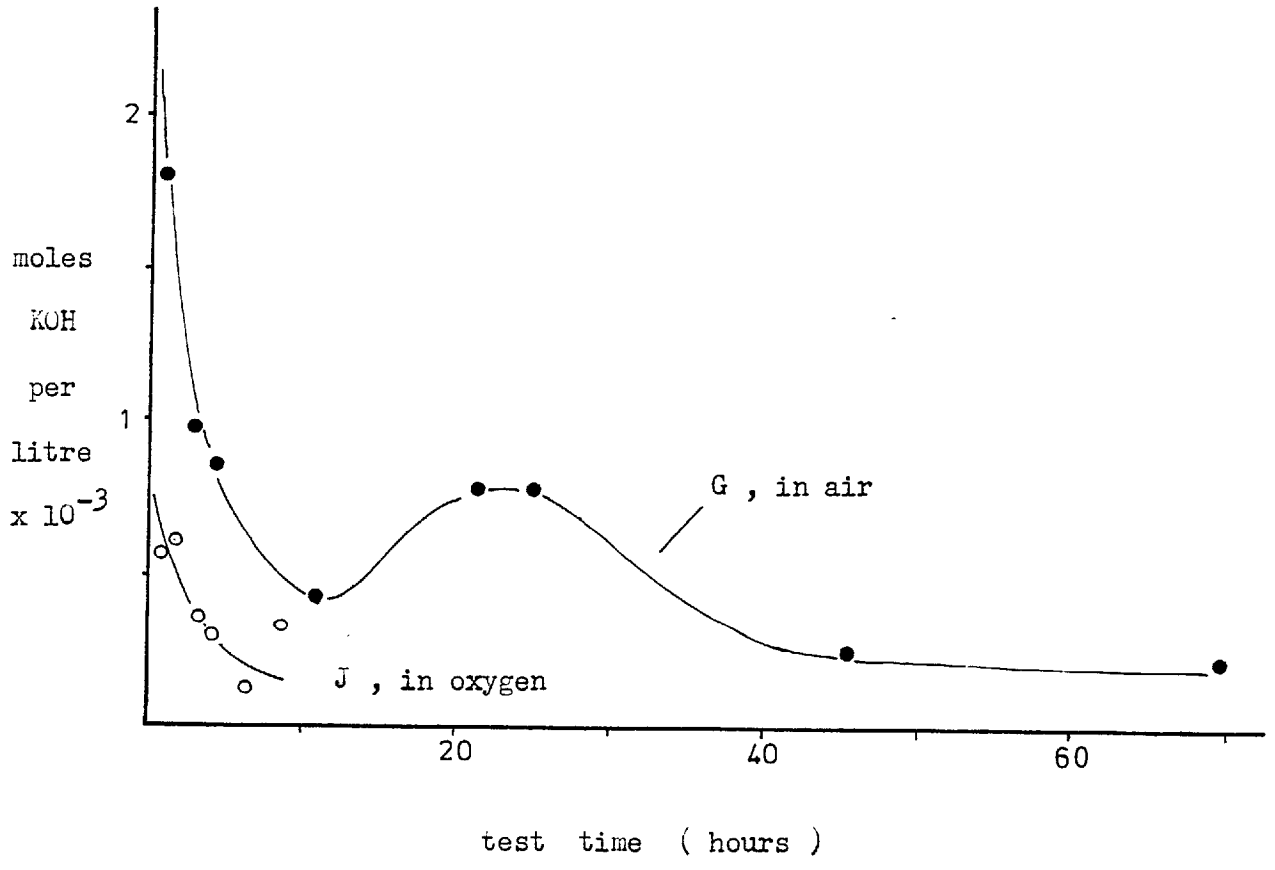

Figure 7.7.2 Hexadecane - Peroxide measurements.

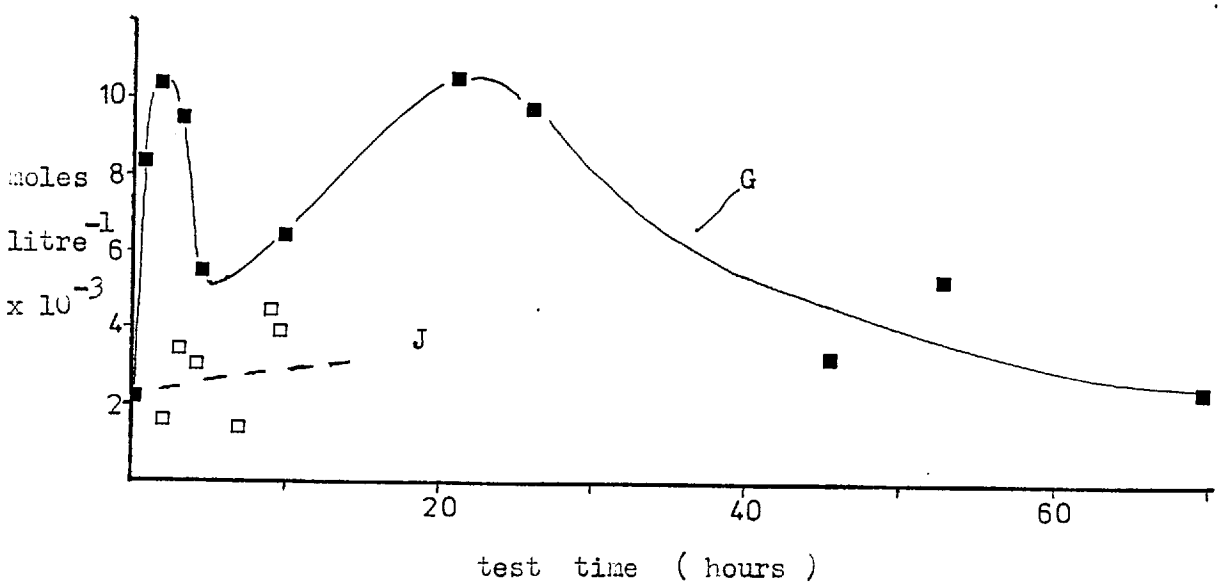

hexadecane onto the metal and debris surfaces. These factors combine to increase the adsorption of polar oxidation products from the lubricant.

(ii) The stability of hexadecane towards oxidation was observed by Stinton[68] to be initially quite high and when oxidised there was a tendency towards polymerisation of oxidation products.

7.8 Tests With Acid Added to Hexadecane

7.8.1 Introduction

It was observed that high concentrations of acid in the ester were associated with a decreased rate of wear. It was decided to test the effect of acid on wear by using purified hexadecane as a solvent for an organic acid.

The acid used was lauric acid (formula $CH_3 (CH_2)_{10} COOH$) - a typical example of the acids formed as a result of hexadecane oxidation[68]. Tests were made with two strengths of solution: 0.19M and 0.01M.

7.8.2 Tests With a Low Acid Content

The tests with the lower acid content gave initial wear rates very similar to pure hexadecane tests over a range of oxygen activities (fig. 7.8.1). The concentration of acid in solution was measured during the tests and has been plotted on the wear graphs (fig. 7.8.2 to 7.8.4). The acidity was observed to increase slightly during the first 5 to 10 hours of tests and decrease thereafter at a rate related to the rapidity of wear. This indicates that adsorption onto the debris is the explanation for the disappearance of acid from solution in hexadecane.

Based on this assumption a calculation similar to

Figure 7.8.1

Wear rates in Hexadecane with added Lauric acid (0.01 M)

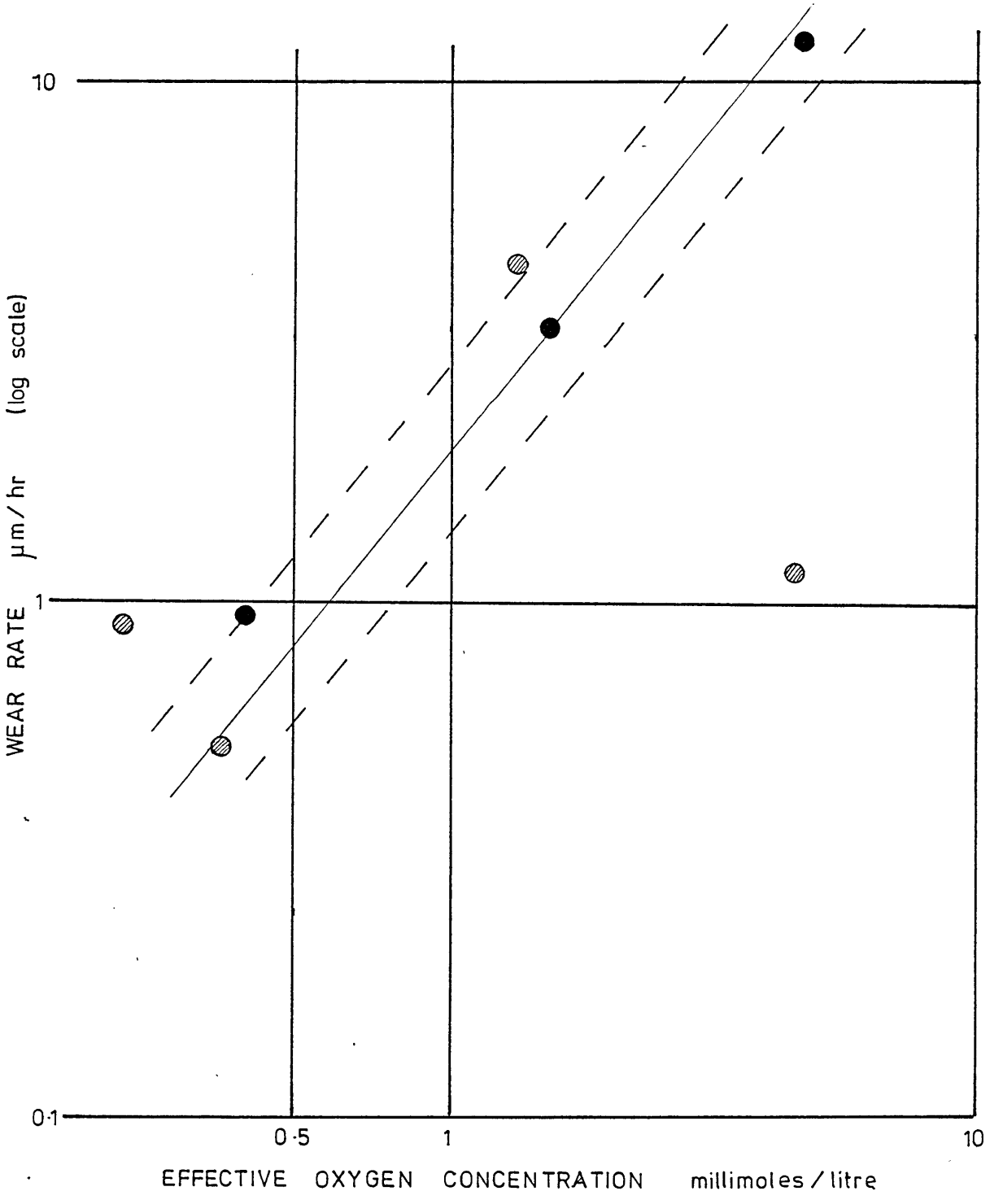

● Initial wear rate
◍ Secondary wear rate

— — —
————— Line of best fit to pure hexadecane results.
— — —

Figure 7.8.2

Test L. Wear and acidity measurements.

Hexadecane plus Lauric acid (0.01 M)

Effective Oxygen concentration : 0.3-0.5 millimoles litre^{-1}

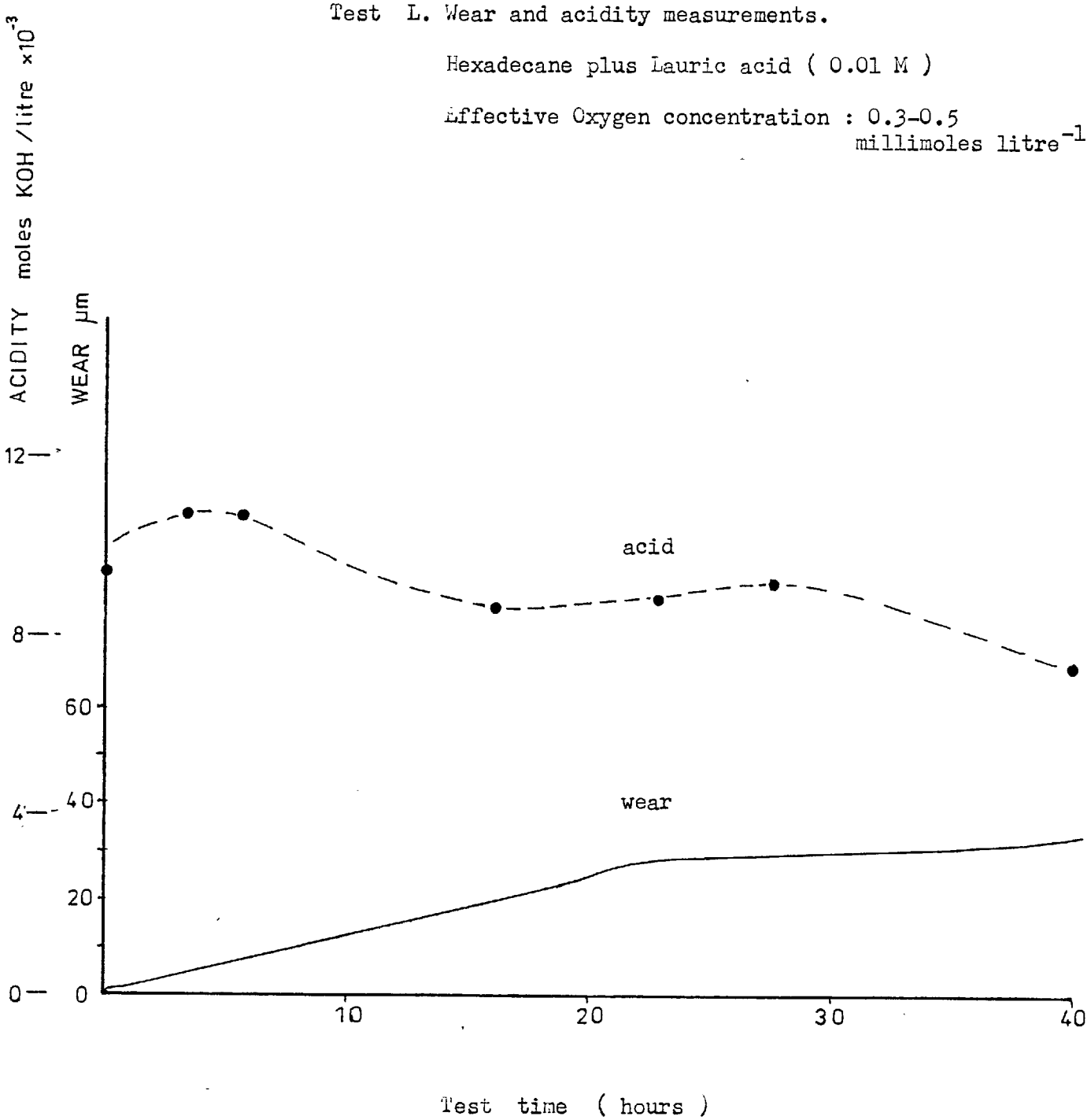

Figure 7.8.3

Test M - Wear and acidity measurements.

Hexadecane plus Lauric acid (0.01 M)

Effective Oxygen concentration : 1.5 - 1.2 millimoles litre^{-1}

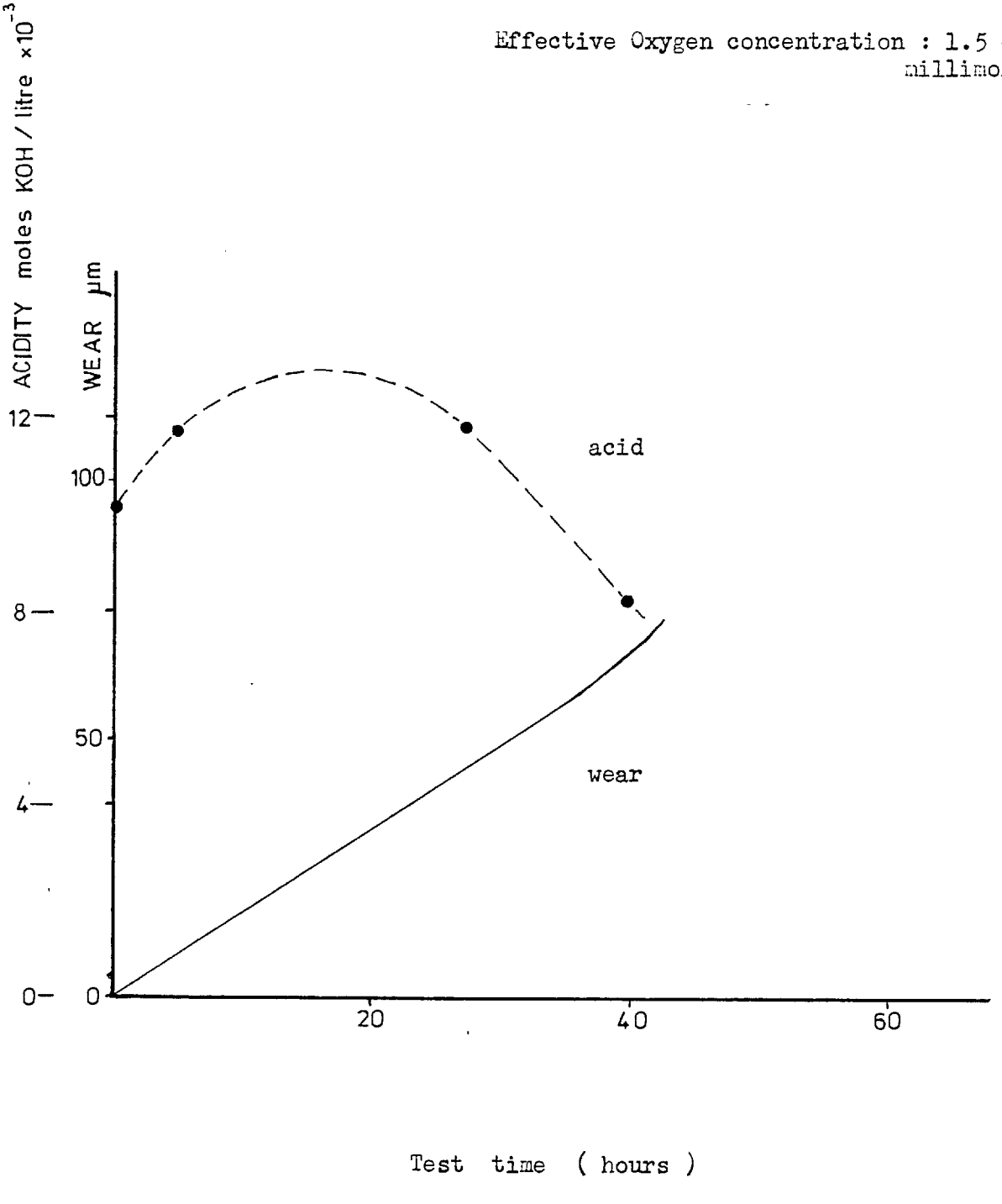

Figure 7.8.4

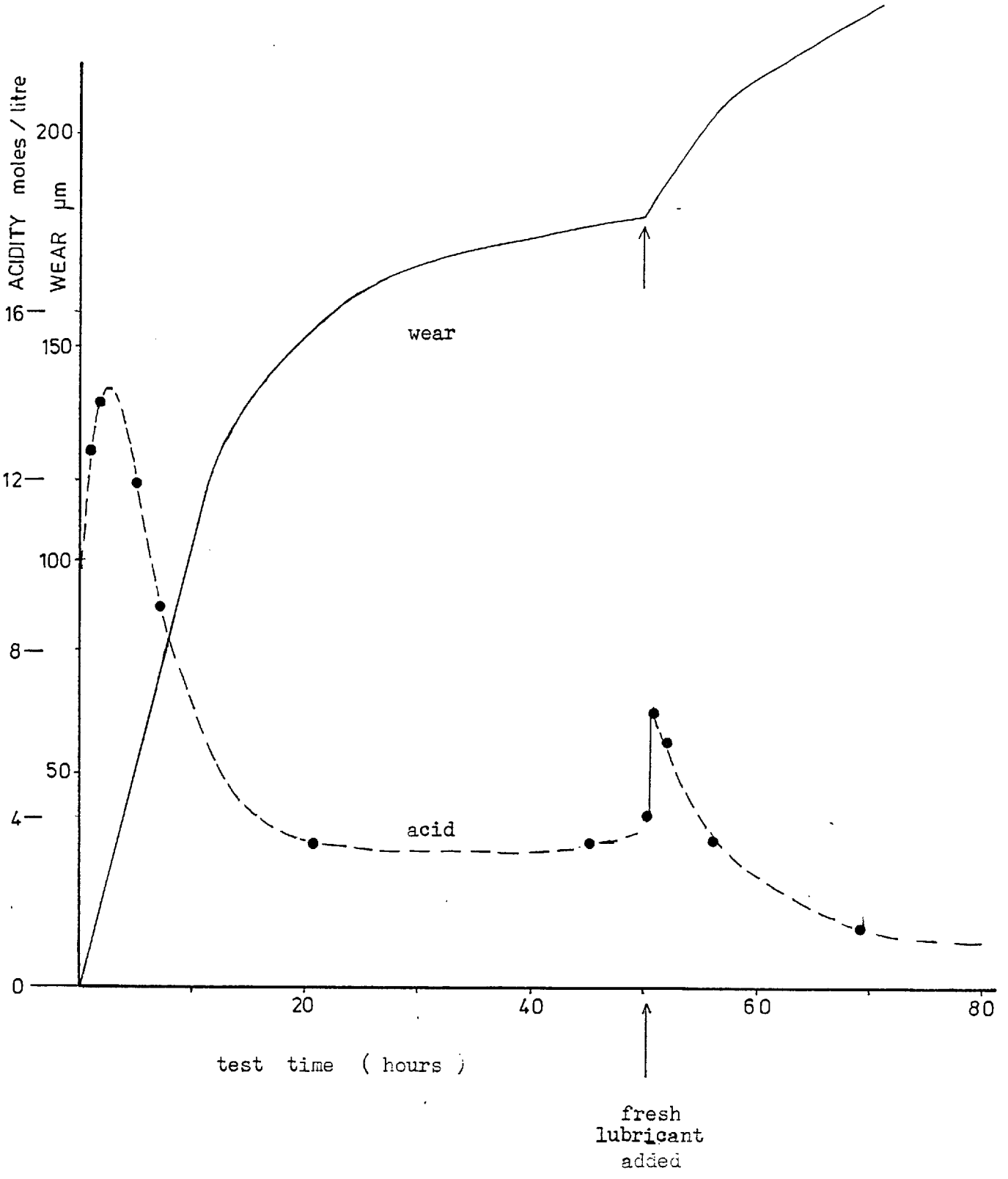

Test N - Wear and acidity measurements.

Hexadecane plus Lauric acid (0.01 M)

Effective Oxygen concentration : 5 millimoles litre^{-1}

that of section 7.4.3 may be made to estimate the particle size of the debris. In this instance it is assumed that acid generation is negligible and the debris is just sufficient to adsorb the acid at the rate observed. In test 'N' the acidity dropped at a maximum rate of 1.3×10^{-3} moles litre^{-1} hour^{-1} whilst a wear rate of 11.3 μm hour^{-1} was recorded.

Calculation

The rig contains about 70 mls of oil

⇒ Number of acid molecules adsorbed in one hour

$= 1.3 \times 10^{-3} \times 7 \times 10^{-2} \times 6 \times 10^{23} = 5.5 \times 10^{19}$

Assuming that each molecule occupies 0.21 nm^2 the area covered = 11.6 m^2.

The volume of debris produced in one hour

$= 12 \times$ tooth area $\times$ wear depth

$= 12 \times 3.2 \times 10^{-5} \times 11.3 \times 10^{-6}$

$= 4.3 \times 10^{-9}$ m^3.

Allowing for oxidation the debris volume may be taken as approximately 6.5×10^{-9} m^3.

Assuming that the debris is spherical and of a size sufficient to just absorb all the acid the radius of such particles may be derived:

$$r = \frac{3 \times V}{A} = \frac{3 \times 6.5 \times 10^{-9}}{11.6} = 1.7 \times 10^{-9} \text{m}$$

Similar calculations on the data presented in figs. 7.8.2 and 7.8.3 yields values for r of 0.88 nm for test 'L' and 1.05 nm for test 'M'. These values are about 5 times greater than those calculated previously (section 7.4.3), but is still well below the size typically reported in fretting wear[1].

Further evidence of adsorption of the acid by debris was furnished by the following test.

A sample of debris was collected from the rig at the end of test 'N'. Any contaminant hexadecane was removed by washing with toluene and then the toluene evaporated off. Thirty mgms of this debris was then shaken vigorously in 10 mls of titration solvent. The acidity of the solution was then determined by titration to be 5 x 10^{-4}M (i.e. 1.7 x 10^{-6} moles mgm^{-1} had desorbed from the debris into the solvent). Thus at the end of this particular fretting test each milligram of debris contained at least as much physically adsorbed acid as was in solution in a millilitre of hexadecane.

The above arguments support the theory that the debris absorbs the acid from the oil. An additional explanation for the disappearance of the acid is the catalysis of polymerisation of the acid by fretting. Evidence in support of this is provided by the results of mass spectra taken of samples of hexadecane from test 'G', which showed an increasing concentration of polymerised products as the test progressed. (See section 6.3.4.)

An interesting footnote to test 'N' is the observation that the addition of 15 mls of fresh oil to replenish losses due to evaporation after 50 hours resulted in a brief increase in wear rate. The oil added contained acid at the initial concentration (10^{-2} M) which resulted in the increase in acidity of the bulk shown in fig. 7.8.4. As the acidity falls away the wear rate returns to a low value. This indicates that either

(i) the increased acidity causes an increase in wear. This is unlikely since initial wear rates are similar with and without added acid.

(ii) the presence of fresh oil causes an increase in wear, i.e. changes take place in the oil after a number of hours which reduce the wear rate from that possible in fresh oil. For further discussion on this point see section 4.9.

7.8.3 Tests With High Acid Content

Tests were conducted with a 0.19 M solution of lauric acid in hexadecane in air and nitrogen atmospheres. In air no wear was observed after the tenth hour of the test and in the period 1-10 hours the wear rate was very low (0.25 $\mu m\ hour^{-1}$). The oxygen activity was increased throughout the tests in an attempt to promote wear up to 1.5 millimoles of oxygen per litre. After about ten hours the oil was observed to have a greenish tinge an indication that organometallics were being formed - probably copper laurate. On dismantling of the rig after the test the copper components of the oil circulation system were found to have been mildly attacked. Measurements of the final acidity found it to be slightly reduced at 0.14 M.

In contrast two tests performed with the lubricant under a nitrogen atmosphere gave rates of wear comparable with or in excess of those recorded with the acid-free hexadecane. As a result the plot of wear rate versus oxygen activity (fig. 7.8.5) shows a sharp fall with increasing oxygen activity, caused it is thought by the formation under oxidising conditions of the metal soap

Figure 7.8.5

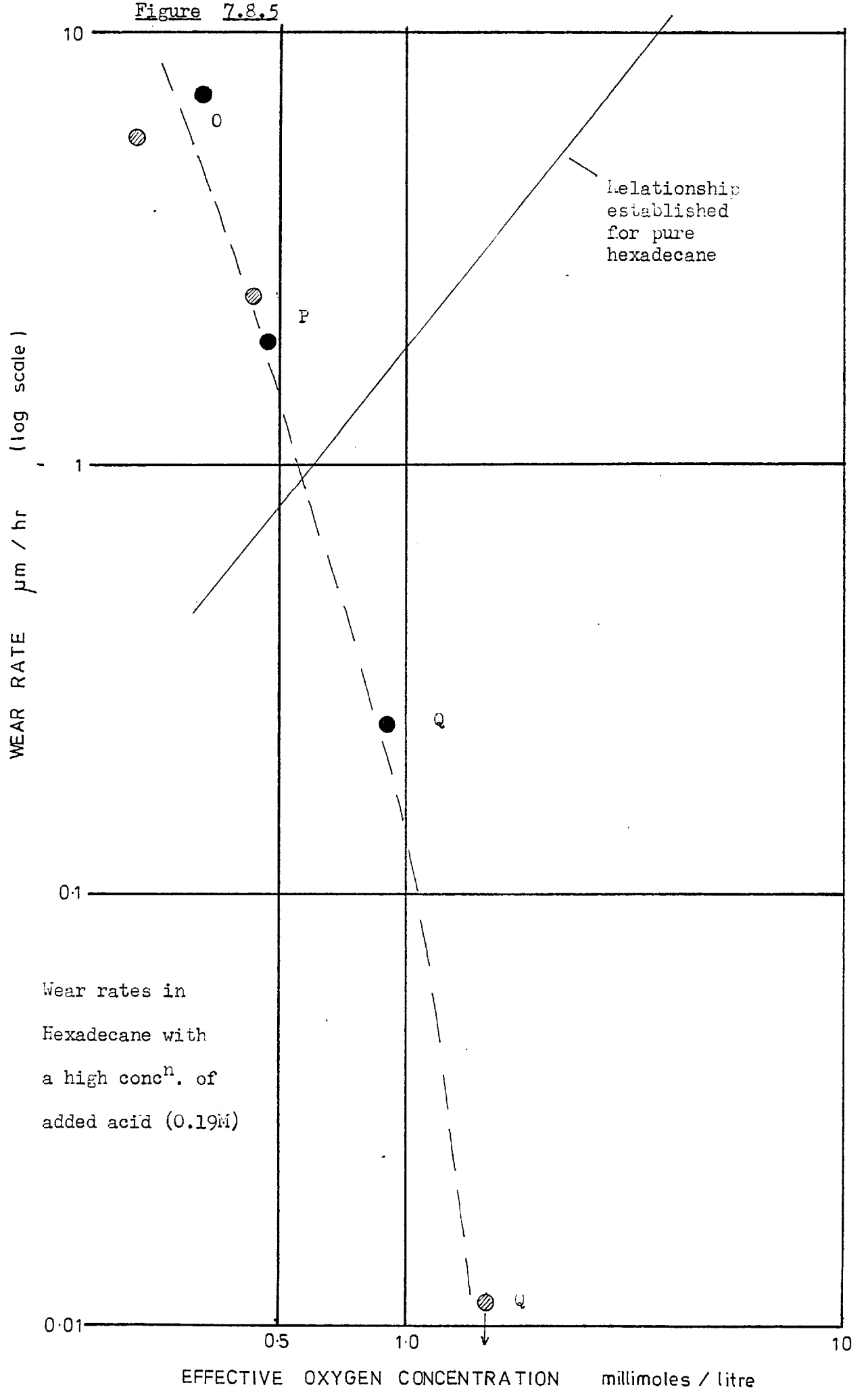
10
1
0·1
0·01
0·5
1·0
10
WEAR RATE μm / hr (log scale)
EFFECTIVE OXYGEN CONCENTRATION millimoles / litre
O
P
Q
Q
Relationship established for pure hexadecane
Wear rates in Hexadecane with a high conc^n. of added acid (0.19M)

Copper Laurate. Russell et al.[104] have shown that the metal soap formed under similar conditions has good anti-wear properties. Wilson and Garner have similarly noted that oxidation is a prerequisite for the reaction of metal with a lubricating oil.[63]

7.9 Conclusions to Section B

The results presented in this section dealing with the effect of acidity on fretting wear are summarised in table 7.4. Consideration of these observations lead to the following conclusions:

(1) Similar behaviour was observed in tests in both pure hexadecane and in hexadecane with a low concentration of added acid.

(2) Therefore the presence of small quantities of acid does not affect fretting wear.

(3) High concentrations of acid leads to a reduction in wear in an air atmosphere but not in nitrogen. This is thought to be due to the formation in oxidising conditions of metal soaps.

(4) A substantial amount of dissolved acid is removed from solution by adsorption onto wear debris.

(5) These tests, however, fail to provide a clear answer to the mechanism of wear reduction at long times. The brief increase in wear following introduction of a fresh quantity of lubricant suggests that after a period of oxidation the oil cannot form the peroxy radicals necessary for metal oxidation.

7.10 General Conclusions

A number of conclusions may be drawn from a

TABLE 7.4

Summary of observations with Hexadecane lubricant.

	ACID	WEAR	OXYGEN effect of an increase in concentration
Pure Hexadecane	i) Rapid disappearance of contaminant acid ii) A low equilibrium value attained.	i) Wear rate depended on the oxygen activity ii) Wear at a secondary (lower) rate.	Wear increased Acid disappeared more rapidly Peak peroxide concentration was lower.
0.01 M Lauric acid in Hexadecane	i) Increased initially, then decreased. ii) A low equilibrium value attained.	Similar wear behaviour observed to that in Hexadecane	Wear increased. Acid disappeared more rapidly.
0.19 M Lauric acid in Hexadecane	No acidity measurements were made. Slow decrease in acidity.	Wear rates similar to those in acid-free Hexadecane. i) Low wear rate ii) Zero wear rate	) Low oxygen) High oxygen*

*The effect of increasing oxygen concentration beyond 0.5 millimoles per litre was to virtually eliminate wear, because of the formation of metal soaps.

comparison of the results presented in parts A and B of this chapter.

7.10.1 Similarities in Behaviour of the Ester and Hexadecane Lubricants

(1) In both lubricants a high concentration of acid was found to inhibit wear, whilst at a low concentration acid had little effect. The transition between these extremes must lie between 0.19 M and 0.01 M in hexadecane and between about 0.06 M and 0.04 M in ester. The latter interval is defined by the acidity at the end of the initial wear period in tests D and E.

The anti-wear action of the acid, initially, is believed to be the reduction of the concentration of peroxy radicals and the adsorption onto the wearing surfaces.

(2) In both lubricants the wear rate was found to depend on the dissolved oxygen concentration but to be independent of the measured hydroperoxide concentration. This implies that hydroperoxides do not themselves take part in metal oxidation.

7.10.2 Differences in Behaviour of Ester and Hexadecane Lubricants

1. Acid

Acid is adsorbed rather than produced in HEXADECANE. The rate of disappearance of added acid increases with increased wear rate.

i.e. A high oxygen concentration $\overset{*}{\longrightarrow}$ High wear
$\longrightarrow$ Rapid disappearance of the acid

Adsorption onto debris is evidently responsible for

$\overset{*}{\longrightarrow}$ denotes "implies"

much of the acid decrease. However, the results of mass spectroscopic analysis and thin layer chromatography show that a fair amount of polymerisation is taking place (e.g. esterification) which also removes acid from solution.

In ESTER acid production shows an induction period after which the acid accumulates at a rate related to the oxygen concentration.

i.e. A high oxygen concentration ⟶ High wear
A high oxygen concentration ⟶ High secondary rate of acid production

2. Hydroperoxide

In HEXADECANE the hydroperoxide concentration peaks and then decreases towards zero, whereas in ESTER the peroxide concentration increases to an equilibrium value and the rate of wear can be correlated with the rate of peroxide increase.

i.e. A high oxygen concentration ⟶ A High rate of peroxide accumulation ⟶ High wear

Here again adsorption mechanisms in hexadecane appear to remove the peroxide from solution.

3. Wear

The end of the initial wear period in ester coincides with the attainment of the equilibrium peroxide concentration and the end of the acid induction period. Whilst a similar reduction in wear at the end of the initial wear period was observed with hexadecane the transition did not relate to any specific acid or hydroperoxide concentration.

7.10.3 The Mechanism of Metal Oxidation Within a Lubricated Contact - A Hypothesis

It is proposed that peroxy radicals which are formed as intermediates in lubricant oxidation, attack and oxidise metal surfaces in a lubricated contact. It is further proposed that such metal oxidation is the controlling factor of fretting wear under the conditions imposed in the spline wear tester.

The foregoing results and observations are compatible with this theory. The actual concentration of peroxy radicals within the fretting contact could not be determined - it was only possible to infer it from the measured hydroperoxide concentration - thus direct evidence to support the hypothesis cannot be obtained.

In the following chapter tests using oil antioxidant additives in ester are described which provide further supporting evidence for this theory.

Chapter 8.
Fretting Tests with Antioxidant Additives

8.1 Introduction

The ability of antioxidants to reduce fretting wear in mineral oil was demonstrated by Weatherford, Valtierra and Ku[12]. However, the mode of action of the additives has not been demonstrated. In Chapter 1 a number of investigations into the effect on sliding wear of antioxidant additives were discussed. The results of Bose et al[9], Klaus and Beiber[5], and Rounds[105] are summarised below.

Bose found that an oxidation inhibitor in mineral oils reduced metallic wear and production of organometallic debris although it was not as effective as the exclusion of oxygen from the oil. In an ester on the other hand, although the organic component of the debris was reduced when an inhibitor was present the quantity of metallic debris was not reduced.

Klaus and Beiber[5] investigated the action of an oxidation inhibitor over a range of oxygen partial pressures and two temperatures in mineral oil. It was found that at 75°C when oil oxidation during a test was not significant the antioxidant had little effect. At 205°C oil oxidation in air was rapid but antioxidants resulted in slightly increased wear whilst preventing oxidation. In nitrogen at the same temperature addition of the additive gave a marked wear reduction. These phenomena were not adequately explained beyond the statement that some little oxidation of a highly refined mineral oil is beneficial. Klaus and Beiber found that additions of an antioxidant to an ester oil had little effect on wear. They suggest at the higher temperatures

the ester degrades to yield acids with good boundary lubricating properties.

In view of these results and those of Ku[12] who showed that substantial fretting wear reductions could be obtained by antioxidant additions to mineral oils, it was considered important to establish whether similar reductions could be obtained with the ester base stock. Most ester lubricants have good thermal stability. It is therefore thought that antioxidant additions should give a marked wear reduction in most ester lubricants.

F. G. Rounds[105] investigated the interaction of antioxidant additives and boundary additives. He found that addition of oxidation inhibitors* to a base oil with a chlorinated wax antifriction additive gave varied results - some combinations proving detrimental, others beneficial. Peroxide decomposers* on the other hand were found to have no interaction with the antifriction additive. It is worth noting therefore that additions of antioxidants to reduce wear should not be made without considering the additive package as a whole.

In this chapter the results of fretting tests with antioxidant additions to the ester lubricant are discussed. It is demonstrated that both the free radical inhibitor and the peroxide decomposer type of antioxidants are effective in reducing wear in the ester base stock. These results, collated with the evidence that has been presented in previous chapters, enables the mode of action of

---

* This terminology will be explained in the following section.

antioxidants as wear-reducers to be identified.

8.2 Antioxidant Types

8.2.1 Oxidation of Hydrocarbons

Oxidation of lubricating oils proceeds by a free radical chain reaction mechanism. The reaction sequence has been explained in a previous chapter (section 4.4) so the reactions are merely summarised below.

Initiation: (1) $RH \longrightarrow R*H$ (an activated state)

Initial propagation: (2) $R*H + O_2 \longrightarrow P$ (an activated complex)

(3) $P + RH \longrightarrow ROOH + R*H$

Termination: (4) $P \longrightarrow$ stable products

Branching: (5) $ROOH \longrightarrow RO\cdot + \cdot OH$

(6) $RO\cdot \longrightarrow R'\cdot +$ carbonyl compounds

Propagation: (7) $R\cdot + O_2 \longrightarrow ROO\cdot$

(8) $ROO\cdot + RH \longrightarrow ROOH + R\cdot$

Termination: (9) $R\cdot + R'\cdot \longrightarrow$ inert products

Now there are three different types of antioxidants which act on different stages of the oxidation process. These will now be described in turn.

8.2.2 Metal Deactivators

It has been shown that metals such as iron and copper catalyse the activation of the RH molecule, perhaps by accepting an electron:

$$RH + M^{2+} \longrightarrow R\cdot + H^{+} + M^{+} \qquad (59)$$

They also catalyse the decomposition of the hydroperoxide

$$ROOH \xrightarrow{M} RO\cdot + HO\cdot$$

or by donating an electron:

$$ROOH + M^{+} \longrightarrow RO\cdot + {}^{-}OH + M^{2+}$$

Metal deactivators prevent metal catalysis by forming metal chelates on metal surfaces and with dissolved metal ions. These chelates are non-reactive towards hydroperoxides and hydrocarbons[8].

8.2.3 Free Radical Inhibitors

Oxidation inhibitors act to break the chain reaction at reactions (3) and (8) above. They are compounds with labile hydrogen which is readily abstracted by the ROO· radical.

$$ROO\cdot + AH \longrightarrow ROOH + A\cdot$$

Effective inhibitors are usually resonance stabilised in the A· state and therefore inactive towards hydrocarbons. Aromatic amines and hindered phenols are the most common types. There is some evidence[106, 107] that aromatic amines inhibit by donating an electron rather than a hydrogen atom.

$$ROO\cdot + \begin{array}{c} | \\ :\!N\!H \\ | \end{array} \longrightarrow ROO^{-} + \begin{array}{c} | \\ (\cdot\!N\!-\!H)^{+} \\ | \end{array}$$

The oxidation inhibitor used in the fretting tests was Phenyl-α-naphthylamine which has the configuration shown in fig. 8.2.1. The aromatic groups are responsible for stabilising the inhibitor.

It is a feature of oxidation inhibitors that they are consumed by the inhibitory process. The inhibitor can react with another radical as follows

Figure 8.2.1

(a) Phenyl-∝-naphthylamine

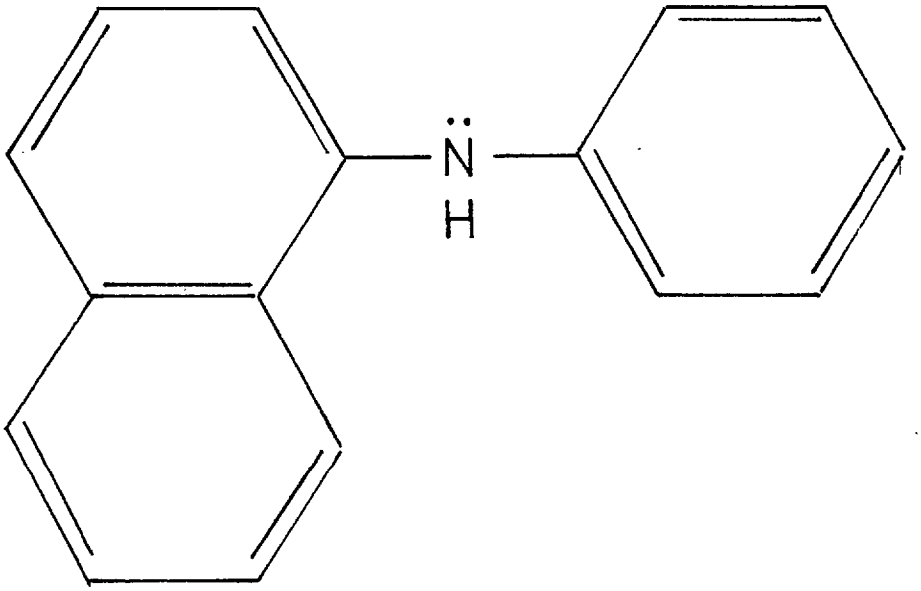

(b) Zinc diethyl dithiocarbamate

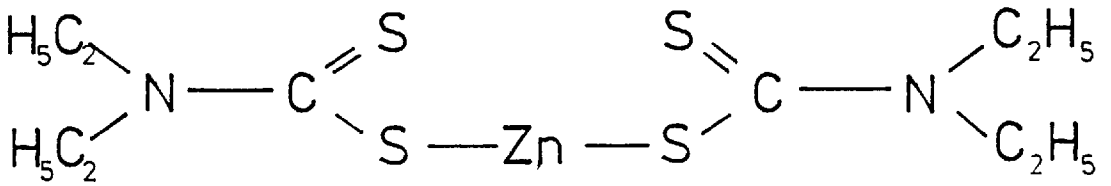

The structure of the antioxidants.

$$A\cdot + ROO\cdot \longrightarrow \text{Inert Products.}$$

8.2.4 Hydroperoxide Decomposers

These antioxidants eliminate hydroperoxides from the oil by decomposing them to inactive products. Thus all oxidation resulting from chain branching (reaction (5) to (8) above) is much reduced. Generally they catalyse the rearrangement of the hydroperoxide[108] and are regenerated by further reaction:

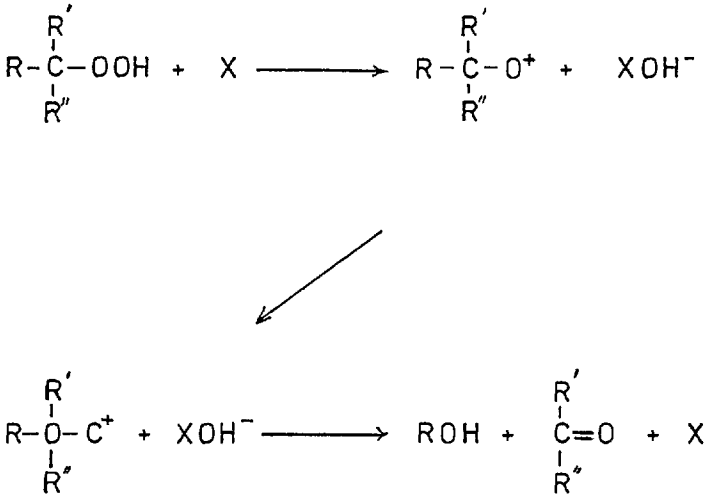

For decomposers containing sulphur the following mechanism is possible. The antioxidant is activated by addition of an electron

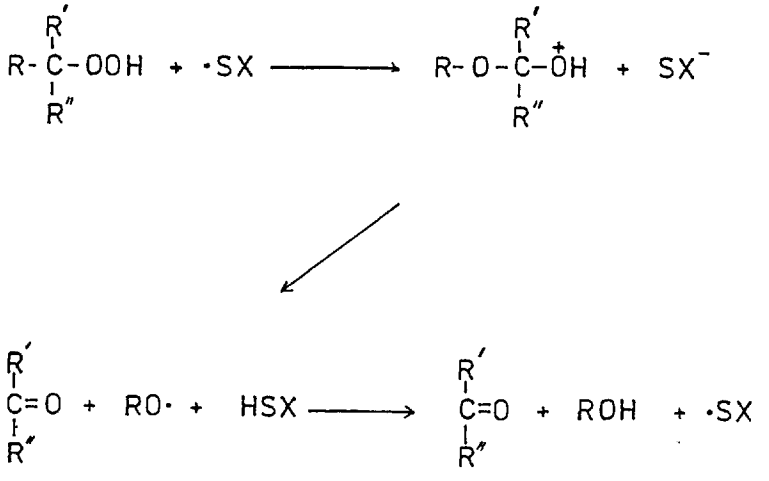

Phenothiazine, an antioxidant commonly used in esters probably acts in this way.

Zinc dialkyldithiophosphates are frequently employed as they also form a protective phosphate layer on rubbing surfaces. Zinc dialkyldithiocarbamate (fig. 8.2.1) has similar antioxidant properties without the ability to form a phosphate layer. The mechanism of hydroperoxide decomposition is not known in detail[8]. Burn[109] has suggested that decomposition occurs via the formation of a complex between the hydroperoxide and the antioxidant in which the double-bonded sulphur plays an important role (fig. 8.2.2).

8.2.5 The Modes of Action of the Inhibitor and the Hydroperoxide Decomposer Antioxidants Contrasted

Phenyl-α-naphthylamine (PαN) and zinc diethyldithiocarbamate (ZDDC) were tested in the fretting rig as additives to the ester base stock. They are examples of the inhibitor type and the hydroperoxide decomposer type of antioxidants respectively and therefore alter the chemical composition of the lubricant during oxidation in different ways.

PαN, the inhibitor, virtually eliminates the ROO· and RO· radicals but does not act to reduce the hydroperoxide concentration except as a result of a lower overall rate of oxidation. ZDDC on the other hand destroys the hydroperoxide, severely curtailing chain-branching, which in turn leads to a low concentration of peroxy radicals.

Whereas inhibitors are consumed in the deactivation of

Figure 8.2.2

The mechanism of action of Zinc diethyldithiocarbamate proposed by Burn, ref. (109)

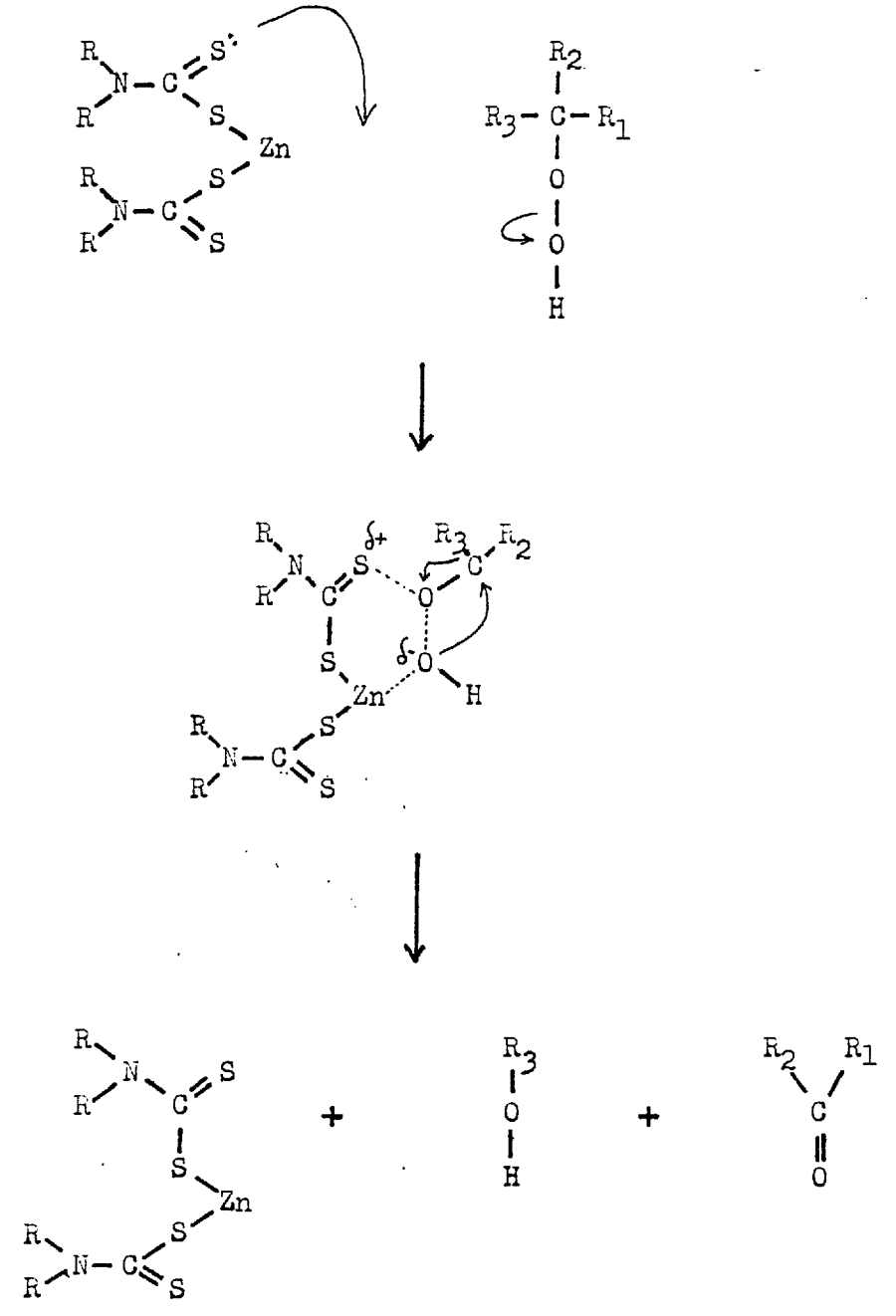

radicals, hydroperoxide decomposers are regenerated and have the capability of many interactions. Hydroperoxide decomposers are therefore relatively more effective than inhibitors and are generally used in lower concentrations.

8.3 Experimental

Fretting tests with the antioxidant additives were conducted at various oxygen partial pressures and under the standard test conditions described in section 4.5. Preliminary tests were performed to determine the concentrations of additive necessary for a clear response. In these tests the oil was air bubbled.

Tests were then performed under controlled atmospheres - the oxygen content of the oils being measured at frequent intervals - with a fixed quantity of the additive. When the tests with phenol-α-naphthylamine were performed the techniques of monitoring the acidity and peroxide content of small samples had not been developed. Therefore, the only measurements made were determinations of the final acidity.

8.4 Results

8.4.1 Preliminary Tests

Weatherford, Valtierra and Ku[16] found that concentrations of 2×10^{-3} moles/litre of zinc diamyl dithiocarbamate and 2×10^{-2} moles/litre phenyl-α-naphthylamine were sufficient to reduce fretting wear. The former additive was not available for this work so the similar zinc diethyldithiocarbamate (ZDDC) was used. In order to determine its effectiveness, concentrations in the ester of 0.03, 0.16 and 1.6 wgt. % were tested. The results of these fretting tests are shown in fig. 8.4.1. For further

Figure 8.4.1

Effect of the concentration of the additive Zinc diethyl-dithiocarbamate on Fretting wear in e.ter.

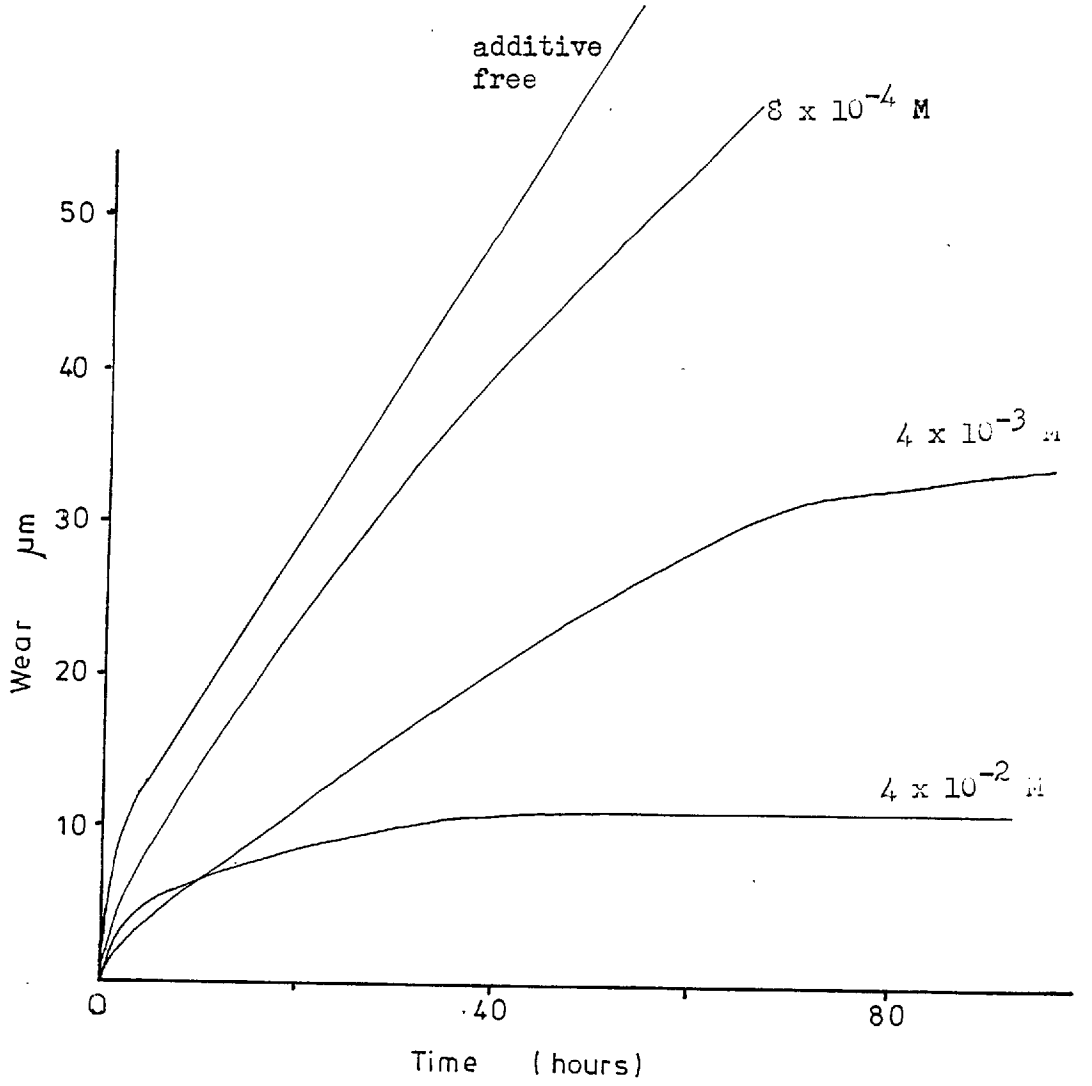

tests it was decided to use a 1.6 wgt. % (4×10^{-2}M) solution of the additive as this gave a positive response (i.e. a clear wear rate reduction) within a fifty hour test. However, because of the low solubility of the additive at this concentration it was necessary to preheat the oil to 60°C before it was introduced into the rig. A higher concentration of additive had to be used in the ester than was used by Ku in a mineral oil to obtain a similar degree of wear reduction, but it should be noted that the wear rate in additive-free ester was only about half that in the additive-free mineral oil.

Figure 8.4.2 shows the results of preliminary trials of phenyl-α-naphthylamine. A 1.9 wgt. % addition did not markedly reduce the wear rate but at double this concentration there was very little wear beyond the first two hours of the test. This concentration (3.8 wgt. %, 0.16M) was used in all subsequent tests.

8.4.2 Tests with a Hydroperoxide Decomposer

Table 8.1 lists the results of tests with a 1.6 wgt. % (4×10^{-2}M) solution of zinc diethyldithiocarbamate in the ester base stock. The wear curves are shown in fig. 8.4.3 and the wear rates taken from these curves are plotted against the dissolved oxygen activity in fig. 8.4.4. The wear rates observed initially fall on a straight line of higher gradient than the ester results:

$$\text{Wear rate} \propto (\text{Oxygen concentration})^{n}$$

where n has a value of between 2 and 3.

Unlike the additive-free ester results, the secondary

Figure 8.4.2

Effect of the concentration of the additive Phenyl-α-naphthylamine on fretting wear in ester.

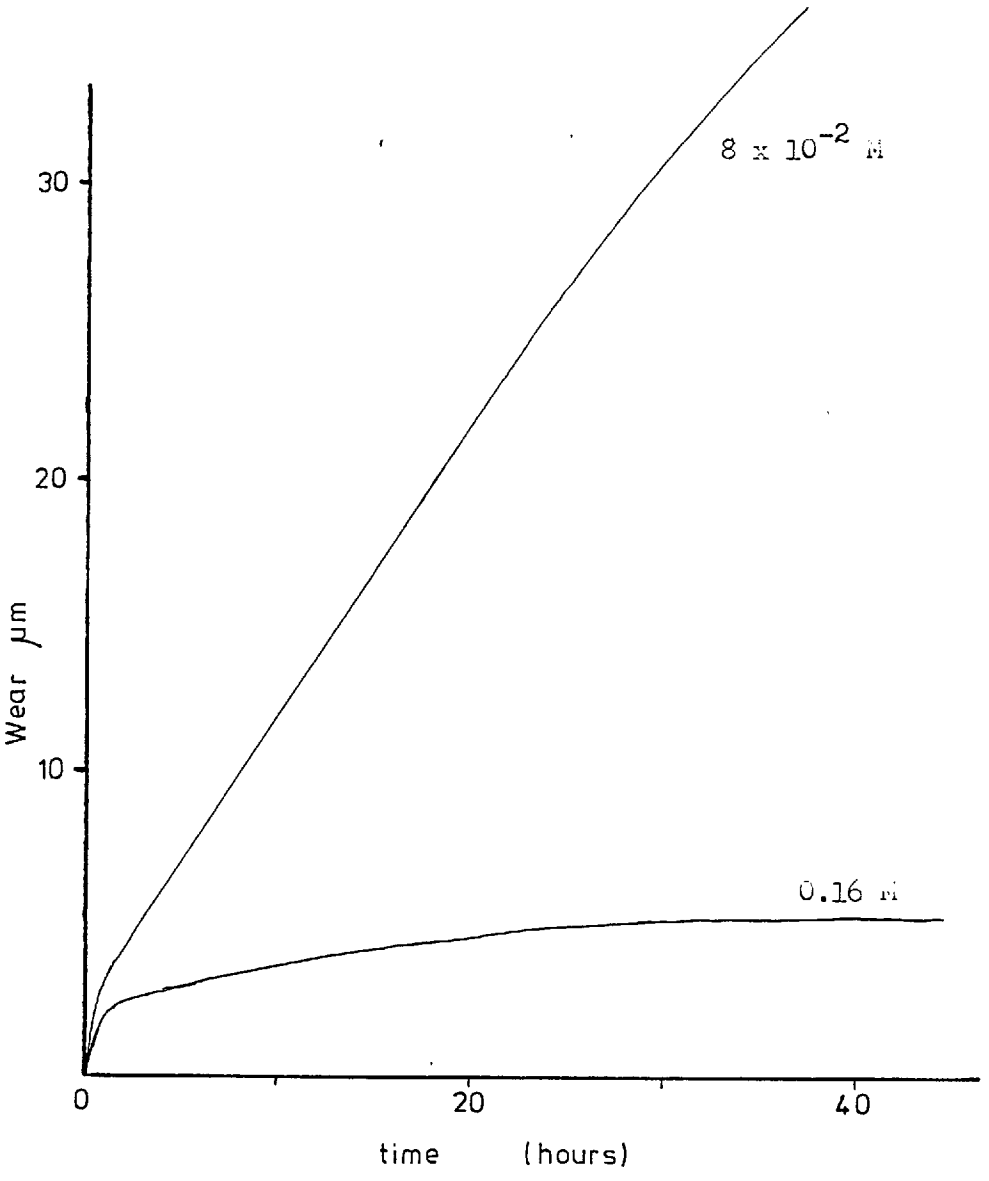

TABLE 8.1

Lubricant : Ester plus Zinc diethyl dithiocarbamate (4×10^{-2} M)

Standard conditions (80° C)

Test code	Test time Hours	Oxygen conc^{n}. mmoles/litre	N	σ	Wear rate µm / hour
W	0 - 6	1.1	5	.07	decreasing
	6 - 44	1 to 1.25	9	-	.097
X	0 -15	4.6	6	0.4	3.93
	18 - 45	1.4	5	0.1	1.24
Y	3 - 22	2.5	)		0.49
	22 - 30	2.5	)20	0.35	increasing
	30 - 57	3.7	15	0.4	3.95

TABLE 8.2

Lubricant : Ester plus Phenylαnaphthylamine (0.16 M)

Standard conditions (80° C)

Test code	Test time Hours	Oxygen conc^{n}. mmoles/litre	N	σ	Wear rate µm / hour
R	0 - 5	0.51	6	0.02	decreasing
	5 - 21	0.35	4	0.08	0.025
S	0 - 24	1.1	)		decreasing
			) 6	0.05	
	24 - 38	1.1	)		0.025
T	0 -12	1.1	)		decreasing
			)		
	12 - 28	1.1	) 10	0.08	0.08
			)		
	28 - 44	1.1	)		0.0
U	2 - 24	2.75	7	0.44	3.1
	24 - 32	4.4	3	0.2	4.6
V	0 - 5	4.5	3	0.5	4.0
	15 - 26	0.83	6	0.03	0.26

N : number of oxygen determinations
σ : standard deviation of the sample values

Figure 8.4.3

Wear curves - Zinc diethyl dithiocarbamate.

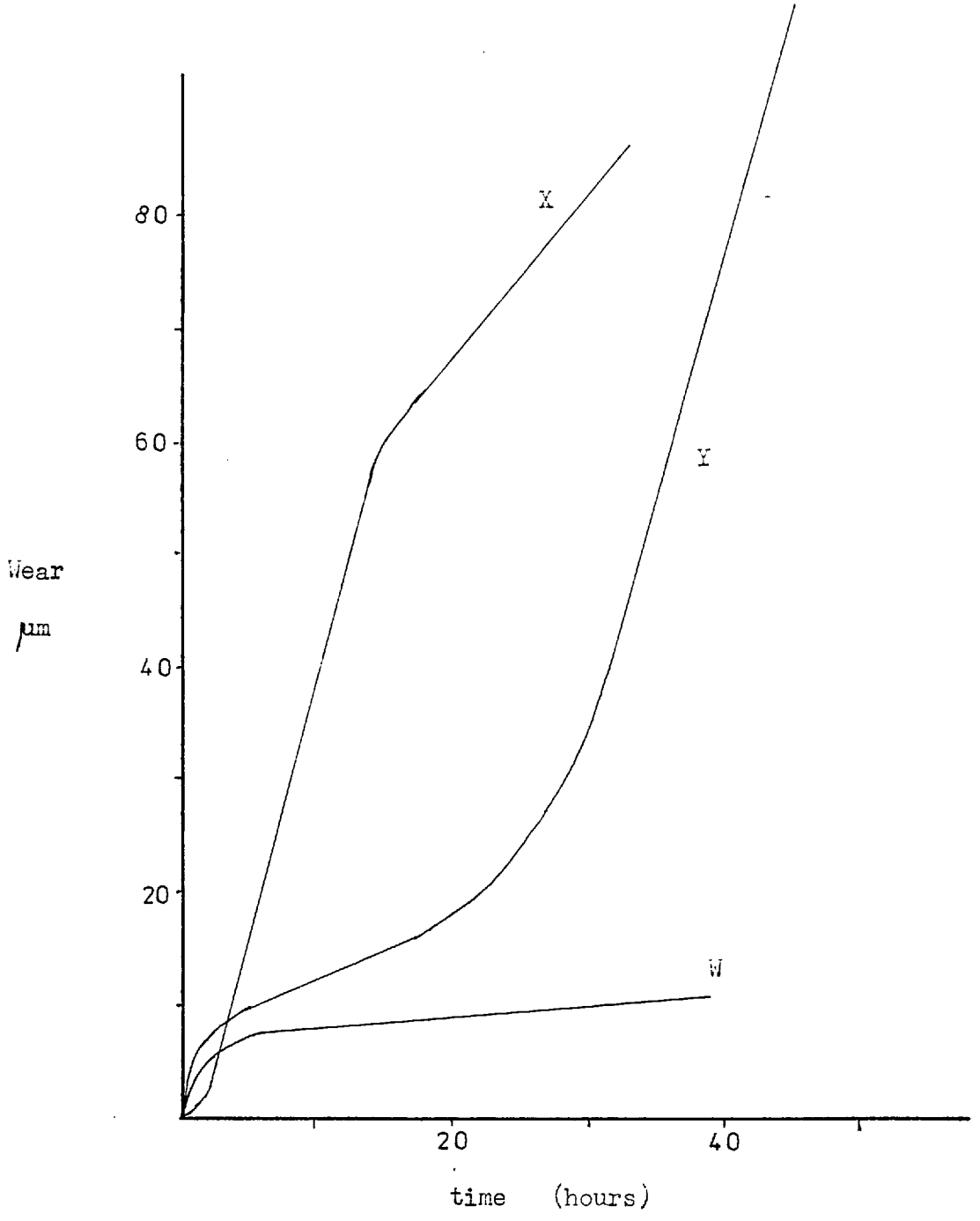

Figure 8.4.4

Relationship between wear rate and oxygen concentration

Ester plus 4×10^{-2} M ZDDC.

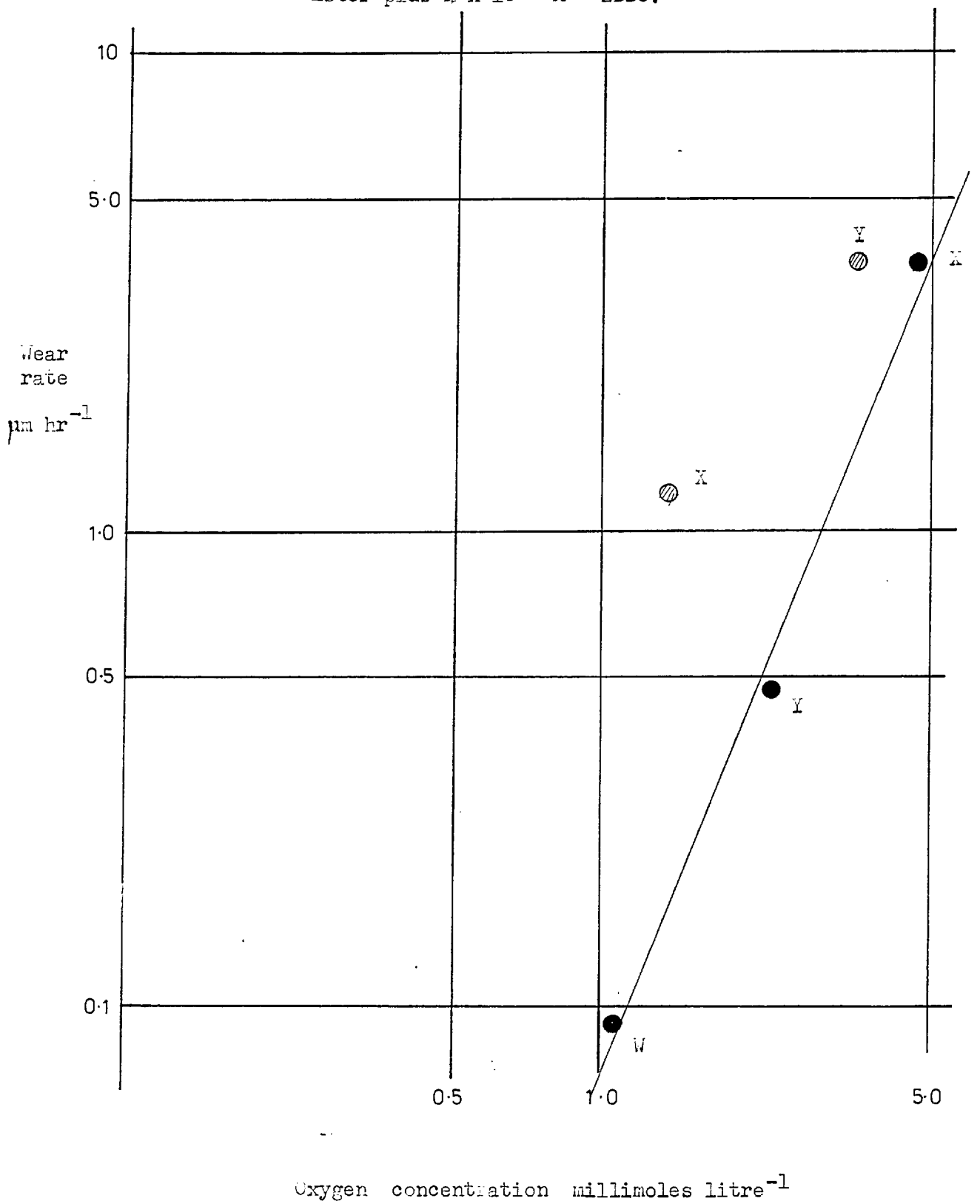

wear rates observed were higher than the initial rates of wear (tests X and Y). These rates are similar to those predicted for additive-free oil under the same oxygen concentrations. It is concluded that after some hours at a high oxygen partial pressure the ZDDC additive loses its ability to suppress lubricant oxidation. Oxidation and wear then proceeds as if the antioxidant were not present. Support for this sequence of events is provided by the measurements of peroxide concentrations.

The peroxide concentration in the lubricant was monitored in tests W and Y. In test W only a very low concentration of peroxide was detected throughout the test (45 hours) (fig. 8.4.5). In the test at high oxygen (Y) similar levels of peroxides were measured for the first twenty hours. Thereafter the peroxide concentration rose quickly to a value of 10^{-1} moles/litre, which was shown in tests with pure ester to be the steady state value (see fig. 7.3.3).

Again there is a marked similarity between the wear curves and the peroxide concentration curves (although in test Y a decrease in wear rate had not been observed when the test was terminated). This is further justification for the argument, put forward in chapter 7 that it is the precursors of peroxides (the peroxy radicals) that are responsible for wear.

8.4.3 Tests with an Inhibitor

Table 8.2 lists the results of tests with a 3.8 wgt. % (0.16M) solution of phenyl-α-naphthylamine in the ester base stock. The wear curves are shown in fig. 8.4.6.

Figure 8.4.5

The build-up of Peroxide concentration in ester plus Zinc diethyl dithiocarbamate.

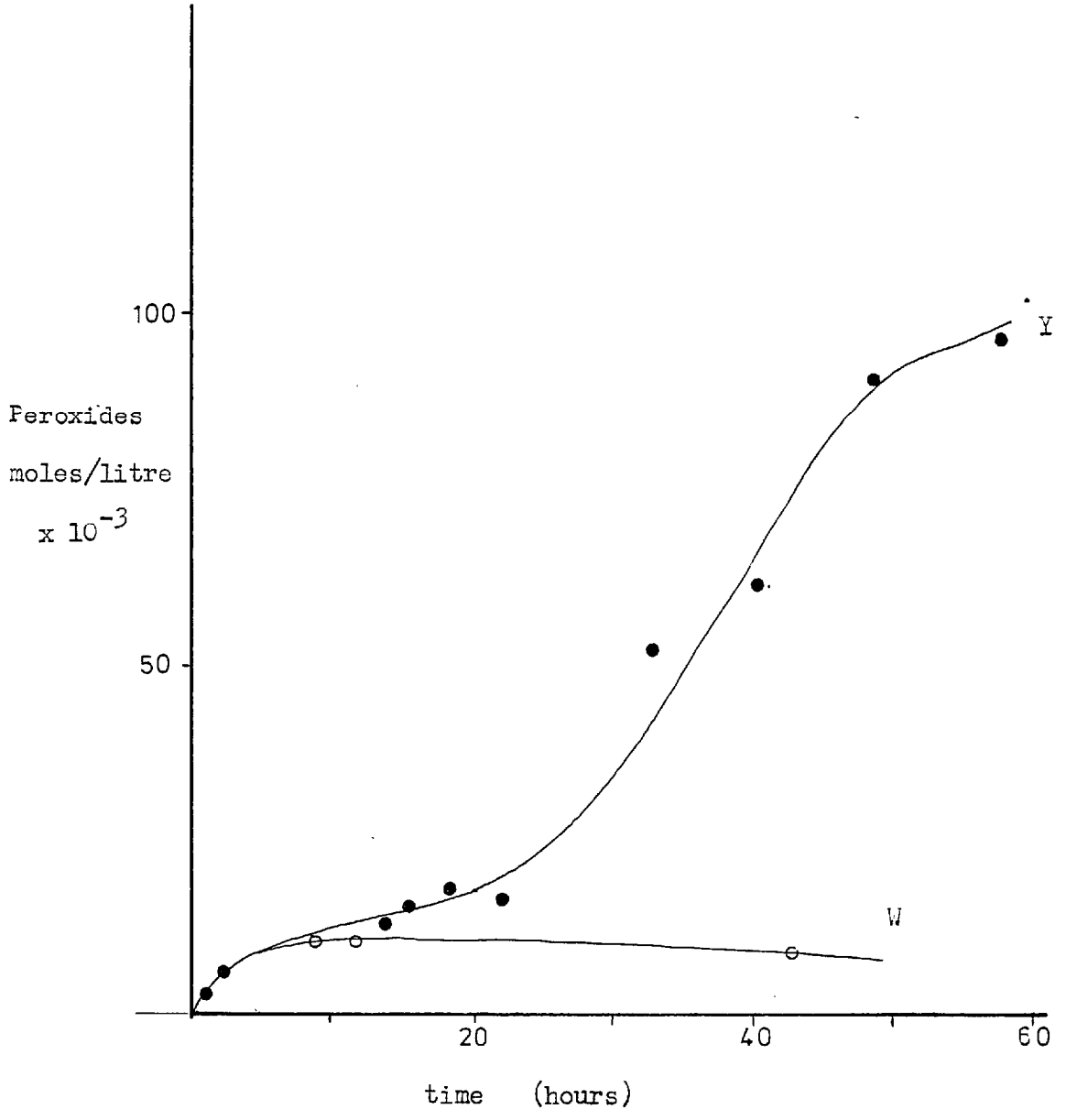

Figure 8.4.6

Wear curves - Phenyl-α-naphthylamine.

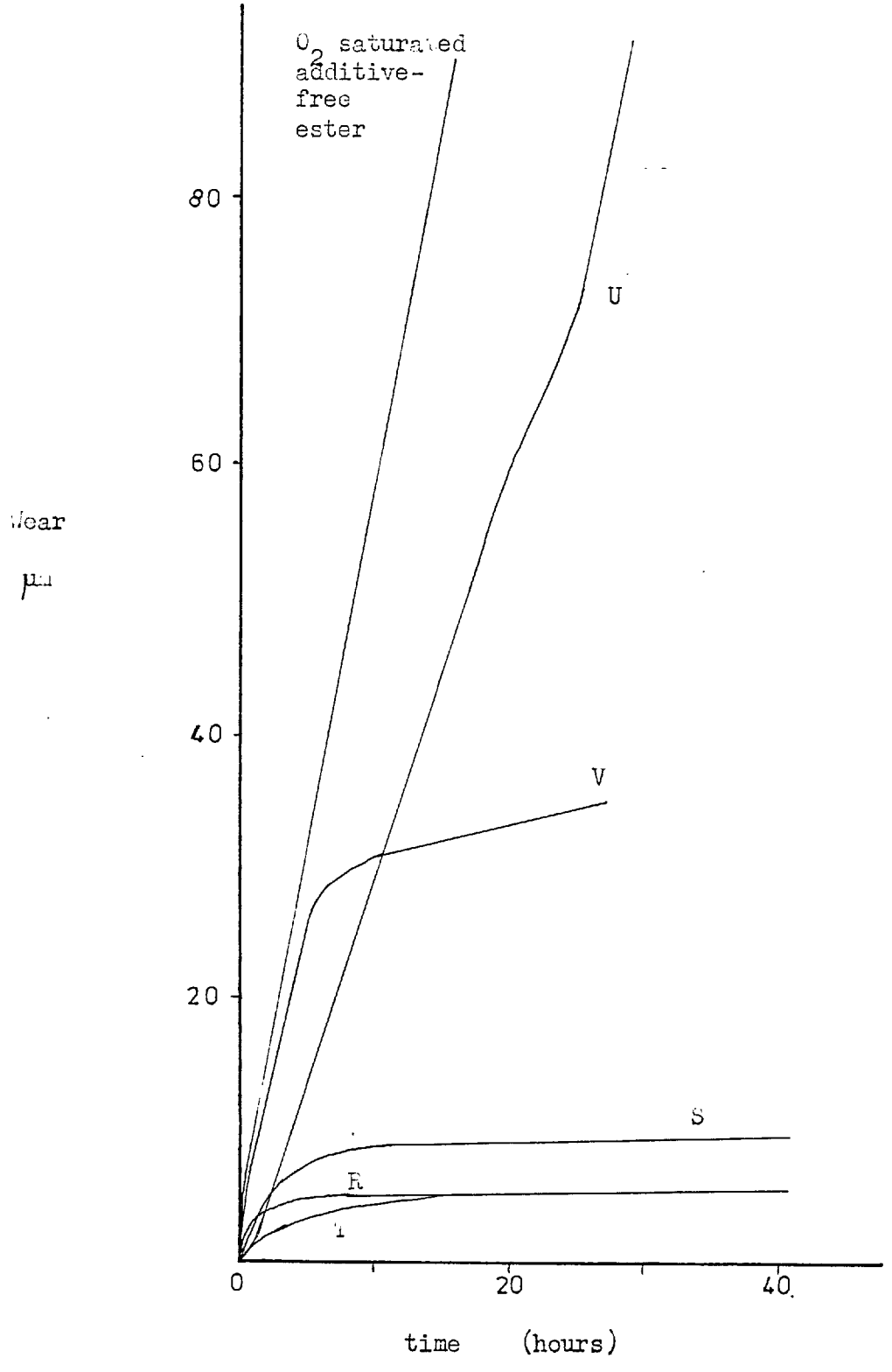

Very low wear rates, approaching zero, were observed at oxygen concentrations of 0.35 millimoles and 1.1 millimoles per litre (tests R, S and T). Under conditions of oxygen saturation of the lubricant a high wear rate was observed. In test V a high initial oxygen concentration was reduced after five hours to air saturated condition and an intermediate wear rate was eventually established. However, the additive appears not to have been totally destroyed or inactivated by exposure to a high oxygen concentration as the subsequent wear rate is significantly lower than in air saturated additive-free oil. The wear rate results (tests R, S, T and U) are shown plotted against oxygen concentration in figure 8.4.7. The low wear rates observed at 1.1 millimoles litre^{-1} and below appear to be independent of the oxygen concentration. It is not clear from these results whether there is a gradual transition from low to high wear with increasing oxygen concentration as was observed with ZDDC.

8.4.4 Results of Acidity Tests

The acidity of the lubricant in tests with added antioxidant was measured at the end of each test. The results are listed in table 8.3 and show a much lower acidity than those measured for tests under similar conditions without additives (section 7.3).

With phenyl-α-naphthylamine the final acidity is related to the exposure time to particular oxygen concentrations. This has been shown by converting the test times to equivalent times at 100% air saturated oxygen. For instance, the oil in test U was 350% air

Figure 8.4.7

Relationship between wear rate and oxygen concentration

Ester plus 0.16 M Phenyl-α-naphthylamine.

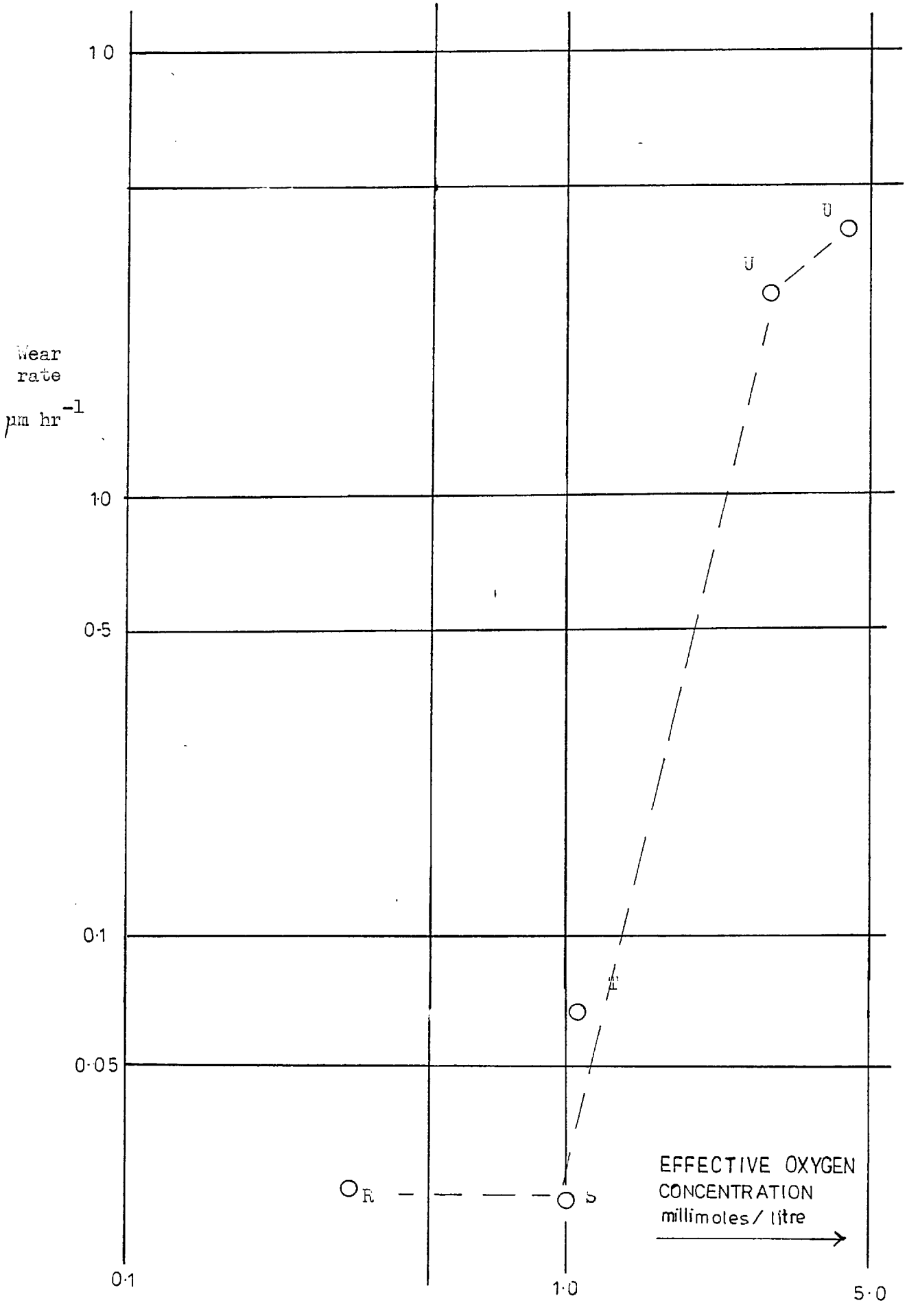

TABLE 8.3

Acidity Tests

Additive	Test Code	Final Acidity		Wear μm	100 % O_2 Hrs.
		$[H^+]$ moles $litre^{-1} \times 10^{-3}$	T.A.N.		
Phenyl-α-naphthylamine	R	1.0	0.06	5.3	12.5
	S	1.47	0.09	9.5	56
	T	1.5	0.095	5.8	62
	U	2.5	0.15	105	130
Zinc diethyldithiocarbamate	W	4.4	0.27	11.9	67.5
	X	104	6.4	84	183
	Y	39	2.4	140	200

saturated for 24 hours and 560% saturated for 8 hours, equivalent, it is proposed to 85 and 45 hours respectively at 100% saturation. These equivalents are tabulated in table 8.3. There is good correlation between acidity and this parameter for the ester inhibited by phenyl-α-naphthylamine (fig. 8.4.8). The lack of correlation when wear is inhibited by ZDDC is probably due to the breakdown of the antioxidant action under high oxygen conditions.

8.5 Discussion of Results

8.5.1 Introduction

The results presented in the previous section confirm that in air saturated oil the presence of antioxidants results in a significant wear reduction. The degree of reduction is dependent on the concentration of the additive and its mode of action. Whereas a 4×10^{-2} M solution of ZDDC, a peroxide decomposer resulted in very low wear, a four times stronger solution of phenyl-α-naphthylamine was required to produce wear reductions of a similar order. However, before explaining these results in terms of the antioxidant action of the additives, two alternative anti-wear properties must be considered.

8.5.2 Alternative Modes of Action of the Additives

(a) Boundary action. The two antioxidant additives tested both have weak boundary lubricating properties. That is, they have a tendency to form adsorbed films on metal surfaces. In order to check that wear reduction was not a result of this action, a 5 wgt. % solution of isopropyl oleate (a powerful boundary additive) in ester was run in the fretting rig under a dry air atmosphere.

Figure 8.4.8

The increase in acidity of ester when inhibited by Phenyl-α-naphthylamine.

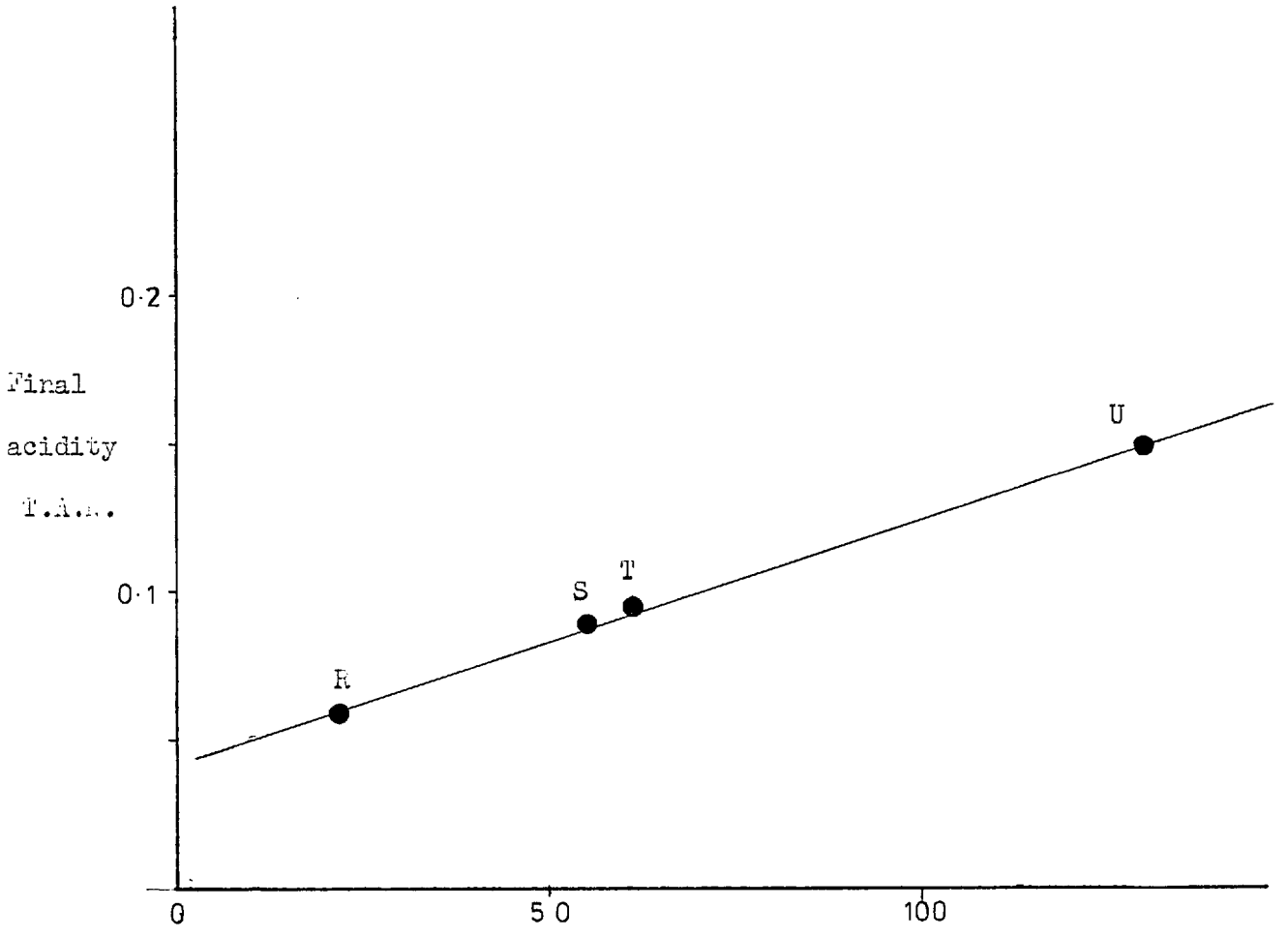

The resulting wear rate (1 μm/hour) is not significantly different from that of the additive-free ester. Since the antioxidants are weaker boundary additives it is unlikely that they could have been reducing wear in this way.

(b) Extreme pressure action. The formation of an e.p. film on the rubbing surfaces by ZDDC must be considered. Many extreme pressure (e.p.) additives contain sulphur and form, by reaction with the metal surface, a wear resistant sulphide layer(67). ZDDC contains 4 atoms of sulphur per molecule and it is conceivable that such a reaction took place.

On the other hand it has been found in a variety of fretting situations that sulphur containing e.p. additives give little decrease and sometimes an increase in wear compared with the additive-free lubricant. This is because reaction with the surfaces merely increases the corrosion rate(16,27,110,123). Furthermore, Hirano(95) has shown that under conditions of oxidation wear a sulphur containing additive (in this case dibenzothiophene or sulphuric acid) was more effective as an oil antioxidant than as an e.p. agent.

8.5.3 The Relationship Between Antioxidant Action and Wear Reduction

The oil oxidation chain reaction mechanism has been outlined previously (sections 4.4, 6.7 and 8.2.1). The propagation stage of oil oxidation may be summarised as shown in fig. 8.5.1. This system is well established except for the proposed reaction (11):

ROO· + metal ⟶ metal oxide ⟶ wear

In chapter 7 it was shown that such a scheme explains the observed relationship between wear and the acid and peroxide concentrations. The results obtained with antioxidant additives are also in agreement with this scheme.

Both types of antioxidamts act to decrease the rate of oil oxidation. Inhibitors such as phenyl-α-naphthylamine do this by inactivating the radical species ROO· and R·. However, they do not directly act on the hydroperoxide ROOH and cannot stop the reaction spreading by chain branching (reaction (5)). The lifetime of ROO· in the presence of an inhibitor will be brief so it is likely that corrosion arises from radicals produced by activation of ROOH or RH within the contact.

The peroxide decomposer catalyses the decomposition of ROOH to stable products (reaction (10)) and so reduces the "spread" of the reaction. Peroxide decomposers are not thought to affect the initiation reactions[108] but are more effective under the severe conditions imposed by fretting because they confine the oxidation to the initiation process. The smaller scale of oxidation leads to a lower concentration of peroxy radicals (ROO·) and a

Figure 8.5.1

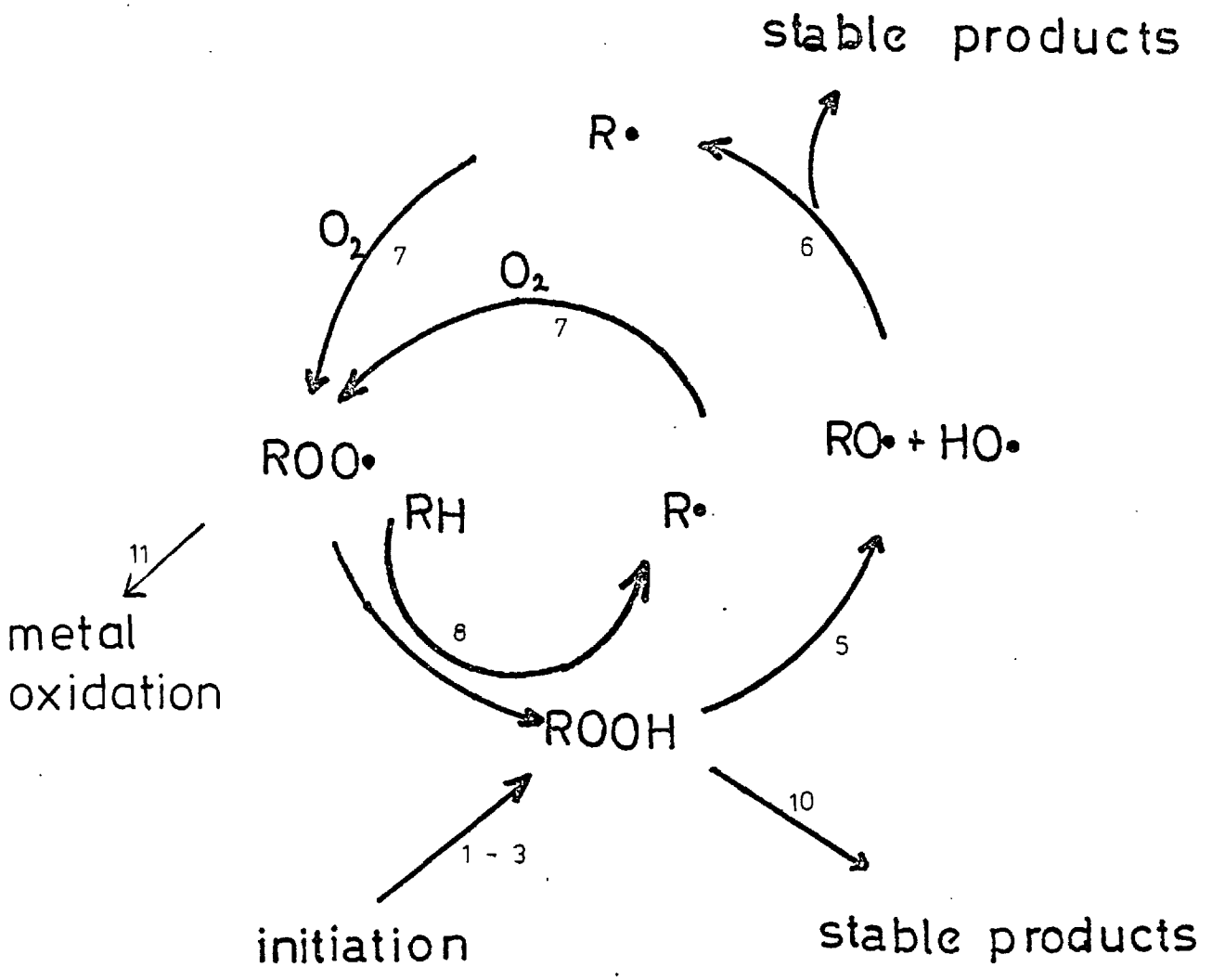

A diagram illustrating the reaction sequence during the steady state propagation stage of hydrocarbon oxidation.

lower wear rate. Thus the solution of 4 x 10^{-2}M ZDDC in ester was as effective as 0.16M phenyl-α-naphthylamine. (Compare figs. 8.4.3 and 8.4.6.)

8.5.4 The Relationship Between Oxygen Activity and Wear Rate

In chapter 4 it was shown that the fretting wear rate was proportional to the activity of the oxygen in solution in the ester*. With the antioxidants different relationships were obtained:

Zinc diethyl dithiocarbamate: Wear $\propto [O_2]^{2.5}$

Phenyl-α-naphthylamine: low wear which appears independent of $[O_2]$

Because of the complex process of ester oxidation it is only possible to derive a theoretical relationship between wear and oxygen activity when steady state conditions may be assumed. The assumption is also made that the wear rate is proportional to the peroxy radical concentration.

In the steady state stage of a reaction the concentration of radical intermediates is approximately constant; in the additive-free ester, steady state conditions apply when oxidation is occurring mainly by the propagation reactions:

$$R\cdot + O_2 \xrightarrow{k_7} ROO\cdot \qquad (7)$$

$$ROO\cdot + RH \xrightarrow{k_8} ROOH + R\cdot \qquad (8)$$

see fig. 8.5.1

---

* Direct attack of the metal by dissolved oxygen would explain this relationship, but not the relationships observed with antioxidants.

It is assumed that the concentration of radicals is approximately constant

$$\Rightarrow \quad \frac{d[ROO\cdot]}{dt} = k_7[R\cdot][O_2] - k_8[ROO\cdot][RH]$$
$$= 0$$

where [RH], the concentration of ester is assumed to be unity and k_7 and k_8 are the reaction rate constants.

$$\frac{[ROO\cdot]}{[R\cdot]} = \frac{k_7}{k_8}[O_2]$$

That is, the steady state concentration of ROO· is proportional to the oxygen concentration. It is worth noting that under these conditions a constant rate of production of hydroperoxide is predicted:

$$\frac{d\,[ROOH]}{dt} = k_8\,[ROO\cdot]\,[RH] = \text{constant.}$$

This was in fact observed during the initial wear period (see chapter 7). The rate of hydroperoxide decomposition becomes more significant as its concentration increases - eventually an equilibrium concentration is attained at which time the above analysis can no longer be applied.

Similarly, when an antioxidant additive is present the oxidation is confined to initiation processes and the steady state propagation stage is not attained. Therefore the simplifying assumptions that enable the dependence of wear rate on oxygen concentration to be predicted, cannot be made.

At high oxygen concentrations it is clear that the additives become increasingly ineffective in reducing

wear. Tests with zinc diethyldithiocarbamate suggested that the additive was being destroyed by oxidation, as wear rates similar to those obtained with the additive-free ester were observed in the later stages of the tests at intermediate oxygen concentrations. This effect was not observed in the tests with phenyl-α-naphthylamine - the acidity results, which showed a significantly lower final acidity than was observed in the additive-free ester, indicate that the additive was still working to some extent under high oxygen conditions. It should be noted, however, that the concentration of the latter additive was some four times greater. An equivalent concentration of ZDDC could not be tested because of its low solubility.

8.6 Conclusions

(1) The antioxidants phenyl-α-naphthylamine and zinc diethyl dithiocarbamate have a beneficial effect on fretting wear and on oil oxidation as measured by oil acidity.

(2) The minimum concentrations in which they are most effective are approximately 0.16 molar for phenyl-α-naphthylamine and 0.04 molar for ZDDC.

(3) The reduction of wear by antioxidants demonstrates that oxidation of the metal by dissolved oxygen is not the mechanism of fretting wear.

(4) A mechanism of oxidative wear is proposed involving oxidation of the metal by peroxy radicals produced as intermediates in oil oxidation. Antioxidants act to reduce wear by decreasing the concentration and lifetime of the ROO· radical.

(5) Results obtained with both additives under varying oxygen concentrations show a non-linear variation of wear rate with oxygen concentration. This contrasts with the behaviour of the additive-free ester lubricant in which the wear rate was found to increase in proportion to the dissolved oxygen concentration.

(6) It is considered that the lifetime of the ROO· radical in the presence of antioxidants is short. Any oxidative wear must therefore result mainly from radicals produced within the vicinity of the wearing surface, activated by the fretting action. It would seem likely therefore that a metal deactivator in combination with either of the two antioxidants would enable the wear to be reduced still further.

(7) The reaction at the surface between the radical and the metal is considered in more detail in the following chapter.

CHAPTER 9 - OXIDATION OF THE STEEL SURFACE

9.1 Introduction

In this chapter the chemical and metallurgical aspects of steel oxidation within the fretting contact are considered in detail. A mechanism is proposed for the reaction of peroxy radicals with metal and oxide surfaces.

In other wear processes the type of oxide formed on steel surfaces has been shown to determine the rate of wear[33, 115, 116]. This chapter describes the tests performed in an attempt to identify the oxides formed on the surfaces of the spline teeth, and as debris, during fretting.

9.2 The Nature of the Oxides

The splines used in the fretting tests were manufactured from EN36C steel. This steel does not contain sufficient chromium to be "stainless", i.e. a protective chromic oxide film is not formed and the majority of the oxides will be compounds of iron.

There are three oxides of iron: FeO (Wustite) Fe_3O_4 (Magnetite) and Fe_2O_3 (Haemetite). FeO is not formed at temperatures below 560°C[111], so will not be considered here. A piece of steel oxidised in air at temperatures below about 180°C will form a duplex oxide film - a layer of Fe_3O_4 beneath αFe_2O_3. Fe_2O_3 has two stable forms:

αFe_2O_3 has a rhombohedral crystal structure [111] and is therefore hard and brittle. There is often an oxygen deficiency with a number of anionic vacancies

balanced by twice as many Fe^{2+} ions. The diffusion of oxygen through the lattice is therefore very much faster than the diffusion of iron. That is, αFe_2O_3 is an n-type conductor.

γFe_2O_3 is formed by oxidation of Fe_3O_4 at temperatures between 200 and 400(111) and has a similar crystal structure to Fe_3O_4 and hence similar properties.

Fe_3O_4 has a spinel structure -- the oxygen ions form a face centred cubic array and the iron ions occupy the interstitial sites. Fe_3O_4 exists with a deficiency of iron - a number of vacant cation sites being balanced by twice as many extra Fe^{3+} ions. It is therefore a p-type conductor, although the diffusion rate of anions is not insignificant. The cubic structure of Fe_3O_4 (and γFe_2O_3) results in relatively high ductility and low hardness.

The difference in crystal structure enables αFe_2O_3 to be distinguished from Fe_3O_4 and γFe_2O_3 by their x-ray diffraction patterns. The details of x-ray diffraction analysis are outlined in this chapter.

The difference in defect structures (n-type and p-type) results in different oxidation processes. Consider a steel covered with a duplex film as shown in fig. 9.2.1 In Fe_3O_4 iron diffuses out from the metal - in αFe_2O_3 oxygen diffuses inwards(112).

The reactions at the interfaces are:

I) $Fe + \boxed{C} \rightarrow Fe^{2+} + 2e^-$ i

Fe^{2+} diffuses by interchange with cation vacancies through Fe_3O_4 towards boundary II. The transfer of electrons may

Figure 9.2.1 Illustration of the duplex film on Iron.
after Kubaschewski and Hopkins, ref. 112

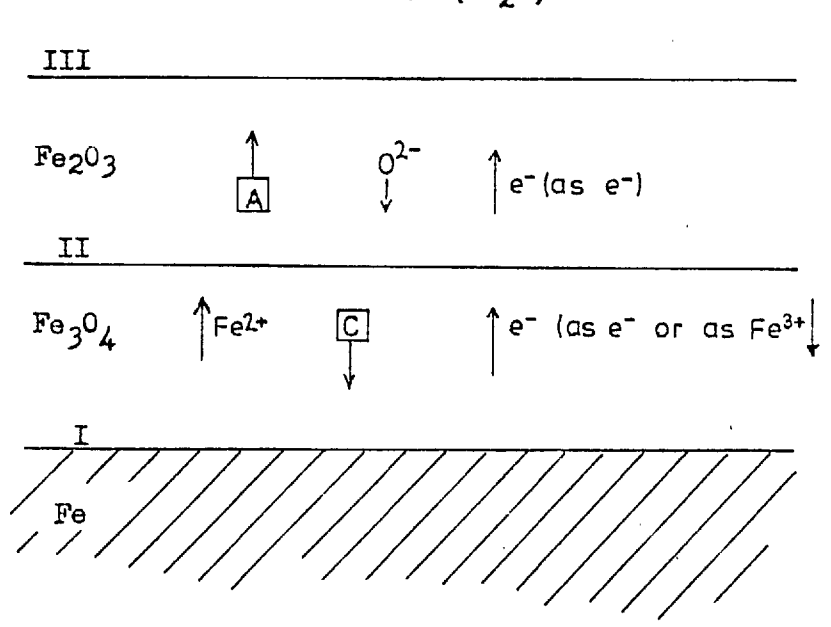

be via the switching $Fe^{2+} \longleftrightarrow Fe^{3+} + e^-$

II $\quad \boxed{Fe^{2+}}_{Fe_3O_4} + O^{2-} \longrightarrow \boxed{Fe^{2+}O^{2-}}_{Fe_3O_4} + \boxed{A}_{Fe_2O_3}$ ii)

$2\boxed{Fe^{2+}O^{2-}}_{Fe_3O_4} + O^{2-} \longrightarrow \boxed{Fe_2O_3}_{Fe_2O_3} + 2\boxed{C}_{Fe_3O_4} + \boxed{A}_{Fe_2O_3}$ iii)

III $\quad \frac{1}{2}O + 2e^- + \boxed{A}_{Fe_2O_3} \longrightarrow \boxed{O^{2-}}_{Fe_2O_3}$ iv

When the environment above the oxide layer is a lubricant the fretting tests indicate that a peroxy radical rather than molecular oxygen takes part in the reaction at boundary III. The following scheme is suggested for the reaction of the peroxy radical with an Fe_2O_3 oxide layer:

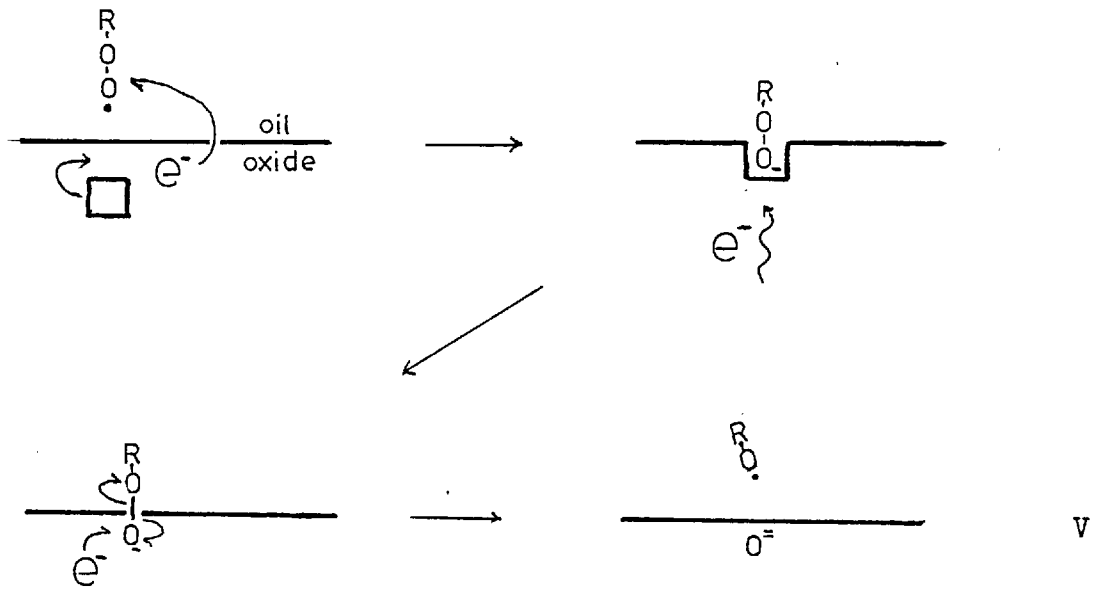

V

The RO· radical may then take part in further oxidation. Under fretting conditions nascent metal and areas of Fe_3O_4 oxide may be exposed to the lubricant as a

result of removal of the oxide layers. Reaction with the peroxy radicals will occur in a similar fashion to v above although as a first step the oxidation of Fe or Fe^{2+} is required:

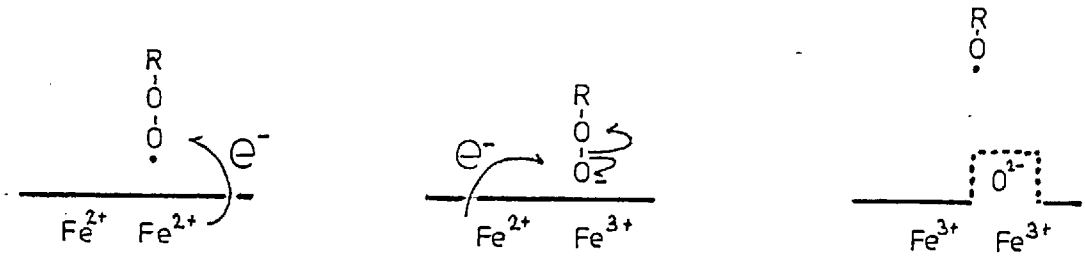

The rate of reaction in this case would not be limited by the rate of diffusion of anionic vacancies.

Whilst the mechanism of reaction v is purely conjectural, it does explain the great reactivity of the peroxy radical, compared with molecular oxygen, towards the metal. In combination with a hydrocarbon the reacting oxygen atom can more readily accept an electron from the oxide than can molecular oxygen. The activation energy required for reaction of the radical is therefore lower.

9.3 Factors Affecting the Oxide Composition

At the interface II the oxides Fe_2O_3 and Fe_3O_4 are in equilibrium. This equilibrium and hence the position

of the interface is dependent on the availability of oxygen in the environment and the reaction temperature. An Ellingham diagram illustrates the equilibrium condition (fig. 9.3.1). At 80°C (the test temperature) Fe_3O_4 and Fe_2O_3 are in equilibrium when the oxygen is reduced below 10^{-50} atmospheres. However, tribological processes are far removed from equilibrium conditions - the rate of supply of oxygen to the surface, and of its reaction there with the metal or with oil radicals, is critical. Tao[60] has calculated that diffusion of dissolved oxygen through a lubricant film as thin as 0.25μm is sufficiently fast to prevent oxygen depletion in a contact. Therefore, formation of Fe_2O_3 would be expected at all the oxygen pressures used in the fretting tests. In addition the increased reactiveness of oxygen in combination with the oil as a peroxy radical would promote the formation of the higher oxide.

On the other hand Kostetskii[114] maintains that, in the presence of a lubricant, formation of lower oxides is promoted. A number of investigations of sliding wear, both lubricated and unlubricated, have shown that under certain conditions αFe_2O_3 is not formed, and also that there is a correlation between the type of oxide formed and the wear rate[115, 116, 33].

Clark, Pritchard and Midgeley[115] found a transition in the friction between unlubricated steel surfaces at a temperature of 200-300°C. There was a corresponding change in the variation of wear with temperature (fig. 9.3.2). They suggested that above the transition

Figure 9.3.1

Ellingham Diagram (113)

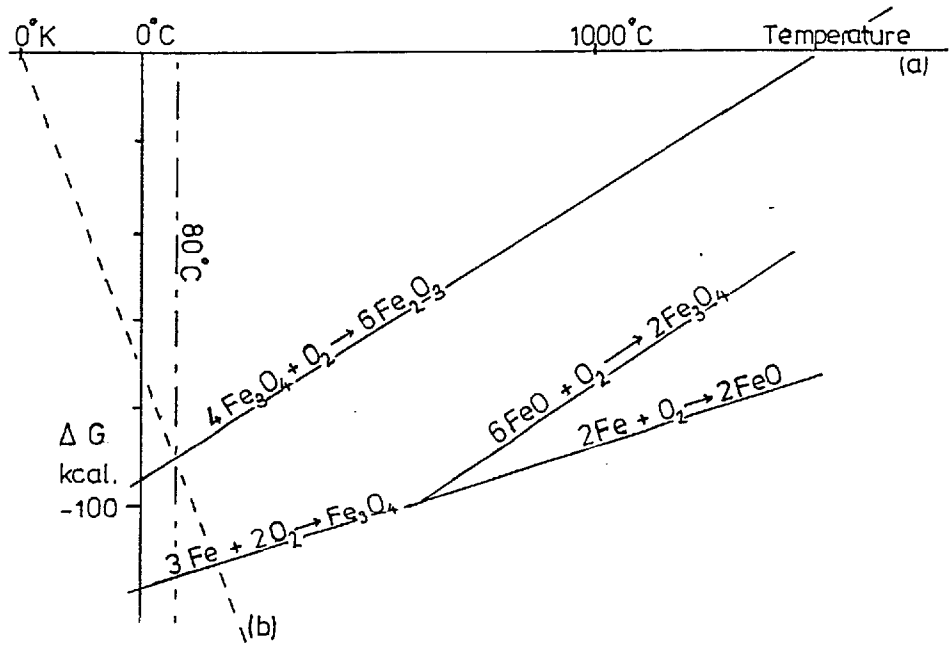

All reactions below and to the left of the Oxygen pressure line, e.g. (a) or (b), will proceed in the direction indicated. Hence if, at 80°C, the oxygen concentration is reduced below that represented by (b) then Fe_3O_4 will not further oxidise to Fe_2O_3.

line (a) represents an oxygen pressure of 1 atmosphere

line (b) represents an oxygen pressure of 10^{-50} atmospheres

Figure 9.3.2 after Clark et al. ref. 115

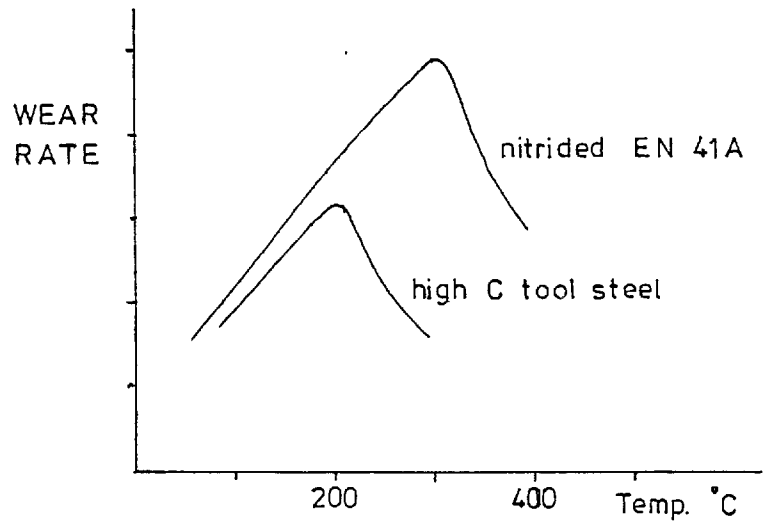

temperature the formation of Fe_3O_4 on the metal surfaces was favoured. As the temperature is increased, Fe_3O_4 replaces Fe_2O_3 on the surface. Tests in carbon dioxide, in which the collected debris was analysed and found to be Fe_3O_4, gave wear two orders of magnitude less than in dry air indicating that the presence of Fe_3O_4 leads to less wear. (Two properties of Fe_3O_4 justify this deduction. It forms a more adherent, more ductile film on metals than Fe_2O_3 and having a lower hardness - 600 VPN as compared with 1100 VPN[38] - is less abrasive). It was shown that the transition temperature varied with the composition of the steel. The presence of alloying elements such as chromium raised the transition temperature.

Similar results were obtained by Quinn et al[116] who investigated the sliding wear of chromium steels in a pin-on-disc rig. A transition in the dependence of wear rate on load occurred at a critical load above which the wear was dramatically reduced. The transition load is said to generate flash temperatures within the contact which coincide with the temperature at which Fe_3O_4 is formed on the steel oxidised in air. Below the transition load the debris was identified as Fe and αFe_2O_3 and the transition load was the lowest at which a Spinel oxide Fe_3O_4 or γFe_2O_3 was identified.

Cullen[33], in wear studies on steels in the presence of a lubricant found a similar transition in wear rate as the lubricant temperature was increased. The transition temperature was load dependent. Again the transition to a low wear rate was associated with the appearance of the

spinel oxide in the debris. The temperature in the contact at transition, a combination of the lubricant temperature and a calculated flash temperature, was 160-180°C.

In lubricated contact a third property of Fe_3O_4 may be responsible for the reduced wear. Namely the greater affinity of Fe_3O_4 over Fe_2O_3 for polar boundary additives in the lubricant. Sakurai et al.(90) has shown that the heat of adsorption of stearic acid onto Fe_3O_4 particles is some ten times greater than onto Fe_2O_3.

In view of the reported large difference in wear rate between the different oxide types and the uncertainty as to the type of oxide formed in lubricated fretting a series of tests was performed to identify the oxide.

9.4 Experimental Techniques

9.4.1 Introduction

The oxides formed on the wearing surfaces during a fretting test may be analysed in situ or by identification of the oxide in the debris. The latter technique has the disadvantage that between removal from the surface and extrusion from the contact the debris undergoes comminution during which further oxidation is possible.

Hence microscopic examination of the debris (see fig. 9.4.1) reveals little about the removal process. However, collected debris may be analysed to determine its composition by the Debye Scherrer x-ray powder diffraction technique. For a number of tests such an analysis was performed but unfortunately for many of the tests the wear was so low that too little debris was collected. In these cases it appeared that only a method of surface analysis

Figure 9.4.1

A Scanning Electron Microscope image of fretting debris.

x 7800

1 µm

The particle size of the debris is estimated to be not greater than 0.7 um

of the very thin oxide films on the fretted teeth could provide answers.

9.4.2 Electron Probe Microanalysis

An electron probe microanalyser (EPMA) was available and has been used previously in lubrication studies[33, 117]. The E.P.M.A. bombards the surface area selected for study with a stream of electrons. The impingement of electrons on the surface excites electrons from the inner shells of the atoms to higher levels. On returning to the ground state the electrons emit radiation of a wavelength characteristic of the particular atom. The analyser is calibrated to be sensitive to the characteristic radiation of specified atoms and gives a reading proportional to the concentration of the atom. However, this technique is not suitable for looking at surface oxide films. E.P.M.A. cannot differentiate between different oxidation states since it relies on excitation of electrons from the inner shells rather than the bonding electrons. In addition the energy of the electron beam (typically 25KV) is such that the electrons penetrate deep into the metal surface. The emitted radiation is therefore characteristic of a layer of depth of the order 10μm in which surface effects are swamped. An E.P.M.A. instrument with a lower beam energy was not available.

9.4.3 Electron Spectroscopy for Chemical Analysis (E.S.C.A.)

Electron spectroscopy for chemical analysis is a method for analysing very thin surface layers. A surface is irradiated with x-rays of known energy under high vacuum (10^{-7} torr). Electrons are liberated with energies

characteristic of their binding energies. Since the energy of the incident x-rays is low only electrons from the outermost shells are ejected and only those very close to the surface of the specimen (1-2nm) escape without collision. The ejected electrons are accelerated towards a target. As the potential of the target is decreased there is a drop in current as those electrons of the lowest energy fail to reach the target. Thus the energy spectrum of emitted electrons may be deduced from the variation of current with voltage. The bonding energies of the electrons are sensitive to the bonding state of the atom so that theoretically the oxidation state of an iron surface can be determined. E.S.C.A. has been applied to studies of e.p. additives on the rubbing surfaces of steel[118] and to studies of the oxidation of steel surfaces in air[119]. In the latter work steel was oxidised by exposure to pure oxygen or air at pressures up to atmospheric. The binding energy of the Iron 2p and the oxygen 1s electrons was measured. It was found that the oxygen spectra was more sensitive than the iron spectra because of the contribution of the sub-surface iron. The results verified that after exposure to air at room temperature and atmospheric pressure both Fe^{3+} and Fe^{2+} were present in the oxide film formed on a clean steel surface.

An E.S.C.A. instrument was used in a trial test to see if any oxide layers could be identified on the fretted surface of spline teeth. The instrument scans a relatively large area (one cm^2) and sums the result. Four teeth were therefore cut from a worn spline and assembled side by

side on a backplate (fig. 9.4.2). The assembly was then inserted into the vacuum chamber on the end of a probe.

It is desirable to transfer the specimens from the rig to the E.S.C.A. instrument in as short a time as is possible with the minimum exposure to atmosphere. Any film on the surface will be susceptible to changes in the environment especially if, as is likely, it is very thin. In the event the experiment was a failure because the fretted surfaces were too rough to give the required intensity of electrons at the detector (most E.S.C.A. studies are performed with highly polished surfaces). Oxygen and carbon peaks were observed, the latter indicating that the surfaces were contaminated with a hydrocarbon film which had not been removed by washing with toluene and acetone. With a cleaning procedure which removed such films there would be a danger of affecting the oxide layer. Unfortunately, further experiments could not be performed because time on the instrument was severely restricted. The development of techniques to enable E.S.C.A. studies of oxide films on worn surfaces would be very valuable.

9.5 Debye-Scherrer X-ray Powder Diffraction Analysis of Fretting Debris

9.5.1 Introduction

The aim of the powder diffraction studies was to determine if there were changes in the oxide composition of the fretting debris as the oxygen activity in the oil was varied. Insufficient debris was produced in the tests with ester at low oxygen concentrations for accurate

Figure 9.4.2

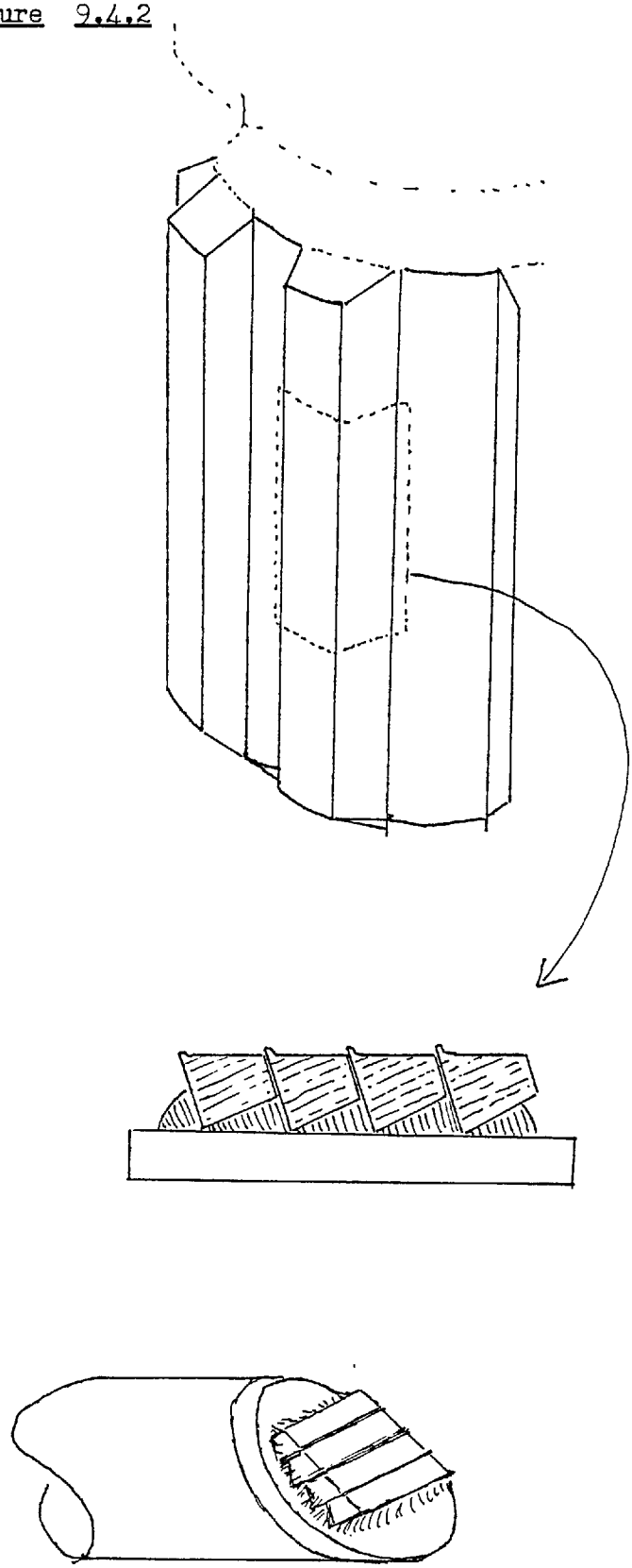

Illustration of the mounting of spline teeth for E.S.C.A.

analysis; therefore debris from the series of tests with hexadecane and hexadecane with acid additives, was analysed.

9.5.2 The Method

X-ray powder diffraction analysis enables identification of the constituents of the wear debris. A monochromatic beam of x-rays directed at the sample is diffracted by it in a family of cones characteristic of its crystal structure. In the Debye Scherrer camera the sample is contained in a Lindemann glass tube, transparent to the x-rays, in the centre of a cylindrical "camera". The cones of diffracted x-rays impinge on a photographic film lining the cylindrical walls and appear as arcs when the film is developed. (See fig. 9.5.1.) Diffraction of the x-ray beam occurs when crystal planes are orientated so as to satisfy the Bragg condition:

$$\Theta = \sin^{-1}\left(\frac{\lambda}{2d}\right)$$

where λ = the wavelength of the incident x-rays

d = the lattice plane spacing

Θ = the angle of the incident beam with respect to the diffracting lattice plane

The dimensions of most cameras are arranged so that the circumference of the camera is 360 cms. Thus the distance between the hole in the film for entry of the x-ray beam and a diffraction line, measured in centimetres, is twice the value of Θ in degrees for the plane giving rise to that line. The Θ values of all lines on the photograph are measured and the lattice spacings (d)

Figure 9.5.1

Diagram of X-ray film - the pattern shown is that from Test 'I'.

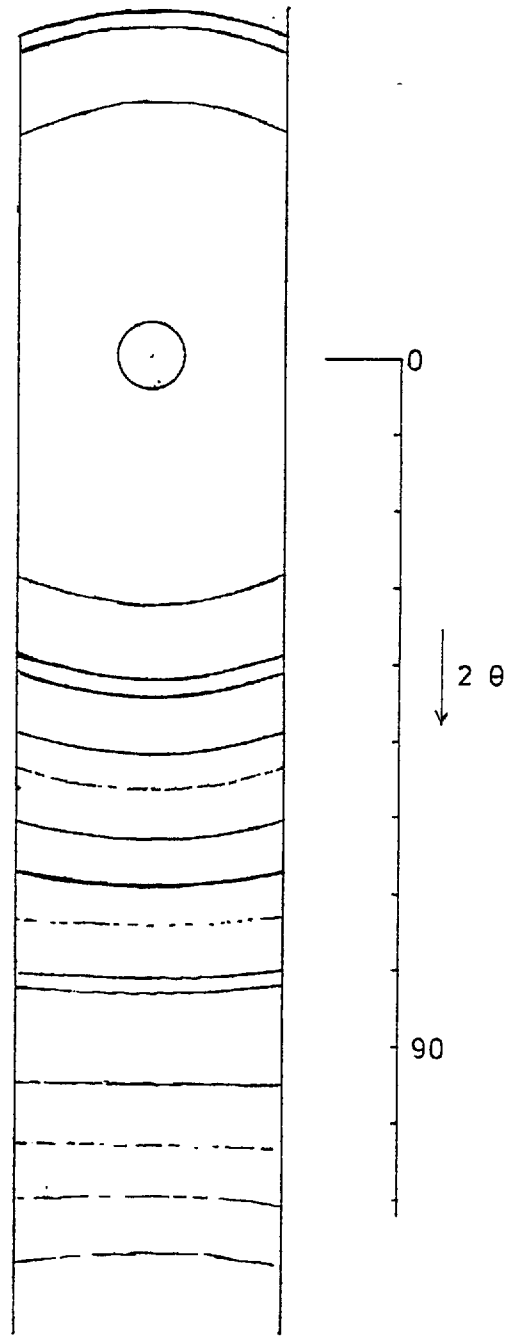

calculated using the Bragg condition.

A pattern of lattice spacings is derived which may be compared with the standard tables in the A.S.T.M. index (120). Note is taken of the intensity of the lines on the film as this plays an important part in the comparison of diffraction patterns.

9.5.3 Experimental Procedure and Results

The debris was prepared for analysis in the following way. It was collected mainly from the bottom of the specimen chamber and by washing of the splines with toluene. It was placed in a broad specimen tube which was filled with toluene. Lubricant contaminating the debris was dissolved by the toluene. Once the debris had settled to the bottom the toluene was pippetted off and a fresh quantity added. When the debris had again settled the toluene was removed and acetone was added. When the debris had settled most of the acetone was removed and the remainder evaporated off. This technique was found to effectively remove hexadecane leaving a dry oxide powder. It was not as successful in treating debris from an ester test leaving a somewhat tarry product, but it was possible to run this in the x-ray machine. The aim of the above process was to prepare the debris for analysis as quickly as possible, as prolonged exposure to atmosphere might have changed the oxidation state. Whilst the iron oxide powders were settling, the specimen tubes were sealed and kept in a cool dark place. The period between removal from the rig and analysis was generally from 24 to 48 hours

The results of the x-ray diffraction studies are tabulated in table 9.1. All the debris consisted of a mixture of iron and one or both of the oxides Fe_2O_3 and Fe_3O_4, except that from a test run in ester with undried air passing through the specimen chamber. In this case the debris was found to contain ferrous hydroxide, $Fe(OH)_2$, in addition to Fe_3O_4 and Fe. Apart from this test Fe_2O_3 was detected in all the debris but Fe_3O_4 was absent after tests at high oxygen concentrations.

The presence in hexadecane of the additive lauric acid does not appear to have affected the composition of the debris. The debris from tests L and P (hexadecane and hexadecane plus acid, at a low oxygen activity) contained an additional substance which was identified as an oxide of chromium. In both these tests the wear was relatively low and only a small sample of debris could be collected. A longer than usual exposure had to be used to obtain a pattern on the film so it is possible that a similar small quantity of chromium oxide was present in all the debris but was only resolved after a long exposure in the camera. The lattice spacings of all the substances identified as given in the A.S.T.M. index are listed in table 9.2.

9.5.4 Assessment of the Relative Quantities of the Oxides

In cases where a sample consists of one or more crystalline substances the relative intensities of the diffraction patterns give some idea of the proportion of each substance present. For instance, the diffraction pattern of the debris from test L contained only the strongest (i.e. most intense) Fe_2O_3 lines, whereas the

TABLE 9.1

Test	Lubricant	Additive	Oxygen Activity m.moles litre^{-1}	Spec. Wgt. Loss mgm.	Oxides Found in Debris
-	Ester	+ water vapour	0.25	16	Fe, $Fe(OH)_2$, Fe_3O_4
F	Hexadecane	-	0.5-1.2	113	Fe, Fe_2O_3, Fe_3O_4
I	"	-	3-4		Fe, Fe_2O_3, Fe_3O_4
L	"	+ 10^{-2}M lauric acid	0.2-0.4	12	Fe, Fe_2O_3, Fe_3O_4, Cr_3O_8
N	"	"	4.5	270	Fe, Fe_2O_3
P	"	+ 0.18M lauric acid	0.2-0.5	13	Fe, Fe_2O_3, Fe_3O_4, Cr_3O_8
U	Ester	Phenyl Naphthyline	3.5-4.2	77	Fe, Fe_2O_3

TABLE 9.2 DIFFRACTION PATTERN INDEX

ANGLE* (2θ)	Subs.A	Subs.B†	Test Code @	F	I	L	N	P	U
23.1	Fe_3O_4							f	
24.4	$Fe(OH)_2$		f						
27.	?							d	
28.8	Cr_3O_8					d		m	
31.	Fe_2O_3		f	v.f	f		m	f	
33.	?					m			
34.	Cr_3O_8					m		m	
36.6	Cr_3O_8					f		f	
38.	Fe_3O_4		f	f	m	m		d	
40.	$Fe(OH)_2$		f						
42.	Fe_2O_3			d	d	v.f	d	d	v.f
45.	Fe_3O_4	Fe_2O_3		v.d	d	d	d	f	f
48.	$Fe(OH)_2$								
52.	Fe_2O_3			v.f	f	f	m		
55.	Fe_3O_4			f	v.f	m		m	
57.	Fe		f	d	d	d	f	f	m
64.	Fe_2O_3			v.f	v.f		m		v.f
69.	Fe_2O_3	Fe_3O_4		d	m		d		f
74.	Fe_3O_4	Fe_2O_3		f	f	v.f	f		v.f
82.	Fe_3O_4	Fe_2O_3		d	m	v.f	m		v.f
84.	Fe_2O_3			f	f		m		v.f
85.	Fe								
96.	Fe_2O_3				v.f		v.f		
98.	Fe_3O_4								
112.	Fe				v.f		v.f		
113.	Fe_2O_3								v.f
116.	Fe_2O_3						v.f		
123.	Fe_2O_3						v.f		
125.	Fe_3O_4								
134.	Fe_2O_3						v.f		
146.	Fe								
157.	Fe_2O_3								

KEY	INTENSITY
v.f	very faint
f	faint
m	medium
d	dark
v.d	very dark

@ Test run in undried air.

*A.S.T.M. values rounded to nearest degree. (Fe K_α radiation)

†Where two substances diffract at the same angle, Substance A is most intense.

Fe_3O_4 pattern is quite marked. This indicates that there is very little Fe_2O_3 present.

A more quantitative estimate of the proportion of oxides present can be made by measuring the intensity of diffraction. Ideally the intensity of the diffracted beams would be measured directly in a diffractometer. As such an instrument was not available, the intensities of the lines on the photographic film were measured using a densitometer, in a comparison of tests F and I. The recorded output of the densitometer is shown in fig. 9.5.2. The peak heights were measured as the distance from the maximum to the notional background level (assumed to be a smooth curve through the points of minimum intensity). These are compared in table 9.3.

Both tests were run with purified hexadecane; during test F the oxygen concentration was maintained in the range 0.94 to 1.40 m.moles litre^{-1} and during test I, at 3 to 5 m.moles litre^{-1}. The absolute intensity of the peaks depends on the quantity of debris in the sample and the exposure time; therefore, the ratio of the peak heights in the two tests has been calculated. The peaks at $2\theta = 45^\circ$, 69°, 74° and 82° cannot be used for comparison as both oxide structures diffract at these angles. Taking the other peaks in order of intensity

Fe_2O_3 has intensity ratios (I/F) 1.65, 1.7, 1.1

Fe_3O_4 has intensity ratios " 1.27, 1.45

Fe has the intensity ratio " 1.52.

The most intense peaks suggest that there is a greater proportion of Fe_2O_3 in the debris from test I.

Figure 9.5.2

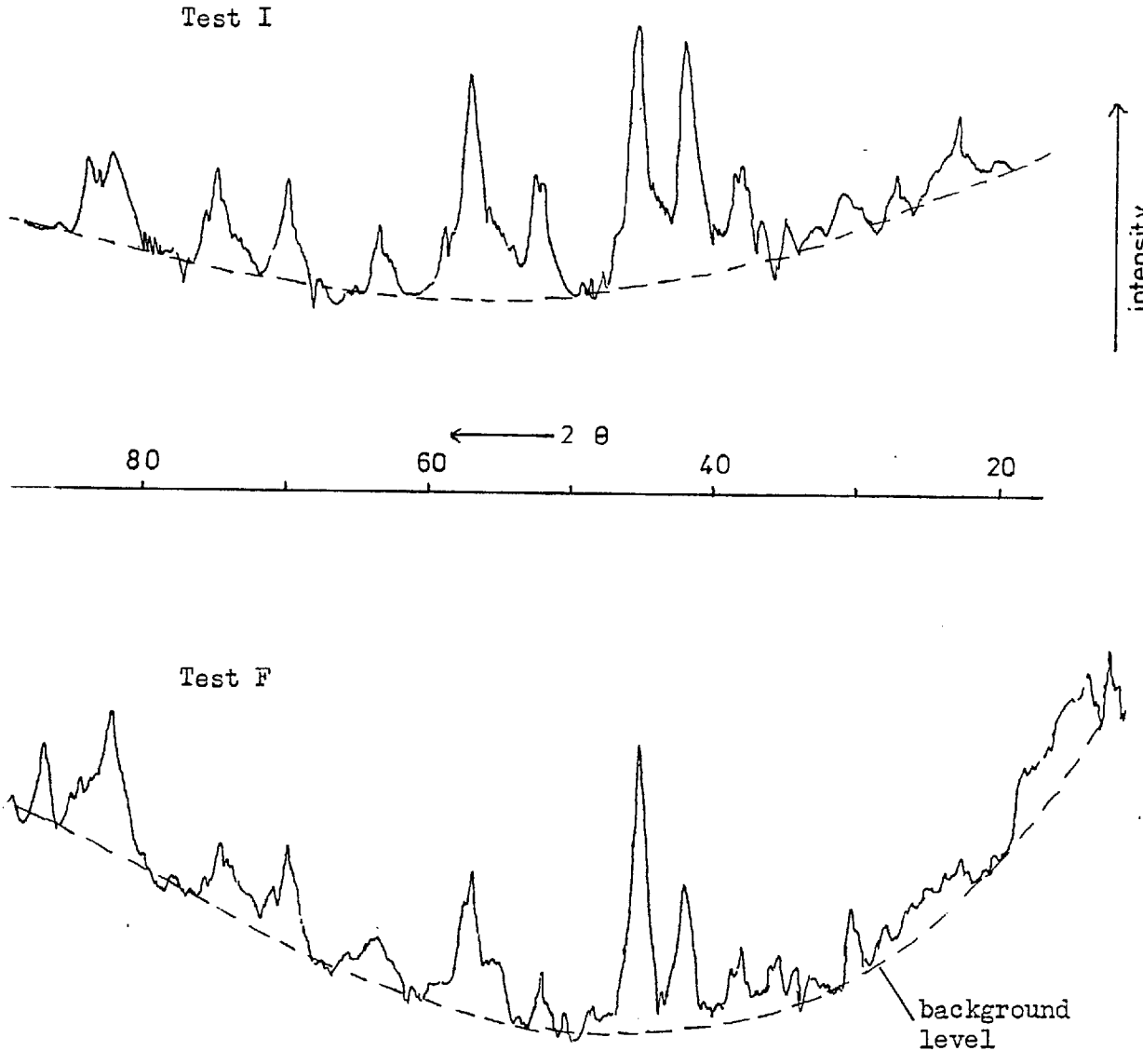

A comparison of Densitometer recordings.

TABLE 9.3 A comparison of the diffraction patterns of debris from tests F and I.

Test conditions:

Test code	Nominal load MN m^{-2}	Oxygen conc^{n} mmoles/litre	Initial wear rate um/hour
F	15	0.48-1.2	1 -1.7
I	15	3 - 4	14.4

Densitometer measurements:

Substance	Diff^{n} angle 2 θ	Peak heights (mm) F	Peak heights (mm) I	Intensity ratios I_F/I_{Fe}	Intensity ratios I_I/I_{Fe}	Intensity ratios I_I/I_F
Fe_3O_4	38	11	14	0.52	0.44	1.27
	55	9	13	0.43	0.41	1.45
Fe_2O_3	42	20	33	0.95	1.03	1.65
	52	10	17	0.48	0.53	1.7
	64	-	10	-	0.31	-
	84	9	10	0.43	0.31	1.1
Fe_2O_3 and Fe_3O_4	45	41	37	1.93	1.14	0.9
	69	14.5	14	0.69	0.44	0.96
	74	10	13	0.48	0.41	1.3
	82	21	13	1.0	0.41	0.62
Fe	57	21	32	1	1	1.52

(i.e. the intensity ratios for Fe_2O_3 $2\theta = 42^\circ, 52^\circ$) are greater than those for Fe_3O_4 ($2\theta = 38^\circ, 55^\circ$). The lower intensity Fe_2O_3 lines at $2\theta = 83.5^\circ$ show the opposite trend. However, the increasing background intensity of the film at high angles makes intensity comparisons less accurate. A similar proportion of iron to iron oxide appears to be present in the samples since the ratios of the intensities of the oxide patterns to the Fe line at $2\theta = 57^\circ$ is about the same for both (table 9.3).

The above analysis demonstrates that there is a decreasing proportion of Fe_2O_3 in the debris as the oxygen concentration in the oil is reduced. There is no evidence for the complete disappearance of this oxide, as it was observed in small quantities at the lowest oxygen concentrations that were obtained in the fretting rig (test L). Whilst every effort was made to analyse the samples without delay, it is possible that during exposure of the debris to atmosphere further oxidation took place.

9.6 Conclusions

(1) Equilibrium conditions predict that a duplex iron oxide film will be formed on the spline surfaces at the test temperature (80°C) over the whole range of oxygen partial pressures used in the fretting tests. It is considered unlikely, however, that equilibrium conditions are attained when fretting wear is occurring.

(2) A mechanism has been proposed for the incorporation of oxygen, supplied by the peroxy radical, into the iron oxides.

(3) Magnetite (Fe_3O_4) has been shown previously to be associated with low rates of sliding wear in both unlubricated and lubricated contact. In some cases a sharp reduction in wear was observed when Fe_3O_4 replaced haemetite (Fe_2O_3) in the debris[33,116].

X-ray diffraction analysis of the debris from a selection of fretting tests showed that Fe_2O_3 was present even at the lowest oxygen concentrations attained in the lubricant, but that the proportion of Fe_2O_3 to Fe_3O_4 decreased with decreasing oxygen activity. Fretting wear tests showed a continuous, rather than a discontinuous, decrease in wear rate with decreasing oxygen activity in the lubricant (see Chapters 4 and 5). It is considered that the reduction in wear rate is due to a combination of a lower rate of metal oxidation due to a decrease in concentration of peroxy radicals and the less abrasive nature of Fe_3O_4 which is formed preferentially at low oxygen activities.

(4) Analysis of the oxides formed on the worn surfaces of the spline teeth by E.S.C.A. was unsuccessful because the fretted surface had an adsorbed hydrocarbon layer which could only have been removed by a cleaning procedure likely to have affected the oxide film. In addition roughening of the metal surface by wear impaired the sensitivity of the E.S.C.A. instrument.

(5) The presence of water vapour in the environment during a fretting test was found to result in the formation of ferrous hydroxide in the debris in addition to magnetite (Fe_3O_4). The wear properties of the

hydroxides and the effect of water vapour on fretting wear have not been investigated here. N.B. Fretting tests run under "standard conditions" were run in an atmosphere from which water vapour had been excluded.

Chapter 10 Conclusions and Suggestions for Further Work

10.1 Conclusions

The work described in this thesis started from the observation by Ku[11, 12] that fretting wear was influenced in some systems by the presence of antioxidants.

The aim was to elucidate this effect by examining the mechanism of fretting and of antioxidant action. This entailed the development of techniques to monitor the activity of dissolved oxygen and the concentration of oxidation products in small samples of oil, and a study of their influence on fretting.

The main conclusions drawn from this work are as follows.

(1) Fretting wear in both ester and hydrocarbon oils is an oxidative process. This is clearly demonstrated by the dependence of wear rate on dissolved oxygen activity.

(2) The transfer of oxygen from solution to the metal is via peroxy radical intermediates. This is shown by an investigation into the effect of antioxidants on fretting and by monitoring of the oxidation products during fretting.

(3) Peroxides which are more stable than peroxy radicals are not directly responsible for oxidation of the metal. The fretting wear rates are shown to be independent of the peroxide concentration.

(4) The removal of oxidised material in fretting is carried out by an abrasive process. Evidence of abrasive wear is shown in Scanning Electron Microscope studies of the worn surface.

(5) High wear rates are associated with three body abrasion and the production of quantities of ferric oxide

debris (Fe_2O_3), whilst low wear rates are associated with two-body abrasion and a high proportion of ferrous oxide (Fe_3O_4) in the debris.

(6) Two-body and three-body abrasive regimes may coexist during fretting at intermediate oxygen activities. Separate regions have been observed on the same tooth surface. It is likely that the transition from 2 to 3 body abrasive wear coincides with the accumulation of a critical quantity of debris.

(7) As a result of this combination of abrasive mechanisms there is no sudden transition from mild to severe wear as the oxygen concentration is increased.

10.2 Practical Relevance of Fretting Wear Results

This work has considerable relevance in lubrication since it suggests ways by which fretting can be reduced.

It has been shown that a prerequisite for severe fretting wear is the presence of a high concentration of dissolved oxygen. Reducing the level of oxygen can dramatically limit fretting but generally this is not a practical possibility. However, it is also possible to reduce fretting by blocking the chemical pathway by which oxygen reacts with the metal. Peroxy radicals have been implicated as the most important intermediates in this pathway and suitable antioxidants are capable of suppressing these species.

10.3 Suggestions for Further Work

The mechanism of fretting wear of the splines has been established. The influence of three parameters on

this mechanism could usefully be investigated.

1. Effect of temperature. Preliminary tests have shown that there is an increase in the wear rate at increased oil temperatures. In view of the changes in lubricant properties with temperature, an investigation of this effect would be valuable.

2. Wear under increased load. An increase of applied load gives an increase in wear rate[12] (fig. 10. 3.1). An increased load could be used in tests at very low oxygen concentrations to explore the low wear regimes. Increased wear under these conditions will improve the sensitivity of the recording system to changes in wear rates. In addition, the production of more debris would aid X-ray diffraction analysis of its composition.

3. Wear of hardened steel specimens. The use of hardened steel splines will reduce wear by abrasion although damage by fatigue processes may well be increased. It is likely that there is an optimum hardness for minimum wear.

10.4 Investigation of Additive Combinations

The complex nature of the fretting process in the spline wear rig made it essential to study at first some simple lubricating systems. The addition of antioxidants to the base stock is effective in reducing wear, although the concentrations required for maximum effect are larger than are used in practice. However, it is known that a combination of the two types of antioxidant is generally more effective in reducing oil oxidation than is one of the additives alone[8]. There is scope

Figure 10.3.1

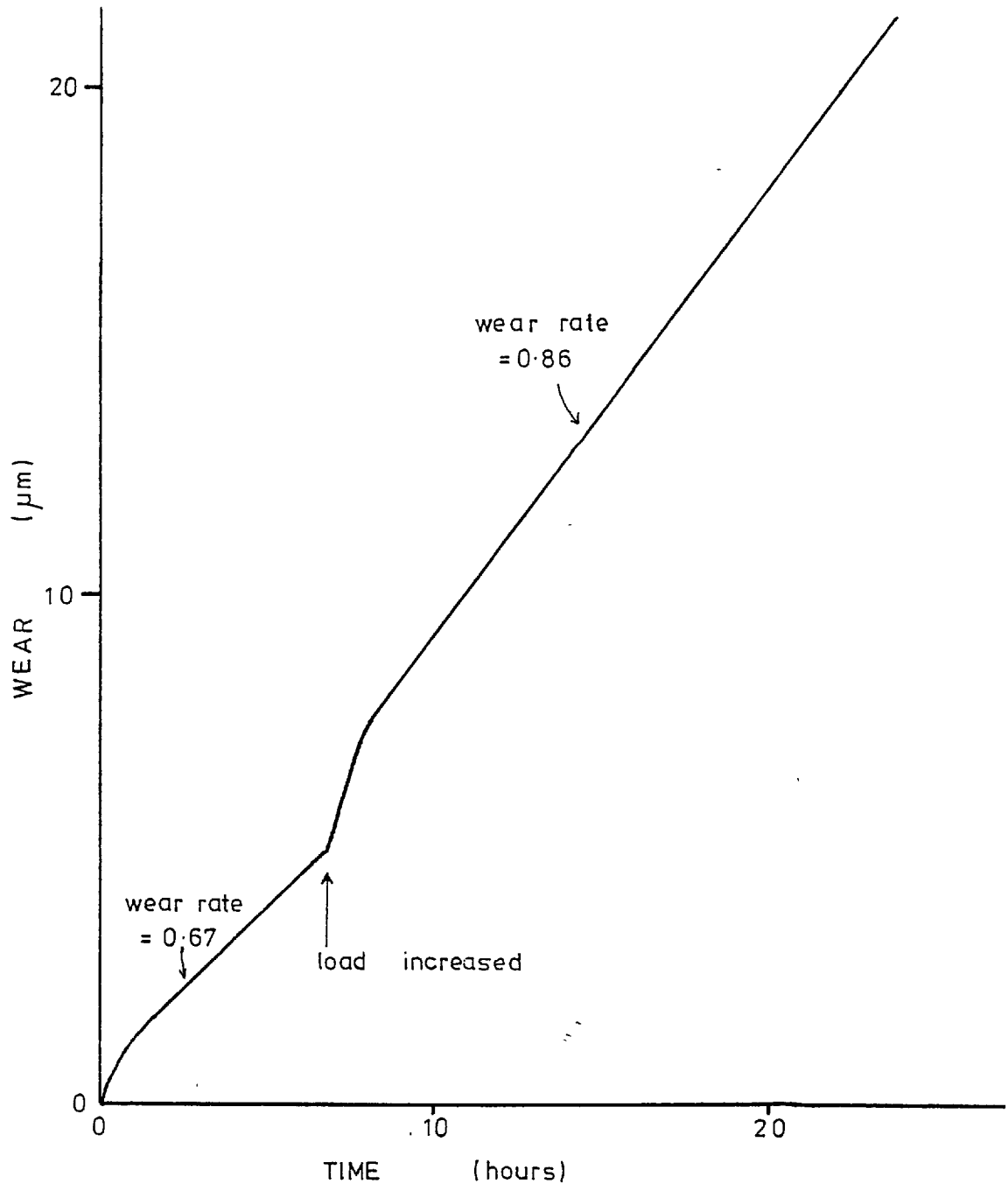

Wear graph of a test in which the tooth loading was increased after 7 hours from 15 MN m^{-2} to 22.5 MN m^{-2}.

Lubricant : Ester

Oxygen concentration : 0.29 mmoles $litre^{-1}$

for investigation of such synergistic effects. In view of the part played by metals in catalysis of oil oxidation the inclusion of a metal deactivator in the additive package should prove beneficial.

Finally, the effect of the gamut of additives (dispersants, detergents, antifoam agents, etc.) which make up a commercial package have yet to be rigorously tested in the fretting rig. It is hoped that the work in this thesis provides a useful foundation for such development.

REFERENCES

1. R. B. Waterhouse 'Fretting Corrosion' publ. Pergamon Press 1972
2. P. L. Hurricks 'The mechanism of fretting - a review' Wear 15 1970 p.389
3. Specialist meeting on fretting in aircraft systems AGARD conference proc. no. 161 1974
4. N. Ohmae and T. Tsukizoe 'Effect of slip amplitude on fretting' Wear 27 1974 p.281
5. E. E. Klaus and H. E. Bieber 'Effect of some physical and chemical properties of lubricants on Boundary Lubrication' A.S.L.E. Trans. 7 1964 p.1-10
6. S. G. Rudston and R. D. Whitby 'The effect of model lubricating oil constituents on the wear of steel' J. Inst. Pet. 57 1971 p. 189-203
7. A. R. Lansdown and P. L. Hurricks 'Interaction of lubricants and materials' Trans. Inst. Marine Eng. 85 1973 p.1-7
8. J. F. Ford 'Lubricating oil additives - a Chemist's eye view' J. Inst. Pet. 54 1968 p.198-210
9. A. C. Bose, E. E. Klaus and E. J. Tewksbury 'Evaluation of wear products produced by some chemical reactions in Boundary Lubrication' A.S.L.E. Trans. 19 1976 p.287-292
10. R. W. Mould and H. B. Silver 'The effect of oil deterioration on the fatigue life of EN31 steel

using the Rolling Four Ball Machine'
Wear 31 1975 p.295-306

11. W. D. Weatherford, M. L. Valtierra and P. M. Ku 'Experimental study of spline wear and lubrication effects'
A.S.L.E. Trans. 9 1966 p.171-178

12. W. D. Weatherford, M. L. Valtierra and P. M. Ku 'Mechanisms of wear in misaligned splines'
J. Lub. Tech., Trans. A.S.M.E. 90F 1968 p.42-48

13. M. L. Valtierra, A. Pakvis and P. M. Ku 'Spline wear in jet fuel environment'
Lub. Engineering 31 1975 p.136-142

14. J. K. Appeldoorn, I. B. Goldman and F. F. Tao 'Corrosive wear by oxygen and moisture'
A.S.L.E. Trans. 12 1969 p.140-150

15. W. W. Seifert and V. C. Westcott 'A method for the study of wear particles in lubricating oil'
Wear 21 1972 p.27-42

16. J. R. McDowell 'Fretting of hardened steel in oil'
A.S.L.E. Trans. 1 1958 p.287-295

17. J. C. Gregory 'A salt bath treatment to improve resistance of ferrous metals to scuffing wear, fretting and fatigue'
Wear 9 1966 p.249-279

18. R. O. Bjerk 'Oxygen - an extreme-pressure additive'
A.S.L.E. Trans. 16 1973 p.97-106

19. D. Godfrey and M. Bailey 'Early stages of fretting of Copper, Iron and Steel'

Lubr. Eng. 10 1954 p.155

20. B. Bethune and R. B. Waterhouse 'Adhesion of metal surfaces under fretting conditions' Wear 12 1968 p.289 and 369

21. I. F. Stowers and E. Rabinowicz 'The mechanism of fretting wear' J. Lub. Tech., Trans. A.S.M.E. 95 1973 p.65-70

22. D. H. Buckley 'Effect of various material properties on the adhesive stage of fretting' N.A.S.A. publ. T.M. x -71582 1974

23. R. C. Bill 'Study of fretting wear in Titanium, Monel-400 and Cobalt-25% Mo using the scanning electron microscope' A.S.L.E. Trans. 16 1973 p.286-290

24. J. T. Burwell and C. D. Strang 'Metallic wear' Proc. Roy. Soc. A 212 1952 p.470-477

25. J. F. Archard 'Contact and rubbing of flat surfaces' J. Appl. Phys. 24 1953 p.981-988

26. N. P. Suh 'The delamination theory of wear' Wear 25 1973 p.111-124

27. R. A. Burton and J. A. Russell 'Lubricant effects on fatigue in a stationary concentrated contact under vibratory loading' J. Basic Eng., Trans. A.S.M.E. 88 1966 p.573-580

28. P. L. Hurricks 'The fretting wear of Mild Steel from room temperature to 200°C' Wear 19 1972 p.207-229

29. H. Pittroff 'Fretting corrosion caused by

vibration with rolling bearings stationary'
J. Basic Eng., Trans. A.S.M.E. 87 1965 p.713-723

30. R. B. Waterhouse and D. E. Taylor 'Fretting debris and the Delamination Theory of Wear'
Wear 29 1974 p.337-344

31. J. E. Bowers, N. J. Finch and A. R. Goreham 'The prevention of fretting fatigue in Aluminium Alloys'
Proc. Inst. Mech. Eng. 182 pt. 1 1967-68 p.703-714

32. J. S. Halliday 'Experimental investigation of some processes involved in fretting corrosion'
Conference on Lubrication and Wear, Paper 39.
Inst. Mech. Eng. 1957

33. J. M. Cullen 'Wear mechanism of Salt Bath Carbonitrided Steel'
PhD. thesis. Univ. of London 1976

34. J. F. Hildebrand and W. H. Watson 'Fretting causes failure of a WC-Co coated slide bearing'
Wear 8 1964 p.34

35. D. M. Waters and J. E. Field 'Fretting fatigue strength of EN 26 steel'
N.E.L. Report No. 275 1967

36. B. I. Kostetskii et al. 'The fretting process'
Russ. Eng. Jour. 50 No. 6 1970 p.46-49

37. A. Desetret, G. Vallier and G. H. Wagner 'Fretting corrosion of Stainless Steel in seawater'
Mécan. Mat. Elect. 296/297 1974 p.3-13

38. P. Hancock and R. Hurst 'Surface oxide films at elevated temperatures' Chapter of 'Advances in Corrosion Science and Technology'

Ed. M. G. Fontana and R. W. Staehle Vol. 4 Plenum Press 1974

39. D. Hull 'Introduction to dislocations' Pergamon Press publ. 1965

40. A. H. Keh and S. Weissmann 'Deformation substructures in Body-centred cubic metals' Electron Microscopy and Strength of Crystals p.231 publ. Wiley 1963

41. H. H. Uhlig 'Mechanism of Fretting Corrosion' J. Appl. Mech., Trans. A.S.M.E. 21 1954 p.401-407

42. D. Godfrey 'A study of fretting wear in mineral oil' Lubr. Eng. 12 1956 p.37-42

43. N. Golego, A. Ya. Alyab'ev and V. V. Shevelya 'Role of electrochemical processes in the fretting corrosion of metals' Fziko-Khim. Mekhan. Mat. 8 1972 p.9-15

44. F. Hirano and S. Goto 'Fatigue cracks of bearing metals caused by Reciprocating Rubbing' 5th Conv. Lubr. and Wear. Proc. Inst. Mech. Engrs. 181 3,0 1967 p.31-40

45. I. M. Feng and B. G. Rightmire 'An experimental study of fretting' Proc. Inst. Mech. Engrs. 170 1956 p.1055

46. K. Muller ' How to reduce Fretting Corrosion -- Influence of lubricants' Tribology International April 1975

47. D. E. Taylor and R. B. Waterhouse 'An electrochemical investigation of fretting corrosion of a number of pure metals in 0.5M Sodium Chloride'

Corrosion Science 14 1974 p.111-122

48. G. H. G. Vaessen, C. P. L. Commissaris and A. W. de Gee 'Fretting Corrosion of Cu-Ni-Al against plain carbon steel'
Paper 15 Tribology Conv. Proc. Inst. Mech. Eng. 183 3p 1968/69

49. L. Toth 'The investigation of the Steady Stage of steel fretting'
Wear 20 1972 p.277-286

50. I. M. Feng and H. H. Uhlig 'Fretting Corrosion of Mild Steel in air and nitrogen'
J. Appl. Mech. Trans. A.S.M.E. 21 1954 p.397

51. R. W. Heinemann and R. Shultz 'Studies of fretting wear. The effect of physical variables'
Schmiertechnik 14 1967 p.239

52. G. C. Hite, H. H. Mabie, N. S. Eiss and C. J. Hurst 'The vibration and fretting corrosion of instrument ball bearings'
A.S.L.E. Trans. 15 1972 p.25-36

53. J. S. Halliday and W. Hirst 'The Fretting Corrosion of Mild Steel'
Proc. Roy. Soc. A 236 1956 p.411-425

54. K. Nishioka and K. Hirakawa 'Fundamental investigations of fretting fatigue. Part II'
Bulletin J.S.M.E. 12 1969 p.180-187

55 P. L. Hurricks and K. S. Ashford 'The effect of temperature on the fretting wear of Mild Steel'
Tribology Conv. Proc. Inst. Mech. Engrs. 184 3L 1970 p.165-175

56 T. Mills
Presentation at the "Limits of Lubrication" Conference 1977 (unpublished)

57. W. A. Graham 'An investigation of the effect of hardness on the fretting corrosion of plain steel' MSc. Thesis Univ. of Oklahoma 1963 (see ref. (1) p.120)

58. R. S. Fein and K. L. Kreuz 'Chemistry of Boundary Lubrication of steel by hydrocarbons' A.S.L.E. Trans. 8 1965 p.29-38

59. F. Morton and R. T. T. Bell 'The low temperature liquid phase oxidation of hydrocarbons: a literature survey' J. Inst. Pet. 44 1958 p.260-272

60. F. F. Tao 'The role of diffusion in corrosive wear' A.S.L.E. Trans. 11 1968 p.121

61. R. W. Mould and H. B. Silver 'A study of the effect of acids on the fatigue life of EN31 steel balls' Wear 37 1976 p.333-343

62. I. Koved 'The effect of three Mineral base oils on roller bearing fatigue life' A.S.L.E. Trans. 9 1966 p.222

63. B. S. Wilson and F. H. Garner 'The role of Peroxides in the corrosion of Lead by lubricating oils' J. Inst. Pet. 37 1951 p.225

64. G. L. Goss and D. W. Hoeppner 'Characterisation of Fretting Fatigue damage by S.E.M. analysis'

Wear 24 1973 p.77-95

65. 'Metallic materials specification handbook'
ed. R. B. Ross publ. Spon Ltd. 1972

66. 'Properties of the EN Steels' Vol. 2
publ. The British Iron and Steel Research Association

67. H. A. Spikes 'Physical and chemical adsorption in Boundary Lubrication'
PhD. thesis Univ. of London 1972

68. C. Stinton
'Chemical reactions in lubricated sliding contacts.'
PhD. theses Univ. of London 1978

69. D. D. Fuller 'Theory and practice of lubrication for engineers'
publ. Wiley 1956

70. A. Jackson 'Optical elastohydrodynamics of rough surfaces'
PhD. thesis Univ. of London 1974

71. H. Blok 'Theoretical study of temperature rise at surfaces of actual contact under oiliness lubricating conditions'
Inst. Mech. Eng. General Discussion on Lubrication 2
1937 p.222

72. J. F. Archard 'The temperature of rubbing surfaces'
Wear 2 1958/59 p.438

73. A. Ya. Alyab'ev, Yu. A. Kazimirchik, V. P. Onoprienko
'Thermal phenomena in the fretting corrosion of metals'
Sbornik Nauchn. Trudov, Kiev Inst. Inzh Gradch Aviatsii
2 1971 p.24-28

74. J. A. Petrocelli, D. H. Licktenfels 'Determination of dissolved gases in petroleum fractions by

Gas Chromatography'
Anal. Chem. 31 1959 p.2017-2019

75. P. G. Elsey 'Gas Chromatography determination of dissolved oxygen in lubricating oils'
Anal. Chem. 31 1959 p.869-870

76. J. E. Jolley and J. W. Hildebrand 'Solubility, Entropy and Partial Molal Volumes in solution of gases in non-polar solvents'
J. Am. Chem. Soc. 80 1958 p.1050-1054

77. J. H. Hildebrand and R. L. Scott 'Regular Solutions'
publ. Prentice Hall. New Jersey 1962

78. 'Standard method of test for solubility of fixed gases in liquids'
A.S.T.M./I.P. Test no. D 2780 publ. 1972 Annual Book of A.S.T.M. Standards Philadelphia Pa.

79. A. A. Kilner 'Measurement of absorbed gases in chemical engineering research'
British Chem. Eng. 10 1965 p.537

80. 'Determination of oxygen in water'
Standard Methods of Chemical Analysis N. H. Furmane, F. J. Welcher eds. publ. Van Nostrand 6th ed. Vol. 1 1962 p.784-786

81. K. H. Mancy, D. A. Okun and C. N. Reilley
'A galvanic Cell oxygen analyzer'
J. of Electroanalytical Chemistry 4 1962 p.65-92

82. A. T. J. Hayward 'Two new instruments for measuring the air content of oil'
J. Inst. Pet. 47 1961 p.99

83. W. G. Dukek and A. H. Popkin 'Dibasic acid esters'
Chapter 5 of 'Synthetic Lubricants'. Gunderson and Hart (eds.) publ. Reinhold P.C. 1962

84. R. L. Johnson, M. A. Swikert and E. E. Besson
Lubr. Eng. 9 1953 p.144

85. M. W. Rigg and H. Gisser ' Autoxidation of the saturated aliphatic diesters'
J. Am. Chem. Soc. 75 1953 p.1415-1420

86. A. D. Walsh 'Processes of oxidation in hydrocarbon fuels - I'
Trans. Faraday Soc. 42 1946 p.269

87. P. J. Sniegoski 'Selectivity of the oxidative attack on a model ester lubricant'
A.S.L.E. Trans. 20 1977 p.282-286

88. L. I. Ermolaeva and B. G. Freidin 'Oxidation of Dimethyl Sebacate'
J. Appl. Chem. of U.S.S.R. 41 1968 p.1542

89. C. D. Wagner, R. H. Smith and E. D. Peters
'Determination of organic peroxides. Evaluation of a modified Iodometric method'
Anal. Chem. 19 1947 p.976-979

90. S. Hironaka, Y. Yahagi and T. Sakurai 'Heats of adsorption and anti-wear properties of some surface active substances'
Bull. Jap. Petr. Inst. 17 1975 p.201-205

91. D. Play and M. Godet 'Coexistence of different wear mechanisms in a simple contact'
Wear 42 1977 p.197-198

92. G. H. Denison 'Oxidation of lubricating oils'
Indust. Eng. Chem. 36 1944 p.477

93. N. K. Chakravarty 'The influence of Lead, Iron, Tin and Copper on the oxidation of lubricating oils - Part II On the metal catalysed oxidation of oils'
J. Inst. Pet. 49 1963 p.353-357

94. M. R. Fenske 'New chemicals and fuels by oxidation'
J. Inst. Pet. 52 1966 p.5

95. Y. Yamamoto and F. Hirano 'The effect of Sulphur compounds at very low concentrations in lubricants on scoring resistance'
Parts I and II Wear 42 p.71-90

96. R. W. Hiley 'Polysulphides and Extreme Pressure Lubrication'
PhD. thesis Univ. of London 1976

97. H. C. Hill 'Introduction to Mass Spectroscopy'
publ. Heyden and Son Ltd. London 2nd Ed. 1972

98. F. W. McLafferty 'Mass Spectral Correlations'
publ. American Chemical Soc. Washington 1963

99. J. H. Beynon 'Mass Spectrometry and its application to organic chemistry'
publ. Elsevier Publ. Co. Ltd. 1960

100. Neutralisation Number by Colour-Indicator Titration
Institute of Petroleum Test No. 139

101. D. H. Wheeler
Oil and Soap 9 1932 p.89

102. J. J. Bikerman
Surface chemistry. Theory and applications
publ. Academic Press inc. 1958

103. L. I. Osipow
Surface Chemistry
publ. Reinhold Publishing Corp. 1962

104. J. A. Russell, W. E. Campbell, R. A. Burton, P. M. Ku
'Boundary Lubrication behaviour of organic films at low temperatures'
A.S.L.E. Trans. 8 1965 p.48-58

105. F. G. Rounds 'Effect of additives on the friction of steel on steel II,- Additive-Base oil interactions'
A.S.L.E. Trans. 8 1965 p.21

106. C. J. Pedersen 'Mechanism of antioxidant action in gasoline'
Industrial and Eng. Chemistry 48 1956 p.1881

107. J. R. Lodwick 'Chemical additives in petroleum fuels. Some uses and action mechanisms'
J. Inst. Pet. 50 1964 p.297-299

108. G. W. Kennerly and W. L. Patterson Jnr.
'Kinetic studies of petroleum antioxidants'
Industrial and Eng. Chemistry 48 1956 p.1917-1924

109. A. J. Burn 'Mechanism of antioxidant action of Zinc Dialkyl dithiophosphates'
Tetrahedron 22 1966 p.2153

110. N. A. Scarlett 'Lubricants for preventing fretting wear'
Erdol und Kohle Erdgas Petrochemie 15 1962 p.538-541

111. M. Hansen 'Constitution of binary alloys'
p.687 publ. McGraw-Hill Book Co. Inc. New York 2nd Ed.

112. O. Kubaschewski and B. E. Hopkins
'Oxidation of Metals and Alloys'
p.108-113 publ. Butterworths London 2nd Edition 1967

113. L. S. Darken and R. W. Gurry
'Physical Chemistry of Metals'
McGraw Hill Book Co. 1953 p. 349.

114. B. I. Kostetskii and P. K. Topekha
'Oxidation processes during friction and wear of metals'
Friction and Wear in Machinery 19 1965 p.65

115. W. T. Clark, C. Pritchard and J. W. Midgeley
'Mild wear of unlubricated hard steels in air and nitrogen'
Tribology Conv. Proc. Inst. Mech. Engrs. 182 pt.3N 1968 p.97-106

116. T. F. J. Quinn, A. R. Baig, C. A. Hogarth and H. Müller 'Transitions in the friction coefficients, the wear rates, and the compositions of the wear debris produced in the unlubricated sliding wear of chromium steels'
A.S.L.E. Trans. 16 1973 p.239-244

117. A. Roberts 'The role of Tin in the Boundary Lubrication of bronzes'
PhD. Thesis Univ. of London 1974

118. R. J. Bird and G. D. Galvin 'The application of Photoelectron spectroscopy to the study of e.p. films on lubricated surfaces'
Wear 37 1976 p.143-167

119. A. Nishijima, Y. Nihei, M. Kudo and H. Kamada 'Application of Photoelectron Spectroscopy to some metallic surfaces and their oxidations' Proc. 2nd Conf. on Solid Surfaces. Japan J. of Appl. Physics Supplement 2 pt.2 1974 p.93-96

120. 'X-ray Powder Data file' A.S.T.M. Special Publication 48.J publ. A.S.T.M. Philadelphia

121. N. P. Suh et al 'A series of papers on the topic of the Delamination Theory of Wear' Wear 44 1977 p.1-162

122. J. P. Hirth and D. A. Rigney 'Crystal plasticity and the Delamination Theory of Wear' Wear 39 1976 p.133-141

123. K. H. R. Wright 'Fretting corrosion of Cast Iron' Proc. Inst. Mech. Engrs. Conf. on Lubrication and Wear 1st-3rd Oct. 1957 Paper 26

124. I. B. Goldman, J. K. Appeldoorn and F. F. Tao 'Scuffing as influenced by oxygen and moisture' A.S.L.E. Trans. 13 1970 p.29

125. F. F. Tao and J. K. Appeldoorn 'An experimental study of the wear caused by loose abrasive particles in oil' A.S.L.E. Trans. 13 1970 p.169

126 'Gear Design and Application' N. P. Chironis ed. McGraw Hill Book Co. 1967 p.316-319